ENVISIONING THE FUTURE OF INDUSTRIAL BIOPROCESSES THROUGH BIOREFINERY

EDITED BY: Sónia Patrícia Marques Ventura, Nicolas Papaiconomou and Jorge Fernando Brandão Pereira

PUBLISHED IN: Frontiers in Bioengineering and Biotechnology

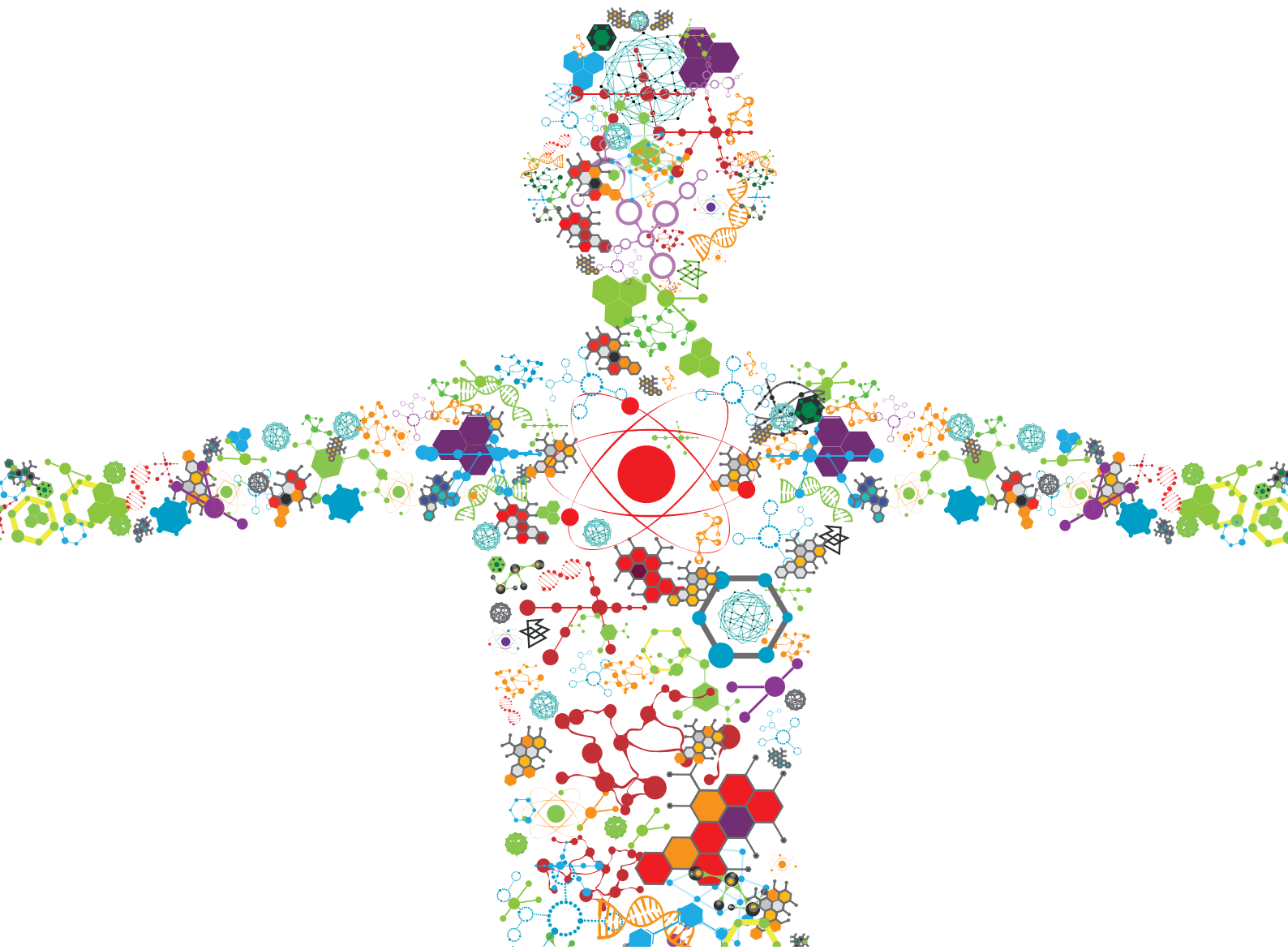

frontiers Research Topics

frontiers

ISSN 1664-8714
ISBN 978-2-88966-670-6
DOI 10.3389/978-2-88966-670-6

About Frontiers

Frontiers is more than just an open-access publisher of scholarly articles: it is a pioneering approach to the world of academia, radically improving the way scholarly research is managed. The grand vision of Frontiers is a world where all people have an equal opportunity to seek, share and generate knowledge. Frontiers provides immediate and permanent online open access to all its publications, but this alone is not enough to realize our grand goals.

Frontiers Journal Series

The Frontiers Journal Series is a multi-tier and interdisciplinary set of open-access, online journals, promising a paradigm shift from the current review, selection and dissemination processes in academic publishing. All Frontiers journals are driven by researchers for researchers; therefore, they constitute a service to the scholarly community. At the same time, the Frontiers Journal Series operates on a revolutionary invention, the tiered publishing system, initially addressing specific communities of scholars, and gradually climbing up to broader public understanding, thus serving the interests of the lay society, too.

Dedication to Quality

Each Frontiers article is a landmark of the highest quality, thanks to genuinely collaborative interactions between authors and review editors, who include some of the world's best academicians. Research must be certified by peers before entering a stream of knowledge that may eventually reach the public - and shape society; therefore, Frontiers only applies the most rigorous and unbiased reviews.
Frontiers revolutionizes research publishing by freely delivering the most outstanding research, evaluated with no bias from both the academic and social point of view. By applying the most advanced information technologies, Frontiers is catapulting scholarly publishing into a new generation.

What are Frontiers Research Topics?

Frontiers Research Topics are very popular trademarks of the Frontiers Journals Series: they are collections of at least ten articles, all centered on a particular subject. With their unique mix of varied contributions from Original Research to Review Articles, Frontiers Research Topics unify the most influential researchers, the latest key findings and historical advances in a hot research area! Find out more on how to host your own Frontiers Research Topic or contribute to one as an author by contacting the Frontiers Editorial Office: frontiersin.org/about/contact

ENVISIONING THE FUTURE OF INDUSTRIAL BIOPROCESSES THROUGH BIOREFINERY

Topic Editors:
Sónia Patrícia Marques Ventura, University of Aveiro, Portugal
Nicolas Papaiconomou, Université Côte d'Azur, France
Jorge Fernando Brandão Pereira, Chemical Process Engineering and Forest Products Research Centre (CIEPQPF), Portugal

Citation: Ventura, S. P. M., Papaiconomou, N., Pereira, J. F. B., eds. (2021). Envisioning the Future of Industrial Bioprocesses Through Biorefinery. Lausanne: Frontiers Media SA. doi: 10.3389/978-2-88966-670-6

Table of Contents

frontiers in Bioengineering and Biotechnology

EDITORIAL
published: 26 February 2021
doi: 10.3389/fbioe.2021.617999

Editorial: Envisioning the Future of Industrial Bioprocesses Through Biorefinery

Jorge F. B. Pereira[1], *Nicolas Papaiconomou*[2] *and Sónia P. M. Ventura*[3]*

[1] Chemical Process Engineering and Forest Products Research Centre (CIEPQPF), Department of Chemical Engineering, University of Coimbra, Coimbra, Portugal, [2] Institut de Chimie de Nice, UMR 7272, Université Côte d'Azur, CNRS, Nice, France, [3] Aveiro Institute of Materials - CICECO, Chemistry Department, University of Aveiro, Aveiro, Portugal

Keywords: residues, biomass, circular economy, Biorefinery, downstream processes

Editorial on the Research Topic

Envisioning the Future of Industrial Bioprocesses Through Biorefinery

Biorefinery is generally described as a facility integrating the conversion of biomass into new chemicals, fuels, and other commercial products and commodities. Supported by the Circular Economy concept, the Biorefinery scope is now enlarging to the conversion of residues, co-products and wastes. Worldwide, academia and industry believe that Biorefinery will soon play a crucial role in the economy, considering the outstanding growth of population and the increased needs for food, energy, chemicals, materials, pharmaceuticals, and other products, as well as acknowledging that society is moving toward a bio-based economy. For a successful market implementation of an integrated Biorefinery, all process unit operations must be technically improved. Moreover, the sustainability of the biomass-to-products chain must be guaranteed. This requires proposing new process developments ensuring both economically profitable bioprocesses and an absence of adverse environmental impacts.

Forestry, food, marine, and freshwater sectors are some of the most relevant players under the concept of Biorefinery, but they have been until now largely unexplored. Experts are working worldwide on the development of new or improved processes in order to address most issues attributed to so-called Biorefinery failure. Their efforts, however, are often not recognized and the resulting potential development of new products included in cosmetics, pharmaceutical, food, feed, medicine, and nutraceutical sectors are compromised. With this in mind, this Research Topic intends to call the attention of academia, industry and society for the chemical wealth that is yet being neglected, not only by the producers of these residues and raw materials, but also by the players of the principal sectors of activity worldwide. This Research Topic presents and discusses the relevant actions under development considering the theme of Biorefinery, particularly, through the analysis of the three main ivory towers of Biorefinery: (i) raw materials and residues; (ii) new or improved processes; and (iii) new products for old markets and old products for new markets. Contributions focused on microalgae, marine residues, and agro-food residues that are explored within a Biorefinery concept.

Agro-food residues and their biotechnological processing to obtain added-value products are central in industrial bioprocesses toward a more "ecofriendly" perspective, this considering the economic and environmental footprints. In this sense, this Research Topic started (Li et al.) by investigating the methane production by processing different parts of corn stover and using a simple co-culture of *Pecoramyces* and *Methanobrevibacter* species. The use of this simple co-culture of anaerobic and methanogen microorganisms allowed high methane conversion rates to be obtained from both the leaf blade and stem pith of corn stover, thus demonstrating its potential to convert lignocellulosic substrates into energy. The focus on other products than the

OPEN ACCESS

Edited and reviewed by:
Georg M. Guebitz,
University of Natural Resources and Life Sciences Vienna, Austria

***Correspondence:**
Sónia P. M. Ventura
spventura@ua.pt

Specialty section:
This article was submitted to Industrial Biotechnology, a section of the journal Frontiers in Bioengineering and Biotechnology

Received: *15 October 2020*
Accepted: *08 February 2021*
Published: *26 February 2021*

Citation:
Pereira JFB, Papaiconomou N and Ventura SPM (2021) Editorial: Envisioning the Future of Industrial Bioprocesses Through Biorefinery. Front. Bioeng. Biotechnol. 9:617999. doi: 10.3389/fbioe.2021.617999

production of bioenergy was reviewed by Mayolo-Deloisa et al.. In this work, the authors reported the valorization of by-products from the food industry (e.g., wastewater) as sources of laccase, a multi-copper oxidase that catalyzes the oxidation of a wide range of phenolic compounds. In this work, the authors focused on the enzyme bioprocessing, industrial potential and biotechnological applications in the food industry, calling the attention for the great potential of laccase to oxidize lignin, as a pretreatment of agro-food-wastes, greatly fitting the "reduce-reuse-recycle" strategy.

The valorization of freshwater biomass, particularly microalgae was also investigated in this Research Topic. Woortman et al. analyzed the total folate content and vitamer distribution in marine microalgae using stable isotope dilution assay (SIDA) accoupled to LC-MA/MS. High amounts of folate were detected in different microalgae, confirming the use of microalgae as a promising source of food-based compounds, as reported by Desai et al. In this second work focusing the valorization of microalgae, the feasibility of using aqueous solutions of ionic liquids based on imidazolium and phosphonium cations in order to separate hydrophilic and hydrophobic components from *Neochloris oleoabundans* was demonstrated. Results showed the capacity of ionic liquids to permeabilize and disrupt the microalgae cells, allowing the effective extraction of intracellular lipids, proteins and carbohydrates, under a multi-product scenario, and following the scope of a Biorefinery approach.

Interestingly, the use of ionic liquids was widely explored in this Research Topic. Shamshina and Berton scrutinized the recovery, dissolution, and treatment of chitin in ionic liquids. In this review, recent developments in the processing of chitin, particularly using ionic liquid-based techniques (as solvents, co-solvents, or catalysts) were highlighted, demonstrating how this type of solvents improves the chitin processing. The importance of valorization of biomass in a circular economy and bioeconomy precepts was also underlined by both authors, specially, emphasizing the "paradigm shift" needed to balance the oil- to biopolymer-based chemicals, such as chitin for example. The positive impact of ionic liquids in biotechnological processes was also the focus of the original work of Dinis et al. Here, the authors investigated the use of aqueous solutions of ionic liquids as potential media on the DNA stability. The main results have confirmed pH as the most significant condition impacting the DNA stability, and cholinium-based ionic liquids as the most promising preservation agents. While in this work, the authors studied the DNA stability, this investigation also shed light on the interesting potential of using ionic liquids as preservation agents and stabilizing solvents for other molecules of interest, namely proteins and enzymes extracted from different biomasses (e.g., micro and macroalgae). The seventh work composing this Research Topic looked to another perspective of biotechnology industry, though strongly connected to the potential valorization of bioactive products of freshwater and marine origin. In this specific work, the authors developed a purification process able to obtain antigens for vaccine production. After a careful optimization, the authors were able to improve the purification of these antigens (pneumococcal capsular polysaccharides) by integrating an ultrafiltration with precipitation, demonstrating a higher immunogenicity of the conjugate vaccine prepared. In the end, the quality of the results, protocols, and reviews compiled in this Research Topic have caught our interest, and we hope that these will stimulate all scientific communities related to Biotechnology to move forward the investigation based on sustainability and circularity concepts associated with the industrial biorefineries.

AUTHOR CONTRIBUTIONS

SV, JP, and NP have contributed equally for this Editorial. All authors contributed to the article and approved the submitted version.

FUNDING

This work was developed within the scope of the project CICECO-Aveiro Institute of Materials, UIDB/50011/2020 & UIDP/50011/2020, financed by national funds through the Portuguese Foundation for Science and Technology/MCTES.

ACKNOWLEDGMENTS

SV thank FCT for the financial support through the project PTDC/BTA-BTA/30914/2017.

Conflict of Interest: The authors declare that the research was conducted in the absence of any commercial or financial relationships that could be construed as a potential conflict of interest.

frontiers in Bioengineering and Biotechnology

ORIGINAL RESEARCH
published: 25 October 2019
doi: 10.3389/fbioe.2019.00284

Mild Fractionation of Hydrophilic and Hydrophobic Components From *Neochloris oleoabundans* Using Ionic Liquids

Rupali K. Desai[1], *Maria Salvador Fernandez*[1], *Rene H. Wijffels*[1,2] *and Michel H. M. Eppink*[1]*

[1] Bioprocess Engineering, AlgaePARC, Wageningen University, Wageningen, Netherlands, [2] Faculty of Biosciences and Aquaculture, Nord University, Bodø, Norway

Microalgae are a promising source for proteins, lipids, and carbohydrates for the food/feed and biofuel industry. To make microalgae production economically feasible, it is necessary to optimally use all produced compounds keeping full functionality. Therefore, biorefining of microalgae is the key to lower the cost of algal products using mild and effective processing techniques. In this article, we have tested the feasibility of aqueous solutions of imidazolium and phosponium ionic liquids to selectively milk the hydrophobic lipids from *Neochloris oleoabundans* biomass out of intact cells and recover after cell disruption the hydrophilic fraction containing proteins and carbohydrates. The results showed that the ionic liquid tributylmethylphosphonium methylsulfate (TBP SO_4; Cyphos 108) is able to permeabilize fresh intact cells of *N. oleoabundans* for extracting 68% of total lipids out of the cells, whereas, after cell disruption, 80% of total proteins, and 77% of total carbohydrates could be obtained in aqueous buffers. This concept kept the recovered proteins in their native form without interacting with the ionic liquids that will denature the proteins. Selective biorefinery of different components from microalgae using ionic liquid TBP SO_4 explains the novelty of this concept.

Keywords: biorefinery, hydrophobic compounds, hydrophilic compounds, ionic liquids, microalgae

OPEN ACCESS

Edited by:
Sónia Patrícia Marques Ventura, University of Aveiro, Portugal

Reviewed by:
Pau Loke Show, University of Nottingham, United Kingdom
Jürgen Andreaus, Regional University of Blumenau, Brazil

Revathy A/P Sankaran contributed to the review of Pau Loke Show

***Correspondence:**
Michel H. M. Eppink
michel.eppink@wur.nl

Specialty section:
This article was submitted to Industrial Biotechnology, a section of the journal Frontiers in Bioengineering and Biotechnology

Received: *19 July 2019*
Accepted: *07 October 2019*
Published: *25 October 2019*

Citation:
Desai RK, Fernandez MS, Wijffels RH and Eppink MHM (2019) Mild Fractionation of Hydrophilic and Hydrophobic Components From Neochloris oleoabundans Using Ionic Liquids. Front. Bioeng. Biotechnol. 7:284. doi: 10.3389/fbioe.2019.00284

INTRODUCTION

Microalgae are promising feedstocks for biofuel production. These photosynthetic microorganisms have high lipid productivity and do not compete for arable land when compared to terrestrial oleaginous crops (Wijffels and Barbosa, 2010). Microalgae have a very tough cell wall and thus require energy-intensive unit operations to break open the cell and release the intracellular content. Thus, despite the high lipid productivity, the energy input to separate the lipids is much higher than the energy obtained from the biomass, indicating the necessity to use less energy-intensive unit operations. Apart from lipids, microalgae are also good sources of proteins, carbohydrates, and pigments. Utilization of these value-added co-products for food, cosmetics, health, and chemicals would help in making the process economically feasible (Vanthoor-Koopmans et al., 2012).

The current process focuses on recovery of a single component from microalgae, i.e., lipids for biodiesel production (Cuellar-Bermudez et al., 2015). Most commonly, organic solvents are used for extraction of lipids. The Soxhlet (1879) method uses hexane as a solvent and the Bligh and Dyer's (1959) method uses chloroform and methanol mixture as a solvent for extraction. As these processes are designed to extract one component (lipids), it degrades the biomass, making it

unsuitable for recovering other components (e.g., proteins, carbohydrates). Additionally, lipids can also be extracted using sub- and super-critical fluids (Herrero et al., 2006); however, these methods have high energy requirements and thus impact the overall economics of the process. In a study done by Ursu et al. (2014), protein extraction was performed using alkaline condition. However, the proteins precipitate and hydrolyzes under alkaline condition and had lower functional properties (Ursu et al., 2014). It is thus prudent to develop a mild process to fractionate the biomass into its components such that their value and functional integrity are retained.

Conventional extraction processes based on volatile organic solvents pose safety concerns, are toxic, and denature proteins. It is thus necessary to develop newer methods to address these issues. Some of the newer methods include use of supercritical fluids and, recently, ionic liquids (ILs).

ILs are salts that are liquid at temperatures below 100°C. They are composed of cations and anions and have negligible vapor pressure. They are known as designer solvents as their properties such as polarity and viscosity can be tailored by using a different combination of cation and anion (Freemantle, 1998). This makes IL an attractive solvent for liquid–liquid extraction.

ILs were used for lipid extraction from microalgae at elevated temperatures and together with co-solvents such as methanol (Young et al., 2010; Kim et al., 2012). Studies using mixtures of ILs have also been performed to extract lipids from algae biomass (Choi et al., 2014; Yu et al., 2015) and dissolution of microalgae in ILs were also demonstrated (Fujita et al., 2013). Teixeira in his studies have shown energy-efficient deconstruction of algae biomass by dissolution and hydrolysis of microalgae in ILs at temperatures above 100°C (Teixeira, 2012). Olkiewicz et al. (2015) showed ∼75% lipid and 93% FAMEs recovery using hydrated phosphonium IL under ambient temperature conditions. All these studies together with some recent investigations (Orr and Rehmann, 2016; Orr et al., 2016; Wahidin et al., 2016; To et al., 2018) have established the potential of ILs to extract lipids from microalgae with high efficiency. While both Teixeira (2012) and Olkiewicz et al. (2015) have qualitatively demonstrated that all components of microalgae (lipids, proteins, and carbohydrates) can be recovered in one process after hydrolyzing the microalgae, it does not give any indication about recovery of proteins and carbohydrates and the stability of the more fragile proteins. Most of these studies address the recovery and extraction efficiency of lipids from microalgae showing a single-component isolation strategy. While recovery of other components such as the high-value proteins and carbohydrates are not addressed or that such harsh conditions are used (Wang and Zhang, 2012; Lee et al., 2017; To et al., 2018), the products are degraded/denatured. A recent study by Yu et al. (2015) reported energy-efficient extraction of lipids from *Chlorella vulgaris* using IL combined with CO_2 capture. The study showed ∼75% lipid (∼89% FAMEs) recovery but the proteins were denatured in the process. Therefore, to be able to recover all components in their full functional state from microalgae biomass, it is necessary to use mild techniques. Majority of the articles discussed above are focused on lipid extraction from microalgae with ILs using harsh methods such as high temperature (100°C) that degrades the more fragile proteins and not biorefining all the functional biomass components. There is thus need to develop a process that is mild, i.e., does not degrade the proteins and thus helps recovering all components.

The primary objective of this article is to develop a novel mild biorefinery concept whereby the algal biomass is fractionated into a hydrophobic fraction (lipids) by milking the lipids out of intact cells using mild pre-treatment at low temperature with an aqueous solution of IL followed by cell disruption with bead milling to obtain the more fragile hydrophilic fraction (proteins, carbohydrates) in their functional state with aqueous buffer solutions (**Figure 1**).

This study is in-line with a recent study we performed by developing a technology able to separate the hydrophilic (e.g., proteins, carbohydrates) and hydrophobic (e.g., pigments) components in their functional state after complete cell disruption with bead milling using emulsion-based IL separations (Desai et al., 2018). The microalgae strain used in this study is *Neochloris oleoabundans*, which is a high lipid- and protein-producing strain (Gouveia et al., 2009). Both fresh and freeze-dried algae were studied to understand the influence of IL pre-treatment on extraction efficiency of individual components and the stability of proteins.

MATERIALS AND METHODS

Description of the Materials

The ILs used in this study were ≥95% pure and used without further purification. All the ILs listed in **Table 1** were purchased from Iolitec. Chemicals and organic solvents used in the study, ethyl acetate, hexane, chloroform, methanol, sulfuric acid, phenol, and fatty acid standards were bought from Sigma.

Microalgae Cultivation

Neochloris oleoabundans was cultivated in the laboratory in fresh water medium as described by Breuer et al. (2012) and the algae were stressed to have a higher lipid content. The microalgae were then harvested by centrifugation (4,000 rpm for 10 min). The microalgae were freeze-dried and used for extraction studies. For the study, using fresh cells, the algae were grown at the AlgaeParc pilot facility, Wageningen, The Netherlands. The cell suspension was centrifuged at 4,000 rpm for 10 min and used for the study.

Pre-treatment With ILs and Fractionation of Biomass

As shown in **Figure 2**, two studies were performed, lipid extraction efficiency of IL from intact microalgae cells at two different IL concentrations (A) and IL pre-treatment of microalgae followed by subsequent fractionation into hydrophilic and hydrophobic components (B).

Neochloris oleoabundans cells (∼10 mg) (freeze dried and/or fresh cells) were treated with 1.5 ml of aqueous solution of IL (see **Table 1**) at 45°C for 30 min. Fresh and freeze-dried cells used in the study were from different batches.

Abbreviations: IL, Ionic Liquid; TBP SO_4, Tributylmethylphosphonium methylsulfate; BMIM DBP, 1-Butyl-3-methylimidazolium dibutylphosphate.

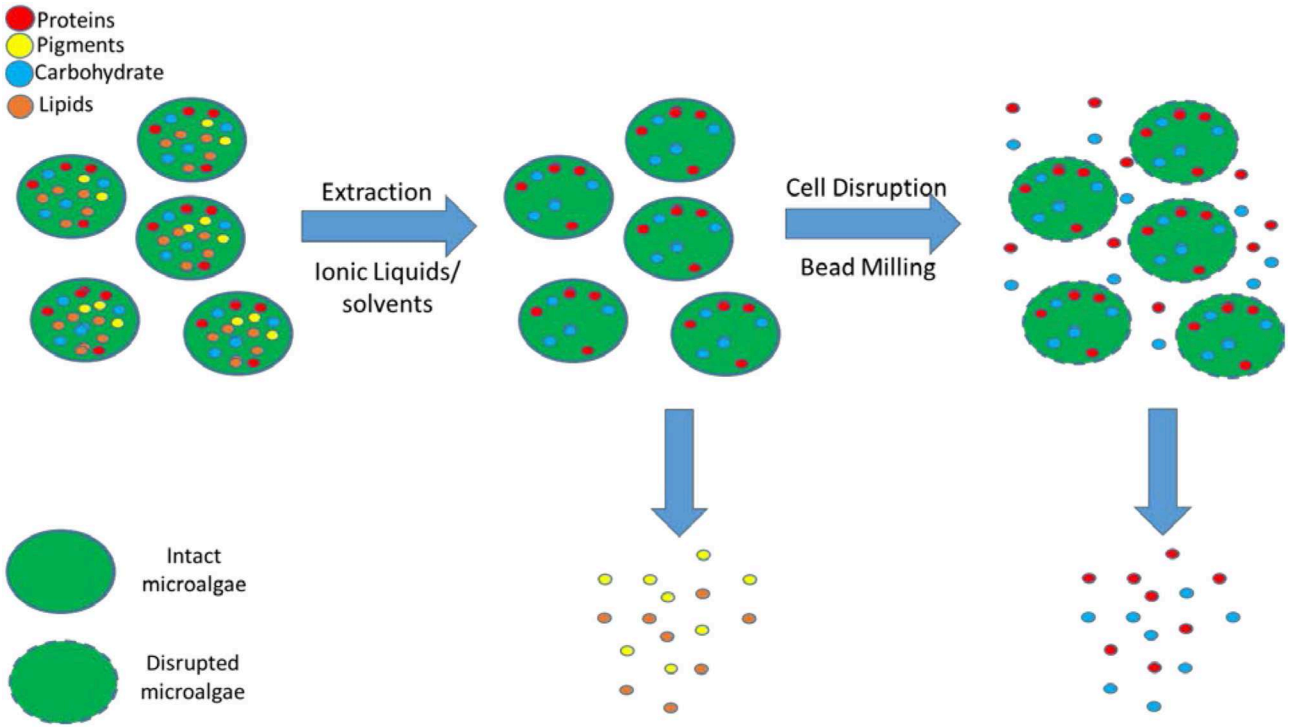

FIGURE 1 | Extraction of the hydrophobic compounds (lipids, pigments) after pre-treatment with ILs/solvents followed by cell disruption with bead milling for the recovery of hydrophilic (proteins, carbohydrates) compounds.

TABLE 1 | Ionic liquids used in the study.

	Ionic liquid names	Abbreviations
1	Tributylmethylphosphonium methylsulfate (Cyphos 108) >95%	TBP SO_4
2	Triisobutylmethylphosphonium tosylate (Cyphos 106) >95%	TBP TOS
3	1-Butyl-3-methylimidazolium dibutylphosphate 97%	BMIM DBP
4	1-Ethyl-3-methylimidazolium dibutylphosphate 97%	EMIM DBP
5	1-Butyl-3-methylimidazolium acetate >98%	BMIM acetate
6	1-Butyl-3-methylimidazolium dicyanamide >98%	BMIM DCA

In study A, preliminary screening studies on IL pre-treatment of microalgae were conducted using the ILs in **Table 1**. The cells were pre-treated with 1.5 ml of 40% aqueous solution of IL at 45°C for 30 min followed by centrifugation at 3,000 rpm for 10 min removing the IL and then contacted with 3 ml of solvent (ethyl acetate) for 2 h. The hydrophobic components from microalgae (lipids) were extracted in the solvent phase and the amount of lipids extracted in the IL phase was determined by measuring the residual amount of lipids remaining in the cells (section Fatty Acid Determination). After the preliminary screening studies, TBP SO_4 and BMIM DBP were selected and further studied, whereby the cells were pre-treated with 1.5 ml of 40 and 80% aqueous solution of IL at 45°C for 30 min. The cells, after pre-treatment, were separated from ILs by centrifugation at 3,000 rpm for 10 min and then contacted with 3 ml of solvent (ethyl acetate) for 2 h. The hydrophobic components from microalgae (lipids) were extracted in the solvent phase and lipid content was determined.

In the B study, the cells were pre-treated with 1.5 ml of 40% aqueous solution of BMIM DBP and TBP SO_4 at 45°C for 30 min. The cells, after pre-treatment, were separated from ILs by centrifugation at 3,000 rpm for 10 min and then contacted with 3 ml of solvent (ethyl acetate) for 2 h. The hydrophobic components from microalgae (lipids) were extracted in the solvent phase and lipid content was determined. The microalgae cells remaining after pre-treatment, containing the hydrophilic components mainly proteins and carbohydrates, were suspended in buffer, beaten, and finalized by analyzing the protein (section Protein Content) and carbohydrate (section Carbohydrate Analysis) content.

Fatty Acid Determination

The total fatty acids (FA) present in the microalgae were determined by treating the cells with $CHCl_3$-MeOH as described by Breuer et al. (2013). For concentration studies, the total amount of fatty acids extracted in the IL phase was determined by measuring the residual amount of fatty acids remaining in the cells after pre-treatment with IL and is expressed as follows:

$$\%\text{Total FA extracted in IL per mg of biomass} = \%\text{Total FA in control sample} - \%\text{Total residual FA in the cells after pretreatment} \quad (1)$$

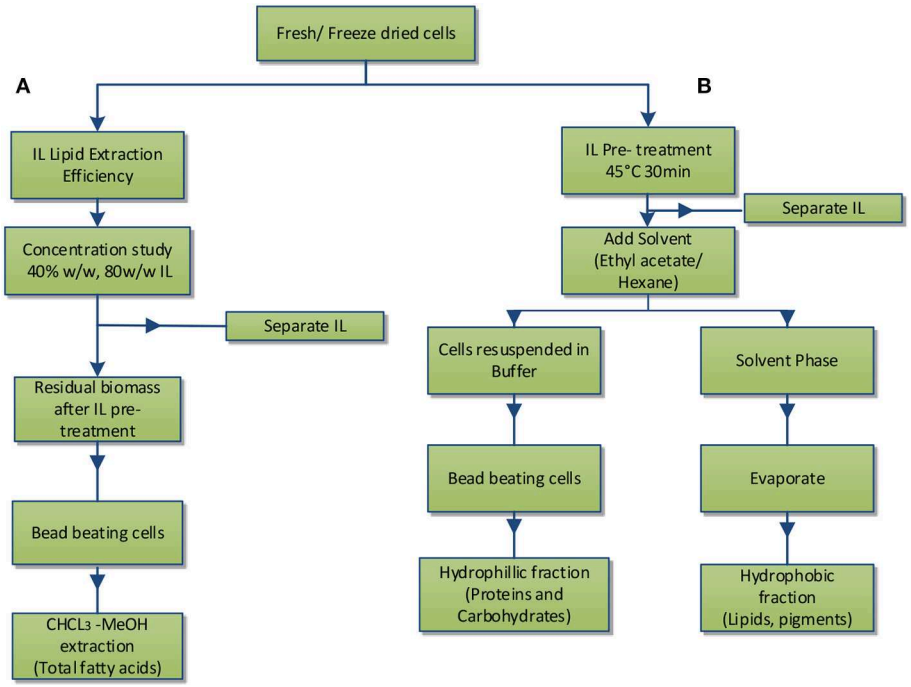

FIGURE 2 | Experimental scheme: **(A)** IL lipid extraction efficiency; **(B)** IL pre-treatment and separation of hydrophobic and hydrophilic components.

For calculating the total FA content of IL and solvent-treated cells, the solvent phase (ethyl acetate/hexane) was evaporated under N_2 stream and the residue was analyzed for total FA content after transesterification. The samples were measured in duplicate. The samples were analyzed in the GC (Agilent 7890A) and the run time was 30 min. For control sample, the fatty acid content was determined by treating the cells with $CHCl_3$-MeOH as described by Breuer et al. (2013).

Protein Content

Protein content was determined with a commercial assay kit (DC™ Protein assay, Bio-Rad, U.S.) using bovine serum albumin (Sigma–Aldrich A7030) as protein standard. The microplate assay protocol was used and the absorbance was measured at 750 nm using a microplate reader (Infinite M200, Switzerland). The cells after pre-treatment with IL were suspended in 1 ml of lysis buffer, 60 mM Tris, and 2% SDS, pH 9, in lysing matrix D tubes (6,913–500, MP Biomedicals Europe). The sample was bead beated for 3 cycles of 60 s at 6,500 rpm with a pause of 120 s between each cycle (Precellys 24, Bertin Technologies). The cell suspension was than heated at 100°C for 30 min. The cell suspension was separated by centrifugation and the supernatant was analyzed for protein content using the DC™ Protein assay. To determine the total protein content (control sample), the cells were directly resuspended in the lysis buffer, and analyzed as described above without any pre-treatment of cells. The samples were measured in duplicate. The protein is expressed as the % of total protein in the cells:

$$\%\ \text{of Total protein} = \left(\frac{\text{Total protein after pretreatment}}{\text{Total protein in cell} - \text{control}}\right) \times 100$$

Gel Electrophoresis

The stability of the proteins after pre-treatment with IL was confirmed by native gel electrophoresis. The cells after pre-treatment were suspended in 50 mM phosphate buffer and disrupted by bead beating (see procedure in section Protein Content). The supernatant was diluted 1:1 with native sample buffer. The diluted sample (~25 µl) was then applied on 4–20% Criterion TGX, Tris glycine precast gel and run with 10× Tris glycine native buffer at 125 V for 75 min. The gel was stained with Pierce™ Silver Stain Kit. The material for electrophoresis was bought from Bio-Rad and staining kit was purchased from Thermo Fisher Scientific.

Carbohydrate Analysis

The total carbohydrate content of IL pre-treated cells was determined by acid hydrolysis, adapted from Dubois et al. (1951). The IL pre-treated cells were suspended in water such that the final cell concentration was 1 mg/ml and disrupted by bead milling (see procedure in section Protein Content). To 50 µl of this suspension, 450 µl water, 500 µl of 5% phenol solution, and 2.5 ml of concentrated sulfuric acid were added. The mixture was incubated at room temperature for 10 min and then at 35°C in a water bath for 30 min. The carbohydrates react with acidic phenol to give a yellow orange color that was then measured at 483 nm using a UV spectrophotometer (Beckman). For control process, the cells were directly suspended in water without any pre-treatment. Starch samples were measured as positive controls. All samples were measured in duplicate. The calibration curve was prepared

TABLE 2 | Effect of different ILs on *N. oleoabundans* permeability (lipid extraction).

	Control*	TBP SO_4	TBP TOS	BMIM DBP	EMIM DBP	BMIM DCA	EA
% of fatty acids/mg biomass	∼25	∼10	∼2	∼9	∼1	∼2	∼0

*Chloroform-MeOH extraction of lipids.

using glucose as the standard. The total carbohydrate content is expressed as:

$$\%\ \text{Total carbohydrate content} = \left(\frac{\text{Total carbohydrate after pretreatment}}{\text{Total carbohydrate in the cell} - \text{control}}\right) \times 100$$

RESULTS

Overview

Extraction efficiency of different components (e.g., proteins, carbohydrates, lipids) after IL pre-treatment is studied and the protein stability is determined by electrophoresis. The study discusses the impact of ILs on lipid extraction efficiency and impact of pre-treatment using ILs on separation of different components from microalgae.

IL Lipid Extraction Efficiency

Preliminary screening of two IL classes, imidazolium-, and phosphonium-based ILs (see **Table 1**), on lipid extraction from intact freeze-dried *N. oleoabundans* shows in **Table 2** the highest lipid extraction efficiency for TBP SO_4 and BMIM DBP (experiments carried out in duplicate).

Further pre-treatment studies of freeze-dried *N. oleoabundans* with imidazolium (BMIM DBP)-based IL showed better lipid extraction efficiency compared to phosphonium (TBP SO_4)-based ILs (see **Figure 3**) at concentrations of 40 and 80% w/w and at a temperature of 45°C. However, TBP SO_4 could have an impact on the cell wall and was hence selected for further studies.

IL Pre-treatment and Extraction of Microalgae Components

Microalgae biomass also contains a large amount of proteins and carbohydrates besides lipids. Additional studies were performed to recover these components in their native form after biomass pre-treatment with ILs.

Pre-treatment studies were done on both fresh and freeze dried *N. oleoabundans* cells using 40% w/w solution of BMIM DBP and TBP SO_4. Hydrophobic components were subsequently extracted with ethyl acetate and then the cells were mechanically disrupted to recover hydrophilic components. The amount of fatty acid extracted after pre-treatment was compared with the Bligh and Dyer (control using $CHCl_3$-MeOH) method. The amount of lipid extracted from fresh biomass after pre-treatment was 11.4% and 17.7% per milligram of biomass for BMIM DBP and TBP SO_4 compared to 26% per milligram of biomass using the Bligh and Dyer method. For the freeze-dried biomass, the amount of lipid extracted after pre-treatment was 10.5 and 15.9% per milligram of biomass for BMIM DBP and TBP SO_4 compared to 18.2% per milligram of biomass using the Bligh and Dyer method. The results (see **Figure 4**) show that lipid recovery was better with TBP SO_4 in comparison to BMIM DBP for both fresh and freeze-dried cells.

The hydrophilic components, proteins, and carbohydrates after lipid extraction were recovered by cell disruption. The percentage of total protein recovered after pre-treatment using BMIM DBP and TBP SO_4 was 76.8 and 80.3% for fresh cells, and for freeze dried cells, 33.8 and 62.5%, respectively (see **Figure 5**), were observed.

The proteins recovered after extraction of lipids were run on a native gel and detected using silver stain (see **Figure 6**) and the multi-component protein Rubisco indicated.

Additionally, the aqueous phase after cell disruption was analyzed for carbohydrate content. The percentage of total carbohydrate recovered after pre-treatment using BMIM DBP and TBP SO_4 was 49 and 77.1% for fresh cells and 74.6 and 64.8%, respectively, for freeze-dried cells (see **Figure 7**).

A summary of the biomass components separated by IL pre-treatment is presented in **Table 3**. The results thus show that the microalgae components lipids, proteins, and carbohydrates can be selectively fractionated after IL pre-treatment and whereby the proteins retain their full functional composition.

A schematic overview of the IL pre-treatment studies with TBP SO_4 for both fresh and freeze-dried cells using the data of **Table 3** is shown below in **Figure 8**. This scheme shows the different products as a hydrophilic/hydrophobic fraction.

DISCUSSION

IL Lipid Extraction Efficiency

In this study, the extraction efficiencies of BMIM DBP (imidazolium)- and TBP SO_4 (phosphonium)-based ILs were investigated after initial screening with different ILs (see **Table 1**). As the concentration of IL increases from 40 to 80% w/w at 45°C, the amount of lipid extracted increases from 2.61 to 9.89% per milligram of biomass for BMIM DBP and from 1.28 to 3.27% per milligram of biomass for TBP SO_4 (see **Figure 3**). This increase in extraction capacity could be attributed to the increase in hydrophobicity of the IL solution. IL solutions under mild conditions were able to extract lipids from intact microalgae cells; the maximum amount extracted was ∼42% of the total fatty acid present in the cells (this value is calculated as % of total fatty acid in the cells, wherein the total fatty acid in cell is measured by Bligh and Dyer—control). Based on the results in **Figure 3**, BMIM DBP could permeabilize the cells and extract lipids better than TBP SO_4, indicating that the cation and anion influences the extraction efficiency, but to a different degree. The results also confirm that the lipid solubility in aqueous solution of ILs is low. Although TBP SO_4 shows low lipid extraction efficiency, it might still have an influence on the cell wall. The hypothesis is that the hydrogen bonding network of the cell wall is disrupted, leading to the formation of pores through which lipids can leak out. ILs are known to solubilize natural polymers such as cellulose and pectin by direct IL interaction. Hydrophilic ILs displaying

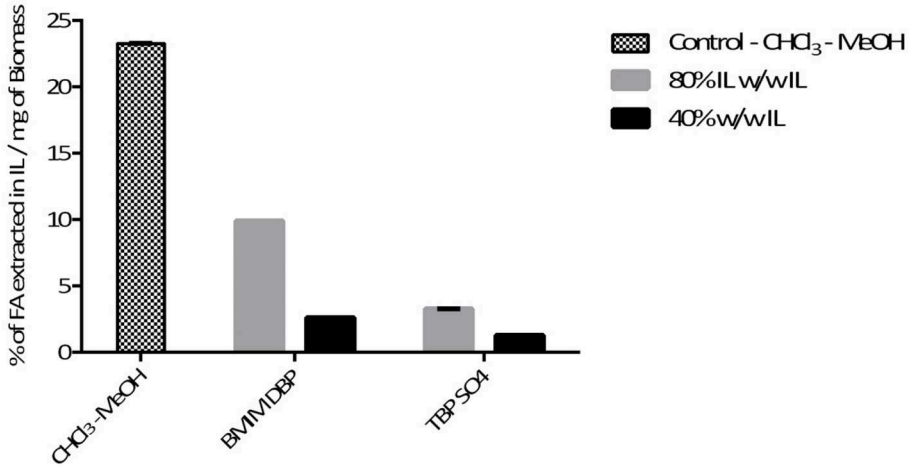

FIGURE 3 | Effect of IL concentration on extraction of lipids at 45°C.

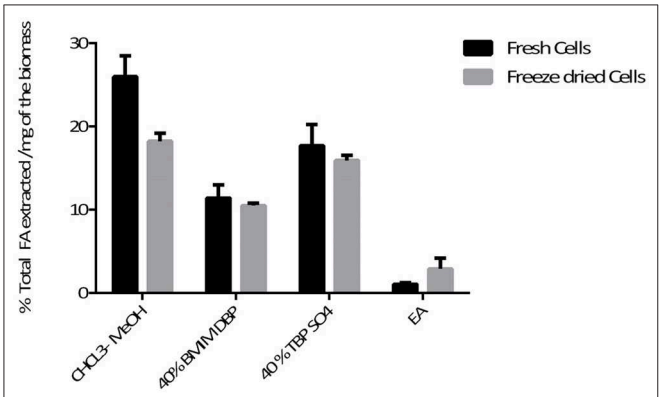

FIGURE 4 | Total lipids extracted with ethyl acetate after IL pre-treatment at 45°C.

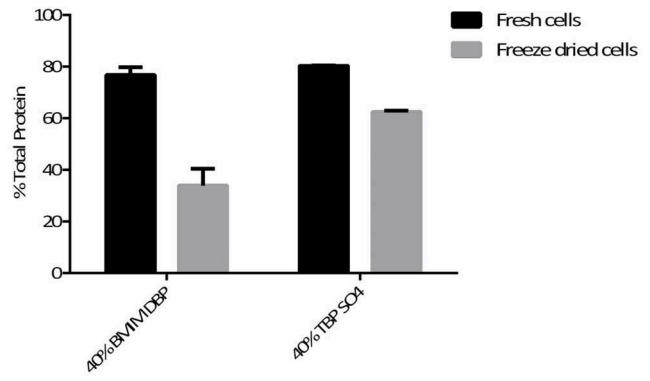

FIGURE 5 | Total proteins in the biomass after IL pre-treatment at 45°C.

low viscosities and high hydrogen bond capacity are reported to be more efficient in the solubilization process (Brandt et al., 2013; Lee et al., 2017). In other studies by different authors (Kim et al., 2012; Teixeira, 2012; Fujita et al., 2013; Choi et al., 2014; Olkiewicz et al., 2015) wherein the IL pre-treatment was done at temperatures close to 100°C, lipids released were extracted with organic solvent and extraction efficiency was >90% of the total fatty acid content. Thus, it indicates that temperature is indeed an important factor influencing the extraction efficiency.

IL Pre-treatment and Extraction of Microalgae Components

The above studies showed that aqueous IL solutions could permeabilize the cells as well as extract the lipids without cell disruption. This observation is in accordance with our previously published studies (Desai et al., 2016) that aqueous IL solutions could permeabilize the intact microalgae cells under mild conditions and release the intracellular hydrophobic pigments (Desai et al., 2016).

Microalgae biomass also contains a large amount of proteins and carbohydrates besides lipids. Additional studies with fresh and freeze-dried cells were performed to recover these components in their native form after biomass pre-treatment with ILs. The results (see **Figure 4**) show that lipid recovery was better with TBP SO_4 in comparison to BMIM DBP for both fresh and freeze-dried cells. This shows that TBP SO_4, which has a low lipid extraction capacity, even at 40% w/w concentration, is able to permeabilize the cells and released lipids are subsequently extracted with ethyl acetate. The release of intracellular content with freeze-dried cells could be attributed partially to the drying effect of the cell walls, which makes it more permeable. The results also show that ethyl acetate alone is not able to permeabilize the cells and extract the lipids. Additionally, studies using hexane instead of ethyl acetate for extracting lipids after IL pre-treatment were performed (not shown). The results indicated that no lipids were extracted in the hexane phase,

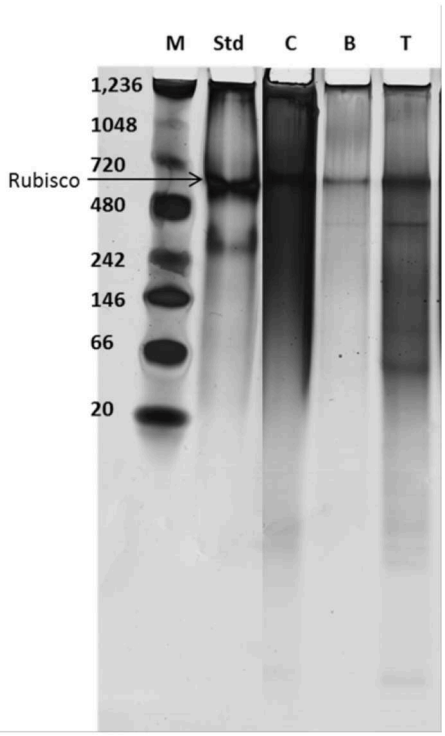

FIGURE 6 | Protein stability determined by native gel electrophoresis; M, marker; Std, standard Rubisco; C, control supernatant after bead beating the cells; B and T, After treatment with BMIM DBP and TBP SO_4, respectively, cells suspended in water and bead beated.

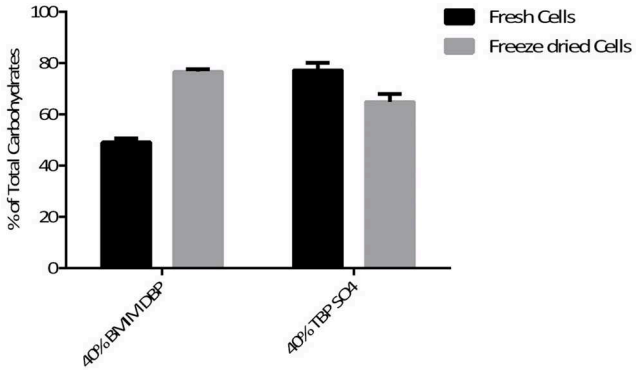

FIGURE 7 | Total carbohydrates in biomass after IL pre-treatment at 45°C.

and this could prove a possible cooperative role of ethyl acetate together with IL in permeabilizing the cell wall so that lipids can be efficiently extracted.

The hydrophilic components, proteins, and carbohydrates after lipid extraction are recovered after cell disruption. The percentage of total protein recovered after pre-treatment using BMIM DBP and TBP SO_4 was 76.8 and 80.3% for fresh cells and 33.8 and 62.5% for freeze-dried cells, respectively (see **Figure 5**). The decrease in protein recovery for freeze-dried cells could be due to direct contact of IL with proteins in the already compromised cell wall. In a separate study, aqueous solution of BMIM DBP (results not shown) and TBP SO_4 (Desai et al., 2014) in contact with Rubisco (Ribulose-1,5-bisphosphate carboxylase/oxygenase) causes aggregation/precipitation of the protein molecule. These results thus indicate that TBP SO_4 effectively permeabilizes the cell wall such that proteins remain intact inside the cell and can be recovered in their functional state after cell disruption. The proteins recovered after extraction of lipids were run on a native gel and detected using silver stain (see **Figure 6**). Although microalgae contains other proteins, Rubisco is used as the known biomarker protein for microalgae. The native gel shows that Rubisco remains intact and is not dissociated into its subunits, indicating that proteins recovered after IL pre-treatment retains its native form.

Additionally, the aqueous phase after cell disruption was analyzed for carbohydrate content. The percentage of total carbohydrate recovered after pre-treatment using BMIM DBP and TBP SO_4 was 49 and 77.1% for fresh cells and 74.6 and 64.8%, respectively, for freeze-dried cells (see **Figure 7**).

A summary of the biomass components separated by IL pre-treatment is presented in **Table 3**, and for the IL TBP SO_4, a schematic is also presented in **Figure 8**. The results thus show that the microalgae components lipids, proteins, and carbohydrates can be selectively fractionated after IL pre-treatment and whereby the proteins retain their full functional composition.

CONCLUSION

In this article, pre-treatment of *N. oleoabundans* using ILs and subsequent fractionation into hydrophilic and hydrophobic components was studied for both fresh and freeze-dried biomass. Additionally, the lipid extraction efficiency of aqueous IL solution under different concentration conditions was studied. We have demonstrated that aqueous solution of imidazolium- and phosphonium-based ILs was able to extract lipids from intact microalgae, albeit to a different degree. We have also shown that pre-treatment of microalgae with BMIM DBP and TBP SO_4 at low concentration (40% w/w) results in permeabilization of cells. The biomass can then be fractionated into hydrophilic and hydrophobic components whereby the proteins were recovered without losing their nativity. The recovery of total fatty acids was ∼68% and that of proteins and carbohydrates was ∼80 and 77%, respectively, of the total amount present in the cells, after pre-treatment of fresh biomass with TBP SO_4. Most of the current processes that use energy-consuming mechanical cell disruption (e.g., bead milling, high-pressure homogenization) (Günerken et al., 2015) and solvents such as methanol/chloroform and hexane (Cuellar-Bermudez et al., 2015) are able to recover only lipids and render the proteins unsuitable for use due to denaturation/degradation. This article is a step forward in establishing the role of ILs in microalgae biorefinery by developing a novel selective fractionation concept for both hydrophobic compounds (e.g., lipids) and hydrophilic compounds (e.g., proteins, carbohydrates).

TABLE 3 | Summary of biomass components separated under different IL pre-treatment.

	Fresh cells			Freeze-dried cells		
	*Control	40% BMIM DBP	40% TBP SO_4	*Control	40% BMIM DBP	40% TBP SO_4
% of total fatty acid/mg of biomass	26.0	11.4	17.7	18.2	10.5	15.9
% of total fatty acid in cells	100	43.9	68.0	100.0	57.6	87.4
Proteins/mg of biomass	16.2	12.4	13.0	21.4	7.2	13.4
% of total protein in cells	100.0	76.8	80.3	100.0	33.8	62.5
Carbohydrates/mg of biomass	16.8	8.2	12.9	21.7	16.6	14.0
% of total carbohydrate in cells	100.0	49.0	77.1	100.0	76.6	64.8

[a]*Control—No pre-treatment with IL. Cells lysed by bead beating and analyzed for content as described in the Materials and Methods section.*

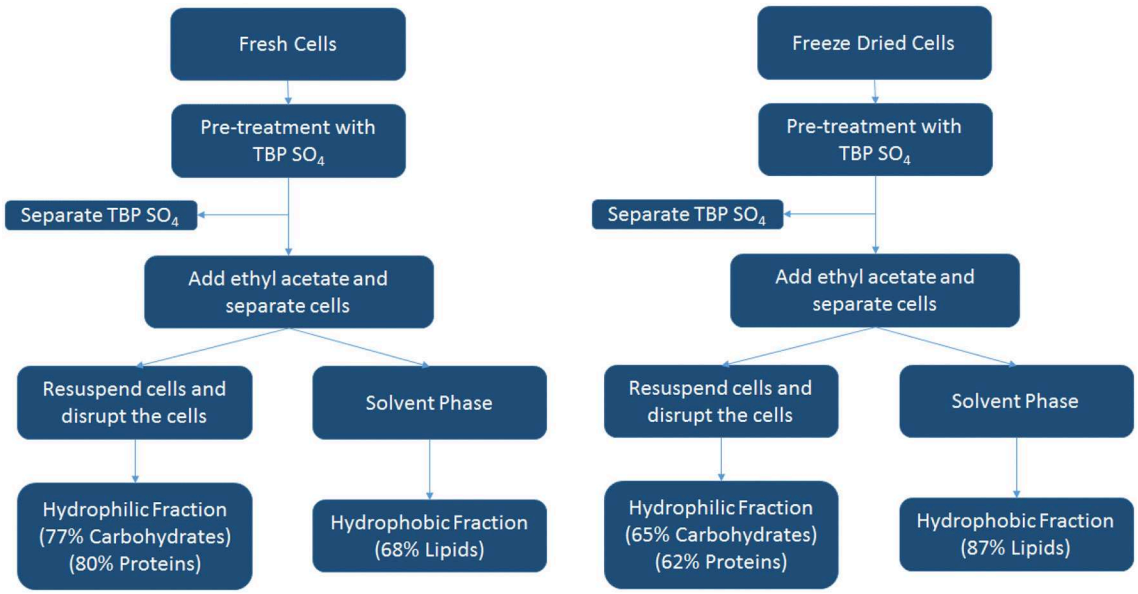

FIGURE 8 | Overview of fractionation process with fresh and freeze-dried cells using the IL TBP SO_4.

Pre-treatment studies as described in this article show the novelty of separating lipids without mechanical disruption and subsequent separation of hydrophilic components (proteins, carbohydrates) in their native form after cell disruption. The process can be optimized further to improve the yields. There are various parameters that influence the efficacy such as biomass loading, time of contact with IL and organic solvent, amount of solvent added, and type of IL, and these should be investigated in detail.

While ILs indeed have a potential role to play in microalgal biorefinery, it can only be realized if they are biocompatible, biodegradable, and economical. The ILs must be tested for their reusability and recyclability so as to make the process economically viable. To be able to judge a process superior than other would require a systematic approach and certain criteria, on basis of which the process is evaluated. Most of these studies are at their infancy and should be evaluated in terms of energy consumption, efficacy, and cost. In the past years, a few studies were published (Ruiz et al., 2016; Chia et al., 2018) about economic and environmental aspects of microalgae biorefinery for biofuel and also on high value product perspectives (Vanthoor-Koopmans et al., 2012; Chew et al., 2017).

DATA AVAILABILITY STATEMENT

The datasets generated for this study are available on request to the corresponding author.

AUTHOR CONTRIBUTIONS

RD and MF performed the experiments. ME and RW analyzed the data. RD wrote a first draft. All authors commented on the manuscript, which was finalized by ME.

ACKNOWLEDGMENTS

The authors would like to thank Technology Foundation STW (Project No. 11410) and Institute for Sustainable Process Technology (ISPT) for the financial support. A Ph.D. thesis with parts of this research was written and mentioned in the Reference list (Desai, 2016).

REFERENCES

Bligh, E. G., and Dyer, W. J. (1959). A rapid method of total lipid extraction and purification. *Can. J. Biochem. Physiol.* 37, 911–917. doi: 10.1139/y59-099

Brandt, A., Grasvik, J., Hallett, J. P., and Welton, T. (2013). Deconstruction of lignocellulosic biomass with ionic liquids. *Green Chem.* 15, 550–583. doi: 10.1039/c2gc36364j

Breuer, G., Evers, W. A. C., de Vree, J. H., Kleinegris, D. M., Martens, D. E., Wijffels, R. H., et al. (2013). Analysis of fatty acid content and composition in microalgae. *J. Vis. Exp.* e50628. doi: 10.3791/50628

Breuer, G., Lamers, P. P., Martens, D. E., Draaisma, R. B., and Wijffels, R. H. (2012). The impact of nitrogen starvation on the dynamics of triacylglycerol accumulation in nine microalgae strains. *Bioresour. Technol.* 124, 217–226. doi: 10.1016/j.biortech.2012.08.003

Chew, K. W., Yap, J. Y., Show, P. L., Suan, N. H., Juan, J. C., Ling, T. C., et al. (2017). Microalgae biorefinery: high value products perspectives. *Bioresour. Technol.* 229, 53–62. doi: 10.1016/j.biortech.2017.01.006

Chia, S. R., Chew, K. W., Show, P. L., Yap, Y. J., Ong, H. C., Ling, T. C., et al. (2018). Analysis of economic and environmental aspects of microalgae biorefinery for biofuels production: a review. *Biotechnol. J.* 13, 1–10. doi: 10.1002/biot.201700618

Choi, S.-A., Oh, Y.-K., Jeong, M.-J., Kim, S. W., Lee, J. S., Park, J. Y., et al. (2014). Effects of ionic liquid mixtures on lipid extraction from *Chlorella vulgaris*. *Renew. Energy* 65, 169–174. doi: 10.1016/j.renene.2013.08.015

Cuellar-Bermudez, S. P., Aguilar-Hernandez, I., Cardenas-Chavez, D. L., Ornelas-Soto, N., Romero-Ogawa, M. A., Parra-Saldivar, R., et al. (2015). Extraction and purification of high-value metabolites from microalgae: essential lipids, astaxanthin and phycobiliproteins. *Microb. Biotechnol.* 8, 190–209. doi: 10.1111/1751-7915.12167

Desai, R. K. (2016). *Ionic liquid pre-treatment of microalgae and extraction of biomolecules* (Ph.D. thesis), Wageningen University, Wageningen.

Desai, R. K., Monteillet, H., Li, X., Schuur, B., Kleijn, J. M., Leermakers, F. A. M., et al. (2018). One-step mild biorefinery of functional biomolecules from microalgae extracts. *React. Chem. Eng.* 3, 182–187. doi: 10.1039/C7RE00116A

Desai, R. K., Streefland, M., Wijffels, R. H., and Eppink, M. H. M. (2014). Extraction and stability of selected proteins in ionic liquid based aqueous two phase systems. *Green Chem.* 16, 2670–2679. doi: 10.1039/C3GC42631A

Desai, R. K., Streefland, M., Wijffels, R. H., and Eppink, M. H. M. (2016). Novel astaxanthin extraction from *Haematococcus pluvialis* using cell permeabilising ionic liquids. *Green Chem.* 18, 1261–1267. doi: 10.1039/C5GC01301A

Dubois, M., Gilles, K., Hamilton, J. K., Rebers, P. A., and Smith, F. (1951). A colorimetric method for the determination of sugars. *Nat.* 168:167. doi: 10.1038/168167a0

Freemantle, M. (1998). Designer solvents. *Chem. Eng. News Arch.* 76, 32–37. doi: 10.1021/cen-v076n013.p032

Fujita, K., Kobayashi, D., Nakamura, N., and Ohno, H. (2013). Direct dissolution of wet and saliferous marine microalgae by polar ionic liquids without heating. *Enzyme Microb. Technol.* 52, 199–202. doi: 10.1016/j.enzmictec.2012.12.004

Gouveia, L., Marques, A. E., da Silva, T. L., and Reis, A. (2009). Neochloris oleabundans UTEX #1185: a suitable renewable lipid source for biofuel production. *J. Ind. Microbiol. Biotechnol.* 36, 821–826. doi: 10.1007/s10295-009-0559-2

Günerken, E., D'Hondt, E., Eppink, M. H. M., Garcia-Gonzalez, L., Elsta, K., and Wijffels, R. H. (2015). Cell disruption for microalgae biorefineries. *Biotechnol. Adv.* 33, 243–260. doi: 10.1016/j.biotechadv.2015.01.008

Herrero, M., Cifuentes, A., and Ibañez, E. (2006). Sub- and supercritical fluid extraction of functional ingredients from different natural sources: plants, food-by-products, algae and microalgae: a review. *Food Chem.* 98, 136–148. doi: 10.1016/j.foodchem.2005.05.058

Kim, Y.-H., Choi, Y.-K., Park, J., Lee, S., Yang, Y. H., Kim, H. J., et al. (2012). Ionic liquid-mediated extraction of lipids from algal biomass. *Bioresour. Technol.* 109, 312–315. doi: 10.1016/j.biortech.2011.04.064

Lee, S. Y., Show, P. L., Ling, T. C., and Chang, J. S. (2017). Single-step disruption and protein recovery from *Chlorella vulgaris* using ultrasonication and ionic liquid buffer aqueous solution as extractive solvents. *Biochem. Eng. J.* 124, 26–35. doi: 10.1016/j.bej.2017.04.009

Olkiewicz, M., Caporgno, M. P., Font, J., Legrand, J., Lepine, O., Plechkova, N. V., et al. (2015). A novel recovery process for lipids from microalgae for biodiesel production using a hydrated phosphonium ionic liquid. *Green Chem.* 17, 2813–2824. doi: 10.1039/C4GC02448F

Orr, V. C. A., Plechkova, N. V., Seddon, K. R., and Rehmann, L. (2016). Disruption and wet extraction of the microalgae *Chlorella Vulgaris* using room-temperature ionic liquids. *ACS Sustain. Chem. Eng.* 4, 591–600. doi: 10.1021/acssuschemeng.5b00967

Orr, V. C. A., and Rehmann, L. (2016). Ionic liquids for the fractionation of microalgae biomass. *Curr. Opin. Green Sustain. Chem.* 2, 22–27. doi: 10.1016/j.cogsc.2016.09.006

Ruiz, J., Olivieri, G., de Vree, J., Bosma, R., Willems, P., Reith, J. H., et al. (2016). Towards industrial products from microalgae. *Energy Environ. Sci.* 9, 3036–3043. doi: 10.1039/C6EE01493C

Soxhlet, F. (1879). Die gewichtsanalytische Bestimmung des Milchfettes. *Dingler's Polytechnisches J.* 232, 461–465.

Teixeira, R. E. (2012). Energy-efficient extraction of fuel and chemical feedstocks from algae. *Green Chem.* 14, 419–427. doi: 10.1039/c2gc16225c

To, T. Q., Procter, K., Simmons, B. A., Subaschchandrabose, S., and Atkin, R. (2018). Low cost ionic liquid-water mixtures for effective extraction of carbohydrate and lipid from algae. *Faraday Discuss.* 206, 93–112. doi: 10.1039/C7FD00158D

Ursu, A.-V., Marcati, A., Sayd, T., Sante-Lhoutellier, V., Djelveh, G., Michaud, P., et al. (2014). Extraction, fractionation and functional properties of proteins from the microalgae *Chlorella vulgaris*. *Bioresour. Technol.* 157, 134–139. doi: 10.1016/j.biortech.2014.01.071

Vanthoor-Koopmans, M., Wijffels, R. H., Barbosa, M. J., and Eppink, M. H. (2012). Biorefinery of microalgae for food and fuel. *Bioresour. Technol.* 135, 142–149. doi: 10.1016/j.biortech.2012.10.135

Wahidin, S., Idris, A., and Shaleh, S. R. M. (2016). Ionic liquid as a promising biobased green solvent in combination with microwave irradiation for direct biodiesel production. *Bioresour. Technol.* 206, 150–154. doi: 10.1016/j.biortech.2016.01.084

Wang, X., and Zhang, X. (2012). Optimal extraction and hydrolysis of *Chlorella pyrenoidosa* proteins. *Bioresour. Technol.* 126, 307–313. doi: 10.1016/j.biortech.2012.09.059

Wijffels, R. H., and Barbosa, M. J. (2010). An outlook on microalgal biofuels. *Science* 329, 796–799. doi: 10.1126/science.1189003

Young, G., Nippgen, F., Titterbrandt, S., and Cooney, M. J. (2010). Lipid extraction from biomass using co-solvent mixtures of ionic liquids and polar covalent molecules. *Separ. Purif. Technol.* 72, 118–121. doi: 10.1016/j.seppur.2010.01.009

Yu, X., Yang, J., Lu, H., Tu, S.-T., and Yan, J. (2015). Energy-efficient extraction of fuel from *Chlorella vulgaris* by ionic liquid combined with CO_2 capture. *Appl. Energy* 160, 648–655. doi: 10.1016/j.apenergy.2015.04.074

Conflict of Interest: The authors declare that the research was conducted in the absence of any commercial or financial relationships that could be construed as a potential conflict of interest.

frontiers in Bioengineering and Biotechnology

ORIGINAL RESEARCH
published: 21 January 2020
doi: 10.3389/fbioe.2019.00481

Microalgae a Superior Source of Folates: Quantification of Folates in Halophile Microalgae by Stable Isotope Dilution Assay

Dirk Volker Woortman[1†], Tobias Fuchs[1†], Lisa Striegel[2†], Monika Fuchs[1], Nadine Weber[2], Thomas B. Brück[1] and Michael Rychlik[2,3*]*

[1] Werner Siemens-Chair of Synthetic Biotechnology, Technical University of Munich, Garching, Germany, [2] Chair of Analytical Food Chemistry, Technical University of Munich, Freising, Germany, [3] Centre for Nutrition and Food Sciences, Queensland Alliance for Agriculture and Food Innovation, The University of Queensland, Brisbane, QLD, Australia

OPEN ACCESS

Edited by:
Sónia Patrícia Marques Ventura, University of Aveiro, Portugal

Reviewed by:
Minnamari Edelmann, University of Helsinki, Finland
Michael Lakatos, Hochschule Kaiserslautern University of Applied Sciences, Germany

***Correspondence:**
Thomas B. Brück
brueck@tum.de
Michael Rychlik
michael.rychlik@tum.de

[†]These authors have contributed equally to this work and share first authorship

Specialty section:
This article was submitted to Industrial Biotechnology, a section of the journal Frontiers in Bioengineering and Biotechnology

Received: 28 May 2019
Accepted: 23 December 2019
Published: 21 January 2020

Citation:
Woortman DV, Fuchs T, Striegel L, Fuchs M, Weber N, Brück TB and Rychlik M (2020) Microalgae a Superior Source of Folates: Quantification of Folates in Halophile Microalgae by Stable Isotope Dilution Assay. Front. Bioeng. Biotechnol. 7:481. doi: 10.3389/fbioe.2019.00481

A multitude of human nutritional supplements based on *Chlorella vulgaris* biomass has recently been introduced to the specialty food market. In this study, an analysis of total folate contents in *Chlorella* sp. and a series of marine microalgae was conducted to evaluate folate content in alternative algae-based food production strains. For the first time, total folate content and vitamer distribution in microalgae were analyzed by stable isotope dilution assay (SIDA) using LC-MS/MS, which has demonstrated its superiority with respect to folate quantification. Consistently, high folate contents were detected in all examined microalgae samples. High folate concentrations of 3,460 ± 134 μg/100 g dry biomass were detected in freshly cultivated *Chlorella vulgaris*, notably also in other well-researched microalgae strains. To that end, the highest folate content currently documented for any algae sample was measured in the marine microalgae *Picochlorum* sp. isolate with values of 6,470 ± 167 μg/100 g dry biomass. This calls for alternative products based on other algae biomass. Our data indicate that freshwater and marine microalgae provide extremely high concentrations of folates, which warrant further studies on the regulation of pteroylpolyglutamates in algae as well as on bioaccessibility, absorption, and retention in humans.

Keywords: stable isotope dilution assay, microalgae, folates, *Chlorella*, *Dunaliella*, *Picochlorum*

INTRODUCTION

With an ever-growing global population and increasing limiting availability of agricultural land, there is a growing demand for edible biomass that contains high concentrations of macro- and micronutrients (Tilman et al., 2002; Foley et al., 2011; Lipper et al., 2014). This situation is further aggravated by climate change effects, which ultimately lead to a shift and total reduction of agricultural lands (Tilman et al., 2001). Hence, generating nutrient concentrated, edible biomass on non-agricultural landmass is a pivotal role for a food-centered, future biorefinery approach (Laurens et al., 2017; Sheppard et al., 2019). To that end, microalgae potentially yield at least five times more biomass than terrestrial plants on the equivalent land surface and can be cultivated without the need for freshwater (Benedetti et al., 2018). Therefore, microalgae cultivation does not compete with terrestrial agricultural activity but can act synergistically to generate

concentrated food resources (Vanthoor-Koopmans et al., 2013). Hence, generating a microalgae-based biorefinery that generates various performance nutrient outlets, such as proteins, sugars and polyunsaturated fatty acids can significantly contribute to meet food demands of future generations (Subhadra and Grinson-George, 2011). While microalgae-based production of macronutrients such as sugars and proteins has been elucidated extensively in the literature, detailed studies on micronutrient, such as vitamins, which add significant economic and nutritional value to food-centered microalgae biorefinery, have been limited (Pulz and Gross, 2004; Draaisma et al., 2013; van der Spiegel et al., 2013). In that respect, Vitamin B9 (Folate) is of extensive importance due to its function in human development and health maintenance. The marine microalgae have recently been flagged as concentrated food production platforms for human and animal nutrition due to their high concentration of health-promoting nutrients, such as proteins and polyunsaturated fatty acids (PUFAs) (Harun et al., 2010; Grosso et al., 2014; Kent et al., 2015; Marventano et al., 2015). It has been reported that high vitamin containing algae biomass could be used to address malnutrition in populations at risk, which not only encompass pregnant women with higher nutritional demands, but also poverty-stricken populations (Pratt and Johnson, 1965; Brown et al., 1999; Becker, 2003; Christaki et al., 2011). A multitude of human nutritional supplements based on algae biomass has recently been introduced. Nevertheless, the often-cited nutritional value of algae food supplements with respect to their micronutrient content and bioavailability is still a matter of scientific debate (Brown et al., 1999; Wells et al., 2017).

Folate vitamins are essential to human nutrition and necessary for many one carbon metabolic pathways, particularly in the synthesis of amino acids and nucleotides (Shane, 1989). A deficiency of folates in women before and during pregnancy is related to an increased prevalence of neural tube defects (NTDs) in newborns. In contrast to humans, plants synthesize folates *de novo* and, therefore, provide dietary folates for humans. These compounds are accruing in all cellular compartments, such as mitochondria, cytoplasm, and nucleus, where they carry out distinct biochemical functions (Selhub, 2002). Folates consist of three different chemical building

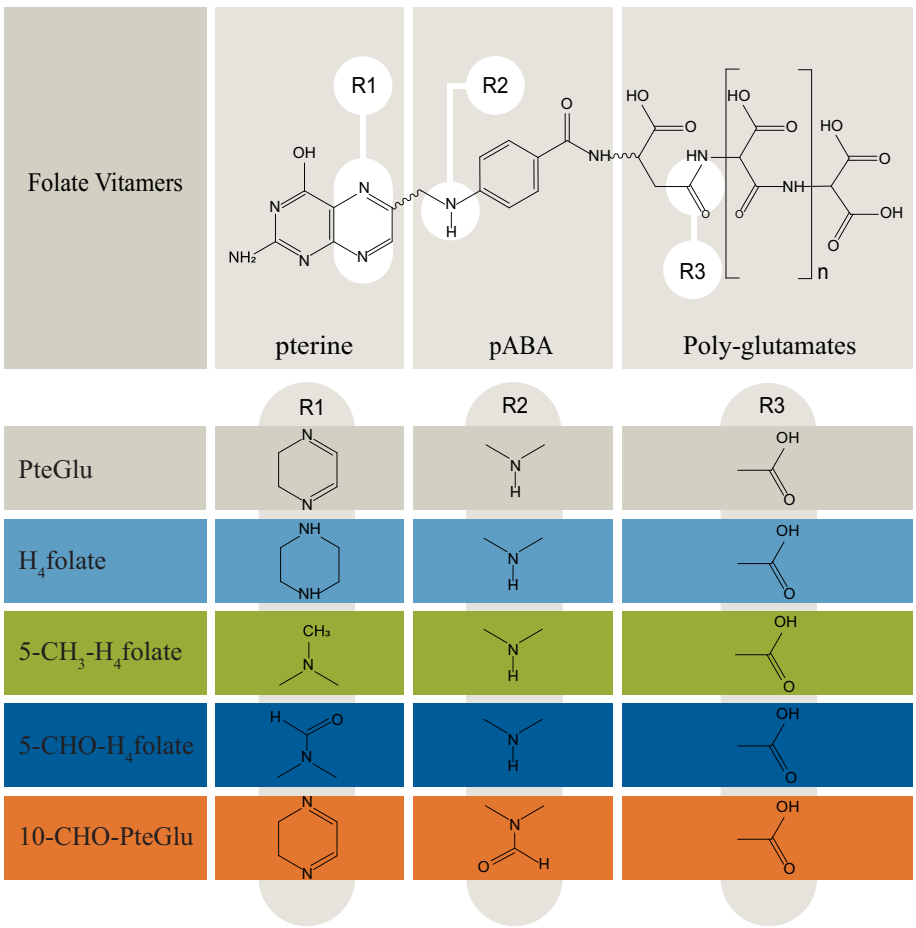

FIGURE 1 | Overview of folate vitamers chemistry (Delchier et al., 2016). Folates are mostly present in the polyglutamated form, which need to be cleaved during sample preparation for quantitative LC-HRMS measurements. pABA, para-aminobenzoic acid. *n*, number of glutamates: 1–8.

blocks, i.e., pterin, para-amino benzoic acid (pABA), and varying numbers of glutamate residues. Depending on the oxidation state, various C1 substituents, and the polyglutamyl tail lengths, the most abundant forms in plants are H_4folate (tetrahydrofolic acid; 2-((4-((2-Amino-4-oxo-5,6,7,8-tetrahydro-1H-pteridin-6-yl)methylamino)benzoyl)-amino)pentandisäure), 5-CH_3-H_4folate (5-methyltetrahydrofolate; (2S)-2-[[4-[(2-Amino-5-methyl-4-oxo-1,6,7,8-tetrahydropteridin-6-yl) methylamino]benzoyl]amino]pentanedioic acid), 5-CHO-H_4folate (5-formyltetrahydrofolate, 2-[[4-[(2-amino-5-formyl-4-oxo-3,6,7,8-tetrahydropteridin-6-yl)methylamino]benzoyl]amino]pentanedioic acid), 10-CHO-PteGlu (10-formyl-folate (2S)-2-[[4-[(2-amino-4-oxo-3H-pteridin-6-yl)methyl-formylamino]benzoyl]amino]pentanedioic acid), and PteGlu (pteroylglutamate (2*S*)-2-[[4-[(2-amino-4-oxo-3*H*-pteridin-6-yl)methylamino]benzoyl]amino]pentanedioic acid) (Hanson and Gregory, 2002). The structures of folate vitamers analyzed throughout this study are illustrated in **Figure 1**.

Since there is an increased interest in the use of microalgae as functional food, the quantitative analysis of folates in well-characterized strains would add significantly to knowledge about the nutritional composition and value of microalgae. At present, there is only scattered information about the total folate content of microalgae biomass. Two publications presented microbiological assays for quantification with limited analytical robustness (Brown et al., 1999; Fujii et al., 2010). Folate quantification by microbiological assays are sensitive, but the results are biased by choice of the calibrants and reagents (Ringling and Rychlik, 2017a). Recently, Edelmann et al. published reliable folate data on commercially available microalgae using microbiological assay and an UHPLC method (Edelmann et al., 2019). However, using UHPLC, particular attention to a complete deconjugation of polyglutamates to the respective monoglutamates need to be paid as only monoglutamates can be detected (Ringling and Rychlik, 2017a). For a direct, reliable, and sensitive analysis, we applied a mass spectrometry-based stable isotope dilution assay (SIDA), which has demonstrated its superiority in folate quantification (Rychlik, 2011). SIDA is based on the application of isotopologic labeled internal standards, which present almost identically chemical and physical properties. As pointed out above SIDA has key advantages such as a complete compensation for losses of analytes during extraction and for ion suppression during LC-MS/MS measurements. Folate analysis using SIDA enables differentiation of the folate pattern (Asam et al., 2009) as well as the detection of an incomplete deconjugation by LC-MS/MS (Ringling and Rychlik, 2017a).

This study evaluates the differential folate content of industrial processed microalgae biomass including fresh biomass and strains isolated from the environment. We examined the folate content of lab-grown microalgae, in particular also marine microalgae as these organisms display higher process robustness in extreme saline media, and can be cultivated on non-arable land using sea, brackish or wastewater (Schenk et al., 2008). Additionally, it prevents culture instability in open pond reactor systems as many terrestrial contaminants, such as bacteria and filamentous fungi, cannot thrive in this medium (Rothschild and Mancinelli, 2011). Therefore, the large scale halophilic algae cultivation potentially shows better economic and ecological benchmarks than its freshwater equivalents (Schenk et al., 2008; Apel and Weuster-Botz, 2015). At present, there is little literature evidence of the nutritional value, specifically focused on folate production and vitamers with respect to halophilic algae strains (Kay and Barton, 1991; Brown et al., 1999; Fujii et al., 2010; Wells et al., 2017). We hypothesize, that in general halophilic green microalgae contain higher excess of folates compared to terrestrial, folate containing food sources, such as rice, strawberries and liver. In this context, it is noteworthy that there is currently no systematic study that elucidates algae strains with a specific analytical procedure that can distinguish folate vitamer species. Moreover, it has not been elucidated yet if processed biomass retains high folate contents compared to its freshly harvested counterpart. Thus, we analyzed total folates contents in freshwater and marine microalgae by SIDA using LC-MS/MS and examined the effects of different industrially applied cultivation conditions on total folate content.

MATERIALS AND METHODS

Commercial Grade Food Supplements

Biomass was sampled from algae food supplement products obtained from Terra Elements GmbH, Munich, Germany (*Chlorella vulgaris*) and Feelgood Shop BV, RK Venlo, Netherlands (*Chlorella vulgaris*). A single batch analysis was performed. The products were bought as dried powders and analyzed unprocessed.

Cultured Reference Strains

Reference microalgae strains found in **Table 1** were obtained from the Sammlung von Algenkulturen der Universität Göttingen (SAG) and the Culture Collection of Algae and Protozoa (CCAP). Sample strains were transferred and adapted under sterile culture conditions to growth media.

Cultured Isolated Strains

Isolated microalgae strains were enriched and purified from Australian environmental samples obtained in August 2014 by Thomas Brueck and coworkers under permission of the Australian government. Preparation of repeated serial dilution cultivations resulted in unialgal cultures after sampling. Maintained unialgal cultures were checked for purity by microscopy (Zeiss AxioLab, Carl Zeiss AG, Oberkochen, Germany) and in high throughput by fluorescence-activated cell sorting analysis (Biorad S3 Sorter, Bio-Rad Laboratories, Inc., Hercules, USA).

Microalgae Cultivation

All reference and isolated microalgae samples were cultured in 500 ml Erlenmeyer flasks with a fill volume of 200 ml in New Brunswick Innova 44 series shakers (26°C, 120 rpm) fitted with light emitting diodes (Future LED GmbH, Berlin, Germany) (**Figure S1**). The cultures were inoculated with

TABLE 1 | Overview of analyzed microalgae biomass.

Genus; species; strain	Origin [country, place (CC ID)]	GPS coordinates (DMS)	Medium	NaCl content (w/v)
COMMERCIAL GRADE FOOD SUPPLEMENTS				
Chlorella vulgari	Terra Elements GmbH, Munich, Germany	n.a.	n.a.	n.a.
Chlorella vulgaris	Feelgood Shop BV, Venlo, Netherlands	n.a.	n.a.	n.a.
CULTURED REFERENCE STRAINS				
Chlorella vulgaris	n.a. (SAG 211-12)	n.a.	BG11	0%
Porphyridium purpureum	UK, Brixham (CCAP 1380/3)	n.a.	ASW	3%
Microchloropsis salina	UK, Isle of Cumbrae (SAG 40.85)	N 055° 46.081′, W 004° 55.18464	BG11	3%
CULTURED ISOLATED STRAINS				
Picochlorum sp. isolate	Australia, Salt Creek	S 036° 09.6874′, E 139° 38.8328′	ASP-M	5%
Dunaliella salina isolate	Australia, Salt Creek	S 036° 09.6874′, E 139° 38.8328′	J/1	5%
Tetradesmus sp. isolate	Australia, Salt Creek	S 036° 09.6874′, E 139° 38.8328′	BG11	3%
Chlorella sp. isolate	Australia, Brisbane River	n.a.	BBM	0%

n.a., not available; NaCl, Sodium chloride; CC ID, Culture collection identification; DMS, Degrees-Minutes-Seconds.

fresh cultivars at a starting optical density of 0.1 (OD_{750}). A constant visible sunlight spectrum approximation illumination at a Photosynthetic Photon Flux Density (PPFD) of 200 μmol m^{-2} s^{-1} was applied. Individual aeration with 1% v/v CO_2 enriched air was controlled by a DASGIP® MX module (Eppendorf AG, Hamburg, Germany). A constant gas flow equivalent to 6 head volume exchanges per hour was applied. After 14 days of cultivation, the resulting algae biomass was harvested by centrifugation (2,450 × g, 5 min). No washing steps were applied. Subsequently, the frozen pellet (−80°C) *Chlorella* sp. isolate was freeze-dried for 24 h. Dried samples were sealed under nitrogen-enriched air, subdued light and stored at −80°C until further processing. Moreover, the analysis of folate content and vitamer distribution after 14 days of cultivation and subsequent 24-h osmotic stress, nitrogen limitation and light spectrum shift was studied. A batch of 15 Erlenmeyer flask cultures where combined after 14 days. The homogeneous culture was pelleted by centrifugation (2,450 × g, 5 min) in individual batches and re-suspended in BBM medium for the control, green light and blue/pink light groups in triplicates. Nitrogen limited conditions were initiated by resuspension in $NaNO_3$ free BBM media. Osmotic stress was initiated by resuspension in 1% NaCl containing BBM media. After 24 h the cultures were harvested and stored for folate analysis as described above. LED spectrum is shown in **Figure S2**.

All cultivation media were prepared sterile. The microalgae media BG11 [Blue-Green Medium] (Allen, 1968), J/1 [Johnson's media] (Allen, 1968), ASW [Artificial Seawater] (Allen and Nelson, 1910), ASP-M [Artificial Seawater medium by Provasoli] (Provasoli et al., 1957) and BBM [Bold's Basal Medium] (Bischoff and Bold, 1963) were prepared as published, but without organic nutrients, vitamins or complex components; all media recipes where adapted accordingly and obtained from: BG11 and J/1 (Borowitzka and Borowitzka, 1988); BBM, ASW and ASP-M (Anderson, 2005). The salinities were adjusted by the addition of sodium chloride as listed in **Table 1**.

Phylogenetic and Fatty Acid Profile Characterization of Analyzed Biomass

Genomic DNA extracts were prepared using the InnuPrep plant DNA extraction kit (Analytic Jena AG, Jena, Germany, 845-KS-1060050). 18S rDNA amplification by PCR (Eppendorf AG, Germany, Mastercycler nexus) was conducted using the primers EukA (21F) (5′- AACCTGGTTGATCCTGCCAGT-3′) (Medlin et al., 1988) and EukB (1791R) (5′-TGATCCTTCTGCAGG TTCACCTAC-3′) (Medlin et al., 1988). The purified amplicons were sequenced by capillary sequencing (Eurofins Genomics GmbH, Ebersberg, Germany). The reads were searched against the GenBank database by the BLASTn (Altschul et al., 1990) algorithm. The nearest ancestral microalgae sequence hits of isolates were used for the lineage assignments. The phylogenetic tree was built with Geneious Tree Builder (Biomatters Ltd., New Zealand, Geneious software version 11.1.3). 18S rDNA data was included from deposited reference strains which are obtainable from SAG, UTEX, CCAP.

The Fatty Acid Methyl Esters (FAME) were prepared according to reported methods applied to microalgae biomass with the following modification (Griffiths et al., 2010): 10 mg lyophilized biomass of each sample was used; the internal standard C17-TAG was replacement by C19-TAG Sigma Aldrich T4632 (Merck AG, Darmstadt, Germany). Initial extraction with GC grade toluene was assisted by sonification for 40 min in an ice bath. BF_3 methanol was replacement by a HCl/Methanol Supleco 17935 solution (Merck AG, Darmstadt, Germany). After transesterification FAMEs were extracted with GC grade hexane by vortexing with glass beads for 10 s at RT. After centrifugation for 5 min at 1,000 rpm, the hexane phase was transferred to GC-vails. The fatty acid profiles were measured with a Shimadzu GC-2025 equipped with a AOC-20i autosampler and FID detector (245°C) (Shimadzu, Kyoto, Japan). For each sample, 1 μl was injected with a split ratio of 1:10 at a temperature of 240°C and loaded on a Zebron ZB-WAX column (30 m × 0.32 mm, thickness of 0.32 μm, Phenomenex, Torrance, USA). The column oven temperature was set to 150°C for 1 min, a ramp of 5°C/min increased the temperature to a final target of 240°C. Thereafter

holding the final temperature for 6 min. Hydrogen 5.0 was used as carrier gas at a constant flow rate of 35 ml/min. Identification of peaks was done by manual calibration with the external standard Marine oil FAME Mix (RestekGmbH, Bad Homburg, Germany). A relative quantification was done by integral FID signal comparison after normalization and exclusion of the internal C19 Fame Standard.

Folate Content and Isoform Distribution Analysis on Microalgae Biomass

For the folate stable isotope dilution assay analysis, the complete information about chemicals, standards, and preparations of solutions as well as validation of the method can be obtained from a previous publication (Striegel et al., 2018b). Briefly, LODs of all analytes were in the range of 0.17 and 0.33 μg/100 g, and LOQs in the range of 0.51 and 0.96 μg/100 g. Inter-injection precision was between 1.96 and 4.46%, intra-day precision between 2.44 and 4.60%, and inter-day precision between 3.04 and 5.06%. 10-CHO-PteGlu was quantified using [$^{13}C_5$]-5-CHO-H_4folate as internal standard. The LODs and LOQs were estimated using the response factor of 5-CHO-H_4folate as a reference value. We calculated a LOD of 0.14 μg/100 g and a LOQ of 0.40 μg/100 g. All results given in the results and discussion section are based on dry biomass.

Sample Preparation for the Folate Analysis of Algae Biomass

The sample extraction was performed under subdued light. Briefly, the freeze-dried algae samples were finely grounded using a mortar and pestle. Ten milligram of resulted biomass were used for each extraction. After addition of 10 ml buffer (200 nmol/l 2-(N-morpholino)ethanlsulfonic acid hydrate (MES), 114 nmol/l ascorbic acid, 0.7 nmol/l DTT, pH 5.0) internal standards ([$^{13}C_5$]-PteGlu, [$^{13}C_5$]-H_4folate, [$^{13}C_5$]-5-CH_3-H_4folate, and [$^{13}C_5$]-5-CHO-H_4folate [used for quantitation of 5-CHO-H_4folate and 10-CHO-PteGlu)] were added to samples in equal amounts (0.004–0.5 nmol) to the anticipated respective analyte content. For deconjugation, an adjusted amount of 1 ml rat serum (used without dilution; endopeptidase used for deconjugation of diglutamates to monoglutamates) and 2 ml chicken pancreas suspension (1 g/l in phosphate buffer (100 mmol/l, 1 g/l ascorbic acid, pH 7); exopeptidase used for deconjugation of polyglutamates to the respective diglutamates) were added, and the samples were incubated overnight for a minimum of 12 h in a water bath at 37°C. After a 10 min boiling step, samples were cooled on ice and transferred into plastic centrifuge tubes with additional 10 ml acetonitrile. After centrifugation (20 min, 4,000 rpm, 4°C), the extracts were applied to a solid-phase extraction (SPE) clean-up using strong anion-exchange (SAX) cartridges (quaternary amine, 500 mg, 3 ml). In short, cartridges were activated with two volumes of methanol, equilibrated with 3 volumes of buffer [10 mmol/l phosphate buffer (consisting of 100 mmol/l sodium hydrogen phosphate and adjusting the solution with 100 mmol/l dipotassium hydrogen phosphate to pH 7.0) was mixed with 1.3 mmol/l DTT], extracts were completely applied, and cartridges were washed again with 3 volumes of buffer for equilibration and run dry. The folates were eluted using 2 ml of buffer for elution (5% sodium chloride, 1% ascorbic acid, 100 mmol/l sodium acetetate, and 0.7 mmol/l DTT), membrane filtered, and measured by LC-MS/MS.

LC-MS/MS

Chromatography was carried out on a Shimadzu Nexera X2 UHPLC system (Shimadzu, Kyoto, Japan) with a Raptor ARC-18 column (2.7 μm, 100 × 2.1 mm, Restek, Bad Homburg, Germany) and a Raptor ARC-18 precolumn (2.7 μm, 5 × 2.1 mm, Restek, Bad Homburg, Germany) as a stationary phase that was kept at 30°C. The mobile phase consisted of (A) 0.1% formic acid and (B) acetonitrile with 0.1% formic acid delivered as a binary gradient at a flow rate of 0.4 ml/min. Gradient concentration started at 3% B and raised linearly to 10% within the next 2.5 min and held at 10% for further 2.5 min. Then, the concentration went up to 15% B within 5 min and then to 50% within 1 min, followed by holding at 50% B for 1 min. Within 1 min, the concentration returned to 3% B and was equilibrated for 4 min. The injection volume was 10 μl.

The LC was interfaced with a triple quadrupole mass spectrometer (LCMS-8050, Shimadzu, Kyoto, Japan). It was operated in the positive ESI mode for all analytes. The specified settings are also described previously (Striegel et al., 2018b). Data acquisition was performed with LabSolutions software 5.8 (Shimadzu, Kyoto, Japan). The ion source paramaters were set as follows: heat block (400°C), dilution line (250°C), interface temperature (300°C), drying gas (10 l/min), heating gas (10 l/min), nebulizing gas (3 l/min), collision-induced dissociation gas (270 kPa), and interface voltage (4 kV), respectively. MS parameters were listed in the previously published paper about the method validation. The mass spectrometer was operated in the multiple reaction monitoring (MRM) mode for MS/MS measurements.

Statistical Evaluation

All folate results are means of technical triplicates ± standard deviation. The received values were tested for normal distribution with the test of Kolmogorov-Smirnov and were tested for outliers by the test of Dixon. A significance test was carried out by the *T*-test after applying the F-test for heteroscedasticity. The level of statistical significance was set to $p < 0.05$.

RESULTS

Within this project, a series of freshwater and marine microalgae were analyzed for their total folate content and vitamer distribution by SIDA based on dry biomass. For all cultured microalgae strains, we validated the lineage assignment by sample-specific fatty acid profiles and 18S rDNA sequence identity. To reflect on the analyzed diversity, we included a phylogenetic tree with reference strains from UTEX, SAG and CCAP collections. The construction of the phylogenetic tree (**Figure 2**) indicates a clustering according to the samples previous lineage assignments or reference. The 18S rDNA

sequences of isolated microalgae strains are deposited in the NCBI database, and the accession numbers are listed in **Table 1**. The reference and environmental microalgae strains cluster with the reference Chlorophyta strains, nearest relatives obtainable from popular culture collections can be deduced from the phylogenetic tree shown in **Figure 2**. For enhanced strain validation and culture status, we determined the fatty acid profile (**Table 2**). All isolated and deposited microalgae samples showed similar fatty acid profiles as reference data (Lang et al., 2011). The red algae *P. purpureum* showed a previously observed 41.9% eicosatetraenoic acid content in total transesterified lipid extracts.

Consistently, high folate contents were detected in all algae biomasses samples, in the range between 539 ± 150 μg/100 g and 6,470 ± 167 μg/100 g. The commercial reference food supplements showed high folate contents of 1,690 ± 17.3 μg/100 g (Supplement 1) and 2,450 ± 52.1 μg/100 g (Supplement 2), respectively. For the cultured reference *Chlorella vulgaris (SAG211-12)* biomass a folate content of 3,460 ± 134 μg/100 g was detected. The highest overall total folate content was observed in *Picochlorum* sp. isolate with a very high value of 6,470 ± 167 μg/100 g in dry biomass thus revealing a significantly higher [$p < 0.05$, $n = 1$ (biological)] total folate content compared to all other samples. The lowest total folate content was observed in *P. purpureum* biomass with a value of 539 ± 150 μg/100 g. The folate contents analyzed in microalgae are graphically shown in **Figure 3** (left), and the detailed values are listed in **Table 3**.

Moreover, we differentially analyzed the main vitamers present in food encompassing PteGlu, H_4folate, 5-CH_3-H_4folate,

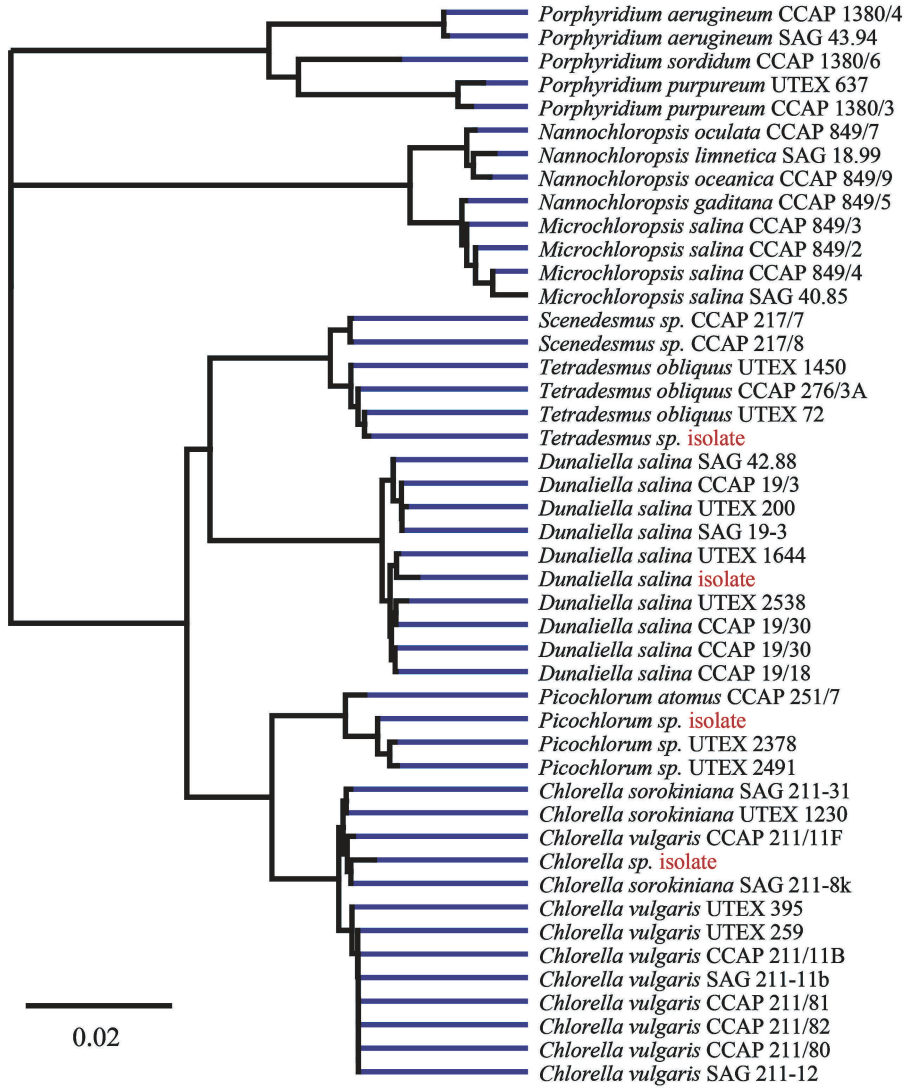

FIGURE 2 | Phylogenetic tree of isolates and reference strains 18S rDNA data build by Geneious Tree Builder [Geneious 11.1.3 (https://www.geneious.com)]. Visualization of global alignment and Neighbor-Joining with 93% similarity cost matrix using the Tamura-Nei distance model.

TABLE 2 | Fatty acid composition of microalgae samples by GC-FID analysis.

Fatty acid methyl esters (FAME) [%]	C16:0	C16:1	C18:0	C18:1	C18:1	C18:2	C18:3	C20:4	C20:5	18S rDNA accession number
CULTURED REFERENCE STRAINS										
Chlorella vulgaris SAG 211-12	24.2	9.1	Trace	5.7	Trace	25.1	34.6	ND	ND	MK971791
Porphyridium purpureum CCAP 1380/3	26.8	Trace	Trace	2.6	Trace	16.8	ND	41.9	8.9	MK971789
Microchloropsis salina SAG 40.85	34.1	5.7	Trace	8.7	Trace	40.7	7.6	ND	ND	MK971790
ISOLATED STRAINS										
Picochlorum sp. isolate	35.9	Trace	1.7	16.8	Trace	23.1	19.5	ND	ND	MK973100
Dunaliella salina isolate	23.0	9.3	1.0	7.8	1.6	25.3	30.1	ND	ND	MK973098
Tetradesmus sp. isolate	31.4	1.0	Trace	26.1	1.1	23.0	13.2	ND	ND	MK973099
Chlorella sp. isolate	24.3	Trace	Trace	7.2	1.8	23.4	31.4	ND	ND	MN365023

ND, not detected; Trace <1%.

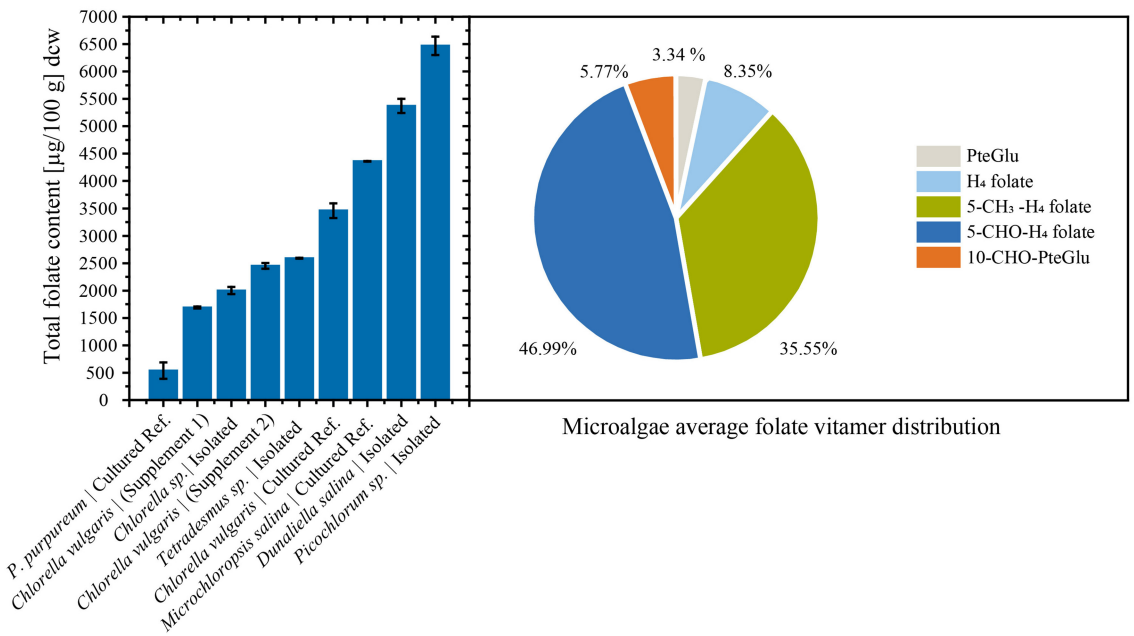

FIGURE 3 | (Left) Total folate content of food supplements, fresh cultured biomass, and isolated strains normalized by dry cell weight (dcw) biomass. **(Right)** Average folate vitamer distribution of the analyzed microalgae.

5-CHO-H_4folate, and 10-CHO-PteGlu. The average vitamer distribution is shown in **Figure 3** (right), and a detailed distribution is listed in **Table 3**. The main vitamers were 5-CH_3-H_4folate (5.43–70.1%) and 5-CHO-H_4folate (18.6–80.9%). The minor vitamers were 10-CHO-PteGlu (1.19–12.6%), H_4folate (0.54–21.2%), and the fully oxidized PteGlu (0.07–13.3%). 5-CH_3-H_4folate was the main vitamer in *Tetradesmus* sp. isolate, *Microchloropsis salina SAG 40.85*, *Chlorella vulgaris SAG 211-12*, and the *Picochlorum* sp. isolate.

Microalgae cultivation often requires product accumulation measures to increase obtainable yields in a technical scale. Particularly, effects of osmotic stress in case of pigment production and nitrogen limitation in case of lipid production are utilized (Borowitzka et al., 1990; Wang et al., 2019). The model microalgae *Chlorella* sp. isolate was used in an additional experiment to evaluate effects of widely applied stressors during late cultivation stages. Osmotic stress for 24 h did have a significant negative effect [$p < 0.05$, $n = 3$ (biological)] on total folates in *Chlorella* sp. isolate (**Figure 4**). Also, nitrogen limitation resulted in reduced [$p < 0.05$, $n = 3$ (biological)] detectable total folate contents. In contrast, light spectrum shift did not show differences on total folate. The detailed values and illumination conditions are shown in **Table S1**.

DISCUSSION

In this study, an analysis of the total folate content of a genetically defined microalgae series with a focus on halophilic Chlorophyta has been carried out. We measured very high total folate contents in all analyzed microalgae samples. The cumulative data indicate that microalgae can serve as a concentrated source of natural folates in form of food supplement products for folate-deficient populations. However, the set of analyzed microalgae species showed high variations in total folate, giving room for process and strain optimization toward concentrated algae

TABLE 3 | The folate content and vitamer distribution of selected microalgae strains, calculated as PteGlu in [μg/100 g].

Genus; species; strain	5-CH_3-H_4folate	5-CHO-H_4folate	10-CHO-PteGlu	H_4folate	PteGlu	Total folate content
COMMERCIAL FOOD SUPPLEMENTS						
Chlorella vulgaris (Supplement 1)	397 ± 11.6	1010 ± 17.3	119 ± 1.81	60.6 ± 6.41	108 ± 7.86	1690 ± 17.3
Chlorella vulgaris (Supplement 2)	631 ± 82.7	1510 ± 65.8	132 ± 7.58	102 ± 17.9	73.3 ± 2.53	2450 ± 52.1
CULTURED REFERENCE STRAINS						
Chlorella vulgaris SAG 211-12	2420 ± 47.8	643 ± 4.29	168 ± 83.9	216 ± 13.6	7.96 ± 3.88	3460 ± 134
Porphyridium purpureum CCAP 1380/3	191 ± 40.3	137 ± 28.4	67.7 ± 75.0	71.0 ± 28.4	71.5 ± 4.74	539 ± 150
Microchloropsis salina SAG 40.85	3050 ± 50.0	1060 ± 50.0	77.2 ± 4.55	147 ± 2.50	23.2 ± 1.45	4360 ± 5.60
CULTURED ISOLATED STRAINS						
Picochlorum sp. isolate	4020 ± 8.87	1990 ± 124	76.9 ± 10.8	285 ± 73.0	96.4 ± 22.1	6470 ± 167
Dunaliella salina isolate	847 ± 33.7	3960 ± 48.0	255 ± 28.6	269 ± 43.3	39.8 ± 23.5	5370 ± 129
Tetradesmus sp. isolate	1410 ± 8.62	731 ± 14.5	82.3 ± 1.48	306 ± 4.54	67.0 ± 0.68	2590 ± 9.59
Chlorella sp. isolate	718 ± 99.9	832 ± 82.3	38.6 ± 4.93	407 ± 40.3	1.40 ± 0.70	2000 ± 66.6

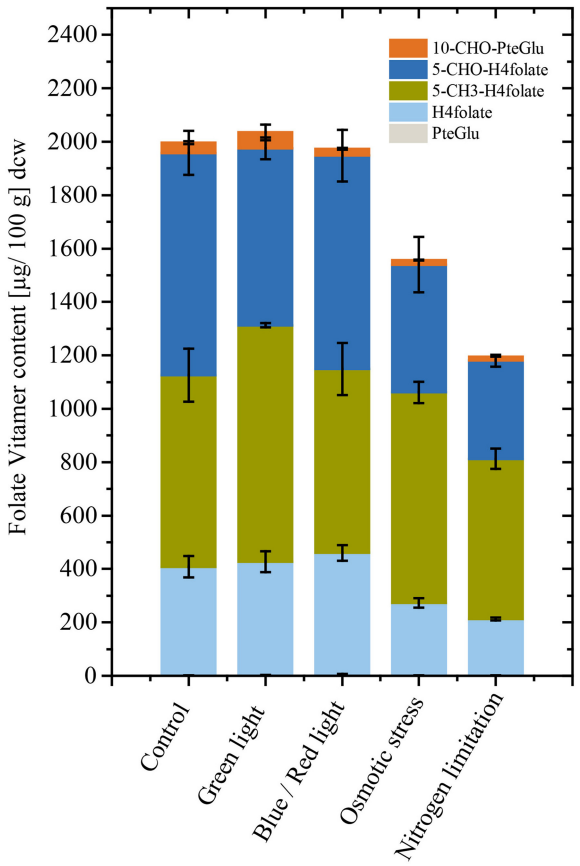

FIGURE 4 | Total folate content and vitamer distribution after conditional changes applied for 24 h in triplicates. *Chlorella* sp. isolate cultivations show reduced folate content when exhibited to osmotic stress and nitrogen limitation. Light wavelength changes did not affect folate contents when shifted for 24 h.

food products. As a reference to our cultivated algae species, we measured the folate content of commercial, algae food supplement products based on *Chlorella* biomass. Interestingly, the industrially processed dried *Chlorella* biomass retained a relatively high folate content, which however was only half of the total amount detected in cultured *Chlorella vulgaris*. *Chlorella* biomass has gained industrial attention in the past due to their generally regarded as safe (GRAS) status declared by the U.S. Food and Drug Administration (FDA). This GRAS status renders novel food approval of these products unnecessary and allows a rapid market rollout of these products. While our isolated halophilic algae strains *Dunaliella* sp. and *Picochlorum* sp. displayed significantly higher folate yields than *Chlorella*, the regulatory barriers for novel food would delay their market entry despite their excellent nutritional content. What is more, the biomass of the *Picochlorum* sp. isolate showed a total folate content of 6,470 μg/100 g, which is currently the highest total folate content detected in algae. This results further emphasizes the importance of halophilic microalgae as an excellent source of micronutrients. Previous publications reported total folate contents within the same order of magnitude as our results. Brown et al. analyzed the vitamin content of four Australian microalgae, inter alia *Nannochloropsis* sp., *Pavlova pinguis*, *Stichococcus* sp., and *Tetraselmis* sp. (Brown et al., 1999). The latter authors detected folate concentrations ranging between 1,700 and 2,600 μg/100 g. Microalgae collected in Japanese ponds were found to contain total folate contents in a range between 1,500 and 3,600 μg/100 g in dry biomass (Fujii et al., 2010). As previous studies applied microbiological assays to determine the folate content, they were not able to determine the folate pattern. Recently, Edelmann et al. analyzed various commercially available microalgae powder using microbiologial assays and an UHPLC methods to differentiate between different vitamers (Edelmann et al., 2019). The group found in average significantly higher total folate contents in *Chlorella* (2,500–4,700 μg/100 g) and *Nannochloropsis gaditana* (2,080 μg/100 g) compared to *Spirulina* (250–470 μg/100 g). The reviewed amounts of *Chlorella* agree with the folate contents in this study.

Furthermore, we found 5-CH_3-H_4folate and 5-CHO-H_4folate as the main vitamers in all algae isolates studied, which is in accordance with Edelmann et al. (2019). The latter authors also quantified 5,10-CH^+-H_4folate and found not negligible amounts of this vitamer in Spirulina samples. This vitamer should be

included in future analysis of microalgae. As previous studies applied microbiological assays or UHPLC methods to determine the folate content, this is the first report of the folate vitamer distribution in microalgae by high-resolution mass spectrometry. As folate vitamers show different stabilities and conversion reactions, the folate pattern can give additional information about the stability of folates in microalgae.

The absorption capacity, as well as the post-absorptive metabolism of different vitamers, lacks deeper understanding (Visentin et al., 2014). However, due to the different stability of folate vitamers, we assume that H_4folate is less bioavailable (Ringling and Rychlik, 2017b). Furthermore, to shed light on the extend of absorption of folates from algae, human trials are required. In the context of species-specific folate concentrations our results for the *Dunaliella* genus exceeded previously reported values (*Dunaliella tertiolecta*, 480 µg/100 g dry biomass) by the factor of ten. In this context it remains to be demonstrated, whether this discrepancy is due to physiological and phenotypic states of the algae or based on subspecies genetic variations.

High folate and vitamin concentration in microalgae biomass is not a generality (Croft et al., 2006); and we observed significantly lower folate content in the studied red algae *P. purpureum*. Osmotic stress and nitrogen limitation during cultivation showed negative effects on total folate content in *Chlorella* sp. As far as we know, this is the first report of precise stress effects during microalgae cultivations, indicating that nitrogen starvation and increased salinity impacts on total folate content negatively in *Chlorella* sp. This is particularly interesting for cultivation processes of microalgae biomass for food and feed. Typical valorization concepts for marine algae biomass includes multiple product streams, and relies on lipid and pigment accumulation, which seems at least in the model algae *Chlorella* sp. to be unfavorable for folate production. Also, *Dunaliella* sp. isolates showed a reduced total folate content when samples were analyzed from the stationary cultures (data not shown). However, only limited and contradictory results on folate accumulation under differential growth conditions are documented (Brown et al., 1999). Folate synthesis is associated with assimilation processes, thus we postulate that highest folate concentrations will be found under unlimited growth conditions (Hjortmo et al., 2008). Further studies are needed to shed light on the underlying metabolic regulation of folates in freshwater and marine microalgae. Product stability is a major concern as degradation of folates is known (Fitzpatrick et al., 2012; Blancquaert et al., 2015) rendering supplement product formulation, packaging, and distribution similar decisive as developments in process and strain optimization (Blancquaert et al., 2015).

Figure 5 depicts a summary of previously analyzed foods and supplements, presented in comparison with our results. In order to reach the European RDA of 300 µg or United States RDA of 400 µg (Krawinkel et al., 2014), an intake of only 6 g *Picochlorum* sp. dry biomass would be required. In contrast, reaching the RDA with high folate content fruits as strawberries

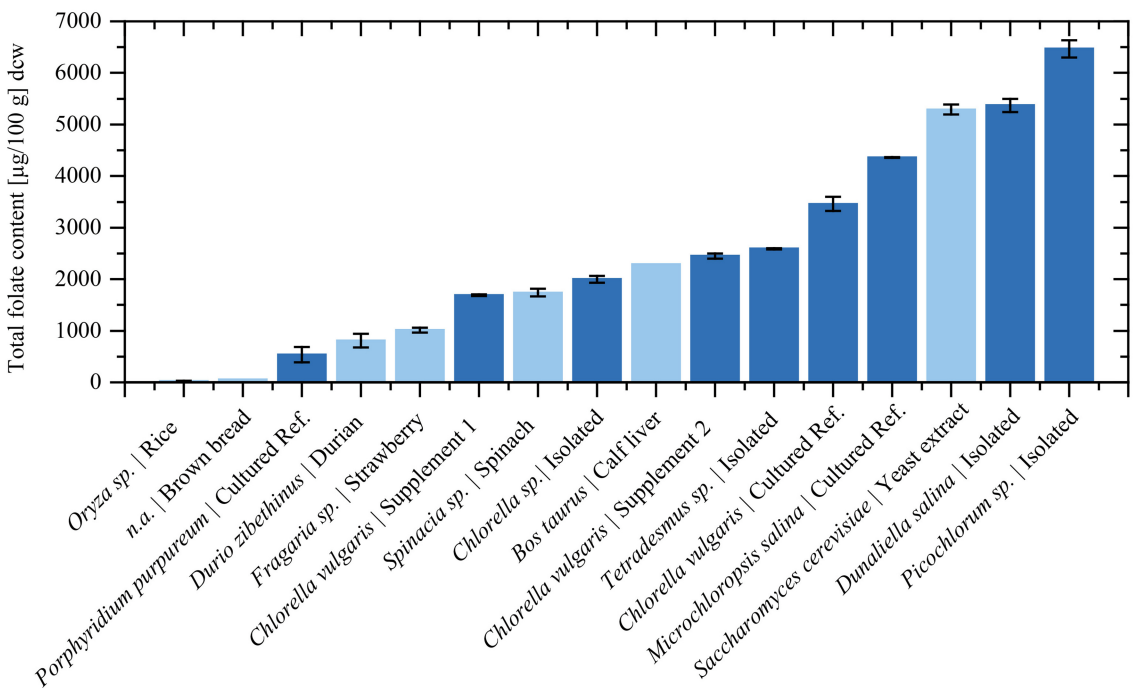

FIGURE 5 | The total folate content in selected food and algae dry biomass. Dark blue bars represent measured values from this study. The total folate content of food products was taken from previous publications using the same quantification method. The total folate contents were adapted to dry biomass according to literature values (Souci et al., 2008): Rice (*Oryza* sp.) from Ringling and Rychlik (2017a), Strawberry (*Fragaria* sp.) from Striegel et al. (2018b), Brown bread from Ringling and Rychlik (2013), Spinach (*Spinacia* sp.) (Ringling and Rychlik, 2013), Durian (*Durio zibethinus*) from Striegel et al. (2018a), Calf liver from Ringling and Rychlik (2017a), Yeast extract from Jacob et al. (2019).

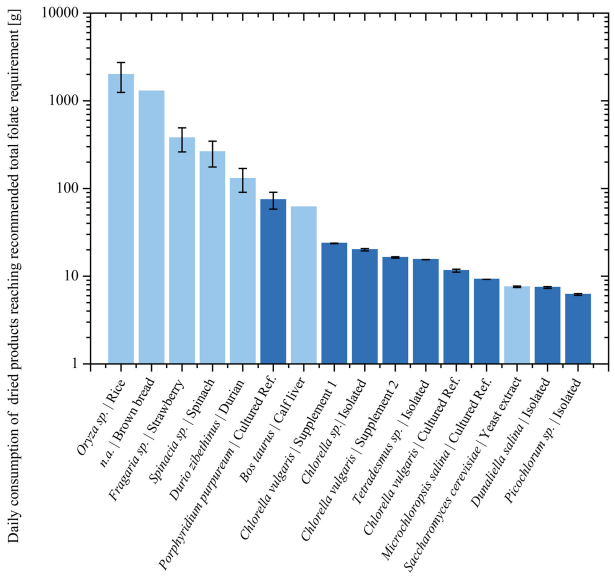

FIGURE 6 | Analyzed food products during this (Dark blue) and previous (Light blue) studies. Required biomass consumption in logarithmic scale according to the U.S. RDA for folate intake.

would require about 400 g dried biomass (**Figure 6**). Thus, it is viable to flag algae as concentrated food and nutrient producing platforms. To the best of our knowledge, we are the first to report the folate content of different microalgae strains using SIDA as quantification method. Microalgae, the potentially highest source of folates, warrant further studies on the distribution of pteroylpolyglutamates as well as on bioaccessibility, absorption, and retention for physiological functions.

DATA AVAILABILITY STATEMENT

Generated sequencing reads can be found at NCBI database: MK971789, MK971790, MK971791, MK973100, MK973098, MK973099, MN365023.

AUTHOR CONTRIBUTIONS

LS, TF, and DW conceived the experiment, analyzed the data, and co-wrote the manuscript. LS, TF, DW, and NW performed experiments. MF reviewed writing. TB and MR supervised the project and reviewed writing.

FUNDING

This work was supported by the German Research Foundation (DFG), the Bavarian Ministry of Economic Affairs, Energy and Technology (20E1507A), the Federal Ministry of Education and Research (033RC012B), and the Technical University of Munich (TUM) in the framework of the Open Access Publishing Program.

ACKNOWLEDGMENTS

We thank Soraya Chebib and Caroline Dumler for their contribution in the lab.

SUPPLEMENTARY MATERIAL

The Supplementary Material for this article can be found online at: https://www.frontiersin.org/articles/10.3389/fbioe.2019.00481/full#supplementary-material

REFERENCES

Allen, E. J., and Nelson, E. W. (1910). On the artificial culture of marine plankton organisms. *J. Mar. Biol. Assoc. U.K.* 8:421. doi: 10.1017/S0025315400073690

Allen, M. M. (1968). Simple conditions for growth of unicellular blue-green algae on plates. *J. Phycol.* 4, 1–4. doi: 10.1111/j.1529-8817.1968.tb04667.x

Altschul, S. F., Gish, W., Miller, W., Myers, E. W., and Lipman, D. J. (1990). Basic local alignment search tool. *J. Mol. Biol.* 215, 403–410. doi: 10.1016/S0022-2836(05)80360-2

Anderson, R. A. (2005). *Algal Culturing Techniques*, *1st Edn*. Burlington, MA; San Diego, CA; London: Elsevier Academic Press.

Apel, A. C., and Weuster-Botz, D. (2015). Engineering solutions for open microalgae mass cultivation and realistic indoor simulation of outdoor environments. *Bioprocess Biosyst. Eng.* 38, 995–1008. doi: 10.1007/s00449-015-1363-1

Asam, S., Konitzer, K., Schieberle, P., and Rychlik, M. (2009). Stable isotope dilution assays of alternariol and alternariol monomethyl ether in beverages. *J. Agric. Food Chem.* 57, 5152–5160. doi: 10.1021/jf900450w

Becker, W. (2003). "Microalgae in human and animal nutrition," in *Handbook of Microalgal Culture*, eds A. Richmond and Q. Hu (Oxford: Blackwell Publishing Ltd.), 312–351.

Benedetti, M., Vecchi, V., Barera, S., and Dall'Osto, L. (2018). Biomass from microalgae: the potential of domestication towards sustainable biofactories. *Microb. Cell Fact.* 17:173. doi: 10.1186/s12934-018-1019-3

Bischoff, H. W., and Bold, H. C. (1963). *Some Soil Algae From Enchanted Rock and Related Algal Species*. Austin, TX: University of Michigan; University of Texas.

Blancquaert, D., Van Daele, J., Strobbe, S., Kiekens, F., Storozhenko, S., De Steur, H., et al. (2015). Improving folate (vitamin B9) stability in biofortified rice through metabolic engineering. *Nat. Biotechnol.* 33, 1076–1078. doi: 10.1038/nbt.3358

Borowitzka, M. A., and Borowitzka, L. J. (1988). *Micro-Algal Biotechnology*. Cambridge, UK: Cambridge University Press.

Borowitzka, M. A., Borowitzka, L. J., and Kessly, D. (1990). Effects of salinity increase on carotenoid accumulation in the green alga *Dunaliella salina*. *J. Appl. Phycol.* 2, 111–119. doi: 10.1007/BF00023372

Brown, M. R., Mular, M., Miller, I., Farmer, C., and Trenerry, C. (1999). The vitamin content of microalgae used in aquaculture. *J. Appl. Phycol.* 11, 247–255. doi: 10.1023/A:1008075903578

Christaki, E., Florou-Paneri, P., and Bonos, E. (2011). Microalgae: a novel ingredient in nutrition. *Int. J. Food Sci. Nutr.* 62, 794–799. doi: 10.3109/09637486.2011.582460

Croft, M. T., Warren, M. J., and Smith, A. G. (2006). Algae need their vitamins. *Eukaryot. Cell* 5, 1175–1183. doi: 10.1128/EC.00097-06

Delchier, N., Herbig, A.-L., Rychlik, M., and Renard, C. M. G. C. (2016). Folates in fruits and vegetables: contents, processing, and stability. *Compr. Rev. Food Sci. Food Saf.* 15, 506–528. doi: 10.1111/1541-4337.12193

Draaisma, R. B., Wijffels, R. H., (Ellen) Slegers, P., Brentner, L. B., Roy, A., and Barbosa, M. J. (2013). Food commodities from microalgae. *Curr. Opin. Biotechnol.* 24, 169–177. doi: 10.1016/j.copbio.2012.09.012

Edelmann, M., Aalto, S., Chamlagain, B., Kariluoto, S., and Piironen, V. (2019). Riboflavin, niacin, folate and vitamin B12 in commercial microalgae powders. *J. Food Compos. Anal.* 82:103226. doi: 10.1016/j.jfca.2019.05.009

Fitzpatrick, T. B., Basset, G. J. C., Borel, P., Carrari, F., DellaPenna, D., Fraser, P. D., et al. (2012). Vitamin deficiencies in humans: can plant science help? *Plant Cell Online* 24, 395–414. doi: 10.1105/tpc.111.093120

Foley, J. A., Ramankutty, N., Brauman, K. A., Cassidy, E. S., Gerber, J. S., Johnston, M., et al. (2011). Solutions for a cultivated planet. *Nature* 478, 337–342. doi: 10.1038/nature10452

Fujii, K., Nakashima, H., and Hashidzume, Y. (2010). Isolation of folate-producing microalgae, from oligotrophic ponds in Yamaguchi, Japan. *J. Appl. Microbiol.* 108, 1421–1429. doi: 10.1111/j.1365-2672.2009.04542.x

Griffiths, M. J., van Hille, R. P., and Harrison, S. T. L. (2010). Selection of direct transesterification as the preferred method for assay of fatty acid content of microalgae. *Lipids* 45, 1053–1060. doi: 10.1007/s11745-010-3468-2

Grosso, G., Pajak, A., Marventano, S., Castellano, S., Galvano, F., Bucolo, C., et al. (2014). Role of omega-3 fatty acids in the treatment of depressive disorders: a comprehensive meta-analysis of randomized clinical trials. *PLoS ONE.* 9:e96905. doi: 10.1371/journal.pone.0096905

Hanson, A. D., and Gregory, J. F. (2002). Synthesis and turnover of folates in plants. *Curr. Opin. Plant Biol.* 5, 244–249. doi: 10.1016/S1369-5266(02)00249-2

Harun, R., Singh, M., Forde, G. M., and Danquah, M. K. (2010). Bioprocess engineering of microalgae to produce a variety of consumer products. *Renew. Sustain. Energy Rev.* 14, 1037–1047. doi: 10.1016/j.rser.2009.11.004

Hjortmo, S., Patring, J., and Andlid, T. (2008). Growth rate and medium composition strongly affect folate content in *Saccharomyces cerevisiae*. *Int. J. Food Microbiol.* 123, 93–100. doi: 10.1016/j.ijfoodmicro.2007.12.004

Jacob, F. F., Striegel, L., Rychlik, M., Hutzler, M., and Methner, F.-J. (2019). Yeast extract production using spent yeast from beer manufacture: influence of industrially applicable disruption methods on selected substance groups with biotechnological relevance. *Eur. Food Res. Technol.* 245, 1–14. doi: 10.1007/s00217-019-03237-9

Kay, R. A., and Barton, L. L. (1991). Microalgae as food and supplement. *Crit. Rev. Food Sci. Nutr.* 30, 555–573. doi: 10.1080/10408399109527556

Kent, M., Welladsen, H. M., Mangott, A., and Li, Y. (2015). Nutritional evaluation of australian microalgae as potential human health supplements. *PLoS ONE.* 10:e0118985. doi: 10.1371/journal.pone.0118985

Krawinkel, M. B., Strohm, D., Weissenborn, A., Watzl, B., Eichholzer, M., Bärlocher, K., et al. (2014). Revised D-A-CH intake recommendations for folate: how much is needed? *Eur. J. Clin. Nutr.* 68, 719–723. doi: 10.1038/ejcn.2014.45

Lang, I., Hodac, L., Friedl, T., and Feussner, I. (2011). Fatty acid profiles and their distribution patterns in microalgae: a comprehensive analysis of more than 2000 strains from the SAG culture collection. *BMC Plant Biol.* 11:124. doi: 10.1186/1471-2229-11-124

Laurens, L. M. L., Markham, J., Templeton, D. W., Christensen, E. D., Van Wychen, S., Vadelius, E. W., et al. (2017). Development of algae biorefinery concepts for biofuels and bioproducts; a perspective on process-compatible products and their impact on cost-reduction. *Energy Environ. Sci.* 10, 1716–1738. doi: 10.1039/C7EE01306J

Lipper, L., Thornton, P., Campbell, B. M., Baedeker, T., Braimoh, A., Bwalya, M., et al. (2014). Climate-smart agriculture for food security. *Nat. Clim. Chang.* 4, 1068–1072. doi: 10.1038/nclimate2437

Marventano, S., Kolacz, P., Castellano, S., Galvano, F., Buscemi, S., Mistretta, A., et al. (2015). A review of recent evidence in human studies of n-3 and n-6 PUFA intake on cardiovascular disease, cancer, and depressive disorders: does the ratio really matter? *Int. J. Food Sci. Nutr.* 66, 611–622. doi: 10.3109/09637486.2015.1077790

Medlin, L., Elwood, H. J., Stickel, S., and Sogin, M. L. (1988). The characterization of enzymatically amplified eukaryotic 16S-like rRNA-coding regions. *Gene* 71, 491–499. doi: 10.1016/0378-1119(88)90066-2

Pratt, R., and Johnson, E. (1965). Production of thiamine, riboflavin, folic acid, and biotin by *Chlorella vulgaris* and *Chlorella pyrenoidosa*. *J. Pharm. Sci.* 54, 871–874. doi: 10.1002/jps.2600540611

Provasoli, L., McLaughlin, J. J. A., and Droop, M. R. (1957). The development of artificial media for marine algae. *Arch. Mikrobiol.* 25, 392–428. doi: 10.1007/BF00446694

Pulz, O., and Gross, W. (2004). Valuable products from biotechnology of microalgae. *Appl. Microbiol. Biotechnol.* 65, 635–648. doi: 10.1007/s00253-004-1647-x

Ringling, C., and Rychlik, M. (2013). Analysis of seven folates in food by LC–MS/MS to improve accuracy of total folate data. *Eur. Food Res. Technol.* 236, 17–28. doi: 10.1007/s00217-012-1849-x

Ringling, C., and Rychlik, M. (2017a). Origins of the difference between food folate analysis results obtained by LC–MS/MS and microbiological assays. *Anal. Bioanal. Chem.* 409, 1815–1825. doi: 10.1007/s00216-016-0126-4

Ringling, C., and Rychlik, M. (2017b). Simulation of food folate digestion and bioavailability of an oxidation product of 5-methyltetrahydrofolate. *Nutrients* 9, 1–19. doi: 10.3390/nu9090969

Rothschild, L. J., and Mancinelli, R. L. (2011). Life in extreme environments. *Nature* 409, 1092–1101. doi: 10.1038/35059215

Rychlik, M. (ed). (2011). *Fortified Foods With Vitamins*. Weinheim: Wiley-VCH Verlag GmbH & Co. KGaA.

Schenk, P. M., Thomas-Hall, S. R., Stephens, E., Marx, U. C., Mussgnug, J. H., Posten, C., et al. (2008). Second generation biofuels: high-efficiency microalgae for biodiesel production. *Bio Energy Res.* 1, 20–43. doi: 10.1007/s12155-008-9008-8

Selhub, J. (2002). Folate, vitamin B12 and vitamin B6 and one carbon metabolism. *J. Nutr. Health Aging* 6, 39–42.

Shane, B. (1989). Folylpolyglutamate synthesis and role in the regulation of one-carbon metabolism. *Vitam. Horm.* 45, 263–335. doi: 10.1016/S0083-6729(08)60397-0

Sheppard, P., Garcia-Garcia, G., Angelis-Dimakis, A., Campbell, G. M., and Rahimifard, S. (2019). Synergies in the co-location of food manufacturing and biorefining. *Food Bioprod. Process.* 117, 340–359. doi: 10.1016/j.fbp.2019.08.001

Souci, S. W., Siegfried W., Fachmann, W., Kraut, H., Kirchhoff, E., Germany Bundesministerium für Ernährung und Landwirtschaft, et al. (2008). *Food Composition and Nutrition Tables*. Stuttgart: MedPharm Scientific Publishers.

Striegel, L., Chebib, S., Dumler, C., Lu, Y., Huang, D., and Rychlik, M. (2018a). Durian fruits discovered as superior folate sources. *Front. Nutr.* 5:114. doi: 10.3389/fnut.2018.00114

Striegel, L., Chebib, S., Netzel, M. E., and Rychlik, M. (2018b). Improved stable isotope dilution assay for dietary folates using LC-MS/MS and its application to strawberries. *Front. Chem.* 6:11. doi: 10.3389/fchem.2018.00011

Subhadra, B., and Grinson-George (2011). Algal biorefinery-based industry: an approach to address fuel and food insecurity for a carbon-smart world. *J. Sci. Food Agric.* 91, 2–13. doi: 10.1002/jsfa.4207

Tilman, D., Cassman, K. G., Matson, P. A., Naylor, R., and Polasky, S. (2002). Agricultural sustainability and intensive production practices. *Nature* 418, 671–677. doi: 10.1038/nature01014

Tilman, D., Fargione, J., Wolff, B., D'Antonio, C., Dobson, A., Howarth, R., et al. (2001). Forecasting agriculturally driven global environmental change. *Science* 292, 281–284. doi: 10.1126/science.1057544

van der Spiegel, M., Noordam, M. Y., and van der Fels-Klerx, H. J. (2013). Safety of novel protein sources (insects, microalgae, seaweed, duckweed, and rapeseed) and legislative aspects for their application in food and feed production. *Compr. Rev. Food Sci. Food Saf.* 12, 662–678. doi: 10.1111/1541-4337.12032

Vanthoor-Koopmans, M., Wijffels, R. H., Barbosa, M. J., and Eppink, M. H. M. (2013). Biorefinery of microalgae for food and fuel. *Bioresour. Technol.* 135, 142–149. doi: 10.1016/j.biortech.2012.10.135

Visentin, M., Diop-Bove, N., Zhao, R., and Goldman, I. D. (2014). The intestinal absorption of folates. *Annu. Rev. Physiol.* 76, 251–274. doi: 10.1146/annurev-physiol-020911-153251

Wang, X., Fosse, H. K., Li, K., Chauton, M. S., Vadstein, O., and Reitan, K. I. (2019). Influence of nitrogen limitation on lipid accumulation and EPA and DHA content in four marine microalgae for possible use in aquafeed. *Front. Mar. Sci.* 6:95. doi: 10.3389/fmars.2019.00095

Wells, M. L., Potin, P., Craigie, J. S., Raven, J. A., Merchant, S. S., Helliwell, K. E., et al. (2017). Algae as nutritional and functional food sources: revisiting our understanding. *J. Appl. Phycol.* 29, 949–982. doi: 10.1007/s10811-016-0974-5

Conflict of Interest: The authors declare that the research was conducted in the absence of any commercial or financial relationships that could be construed as a potential conflict of interest.

frontiers in Bioengineering and Biotechnology

SYSTEMATIC REVIEW
published: 31 January 2020
doi: 10.3389/fbioe.2020.00011

Use of Ionic Liquids in Chitin Biorefinery: A Systematic Review

Julia L. Shamshina[1]* *and Paula Berton*[2]

[1] Mari Signum, Richmond, VA, United States, [2] Chemical and Petroleum Engineering Department, University of Calgary, Calgary, AB, Canada

Lignocellulosic biomass biorefinery is the most extensively investigated biorefinery model. At the same time, chitin, structurally similar to cellulose and the second most abundant polymer on Earth, represents a unique chemical structure that allows the direct manufacture of nitrogen-containing building blocks and intermediates, a goal not accomplishable using lignocellulosic biomass. However, the recovery, dissolution, and treatment of chitin was fairly challenging until the polymer's easy dissolution in ionic liquids (salts that are liquid at room temperature) was discovered. In this systematic review, we highlight recent developments in the processing of chitin, with a particular emphasis placed on methods conducted with the help of ionic liquids used as solvents, co-solvents, or catalysts. Such use of ionic liquids in the field of chemical transformations of chitin not only allows for shorter times and less harsh reaction conditions, but also results in different outcomes and higher product yields when compared with reactions conducted in "traditional" manner. Valorization of biomass in general, and chitin in particular, is a key enabling strategy of the circular economy, due to the importance of the sustainable production of biomass-based goods and chemicals and full chain resource efficiency. Economics is driven by the production of high-value chemicals or chemical intermediates from various biomasses, and chitinous biomass is a valuable potential resource. A fundamental "paradigm shift" will radically change the balance of oil-based chemicals to biopolymer-based chemicals, and chitin valorization is a necessary step aimed toward its full market competitiveness and flexibility.

Keywords: biorefinery, chitin, biomass, ionic liquids, circular economy, biomass valorization

OPEN ACCESS

Edited by:
Sónia Patrícia Marques Ventura, University of Aveiro, Portugal

Reviewed by:
Carla Silva, University of Minho, Portugal
André Miguel Da Costa Lopes, Center for Research in Ceramic and Composite Materials, Department of Chemistry, University of Aveiro, Portugal

***Correspondence:**
Julia L. Shamshina
shams002@gmail.com

Specialty section:
This article was submitted to Industrial Biotechnology, a section of the journal Frontiers in Bioengineering and Biotechnology

Received: *22 July 2019*
Accepted: *08 January 2020*
Published: *31 January 2020*

Citation:
Shamshina JL and Berton P (2020) Use of Ionic Liquids in Chitin Biorefinery: A Systematic Review. Front. Bioeng. Biotechnol. 8:11. doi: 10.3389/fbioe.2020.00011

BIOREFINERY AND CHITIN BIOPOLYMER

Today, there is a strong drive toward the circular economy of producing materials and chemicals from sustainable sources (Mitchell, 2018) caused by the devastating quantity of plastics and the limits of oil resources (North and Halden, 2013). In this regard, biorefining is one of the key enabling strategies of the circular economy, with a primary purpose of developing biomass-based products and chemicals rather than oil-based ones. The concept is similar to petrochemical refineries where feed crude oil, initially consisting of several thousand different organic compounds, is first separated into major streams and then chemically converted into pure building blocks for consumer goods (de Jong and Jungmeier, 2015). Similarly, biomass feedstock can be partially or completely separated into main fractions, followed by the deconstruction of the components into valuable materials, chemicals, and biofuels (Stöcker, 2008; Stark, 2011; North and Halden, 2013; Sun et al., 2017). A great example of biorefinery that uses lignocellulosic biomass is the National

Renewable Energy Laboratory (NREL), where an Integrated Biorefinery Research Facility (IBRF) was built encompassing a pilot plant on site to "develop, test, evaluate, and demonstrate processes and technologies for the production of bio-based products and fuels (NREL, 2019)."

We believe biopolymers, such as chitin, cellulose, or lignin (**Figure 1**), are of great interest due to their unique set of properties and characteristics suitable for direct preparation of functional materials in many fields, and we will always strongly advocate for using unmodified polymers as-is, for the preparation of materials directly (Qin et al., 2010; Barber et al., 2013; Shamshina et al., 2014, 2019; Rogers, 2015; Shen et al., 2016; King C. A. et al., 2017; King C. et al., 2017). However, following the practice with oil-based products, these biopolymers can be cut up into building blocks for production of low-volume, but high-value, chemicals. This is especially true for biopolymers such as lignin, with a highly variable composition. Whereas, a lot of research has been conducted on the topic of lignocellulosic biomass transformation (de Jong and Gosselink, 2014), much less research has been done on the treatment of chitin.

Chitin, the second most copious polysaccharide on Earth (after cellulose) (Elieh-Ali-Komi and Hamblin, 2016), is structurally analogous to cellulose except for the acetamide side chain at the C-2 position (**Figure 1**). It is a linearly assembled 2-(acetylamino)-2-deoxy-D-glucose β-linked polymer (Foster and Webber, 1961), available mostly from shrimp and crab shell waste biomass (15–40%) (Younes and Rinaudo, 2015), where it coexists with proteins (20–40%) and minerals (20–50%) (Rhazi et al., 2000; Ibitoye et al., 2018). Its abundance (*ca*. 0.15 megatons per year) (Roberts, 1992) makes chitin a remarkably valuable potential resource for the production of value-added chemicals. Because chitin has 5–7 wt% of biologically fixed nitrogen (value that depends on its degree of acetylation or DA) (Schoukens, 2009), it is possible to directly produce nitrogen-containing building blocks from this polymer. This is a task which cannot be accomplished using lignocellulosic biomass. Chitin possesses a unique combination of properties and is widely used in preparation of chemicals and materials, mostly for the biotechnology market (Prudden et al., 1970; Peluso, 1994; Jayakumar et al., 2011; Yang, 2011; Vázquez et al., 2013; Wan and Tai, 2013; Shamshina et al., 2018).

Chitin can be transformed into valuable chemicals using transformations shown in **Scheme 1**, such as the hydrolysis to its monomer *N*-acetylglucosamine (GlcNAc), dimer *N*, *N*′-diacetylchitobiose, or longer oligomers, where the hydrolysis of the glycosidic linkages is much faster than deacetylation (Einbu and Vårum, 2008). Also, its deacetylation is widely explored to generate chitosan of different DAs, obtained using more or less harsh conditions, depending on the potential applications (Sivashankari and Prabaharan, 2017). Less explored reactions of chitin include formation of furan derivatives such as 5-hydroxymethylfurfural (5-HMF) and

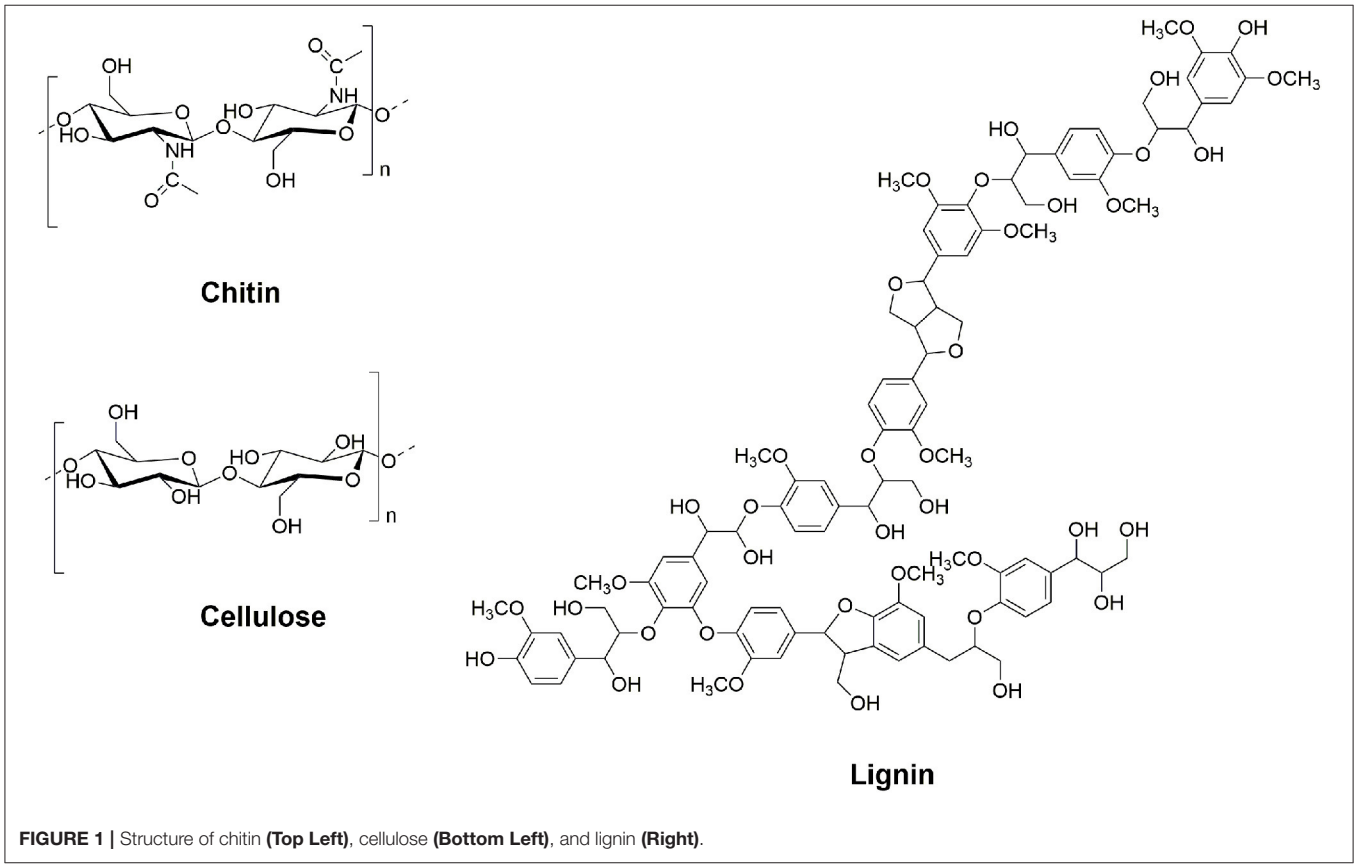

FIGURE 1 | Structure of chitin **(Top Left)**, cellulose **(Bottom Left)**, and lignin **(Right)**.

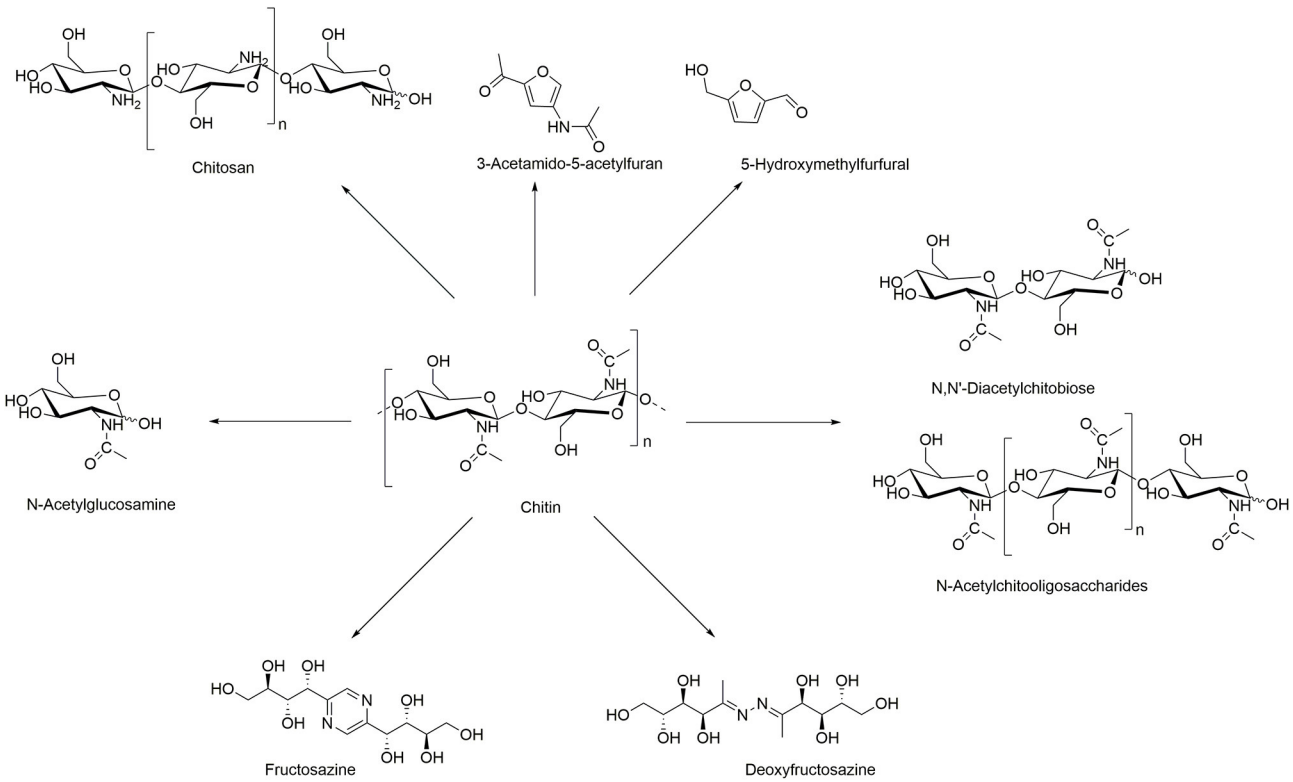

SCHEME 1 | Chitin conversion to high-value chemicals.

nitrogen-containing (*N*-containing) furan derivatives such as 3-acetamido-5-acetylfuran (3A5AF), normally conducted with the use of acidic catalysts and dehydration agents (Omari et al., 2012). Other, less known, chemical transformations include the purification of fructosazine and deoxyfructosazine, normally obtained from glucose under weakly acidic reaction conditions (Tsuchida et al., 1973).

Perhaps one of the main reasons for the limited exploratory work for chitin in comparison with cellulose can be explained by its insolubility in water and most organic solvents (Sieber et al., 2018). In this regard, the field of ionic liquids (ILs, organic salts with melting points below 100°C) (Hayes et al., 2015) offers tremendous potential as a class of solvents suitable for chitin processing. Due to their ability to directly dissolve both biomass (Fort et al., 2007; Kilpeläinen et al., 2007; Sun et al., 2009; V2020 Alternate Feedstock Report, 2019) and purified biopolymers (Phillips et al., 2004; Heinze et al., 2005; Xie et al., 2005, 2006; Zhang et al., 2005; Biswas et al., 2006; Pu et al., 2007; Wu et al., 2008), ILs have opened a door to effectively explore the carbohydrate economy and are widely used for biomass conversion. At the same time, the use of chitin as a sustainable resource assumes employment of more sustainable methods for its processing.

Indeed, the use of ILs for biopolymer processing presents a great advantage. Because ILs are capable of the disruption of chitin's hydrogen bonds, ILs have been shown to act as agents for biopolymer (or biomass) pre-treatment and solvents/co-solvents (Heinze et al., 2005; Biswas et al., 2006; Wu et al., 2008; Sun et al., 2009). Hence, chitin polymer can be pre-treated or even dissolved in the suitable IL prior to its transformation, with its hydrogen bond network being partially or fully destroyed. This provides an amorphous chitin of lower degree of crystallinity and makes the polymer chain "opened" and fully accessible to the reactant(s). ILs are also used as acidic catalysts (e.g., -SO_3H functionalized ILs, where -SO_3H is a part of cation or anion demonstrated high catalytic activity compared with non-functionalized ILs) (Sharghi et al., 2018) and as solvents or co-solvents at the same time. Besides, in many areas, reactions conducted using ILs as solvents, catalysts, or reactants have different outcomes and/or product yields when compared with those done in "traditional" manner. Furthermore, reactions utilizing ILs often require less harsh conditions and shorter reaction times (Maier et al., 2017).

Despite of all these achievements, the field of converting chitin into *chemicals* using ILs is still in its infancy. This fact is rather surprising, considering the structural similarity between chitin and cellulose and the significant efforts from industry and research centers (e.g., Joint Bioenergy Institute, JBEI, 2019)[1] in maximizing the value derived from the lignocellulosic biomass feedstock with the help of ILs. This systematic review will hence focus on the different approaches explored on processing

[1]JBEI. The Joint BioEnergy Institute (JBEI): U.S. Department of Energy (DOE) Bioenergy Research Center. Available online at: https://www.jbei.org/about/ (accessed June 25, 2019).

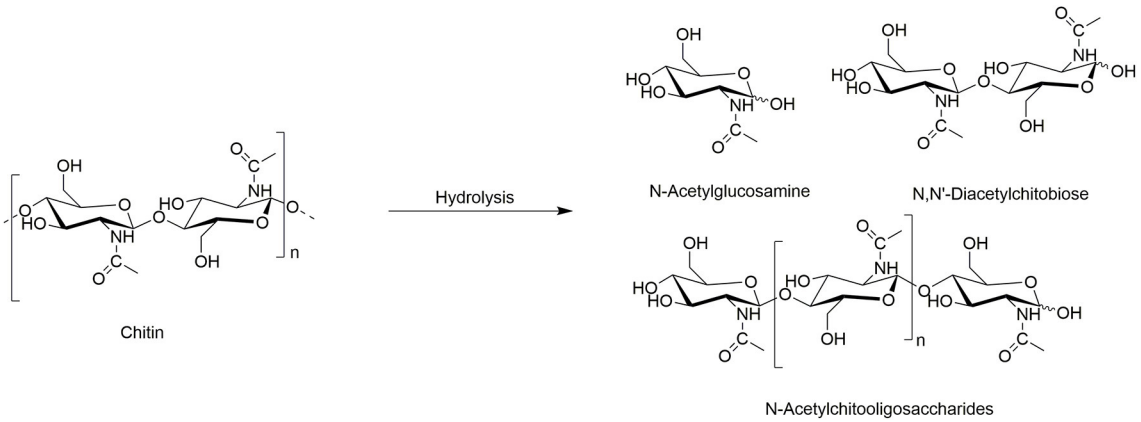

SCHEME 2 | Chitin hydrolysis.

TABLE 1 | Hydrolysis and deacetylation of chitin with the use of ILs.

S.no	Reaction type	Conditions	IL used	IL role	Products	References
1	Enzymatic hydrolysis	*Trichoderma viride* and *Streptomyces griseus* chitinases	$[C_2mim][OAc]$	Pre-treatment agent	GlcNAc, *N*, *N′*-diacetylchitobiose, and oligomers	Husson et al., 2017
2	Enzymatic hydrolysis	*S. griseus* chitinase	$[C_2mim][OAc]$	Used to regenerate chitin using this IL	GlcNAc, *N*, *N′*-diacetylchitobiose, and triacetylchito-biose	Berton et al., 2018
3	Acidic hydrolysis	N/A	$[HOSO_2C_3mim][CF_3SO_3]$; $[HOSO_2C_8mim][NTf_2]$	Solvent and catalyst	GlcNAc	Pischek et al., 2014
4	Enzymatic deacetylation	ChD enzyme from *Absidia orchidis*	[Amim]Cl; $[C_4mim]Br$	Activator of ChD	Fully deacetylated chitosan	Aspras et al., 2016, 2017

the chitin polymer with the help of ILs for production of sugars, aldehydes, nitrogen-containing compounds, and further chemical transformations.

HYDROLYSIS

From polymers, a broad range of monomers can be obtained as a single feedstock making them a good resource for the development of renewable chemicals. Thus, the first step in chitin transformation into various chemicals is its depolymerization, a process where chitin is broken down into its basic building blocks: the monomer GlcNAc, dimer *N*, *N′*-diacetylchitobiose, and longer oligomers (**Scheme 2**). The GlcNAc is used as a food additive in the food industry (as, e.g., antimicrobial and antitumoral food additive) (Nakagawa et al., 2011), joint-pain reliever, osteoarthritis and diabetes cure (Future Market Insights, 2019), and in cosmetic (as, e.g., skin moisturizers). The dimer is known to be a plant elicitor and promote plant induced immune response (Nakagawa et al., 2011); it is also used in research of chitobiose transporter systems and enzymes (Rhodes et al., 2010).

The hydrolysis of chitin can be achieved either by enzymatic or chemical approaches. The former approach for GlcNAc production is less preferred due to its lower product yield than that in the chemical (acidic) hydrolysis. However, the highly corrosive nature of the hydrochloric acid (HCl) generally used in the process requires replacing the equipment after a certain period of time, increasing the final cost of GlcNAc (Future Market Insights, 2019).

A few examples use ILs for the hydrolysis of chitin (**Table 1**). The initial report used the IL 1-ethyl-3-methyl-imidazolium acetate ($[C_2mim][OAc]$) to pre-treat chitin prior to enzymatic hydrolysis (**Table 1**, Entry 1). After pre-treatment, chitin was further hydrolyzed into the GlcNAc monomer using commercially available enzymes from *Trichoderma viride* and *S. griseus* (Husson et al., 2017). The IL-pre-treated (swollen) commercially available chitin resulted in a significant facilitation of, otherwise slow, enzymatic hydrolysis. The products of the reaction were GlcNAc (∼18%), *N*, *N′*-diacetylchitobiose (∼67%), and small amount of oligomers. The study suggested an increase in accessibility of enzymes to the chitin polymer after the IL pre-treatment.

The enzymatic hydrolysis of chitin was also studied using *S. griseus* chitinase but utilized different chitin substrates (**Table 1**, Entry 2) (Berton et al., 2018). One type of chitin was dissolved in $[C_2mim][OAc]$ IL and then reconstituted using water as an antisolvent remaining in amorphous, gel-like, state (amorphous

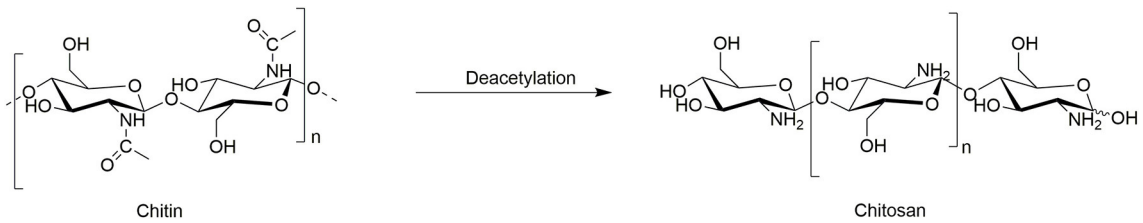

SCHEME 3 | Chitin deacetylation.

wet IL-chitin). The second type of chitin was isolated with the help of [C_2mim][OAc] IL and not otherwise pre-treated or dissolved (IL-dry-chitin). It was found that in both cases, the enzymatic reaction resulted in the formation of GlcNAc and the dimer *N*, *N*′-diacetylchitobiose. However, a longer chain trimer was detected in hydrolysis of regenerated amorphous wet chitin, which might be a result of its slower hydrolysis rate due to its higher hydration degree. This study pointed out the identity of obtained oligomers depending on pre-treatment of chitin with the IL and suggested that control of the hydrolysis products might be achieved using different pre-treatment conditions.

In the reactions where IL and a carbohydrate (e.g., chitin, chitosan, glucosamine, N-acetylglucosamine) is involved, the first, common step is the disruption of the hydrogen bonding of the carbohydrate, both inter- and intramolecular, and the formation of new hydrogen bonds between its hydroxyl groups and the anions of the IL. For the enzymatic hydrolysis reaction, it was shown that the enzymatic activity is strongly governed not only by the enzyme but also by the nature and amount of ionic liquid(s). For example, the enzymatic hydrolysis of chitin that has been pre-treated with [C_2mim][OAc] (either as pretreatment solvent, a co-solvent, or both), was found to be conditioned by the structural changes of the biopolymer induced by the IL. In all cases, the IL disrupted the hydrogen bonding of the chitin molecule and increased the enzymes' accessibility to the chitin substrate. It has also been shown that simultaneous use of the IL as pretreatment solvent and co-solvent was the most efficient and required the least amount of [C_2mim][OAc].

This was also confirmed by Li et al. (2019), who reported a significant decrease in the crystallinity of the polymer after IL pretreatment, and thus higher enzyme activity when compared to non-treated polymer. The authors hypothesized that enzymatic performances were correlated with the polymers' structural changes and depended on polymer's particle size and porosity. They evaluated N-acetylglucosamine solvation in [C_2mim][OAc] by NMR spectroscopy studies and confirmed the disruption of H-bonding network and the formation of new H-bonds between the IL anion and chitin hydroxyl groups as the major forces for the transformation.

An interesting example of an acidic, not enzymatic hydrolysis of chitin into GlcNAc monomer was presented using acidic ILs, namely 3-(1-methyl-1H-imidazol-3-ium-3-yl)propane-1-sulfonate triflate ([$HOSO_2C_3$mim][CF_3SO_3]) and 8-(1-methyl-1H-imidazol-3-ium-3-yl)octane-1-sulfonate bis(trifluoromethylsulfonyl)imide ([$HOSO_2C_8$mim][NTf_2]), that were used as both a solvent and acidic catalyst (Pischek et al., 2014) to produce GlcNAc in moderate yield (**Table 1**, Entry 3). Still, although a good example of the use of the IL as both the catalyst and solvent for the hydrolysis of chitin, this work was presented at a conference, and as such, there is no record of the results (yields) achieved.

DEACETYLATION

The de-*N*-acetylation (or "deacetylation") process can be used on either chitin itself (**Scheme 3**), chitosan, or the *N*-acetylated sugars obtained after the hydrolysis of chitin. We could find only one report where ILs were used in the enzymatic deacetylation using the enzyme chitin deacetylase (ChD) (**Table 1**, Entry 4). In this study, chitosan with degree of acetylation (DA) of 23% was further deacetylated using ChD enzyme isolated from *Absidia orchidis* (Aspras et al., 2016). In this reaction, the authors reported that the [C_4mim]Br IL acts as an activator of chitin deacetylase (ChD) (Aspras et al., 2016). Since chitin deacetylase can function in an IL-free environment, this activation effect takes place via non-essential enzyme activation mechanism. The IL was proposed to bind both the enzyme and the enzyme-substrate complex, although with different binding strength. However, when the concentration of the IL becomes high, this effect decreased, possibly because of some non-specific interactions between the IL and the ChD enzyme, affecting the tertiary structure of the enzyme. Other ILs, such as composed of imidazolium and pyridinium cations (1-alkyl-3-methylimidazolium $[C_2mim]^+$, 1-allyl-3-methylimidazolium $[Amim]^+$, 1-butyl-3-methylimidazolium $[C_4mim]^+$, and 1-ethylpyridinium $[C_2pyr]^+$) combined with halide (chloride Cl^-, bromide Br^-, iodide I^-), bis(trifluoromethane)sulfonimide ($[NTf_2]^-$), and dicyanamide ($[DCA]^-$) anions, were screened for their ability to activate ChD enzyme.

The experiments were carried out using 0.1 wt% chitosan load, 2% (v/v) ChD enzyme, and 10–70% IL in the reaction mixture. While none of the ILs acted as ChD inhibitors, [Amim]-containing ILs were able to significantly increase the activity of ChD. The highest increase in activity was noticed for [Amim]Cl IL (40% increase compared to the reaction conducted in the absence of the IL). [C_4mim]Br IL also demonstrated a significant increase in the activity of ChD (30% increase compared to the reaction conducted in the absence of the IL), while $[C_2mim]^+$ or $[C_2pyr]^+$-derived ILs had no effect on the enzyme activity.

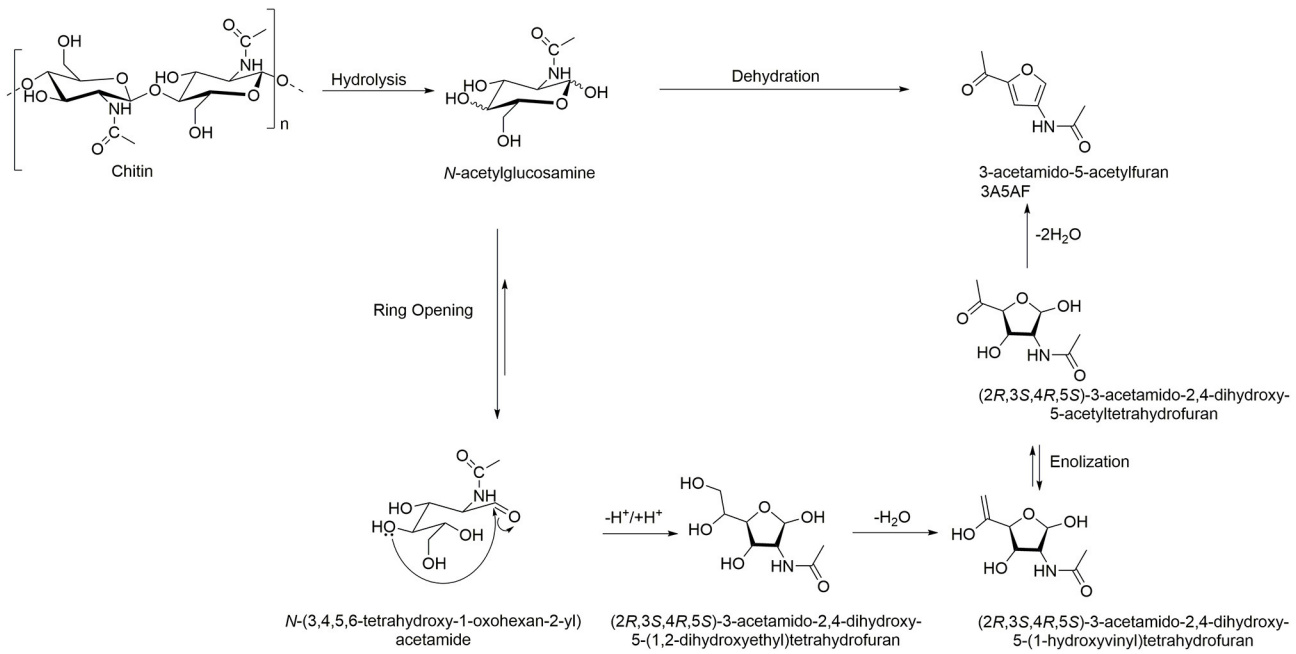

SCHEME 4 | Chitin conversion into 3-acetamido-5-acetylfuran (3A5AF). Adapted from Drover et al. (2012).

A follow up study indicated that the activity of ChD depended on the IL concentration, and at a low concentration, [C_4mim]Br acted as an activator for ChD. Contrarily, with an increase of IL amount, no change in enzyme activity was observed (Aspras et al., 2017).

PRODUCTION OF FURAN DERIVATIVES

Preparation of 3-Acetamido-5-Acetylfuran (3A5AF)

One of the most studied areas of chitin transformation using ILs is its direct conversion into the furan derivative 3A5AF through hydrolysis followed by dehydration (**Scheme 4**, **Table 2**). Generally, this type of reactions is conducted under catalyzed high-temperature conditions or using microwave energy, utilizing dimethylformamide (DMF) or dimethylacetamide (DMAc) as solvents (Chen et al., 1998, 2014; Drover et al., 2012; Omari et al., 2012).

The initial study by Kerton et al. screened six ILs for the conversion of GlcNAc monomer into 5A5AF, prior to testing chitin polymer (**Table 2**, Entries 1–4) (Drover et al., 2012). The ILs featured imidazolium cations and basic anions, namely [C_2mim]Br, [C_2mim][OAc], [C_4mim]Br, [C_4mim]Cl, [C_4mim][OAc], and 1,2-dimethyl-3-butylimidazolium chloride ([C_1C_4mim]Cl). Out of the six tested ILs, those containing Cl^- as the anion showed the best performance for the transformation of the amino-sugar into the *N*-substituted furan; yields of the product were found to be 14.1 and 25.5% in [C_4mim]Cl (at 120°C and 180°C, respectively), and 25.3% in [C_1C_4mim]Cl (at 180°C). Various additives were screened to increase the 3A5AF yield, and it was found that the addition of boric acid ($B(OH)_3$) significantly improved the yield up to 60%.

As continuation of these studies, Kerton et al. used chitin in place of GlcNAc for the formation of 3A5AF using ILs (**Table 2**, Entries 5, 6) (Chen et al., 2015b). The portfolio of ILs was much broader than that in the previous study and consisted of the commercially available imidazolium ILs such as [Amim]Br, [Amim]Cl, [C_4mim][OAc], 1-butyl-3-methylimidazolium tetrafluroborate ([C_4mim][BF_4]), [C_4mim]Cl, 1-butyl-3-methylimidazolium triflate ([C_4mim][CF_3SO_3]), [C_4mim][NTf_2], 1-butyl-3-methylimidazolium hexafluorophosphate ([C_4mim][PF_6]), [C_2mim]Cl, and 1-(2-hydroxyethyl)-3-methylimidazolium chloride ([HOC_2mim]Cl) and the in-house synthesized ILs 1-butyl-3-methylimidazolium hydrogen sulfate ([C_4mim][HSO_4]) and its sulfonated derivative ([$HOSO_2C_4$mim][HSO_4]). The ILs were used with and without additives (e.g., aluminum chloride ($AlCl_3$), calcium chloride ($CaCl_2$), chromium chloride ($CrCl_3$), cobalt chloride ($CoCl_2$), nickel chloride ($NiCl_2$), HCl, and $B(OH)_3$).

For the screening, all reactions were conducted in a multi-cell reactor at 120–180°C using commercially available, low molecular weight (MW) chitin. It was found that conversion into 3A5AF product was successful in ILs featuring Cl^- anion, in which chitin had either partial or complete solubility. These ILs included [Amim]Cl, [C_2mim]Cl, and [C_4mim]Cl. Interestingly, no additive was required for the conversion to occur, although incorporation of an additive into the reaction significantly improved the yield. Here, 400 mol% in respect to chitin using $B(OH)_3$ and 100 mol% in respect to chitin using HCl were the best performing "combinational" additives. The optimum

TABLE 2 | Preparation of chemicals from chitin with the use of ILs[a].

S.no	Substrate	Conditions	Most successful ILs	IL role	Product (Yield, %)	References
1	Commercial GlcNAc monomer	Multi-cell reactor, water/IL, 120°C, 1 h	$[C_4mim]Cl$	Co-solvent	3A5AF (14.1)	Drover et al., 2012
2	Commercial GlcNAc monomer	Multi-cell reactor, water/IL, 180°C, 1 h	$[C_4mim]Cl$	Co-solvent	3A5AF (25.5)	Drover et al., 2012
3	Commercial GlcNAc monomer	Multi-cell reactor, water/IL, 180°C, 1 h	$[C_1C_4mim]Cl$	Co-solvent	3A5AF (25.3)	Drover et al., 2012
4	Commercial GlcNAc monomer	Multi-cell reactor, water/IL, 180°C, $B(OH)_3$, 1 h	$[C_1C_4mim]Cl$	Co-solvent	3A5AF (60.0)	Drover et al., 2012
5	Commercial chitin	Multi-cell reactor, water/IL, 8 wt% chitin load, 180°C, $CrCl_3$, 1 h	[Amim]Cl	Co-solvent	3A5AF (0.5)	Chen et al., 2015b
6	Commercial chitin	Multi-cell reactor, water/IL, 8 wt% chitin load, 180°C, $B(OH)_3$/HCl, 1 h	$[C_2mim]Cl$	Co-solvent	3A5AF (4.5)	Chen et al., 2015b
7	Commercial chitin	Multi-cell reactor, water/IL, 8 wt% chitin load, 180°C, $B(OH)_3$/HCl, 1 h	$[C_4mim]Cl$	Co-solvent	3A5AF (6.2)	Chen et al., 2015b
8	Commercial chitin	Multi-cell reactor, water/IL, 8 wt% chitin load, 180°C, $B(OH)_3$/HCl, 10 min	[Amim]Br for dissolution-regeneration of the polymer then $[C_4mim]Cl$	Co-solvent	3A5AF (28.5)	Chen et al., 2015a
9	Commercial chitin and chitosan	50 mL stainless steel vessel with a Teflon lining, sealed by a screw cap, 4 wt% IL in water, 100 mg chitosan, 180°C, 5 h	$[Hmim][HSO_4]$	Co-solvent/ catalyst	5-HMF (29.5 from chitosan); (19.3 from chitin)	Li et al., 2015
10	Commercial chitin and GlcNAc monomer	50 mL stainless steel vessel with a Teflon lining, sealed by a screw cap, IL in DMSO/water, 100 mg GlcNAc, 20 of [Hmim][HSO4]/GlcNAc molar ratio, 180°C, 6 h	$[Hmim][HSO_4]$	Catalyst	5-HMF (64.6 from GlcNAc); (25.7 from chitin)	Zang et al., 2017
11	Commercial chitin	Synthesis reactor with 3% w/w IL in water, $Fe(ClO_4)_3.xH_2O$ (catalyst), chitin, 6 h, 200°C	$[(CH_2)_4SO_3Hpy][HSO_4]$	Co-solvent	5-HMF (46)	Zang et al., 2015
12	Commercial GlcNAc·HCl	Synthesis reactor with 10 g IL, 20 g GlcNAc·HCl, $H_2O_{2(aq)}$, 80 mL DMSO, 10 days, 20°C	$[C_2mim][OAc]$	Co-solvent/catalyst	Fructosazine (40)	Hou et al., 2015
13	Commercial GlcNAc·HCl	Synthesis reactor with 15 g IL, 35 g NaGlcN-2S, hypobromous acid, 100 mL DMSO, 10 min, 80°C	$[C_4mim][OAc]$	Co-solvent/catalyst	Fructosazine (25)	Hou et al., 2015
14	Commercial chitin	Synthesis reactor with 20 g IL, 200 g chitin, KBrO, 200 mL DMSO, 5 min, 200°C	$[C_2mim][OH]$	Co-solvent/catalyst	Fructosazine (15)	Hou et al., 2015
15	Commercial chitin	Synthesis reactor with 50 g IL, 45 g chitin, $H_2O_{2(aq)}$, 500 mL DMSO, 1 h, 180°C	$[C_6mim][OH]$	Co-solvent/catalyst	Fructosazine (12)	Hou et al., 2015
16	Commercial chitosan	Synthesis reactor with 80 g IL, 60 g chitosan, $H_2O_{2(aq)}$, 800 mL DMSO, 9 h, 100°C	$[C_4mim]_2[CO_3]$	Co-solvent/catalyst	Fructosazine (10)	Hou et al., 2015
17	Commercial chitosan	Synthesis reactor with 70 g IL, 15 g chitosan, $H_2O_{2(aq)}$, 500 mL DMSO, 6 h, 200°C	$[C_4mim][HCO_3]$	Co-solvent/catalyst	Fructosazine (28)	Hou et al., 2015
18	Commercial chitosan	Synthesis reactor with 35 g IL, 25 g chitosan, $KBrO_3$, 10 mL DMSO, 5 h, 170°C	$[C_4mim][C_6H_5COO]$	Co-solvent/catalyst	Fructosazine (54)	Hou et al., 2015
19	Commercial NaGlcN-2S	Synthesis reactor with 20 g IL, 15 g GlcNAc·HCl, $H_2O_{2(aq)}$, 500 mL DMSO, 5 h, 80°C	$[C_2mim][OAc]$	Co-solvent/catalyst	Fructosazine (59)	Hou et al., 2015
20	Commercial GlcNAc·HCl	Synthesis reactor with 10 g IL, 1 g GlcNAc·HCl, 50 mL DMSO, 48 h, 25°C	$[C_2mim][OAc]$	Co-solvent/catalyst	Deoxyfructosazine (60)	Wang et al., 2016
21	Commercial NaGlcN-2S	Synthesis reactor with 25 g IL, 50 g NaGlcN-2S, $Na_2B_4O_7$, 10 mL DMSO, 10 min, 80°C	$[C_2mim][OAc]$	Co-solvent/catalyst	Deoxyfructosazine (55)	Wang et al., 2016

(Continued)

TABLE 2 | Continued

S.no	Substrate	Conditions	Most successful ILs	IL role	Product (Yield, %)	References
22	Commercial NaGlcN-2S	Synthesis reactor with 10 g IL, 5 g NaGlcN-2S, K_2SO_4, 25 mL DMSO, 5 min, 150°C	[C_4mim][OAc]	Co-solvent/catalyst	Deoxyfructosazine (65)	Wang et al., 2016
23	Commercial chitin	Synthesis reactor with 40 g IL, 35 g chitin, HOAc, 10 mL DMSO, 6 h, 150°C	[C_4mim][OAc]	Co-solvent/catalyst	Deoxyfructosazine (15)	Wang et al., 2016
24	Commercial chitin	Synthesis reactor with 50 g IL, 45 g chitin, K_2CO_3, 150 mL DMSO, 4h, 180°C	[C_6mim][OH]	Co-solvent/catalyst	Deoxyfructosazine (10)	Wang et al., 2016
25	Commercial chitosan	Synthesis reactor with 100 g IL, 60 g chitosan, H_3PO_4, Na_2CO_3, 200 mL DMSO, 9 h, 100°C	[C_4mim]$_2$[CO_3]	Co-solvent/catalyst	Deoxyfructosazine (36)	Wang et al., 2016
26	Commercial chitosan	Synthesis reactor with 70 g IL, 15 g chitosan, KH_2PO_4, 10 mL DMSO, 1 h, 200°C	[C_4mim][HCO_3]	Co-solvent/catalyst	Deoxyfructosazine (30)	Wang et al., 2016
27	Commercial chitosan	Synthesis reactor with 35 g IL, 25 g chitosan, phenylboronic acid, 10 mL DMSO, 5 h, 170°C	[C_4mim][C_6H_5COO]	Co-solvent/catalyst	Deoxyfructosazine (45)	Wang et al., 2016

[a] *3A5AF, 3-acetamido-5-acetylfuran; 5-HMF, 5-hydroxymethylfurfural; NaGlcN-2S, Sodium glucosamine Sulfate; $Na_2B_4O_7$, Sodium tetraborate.*

conditions were found to be as follows: 8 wt% chitin load in [C_4mim]Cl IL, $B(OH)_3$/HCl and stirring with heating at 180°C for 1 h. These conditions resulted in a 3A5AF with 6.2% yield.

Chen et al. also reported the formation of 3A5AF from chitin, using [C_4mim]Cl and utilizing the conditions described above, however in this case, chitin was pre-treated by various means prior to the transformation (**Table 2**, Entry 8) (Chen et al., 2015a). The pre-treatment included ball-mill grinding, steam, alkaline and acidic treatments, and decreasing of crystallinity through the dissolution-regeneration of the polymer from [Amim]Br IL. After pre-treatment, the procedures for chitin dehydration in IL solvent were carried out as reported by Kerton et al. (Chen et al., 2015b): 8 wt% chitin in [C_4mim]Cl, $B(OH)_3$/HCl additive at 180°C. After the reaction, 3A5AF product was extracted with ethyl acetate. The yield was improved significantly in IL solvent after ball-milling treatment, with the best yield of 28.5% being achieved within 10 min (vs. 7.5% for untreated chitin).

The first step is based on the disruption of the inter- and intramolecular hydrogen bonding of sugars and the formation of new hydrogen bonds between the carbohydrate hydroxyl protons and the anions of the IL, which facilitates the hydrolysis of chitin to its monomer. In fact, kinetic studies suggest that hydrolysis of the crystalline region of chitin is likely to be a rate-determining step (Chen et al., 2014). Then, the mechanism for formation of 3A5AF from N-acetylglucosamine is analogous to that described elsewhere for other sugars (e.g., fructose and glucose) dehydration processes. Here, complexation of imidazolium (or additive employed) with the hydroxyl oxygen of the sugar facilitates its conversion into the open chain aldose form. The nucleophilic attack by a hydroxyl group to a carbonyl yields the 5-membered heterocyclic ring, which, in turns undergoes subsequent dehydration and keto-enol tautomerization to yield the 3A5AF product.

The produced 3A5AF can be further employed as a building block in a multistep synthesis. New applications and markets for this chemical include its incorporation into active pharmaceutical ingredients (APIs), such as proximicins, aminofuran antibiotics, and anticancer compounds isolated from marine strains MG-37 of the actinomycete *Verrucosispora* (Fiedler et al., 2008). Sadiq et al. developed a safe, sustainable synthesis of proximicin A (Sadiq et al., 2018) from 3A5AF prepared from mechanochemically treated chitin by Chen et al. (2015a) (**Table 2**, Entry 7), i.e., by using [C_4mim]Cl as a solvent, and $B(OH)_3$/HCl additives. The reaction sequence from 3A5AF proceeded through 6 steps, namely the oxidation of 3A5AF into the corresponding ester, selective hydrolysis of respective amide, installation of the methyl carbamate moiety, selective ester hydrolysis, and finally selective formation of amide using ammonium hydroxide coupling with 3-aminofuran. Although an IL was used to generate 3A5AF from chitin, their use in the following steps is still to be explored. Still, the proposed synthesis eliminated the use of toxic chemicals previously employed for this transformation. In addition, the study emphasized the role chitin would be playing in the sustainable production of nitrogen-containing building blocks, which are not directly obtainable from lignocellulosic biomass.

Preparation of 5-Hydroxymethylfurfural (5-HMF)

The direct conversion of chitin into 5-HMF is a traditional reaction usually conducted using metal salts as catalysts ($FeCl_2$, $ZnCl_2$, $AlCl_3$, and $B(OH)_3$) under high temperature, hydrothermal conditions (**Scheme 5**) (Wang et al., 2013; Yu et al., 2016). In 2015, ILs with different cations and anions of varying acidity, hydrogen-bonding capacity, and steric hindrance were tested as catalysts for 5-HMF formation from chitosan as the starting material (**Table 2**, Entry 9). The ILs included [C_4mim][HSO_4], [C_4mim][BF_4], [C_4mim]Cl, [C_4mim]Br, 1,3-bis(4-sulfobutyl)-1H-imidazol-3-ium hydrogen

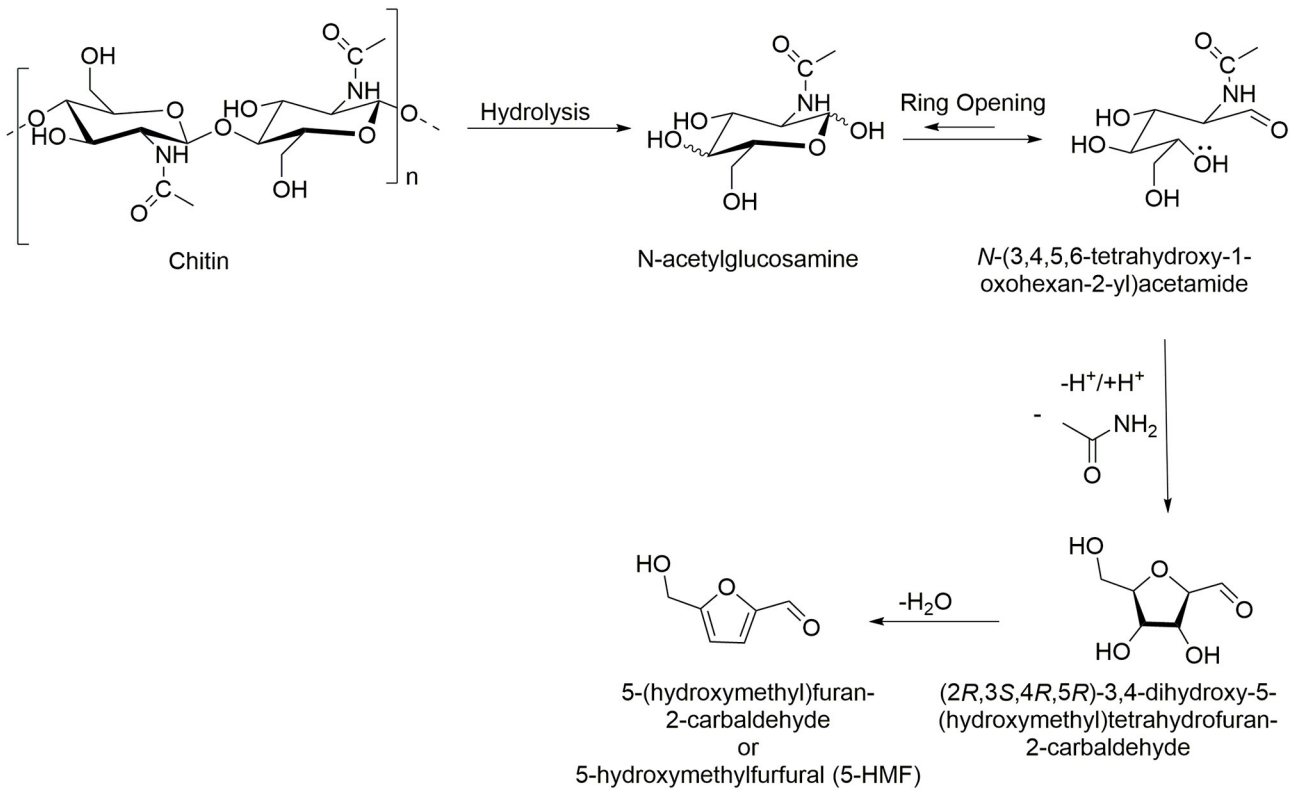

SCHEME 5 | Chitin conversion into 5-hydroxymethylfurfural (5-HMF).

sulfate [$(HOSO_2C_4)_2$im][HSO_4], 3-methyl-1-(4-sulfobutyl)-1H-imidazol-3-ium hydrogen sulfate [$HOSO_2C_4$mim][HSO_4], 1-methylimidazolium hydrogen sulfate ([Hmim][HSO_4]), 1-methylimidazolium chloride ([Hmim]Cl), and 1-carboxymethyl-3-methylimidazolium hydrogen sulfate ([$HOOCCH_2$mim][HSO_4]) (Li et al., 2015).

The nine ILs were initially evaluated using chitosan as a substrate, five of which performed satisfactorily, although the reaction required a high temperature (180°C). The best performances (based on yields) were [Hmim][HSO_4] (21.7% yield at 2 wt% IL loading and 29.5% yield at 4 wt% IL loading) > [C_4mim][HSO_4] (18.9% yield) > [$(HOSO_2C_4)_2$im][HSO_4] (12.8% yield) > [$HOOCCH_2$mim][HSO_4]) (11.5 % yield) > [C_4mim][BF_4] (10.8% yield). After using chitosan for the reaction optimization, the best performing IL, [Hmim][HSO_4], was tested on chitin under the optimized conditions (0.5 wt% chitin suspension in water, 5 h treatment time, 4 wt% [Hmim][HSO_4] IL, at 180°C) resulting in 19% yield of HMF. As a comparison, the reaction in the absence of any catalyst did not form any product, and the yield of the reaction that used $SnCl_4 \cdot 5H_2O$ or $ZnCl_2$ resulted in only 10% yield of HMF.

A series of Brønsted acidic ILs with different structures were also tested for the conversion of chitin and its derivative into 5-HMF (**Table 2**, Entry 10). The ILs included [Hmim][HSO_4], 1-methylimidazolium dihydrogen phosphate ([Hmim][H_2PO_4]), 1-methylimidazolium nitrate ([Hmim][NO_3]), [Hmim]Cl, 4,5-dimethylthiazolium hydrogen sulfate ([TM][HSO_4]), 2-isobutylthiazolium hydrogen sulfate ([TB][HSO_4]), and 4,5-dimethyl-3-(4-sulfonic acid butyl)thiazolium hydrogen sulfate ([$TBSO_3H$][HSO_4]). Initially the reaction was conducted using GlcNAc as a substrate, and then was extended to the use of chitin and chitosan under the best determined conditions.

With exception of [Hmim][HSO_4], the other ILs resulted in a moderate conversion of GlcNAc into 5-HMF (traces to 28.7% yield). The IL [Hmim][HSO_4] exhibited the best catalyst performance (45.2% yield) which, when optimized, reached 64.6% yield without the need of catalysts other than the IL. The reaction was conducted using GlcNAc/water/dimethylsulfoxide (DMSO) ratio of 1/120/80 by weight, under 180°C for 6 h. When chitin was employed as a substrate, the usage of [Hmim][HSO_4] IL resulted in 25.7% yield of HMF under these conditions, providing access to valuable chemicals from chitin for biorefinery purposes.

A patent application (Zang et al., 2015) has also used chitinous raw materials for their catalytic conversion into 5-HMF, employing ILs as co-solvents and catalysts. Both chitin and chitosan were studied: several chotosans with DA in the range of 20–50% and several chitins with DA in the range of 85–95%. Some of the ILs used in this study were the same as previously noted, namely [C_4mim]Cl, [C_4mim][OAc], [Amim][OAc], [Hmim][HSO_4], but also included novel ILs (not previously evaluated for this

application): 3-methyl-1-(4-sulfobutyl)-1H-imidazol-3-ium hydrogen sulfate $[HO_3S(CH_2)_4mim][HSO_4]$, lysine 4-methylbenzenesulfonate $[Lys][pCH_3C_6H_4SO_3]$, 1-carboxy-3-methylimidazolium chloride [HOOCmim]Cl, glycine chloride [Gly]Cl, 1-(4-sulfobutyl)pyridinium hydrogen sulfate $[HO_3S(CH_2)_4Py][HSO_4]$. The reaction was conducted in water as a solvent, with 0.25–0.33 wt% load of chitin or chitosan to form a suspension and 1–20 wt% IL as a co-solvent and acidic catalyst. This reaction was conducted with or without additional catalysts (trace amounts of $La(CF_3SO_3)_3$, $CrCl_3{\cdot}6H_2O$, $Gd(CF_3SO_3)_3{\cdot}H_2O$, $Yb(CF_3SO_3)_3{\cdot}H_2O$, etc.), under 120–200°C heating. Unfortunately, due to the patent being relatively broad, it is not clear which ILs were the best performing. The best reported yield of 5-HMF (46%) was achieved using $[(CH_2)_4SO_3Hpy][HSO_4]$ as co-solvent and $Fe(ClO_4)_3{\cdot}H_2O$ as catalyst.

Similarly for 5-HMF, the first step of the reaction no matter whether it is done from chitin or chitosan is the formation of new hydrogen bonds though the coordination of basic anions with chitin's or chitosan's hydroxyls, which breaks the original hydrogen bonding (This step is similar to all related chitin biorefinery reactions.). Then, the mechanism is very similar to that for formation of 3A5AF from *N*-acetylglucosamine, followed by the released of H^+ and/or electron-rich aromatic, which facilitates the conversion of the carbohydrate into its open chain aldose form; this is the rate-limiting step. This step is followed by the isomerization into enol-intermediate, followed by ring closure with simultaneous deamination. Subsequent keto-enol tautomerization into 4-hydroxy-5-hydroxymethyl-4,5-dihydrofuran-2-carbaldehyde followed by dehydration yields the desired 5-HMF product (Li et al., 2015).

PREPARATION OF COMPLEX COMPOUNDS

The preparation of fructosazine [IUPAC name: 2,5-bis(1,2,3,4-tetrahydroxybutyl)pyrazine]) and deoxyfructosazine (**Scheme 1**) from chitin was also reported (Hou et al., 2015; Wang et al., 2016). These compounds are used as flavoring agents, fragrance compounds, and in medicine for the prevention and treatment of osteoarthritis and as popular anti-inflammatory agents (Leffingwell, 1976; Giordani et al., 2006; Yang and Yan, 2018).

To produce fructosazine (**Table 2**, Entries 12–19), chitin biomass was oxidized with strong oxidizer in DMSO, with an IL catalyst which also played a co-solvent role; traditionally this reaction requires inorganic salts as catalysts (Hou et al., 2015). The ILs evaluated were the imidazolium ILs $[C_2mim][OAc]$, $[C_4mim][OAc]$, 1-ethyl-3-methylimidazolium hydroxide ($[C_2mim][OH]$), 1-butyl-3-methylimidazolium hydroxide ($[C_4mim][OH]$), 1-butyl-3-methylimidazolium carbonate ($[C_4mim]_2[CO_3]$), 1-butyl-3-methylimidazolium bicarbonate ($[C_4mim][HCO_3]$), and 1-butyl-3-methylimidazolium benzoate ($[C_4mim][C_6H_5COO]$). The chitin raw material was loaded into DMSO/IL mixture (DMSO to chitin ratio of 10:1 w/w, IL to chitin ratio of 1:2–100 w/w), and then oxidant added (oxidant to chitin ratio of 1–50:1 w/w). Aqueous hydrogen peroxide, sodium hypochlorite, sodium hypobromite, or potassium hypobromite (30–95% solutions in water) were used as oxidants. The reactants were mixed and then allowed to react at temperatures up to 200°C, for up to 10 days. The product was easily recrystallized from the reaction mixture using acetonitrile, ethanol, propanol, or acetone as recrystallization solvents. Unfortunately, details or more narrow ratios between reagents were not provided as the patent is broad.

Deoxyfructosazine was prepared using very similar conditions as those reported above (**Table 2**, Entries 20–27): DMSO was used as a solvent, ILs as co-solvent/catalyst, and a dehydration agent ($B(OH)_3$, sodium tetraborate, phenylboronic acid, acetic acid, AcOH, carbonic acid or phosphoric acid) (Wang et al., 2016). While the reaction was also attempted in DMF and DMAc, the use of DMSO resulted in the highest product yield. The reaction was carried out in a pressure vessel with a Teflon screw cap. Chitin, DMSO, IL and an additive were placed in a pressure vessel equipped with a magnetic stirring bar, and a reaction was heated in an oil bath (25–200°C) at different time intervals (from 5 min to 2 days). While the ratios of reagents depended on the IL identity and the dehydration agent used in the reaction, in general the ratio of IL:chitin was ca. 1–1.5:1 w/w, 2–50:1 mol/mol dehydrating additive:chitin, IL/DMSO 0.25:1–50 v/v.

Using low MW chitin (MW 250,000 Da), $[C_4mim][OAc]$ IL was employed as catalyst, AcOH as dehydration agent, and the ratio of reagents was 1.2:1 w/w IL:chitin, 2:1 mol/mol AcOH:chitin, 4:1 v/v IL:DMSO, at 150°C for 6 h. In another example, $[C_6mim][OH]$ IL and K_2CO_3 as a dehydration agent were utilized for conversion of high MW chitin (MW 1,000,000 Da). The ratio of reagents was 1.1:1 w/w IL:chitin, 15:1 mol/mol K_2CO_3:chitin, 1:3 w/w IL:DMSO, at 180°C for 4 h. The yield of deoxyfructosazine was determined to be 50–60%. Interestingly, the use of ILs with acidic sulfonic group that are usually used as dehydration agents in similar reactions as catalysts required increase in the reaction temperature and resulted in bond cleavage with formation of formic and levulinic acids, and not deoxyfructosazine (Wang et al., 2016). Recently, selective transformation of chitin and chitosan into levulinic acid has been realized by the catalysis using acidic 1-methyl-3-(3-sulfopropyl)imidazolium hydrogen sulfate ($[HSO_3C_3mim][HSO_4]$) up to a yield of 67.0% (Hou et al., 2019). The authors suggested the IL was not basic enough to completely disrupt H-bonding of the *N*-acetyl groups which shielded the accessibility of glycosidic linkages to the acidic catalyst, thus deacetylation-depolymerization mechanisms occurred only at the outer surface of the polymer.

THE ROLE OF IONIC LIQUIDS

Although enzymatic reactions (hydrolysis and deacetylation) could proceed without use of IL (IL is considered to be non-essential activator), ILs disrupt the H-bonding and thus facilitate the access of the enzyme to the substrate. This results in formation of different products and different product distribution profile (ratio of monomer to dimer to oligomers)

than what is observed without the use of ILs (Husson et al., 2017; Berton et al., 2018). The IL systems also appear to be superior in terms of product yields and reaction speed.

In those cases reporting the formation of small molecule heterocycles (5-HMF, 3A5AF), no product could be formed from chitin using VOCs instead of ILs, even at harsh reaction conditions. Besides, in many cases, the product was not stable at high temperatures or for elongated reaction times, while the use of ILs allows mild reaction conditions (Chen et al., 2015b). For example, no 3A5AF was formed by using organic solvents even at a high temperature (Chen et al., 2015b). One of the reasons for this phenomenon is that there is a strong correlation between the hydrogen-bonding network strength and the reactivity of chitin, and ILs allow an easy disruption of this H-bond network (Chen et al., 2015a).

The pretreatment of chitin may be an essential step in all reactions for chitin deconstruction because it allows faster chitin depolymerization through breaking down the polymer's robust structure and H-bonding network. Considering this, ILs that possess anions that are more basic should be investigated more closely. Rational design directed to functionalization of ILs that could assist in this step may be necessary, in order to improve the reaction yield from chitin, which currently remain low.

RECOVERING OF IONIC LIQUIDS

Contrarily to methods for IL dewatering (Abu-Eishah, 2011; Kuzmina and Hallett, 2016; Zhou et al., 2018), the literature addressing the recyclability of the ILs after deconstruction of chitin polymers into chemicals is scarce. The process of IL recycle would not be as simple as a dewatering of the ILs after formation of chitin *materials*, but instead we envision a two-step process, with the recovery of products and unreacted starting materials first, and then the IL purification and recovery. We will review the methods that were reported by authors of these technologies where available.

The simplest IL recovery strategy would potentially be after enzymatic hydrolysis reaction, where IL is used for the polymer's pretreatment and then is washed out with water prior to the reaction of the sugar with enzymes. Such "pre-treatment" strategy facilitates purification of mono-/oligosaccharides from the reaction media. At the same time, washing chitin out with water not only leads to a production of hydrolysates, which are nearly free of residual ILs, but also results in an IL that is simply "wet." A simple dewatering step could be done to recover of the IL for the next pretreatment cycle. The dewatering strategies for the IL are provided elsewhere (Shamshina, 2019).

In the reactions where small molecule heterocycles (3A5AF or 5-HMF) are formed, the product is normally extracted with a suitable volatile organic solvent (VOC) such as ethyl acetate, diethyl ether, or dichloromethane, after which the IL is recovered together with the additive or catalyst used (Chen et al., 2015a). In this recovery process, the water is removed through evaporation under high-vacuum, usually using a rotary evaporator. The IL/additive that was used as catalyst remained unseparated and are used "as is," in the next catalytic cycle. For instance, in the formation of 5HMF from glucosamine (Li et al., 2019), the recyclability of [Hmim][HSO_4] catalyst was evaluated over five cycles on the "model" reaction, in a DMSO/water mixture. In every cycle, IL/catalyst was recovered, re-used, and the product yield was evaluated. The product yield slightly decreased (*ca.* ∼10% of initial yield) with each re-use cycle, which was attributed to the catalyst mass loss during the recycle procedure. It was found that unreacted starting material and 5-HMF product can be easily removed from the reaction mixture by extraction with ethyl acetate. After removal of the product, the water was evaporated under vacuum and the remaining [Hmim][HSO_4]/DMSO used directly in the next catalytic cycle, under the same reaction conditions.

Although not reported in the literature reviewed for chitin conversion, there are two methods that might be of interest and that would not depend of the components of the mixture to be separated. The first method is the recovery of the IL through the formation of the distillable carbene, patented by BASF (Earle and Seddon, 2001). The method involves the treatment of imidazolium IL with a strong base (such as potassium *tert*-butoxide), which deprotonates the imidazolium cation at C-2 position, forming 1,3-dimethyl-imidazol-2-ylidene carbene. This carbene is distillable and could be distilled out (Earle and Seddon, 2001). Afterwards, the formed carbene reacts with the acid of the desired anion, reforming the imidazolium IL. The method can be used after the desired products have been extracted from the IL, and the IL/residues mixture has been dewatered fully.

Membrane separation might constitute another method for the IL recovery, including the commercially available pervaporation systems (PVs). These systems have been shown to be suitable for the recycling of [C_2mim][Ac] IL after lignocellulosic biomass pretreatment. The inventors of the technology claim separation factors of 1,500 and recycle efficiency of >99.9 wt% IL (Campos et al., 2014). This said, the efficiencies of removing contaminants by membrane separation processes would be dependent on the size and molecular weight of the mixture constituents. Either way, we are convinced that the choice and application of the separation method would depend on the product yield, other contaminants (e.g., starting materials) level, cost of the process, and chemical nature of components.

OUTLOOK

Every so often in the history of society, a paradigm shift, an important change that happens when the traditional way of thinking is replaced by a new and/or different way, takes place. The reason behind such change is that "crisis simultaneously loosens the stereotypes and provides the incremental data necessary for a fundamental paradigm shift" (Kuhn, 1962). Nowadays, it is all about a shift from oil-based economy to biopolymers-based one, caused by depletion of oil resources, and environmental awareness.

Due to numerous worldwide-enforced legislative measures around environmental protection, and public environmental awareness, biopolymers have finally started gaining recognition in multiple industrial sectors. Such replacement of oil-based

chemicals with biopolymer-derived ones, should, however, be done in a clever fashion and careful decisions must be made whether the biopolymers should be used in their unmodified state for high-value products, or in a bio-/chemical transformation for low-value commodity chemicals. For chitin, IL-extracted chitin would be considered a specialty polymer, due to its unprecedented high molecular weight, while pulped chitin would be considered a bulk commodity. In this case, prices for the polymer would differ greatly reflecting not only more expensive process of isolation for IL-extracted chitin, but also development costs for its special molecular weight.

Since market for chemicals made from renewable biopolymers such as cellulose or chitin is driven by a low tech, but high-volume commodity, chitin obtained by pulping (Shamshina et al., 2016) would work as a suitable starting material for chitin conversion into chemicals, and provide access to the chemicals that are cannot be obtained otherwise. It is cheap and commercially available, and thus would be ideal for the purpose (Shamshina et al., 2019). A large number of existing National programs is indeed built around such bio-refineries where biomass feedstock, after partial or complete separation into main fractions, is followed by the deconstruction of the components into valuable chemicals. This includes the program by the National Renewable Energy Laboratory (NREL, 2019), and the program by Joint BioEnergy Institute (JBEI, 2019)[1] which focus on the production of bio-based chemicals. On the other side, we believe in taking advantage of polymers accessible directly from Nature as primary polymer source for the preparation of materials, and not chopping them up into the chemicals. Here, high-cost, high-value medical devices, and implantables of IL-extracted chitin would more than cover the cost of its isolation and other chitin-based products will become more financially attractive.

Review of scientific literature suggests that biopolymers in general, and chitin in particular, are very appealing for overall biorefinery, although further research is needed for proper biopolymers' valorization. Yet, the principle of circular economy encourages its exploitation as an alternative resource for a sustainable future.

AUTHOR CONTRIBUTIONS

JS and PB together created the idea, the first draft, finalized, and templated the article.

REFERENCES

Abu-Eishah, S. I. (2011). "Ionic liquids recycling for reuse," in *Ionic Liquids - Classes and Properties*, ed S. Handy (Rijeka: InTechOpen), 239–274.

Aspras, I., Jaworska, M. M., and Gorak, A. (2017). Kinetics of chitin deacetylase activation by the ionic liquid [Bmim][Br]. *J. Biotechnol.* 251, 94–98. doi: 10.1016/j.jbiotec.2017.04.015

Aspras, I., Kaminska, M., Karzynski, K., Kawka, M., and Jaworska, M. (2016). The influence of selected ionic liquids on activity of chitin deacetylase. *Chem. Proc. Eng.* 37, 77–82. doi: 10.1515/cpe-2016-0008

Barber, P. S., Griggs, C. S., Bonner, J. R., and Rogers, R. D. (2013). Electrospinning of chitin nanofibers directly from an ionic liquid extract of shrimp shells. *Green Chem.* 15, 601–607. doi: 10.1039/c2gc36582k

Berton, P., Shamshina, J. L., Ostadjoo, S., King, C. A., and Rogers, R. D. (2018). Enzymatic hydrolysis of ionic liquid-extracted chitin. *Carbohydr. Polym.* 199, 228–235. doi: 10.1016/j.carbpol.2018.07.014

Biswas, A., Shogren, R. L., Stevenson, D. G., Willett, J. L., and Bhowmik, P. K. (2006). Ionic liquids as solvents for biopolymers: acylation of starch and zein protein. *Carbohydr. Polym.* 66, 546–550. doi: 10.1016/j.carbpol.2006.04.005

Campos, D., Edward, A., Sudipto, F., Majumdar, S., and Nemser, S. M. (2014). *Membrane Separation of Ionic Liquid Solutions*. WO2015066245A1. Newport, DE: CMS Technologies Holdings, Inc.

Chen, J., Wang, M., and Ho, C.-T. (1998). Volatile compounds generated from thermal degradation of N-acetylglucosamine. *J. Agric. Food Chem.* 46, 3207–3209. doi: 10.1021/jf980129g

Chen, X., Chew, S. L., Kerton, F. M., and Yan, N. (2014). Direct conversion of chitin into a N-containing furan derivative. *Green Chem.* 16, 2204–2212. doi: 10.1039/C3GC42436G

Chen, X., Gao, Y., Wang, L., Chen, H., and Yan, N. (2015a). Effect of treatment methods on chitin structure and its transformation into Nitrogen-containing chemicals. *ChemPlusChem* 80, 1565–1572. doi: 10.1002/cplu.201500326

Chen, X., Liu, Y., Kerton, F. M., and Yan, N. (2015b). Conversion of chitin and N-acetyl-D-glucosamine into a N-containing furan derivative in ionic liquids. *RSC Adv.* 5, 20073–20080. doi: 10.1039/C5RA00382B

de Jong, E., and Gosselink, R. J. A. (2014). "Lignocellulose-based chemical products," in *Bioenergy Research: Advances and Applications*, eds V. K. Gupta, C. P. Kubicek, J. Saddler, F. Xu, and M. G. Tuohy (Amsterdam: Elsevier), 277–313. doi: 10.1016/B978-0-444-59561-4.00017-6

de Jong, E., and Jungmeier, G. (2015). "Biorefinery concepts in comparison to petrochemical refineries," in *Industrial Biorefineries and White Biotechnology*, eds A. Pandey, R. Höfer, M. Taherzadeh, K. M. Nampoothiri, and C. Larroche (Amsterdam: Elsevier), 3–33. doi: 10.1016/B978-0-444-63453-5.00001-X

Drover, M. W., Omari, K. W., Murphy, J. N., and Kerton, F. M. (2012). Formation of a renewable amide via direct conversion of N-acetyl-D-glucosamine. *RSC Adv.* 2, 4642–4644. doi: 10.1039/c2ra20578e

Earle, M. J., and Seddon, K. R. (2001). *Preparation of Imidazole Carbene and the Use Thereof for the Synthesis of Ionic Liquids*. WO2001077081A1. Belfast: The Queen's University of Belfast.

Einbu, A., and Vårum, K. M. (2008). Characterization of chitin and its hydrolysis to GlcNAc and GlcN. *Biomacromolecules* 97, 1870–1875, doi: 10.1021/bm8001123

Elieh-Ali-Komi, D., and Hamblin, M. R. (2016). Chitin and chitosan: production and application of versatile biomedical nanomaterials. *Int. J. Adv. Res.* 4, 411–427.

Fiedler, H.-P., Bruntner, C., Riedlinger, J., Bull, A. T., Knutsen, G., Goodfellow, M., et al. (2008). Proximicin A, B and C, novel aminofuran antibiotic and anticancer compounds isolated from marine strains of the actinomycete *Verrucosispora*. *J. Antibiot.* 61, 158–163. doi: 10.1038/ja.2008.125

Fort, D. A., Remsing, R. C., Swatloski, R. P., Moyna, P., Moyna, G., and Rogers, R. D. (2007). Can ionic liquids dissolve wood? Processing and analysis of lignocellulosic materials with 1-n-butyl-3-methylimidazolium chloride. *Green Chem.* 9, 63–69. doi: 10.1039/B607614A

Foster, A. B., and Webber, J. M. (1961). "Chitin," in *Advances in Carbohydrate Chemistry: Volume 70*, eds L. Melville, R. Wolfrom, and S. Tipson (Oxford: Academic Press), 371–393. doi: 10.1016/S0096-5332(08)60192-7

Future Market Insights (2019). *Chitin Market: Agrochemical End Use Industry Segment Inclined Towards High Growth – Moderate Value During the Forecast Period: Global Industry Analysis (2012–2016) and Opportunity Assessment (2017–2027)*. Available online at: https://www.futuremarketinsights.com/reports/chitin-market (accessed July 14, 2019).

Giordani, A., Letari, O., Stefano, P., Roberto, A., Walter, P., Gianfranco, C., et al. (2006). *2,5-bis (Tetrahydroxybutyl) Pyrazines for the Treatment of Osteoarthritis and Rheumatoid Arthritis*. EP1704862A1. Milan: Rottapharm SpA; European Patent Application.

Hayes, R., Warr, G. G., and Atkin, R. (2015). Structure and nanostructure in ionic liquids. *Chem. Rev.* 115, 6357–6426. doi: 10.1021/cr500411q

Heinze, T., Schwikal, K., and Barthel, S. (2005). Ionic liquids as reaction medium in cellulose functionalization. *Macromol. Biosci.* 5, 520–525. doi: 10.1002/mabi.200500039

Hou, W., Zhao, Q., and Liu, L. (2019). Selective conversion of chitin to levulinic acid catalyzed by ionic liquids: distinctive effect of N-acetyl groups. *Green Chem.* 22, 62–70. doi: 10.1039/C9GC02669J

Hou, X., Jia, L., Wang, Y., Qiao, Y., and Qin, Z. (2015). *Method for Preparing Fructosazine Through Chitin-Based Biomass*. *CN*105348205A.

Husson, E., Laclef, S., Lesur, D., Jamali, A., Gottis, S., Sarazin, C., et al. (2017). The effect of room temperature ionic liquids on the selective biocatalytic hydrolysis of chitin via sequential or simultaneous strategies. *Green Chem.* 19, 4122–4131. doi: 10.1039/C7GC01471F

Ibitoye, E. B., Lokman, I. H., Hezmee, M. N. M., Goh, Y. M., Zuki, A. B. Z., and Jimoh, A. A. (2018). Extraction and physicochemical characterization of chitin and chitosan isolated from house cricket. *Biomed. Mater.* 13:025009. doi: 10.1088/1748-605X/aa9dde

Jayakumar, R., Prabaharan, M., Sudheesh Kumar, P. T., Nair, S. V., and Tamura, H. (2011). Biomaterials based on chitin and chitosan in wound dressing applications. *Biotechnol. Adv.* 29, 322–337. doi: 10.1016/j.biotechadv.2011.01.005

Kilpeläinen, I., Xie, H., King, A., Granstrom, M., Heikkinen, S., and Argyropoulos, D. S. (2007). Dissolution of wood in ionic liquids. *J. Agric. Food Chem.* 55, 9142–9148. doi: 10.1021/jf071692e

King, C., Shamshina, J. L., Gurau, G., Berton, P., Khan, N. F. A. F., and Rogers, R. D. (2017). A platform for more sustainable chitin films from an ionic liquid process. *Green Chem.* 19, 117–126. doi: 10.1039/C6GC02201D

King, C. A., Shamshina, J. L., Zavgorodnya, O., Cutfield, T., Block, L. E., and Rogers, R. D. (2017). Porous chitin microbeads for more sustainable cosmetics. *ACS Sustain. Chem. Eng.* 5, 11660–11667. doi: 10.1021/acssuschemeng.7b03053

Kuhn, T. S. (1962). *The Structure of Scientific Revolutions*. Chicago, IL: The University of Chicago Press.

Kuzmina, O., and Hallett, J. (2016). *Application, Purification, and Recovery of Ionic Liquids*. Amsterdam: Elsevier, 59–99.

Leffingwell, J. C. (1976). Nitrogen components of leaf and their relationship to smoking quality and aroma. *Rec. Adv. Tob. Sci.* 1, 1–31.

Li, J., Huang, W.-C., Gao, L., Sun, J., Liu, Z., and Mao, X. (2019). Efficient enzymatic hydrolysis of ionic liquid pretreated chitin and its dissolution mechanism. *Carbohydr. Polym.* 211, 329–335. doi: 10.1016/j.carbpol.2019.02.027

Li, M., Zang, H., Feng, J., Yan, Q., Yu, N., Shi, X., et al. (2015). Efficient conversion of chitosan into 5-hydroxymethylfurfural via hydrothermal synthesis in ionic liquids aqueous solution. *Polym. Degrad. Stab.* 121, 331–339. doi: 10.1016/j.polymdegradstab.2015.09.009

Maier, F., Niedermaier, I., and Steinrücka, H.-P. (2017). Perspective: Chemical reactions in ionic liquids monitored through the gas (vacuum)/liquid interface. *J. Chem. Phys.* 146, 170901-1–170901-14. doi: 10.1063/1.4982355

Mitchell, G. (2018). Biopolymers and the circular economy. *Expert Opin. Environ. Biol.* 7:43. doi: 10.4172/2325-9655-C5-031

Nakagawa, Y. S., Oyama, Y., Kon, N., Nikaido, M., Tanno, K., Kogawa, J., et al. (2011). Development of innovative technologies to decrease the environmental burdens associated with using chitin as a biomass resource: mechanochemical grinding and enzymatic degradation. *Carbohydr. Polym.* 83, 1843–1849. doi: 10.1016/j.carbpol.2010.10.050

North, E. J., and Halden, R. U. (2013). Plastics and environmental health: the road ahead. *Rev. Environ. Health* 28, 1–8. doi: 10.1515/reveh-2012-0030

NREL (2019). *Integrated Biorefinery Research Facility.* Available online at: https://www.nrel.gov/bioenergy/ibrf.html (accessed June 25, 2019).

Omari, K. W., Dodot, L., and Kerton, F. M. (2012). A simple one-pot dehydration process to convert *N*-acetyl-D-glucosamine into a Nitrogen-containing compound, 3-acetamido-5-acetylfuran. *ChemSusChem* 5, 1767–1772. doi: 10.1002/cssc.201200113

Peluso, G. (1994). Chitosan-mediated stimulation of macrophage function. *Biomaterials* 15, 1215–1220. doi: 10.1016/0142-9612(94)90272-0

Phillips, D. M., Drummy, L. F., Conrady, D. G., Fox, D. M., Naik, R. R., Stone, M. O., et al. (2004). Dissolution and regeneration of bombyx mori silk fibroin using ionic liquids. *J. Am. Chem. Soc.* 126, 14350–14351. doi: 10.1021/ja046079f

Pischek, A. M., Goodie, T., and Reichert, M. (2014). "Feedstocks from biomass: an application of ionic liquid-based technology," in *Abstracts of Papers, 247th ACS National Meeting and Exposition* (Dallas, TX), ORGN-195.

Prudden, J. F., Migel, P., Hanson, P., Freidrich, L., and Balassa, L. (1970). The discovery of a potent pure chemical wound-healing accelerator. *Am. J. Surg.* 119, 560–564. doi: 10.1016/0002-9610(70)90175-3

Pu, Y., Jiang, N., and Ragauskas, A. J. (2007). Ionic liquid as a green solvent for lignin. *Wood Chem. Technol.* 27, 23–33. doi: 10.1080/02773810701282330

Qin, Y., Lu, X., Sun, N., and Rogers, R. D. (2010). Dissolution or extraction of crustacean shells using ionic liquids to obtain high molecular weight purified chitin and direct production of chitin films and fibers. *Green Chem.* 2010, 968–971. doi: 10.1039/c003583a

Rhazi, M., Desbrières, J., Tolaimate, A., Alagui, A., and Vottero, P. (2000). Investigation of different natural sources of chitin: influence of the source and deacetylation process on the physicochemical characteristics of chitosan. *Polym. Int.* 49, 337–344. doi: 10.1002/(SICI)1097-0126(200004)49:4<337::AID-PI375>3.0.CO;2-B

Rhodes, R. G., Atoyan, J. A., and Nelson, D. R. (2010). The chitobiose transporter, *chbC*, is required for chitin utilization in *Borrelia burgdorferi*. *BMC Microbiol.* 10:21. doi: 10.1186/1471-2180-10-21

Roberts, G. A. F. (1992). "Preparation of chitin and chitosan," in *Chitin Chemistry* (London: Macmillan Education), 54–84. doi: 10.1007/978-1-349-11545-7_2

Rogers, R. D. (2015). Eliminating the need for chemistry. *CandEN* 93, 42–43. doi: 10.1021/cen-09348-scitech2

Sadiq, A. D., Chen, X., Yan, N., and Sperry, J. (2018). Towards the shell biorefinery: sustainable synthesis of the anticancer alkaloid proximicin A from chitin. *ChemSusChem* 11, 532–535. doi: 10.1002/cssc.201702356

Schoukens, G. (2009). "Bioactive dressings to promote wound healing," in *Woodhead Publishing Series in Textiles, Advanced Textiles for Wound Care*, ed S. Rajendran (Woodhead Publishing), 114–152. doi: 10.1533/9781845696306.1.114

Shamshina, J. L. (2019). Chitin in ionic liquids: historical insights into the polymer's dissolution and isolation. A review. *Green Chem.* 21, 3974–3993. doi: 10.1039/C9GC01830A

Shamshina, J. L., Barber, P. S., Gurau, G., Griggs, C. S., and Rogers, R. D. (2016). Pulping of crustacean waste using ionic liquids: to extract or not to extract. *ACS Sustain. Chem. Eng.* 4, 6072–6081. doi: 10.1021/acssuschemeng.6b01434

Shamshina, J. L., Berton, P., and Rogers, R. (2019). Advances in functional chitin materials: a review. *ACS Sustain. Chem. Eng.* 7, 6444–6457. doi: 10.1021/acssuschemeng.8b06372

Shamshina, J. L., Gurau, G., Block, L. E., Hansen, L. K., Dingee, C., Walters, A., et al. (2014). Chitin - calcium alginate composite fibers for wound care dressings spun from ionic liquid solution. *J. Mater. Chem. B* 2, 3924–3936. doi: 10.1039/C4TB00329B

Shamshina, J. L., Zavgorodnya, O., and Rogers, R. D. (2018). "Advances in processing chitin as a promising biomaterial from ionic liquids," in *Advances in Biochemical Engineering/Biotechnology*, ed T. Scheper (Berlin; Heidelberg: Springer International Publishing AG), 1–22. doi: 10.1007/10_2018_63

Sharghi, H., Shiri, P., and Aberi, M. (2018). An overview on recent advances in the synthesis of sulfonated organic materials, sulfonated silica materials, and sulfonated carbon materials and their catalytic applications in chemical processes. *Beilstein J. Org. Chem.* 14, 2745–2770. doi: 10.3762/bjoc.14.253

Shen, X., Shamshina, J. L., Berton, P., Gurau, G., and Rogers, R. D. (2016). Hydrogels based on cellulose and chitin: fabrication, properties, and applications. *Green Chem.* 18, 53–75. doi: 10.1039/C5GC02396C

Sieber, V., Hofer, M., Brück, W. M., Garbe, D., Brück, T., and Lynch, C. A. (2018). "ChiBio: an integrated bio-refinery for processing chitin-rich bio-waste to specialty chemicals," in *Grand Challenges in Marine Biotechnology. Grand Challenges in Biology and Biotechnology*, eds P. Rampelotto and A. Trincone (Cham: Springer), 575–578. doi: 10.1007/978-3-319-69075-9_14

Sivashankari, P. R., and Prabaharan, M. (2017). "5-Deacetylation modification techniques of chitin and chitosan," in *Chitosan Based Biomaterials, Vol. 1*, eds J. A. Jennings and J. D. Bumgardner (Duxford: Woodhead Publishing), 117–133. doi: 10.1016/B978-0-08-100230-8.00005-4

Stark, A. (2011). Ionic liquids in the biorefinery: a critical assessment of their potential. *Energy Environ. Sci.* 4, 19–32. doi: 10.1039/C0EE00246A

Stöcker, M. (2008). Biofuels and biomass-to-liquid fuels in the biorefinery: catalytic conversion of lignocellulosic biomass using porous materials. *Angew. Chem. Int. Ed*. 47, 9200–9211. doi: 10.1002/anie.200801476

Sun, J., Murthy Konda, N. V. S. N., Parthasarathi, R., Dutta, T., Valiev, M., Xu, F., et al. (2017). One-pot integrated biofuel production using low-cost biocompatible protic ionic liquids. *Green Chem.* 19, 3152–3163. doi: 10.1039/C7GC01179B

Sun, N., Rahman, M., Qin, Y., Maxim, M. L., Rodriguez, H., and Rogers, R. D. (2009). Complete dissolution and partial delignification of wood in the ionic liquid 1-ethyl-3-methylimidazolium acetate. *Green Chem.* 11, 646–655. doi: 10.1039/b822702k

Tsuchida, H., Komoto, M., Kato, H., and Fujimaki, M. (1973). Formation of deoxy-fructosazine and its 6-isomer on the browning reaction between glucose and ammonia in weak acidic medium. *Agric. Biological Chem.* 37, 2571–2578. doi: 10.1271/bbb1961.37.2571

V2020 Alternate Feedstock Report (2019). *V2020 Alternate Feedstock Report Final.* Available online at: https://www.scribd.com/doc/161293770/V2020-Alternate-Feedstock-Report-Final (accessed July 18, 2019).

Vázquez, J. A., Rodríguez-Amado, I., Montemayor, M. I., Fraguas, J., González, M. P., and Murado, M. A. (2013). Chondroitin sulfate, hyaluronic acid and chitin/chitosan production using marine waste sources: characteristics, applications and eco-friendly processes: a review. *Mar. Drugs* 11, 747–774. doi: 10.3390/md11030747

Wan, A. C., and Tai, B. C. (2013). Chitin - a promising biomaterial for tissue engineering and stem cell technologies. *Biotechnol. Adv.* 31, 1776–1785. doi: 10.1016/j.biotechadv.2013.09.007

Wang, Y., Jia, L., Hou, X., Qiao, Y., and Qin, Z. (2016). *Method for Preparing Deoxyfructosazine Through Chitin Biomass*. CN105294579A.

Wang, Y., Pedersen, C. M., Deng, T., Qiao, Y., and Hou, X. (2013). Direct conversion of chitin biomass to 5-hydroxymethylfurfural in concentrated ZnCl2 aqueous solution. *Bioresource Tech.* 143, 384–390. doi: 10.1016/j.biortech.2013.06.024

Wu, Y., Sasaki, T., Irie, S., and Sakurai, K. (2008). A novel biomass-ionic liquid platform for the utilization of native chitin. *Polymer* 49, 2321–2327. doi: 10.1016/j.polymer.2008.03.027

Xie, H., Li, S., and Zhang, S. (2005). Ionic liquids as novel solvents for the dissolution and blending of wool keratin fibers. *Green Chem.* 7, 606–608. doi: 10.1039/b502547h

Xie, H., Zhang, S., and Li, S. (2006). Chitin and chitosan dissolved in ionic liquids as reversible sorbents of CO_2. *Green Chem.* 8, 630–633. doi: 10.1039/b517297g

Yang, H., and Yan, N. (2018). "Transformation of seafood wastes into chemicals and materials," in *Encyclopedia of Sustainability Science and Technology*, ed R. A. Meyers (New York, NY: Springer), 1–23. doi: 10.1007/978-1-4939-2493-6_1012-1

Yang, T. L. (2011). Chitin-based materials in tissue engineering: applications in soft tissue and epithelial organ. *Int. J. Mol. Sci.* 12, 1936–1963. doi: 10.3390/ijms12031936

Younes, I., and Rinaudo, M. (2015). Chitin and chitosan preparation from marine sources. Structure, properties and applications. *Mar. Drugs* 13, 1133–1174. doi: 10.3390/md13031133

Yu, S., Zang, H., Chen, S., Jiang, Y., Yan, B., and Cheng, B. (2016). Efficient conversion of chitin biomass into 5-hydroxymethylfurfural over metal salts catalysts in dimethyl sulfoxide -water mixture under hydrothermal conditions. *Polymer Degrad. Stability* 134, 105–114. doi: 10.1016/j.polymdegradstab.2016.09.035

Zang, H., Feng, J., Yan, Q., Wu, C., and Shi, X. (2015). *Method for Preparing 5-Hydroxymethyl Furfural From Chitin/Chitosan Raw Material. CN*1047 10390A.

Zang, H., Yu, S., Yu, P., Ding, H., Du, Y., Yang, Y., et al. (2017). Hydrothermal conversion of N-acetyl-d-glucosamine to 5-hydroxymethylfurfural using ionic liquid as a recycled catalyst in a water-dimethyl sulfoxide mixture. *Carbohydr. Res.* 442, 1–8. doi: 10.1016/j.carres.2017.02.002

Zhang, H., Wu, J., Zhang, J., and He, J. (2005). 1-Allyl-3-methylimidazolium chloride room temperature ionic liquid: a new and powerful nonderivatizing solvent for cellulose. *Macromolecules* 38, 8272–8277. doi: 10.1021/ma0505676

Zhou, J., Sui, H., Jia, Z., Yang, Z., He, L., and Li, X. (2018). Recovery and purification of ionic liquids from solutions: a review. *RSC Adv*. 8, 32832–32865. doi: 10.1039/C8RA06384B

Conflict of Interest: JS is a former CSO of Mari Signum Mid-Atlantic, LLC.

The remaining author declares that the research was conducted in the absence of any commercial or financial relationships that could be construed as a potential conflict of interest.

frontiers in Bioengineering and Biotechnology

ORIGINAL RESEARCH
published: 04 February 2020
doi: 10.3389/fbioe.2020.00039

Quality Improvement of Capsular Polysaccharide in *Streptococcus pneumoniae* by Purification Process Optimization

Chankyu Lee[1,2†], Hee Jin Chun[1†], Minchul Park[1], Rock Ki Kim[1], Yoon Hee Whang[1], Seuk Keun Choi[1], Yeong Ok Baik[1], Sung Soo Park[2] and Inhwan Lee[1*]*

[1] R&D Center, EuBiologics Co., Ltd., Chuncheon-si, South Korea, [2] Department of Biotechnology, Korea University, Seoul, South Korea

OPEN ACCESS

Edited by:
Jorge Fernando Brandão Pereira, São Paulo State University, Brazil

Reviewed by:
Viviane Maimoni Goncalves, Butantan Institute, Brazil
Norma Suarez, University of the Republic, Uruguay
Elisabeth Cheng, Instituto Butantan, Brazil

***Correspondence:**
Sung Soo Park
sspark@Korea.ac.kr
Inhwan Lee
inhwan@eubiologics.com

[†] These authors have contributed equally to this work

Specialty section:
This article was submitted to Industrial Biotechnology, a section of the journal Frontiers in Bioengineering and Biotechnology

Received: 16 September 2019
Accepted: 16 January 2020
Published: 04 February 2020

Citation:
Lee C, Chun HJ, Park M, Kim RK, Whang YH, Choi SK, Baik YO, Park SS and Lee I (2020) Quality Improvement of Capsular Polysaccharide in Streptococcus pneumoniae by Purification Process Optimization. Front. Bioeng. Biotechnol. 8:39. doi: 10.3389/fbioe.2020.00039

Streptococcus pneumoniae is the causative agent of many diseases, most notably pneumonia. Most of the currently used vaccines to protect against this pathogen employ pneumococcal capsular polysaccharides (CPSs) as antigens, but purifying CPS of sufficient quality has been challenging. A purification process for CPS comprising conventional methods such as ultrafiltration, CTAB precipitation, and chromatography was previously established; however, this method resulted in high cell wall polysaccharide (CWPS) contamination, especially for serotype 5. Thus, a better purification method that yields CPS of a higher quality is needed for vaccine development. In this study, we significantly reduced CWPS contamination in serotype 5 CPS by improving the ultrafiltration and CTAB precipitation steps. Moreover, by applying an acid precipitation process to further remove other impurities, serotype 5 CPS was obtained with a lower impurity such as decreased nucleic acid contamination. This improved method was also successfully applied to 14 other serotypes (1, 3, 4, 6A, 6B, 7F, 9V, 11A, 14, 18C, 19A, 19F, 22F, and 23F). To assess the immunogenicity of the CPS from the 15 serotypes, two sets of 15-valent pneumococcal conjugate vaccines were prepared using the previous purification method and the improved method developed here; these vaccines were administered to a rabbit model. Enzyme-linked immunosorbent assay and opsonophagocytic assay demonstrated higher immunogenicity of the conjugate vaccine prepared using CPS produced by the improved purification process.

Keywords: pneumococcal capsular polysaccharide, purification, cetyltrimethylammonium bromide (CTAB) precipitation, cell wall polysaccharide, vaccine

INTRODUCTION

Streptococcus pneumoniae, which was first isolated by Louis Pasteur and George Sternberg independently in 1880 (Grabenstein and Klugman, 2012), is a gram-positive bacterium and major cause of pneumonia. The bacterium is also responsible for meningitis, otitis media, and other infectious diseases (Örtqvist, 1999; Hortal et al., 2000; Mitchell and Mitchell, 2010; Blasi et al., 2012). One of the most important virulence factors in *S. pneumoniae* is capsular polysaccharide (CPS), the

types of which determine the serotypes of the pneumococcal bacterium (Dubos and Avery, 1931; Henrichsen, 1995). CPS composes the outer layer of *S. pneumoniae*, and more than 90 structurally different serotypes of *S. pneumoniae* have been reported thus far; 11 serotypes are known to cause over 70% of invasive pneumococcal diseases (Geno et al., 2015). Because pneumococcal CPS is a major factor of pathogenicity and involved in the antigen-specific immune response against *S. pneumoniae*, it has been a primary target for the development of pneumococcal disease vaccines by pharmaceutical companies worldwide (Melegaro et al., 2006).

In the cell wall of *S. pneumoniae*, cell wall polysaccharide (CWPS) coexists with CPS and is a common contaminant during the process of CPS purification (Xu et al., 2005). CWPS is a negatively charged molecule and structurally conserved, except for the number of phosphocholine groups, among the serotypes (Vialle et al., 2005; Brown et al., 2013). Because CWPS is known to cause an inflammatory response (Tuomanen et al., 1987) and antibodies against CWPS are known to be not protective despite its high immunogenicity (Nielsen et al., 1993), CWPS must be separated from CPS for pneumococcal vaccine development. However, it is difficult to remove CWPS from CPS because the molecules are covalently bound through peptidoglycan (Sørensen et al., 1990; Larson and Yother, 2017) except for serotypes 3 and 37. In this study, we developed an improved process for CPS purification from the fermentation broth of *S. pneumoniae* that reduces CWPS as well as other contaminants such as nucleic acids and proteins. We exploited the differences in molecular weight and electrostatic properties between CPS and CWPS and successfully improved the quality of isolated CPS. Higher-quality CPS and CPS with high CWPS content were then conjugated to the carrier protein CRM_{197} to overcome the limited effectiveness of polysaccharide vaccines since polysaccharide alone cannot elicit T-cell dependent immune responses (Beuvery et al., 1982; Lesinski and Westerink, 2001). Animal studies were conducted to compare the immunogenicity between the conjugate vaccines produced by the previous and new methods.

MATERIALS AND METHODS

Cell Culture

To produce pneumococcal polysaccharides, each serotypes of *S. pneumoniae* were cultivated in Hemin free media in a 40L fermenter (Sartorius, BIOSTAT, D-DCU, Göttingen, Germany) at 37°C, pH 7.2. All 15 serotype of *S. pneumoniae* (1, 3, 4, 5, 6A, 7F, 9V, 11A, 14, 18C, 19A, 19F, 22 F, 23F) were obtained from Culture Collection University of Gothenburg (CCUG).

Purification

Purification Before Process Optimization

After the cultivation of *S. pneumoniae*, 10% sodium deoxycholate (DOC) was added to the cell broth to achieve a final concentration of 0.1% to lyse the cells, followed by centrifugation at 7000 rpm. The supernatant was filtered using a 0.2 μm cut-off filter and subjected to ultrafiltration/diafiltration (UF/DF) against pure water at 10-fold volume of the supernatant by using a 50 kDa (for serotypes 4, 5, and 14) or 100 kDa (for serotypes 1, 2, 3, 6A, 6B, 7F, 9V, 11A, 18C, 19A, 19F, 22F, and 23A) cut-off cassette membrane filter (Hydrosart, Sartocon Ultrafiltration cassettes, Sartorius, Göttingen, Germany), depending on the size of the CPS. CTAB (10%) was added to achieve a final concentration of 0.7% to the diafiltered solution of CPS. For negatively charged CPS such as 1, 3, 4, 5, 6A, 6B, 9V, 11A, 18C, 19A, 19F, 22F, and 23A, CPS precipitated with some negatively charged impurities, including nucleic acids, and for neutral CPS such as 7F and 14, only impurities precipitated, leaving the CPS remain in the solution. Thus, after centrifugation of CTAB-treated solution, precipitates were collected for negative CPS, and supernatant was collected for neutral CPS. NaCl solution (1 M) was added to the precipitated CPS, and CPS in the supernatant was mixed with NaCl solution to achieve a final NaCl concentration of 1 M. Then, ethanol was added to CPS in 1 M NaCl solution (1st ethanol CPS precipitation) to a final concentration of 75% to precipitate CPS. Precipitates were recovered by centrifugation and dissolved in water. After treating 6% (w/v) sodium acetate and 0.5% (w/v) DOC, the pH of the solution was adjusted to 6.4 using 8 M acetic acid. Ethanol was added to this solution (ethanol impurity precipitation) to a final concentration of 20% (1, 3, 4, 5, 19A, and 19F) or 33% (6A, 6B, 7F, 9V, 11A, 14, 18C, 22F, and 23A) to precipitate the impurities. After centrifugation, the supernatant was collected and mixed with 6% (w/v) sodium acetate, and ethanol was added (2nd ethanol CPS precipitation) to achieve a final concentration of 75%. As in the 1st ethanol CPS precipitation process, in the 2nd ethanol CPS precipitation, CPS were precipitated, and these precipitates were collected by centrifugation and dissolved in water. Then, this CPS solution was sequentially diafiltered against Buffer I (50 mM Tris–HCl, 2 mM EDTA, 0.3% DOC), Buffer II (50 mM Tris–HCl, 2 mM EDTA), and Buffer III (150 mM NaCl). Afterward, buffer exchange to water was performed by diafiltration for hydroxyapatite (HA) chromatography, during which impurities will bind to the column. For the HA chromatography, column was equilibrated with PBS (10 mM phosphate buffer, 150 mM sodium chloride, pH 7.4) before sample loading. The flow through (F/T) was recovered for the final UF/DF and formulation.

Improved Purification Method

To improve the process, after cell lysis, acid precipitation was performed, during which the pH of the cell broth was adjusted to 5.0 by adding acetic acid to remove impurities such as soluble proteins. After the acid precipitation, extensive UF/DF against pure water at 20-fold volume of the supernatant, which was twice the volume used in the former method, was performed to remove low molecular weight molecules including CWPS. CTAB concentration was also increased, from 0.7 to 2%. The purification steps before and after optimization are presented in **Figure 1**.

Gel Permeation Chromatography (GPC)

To determine the molecular sizes of pneumococcal CPS from each serotype, gel permeation chromatography (GPC)

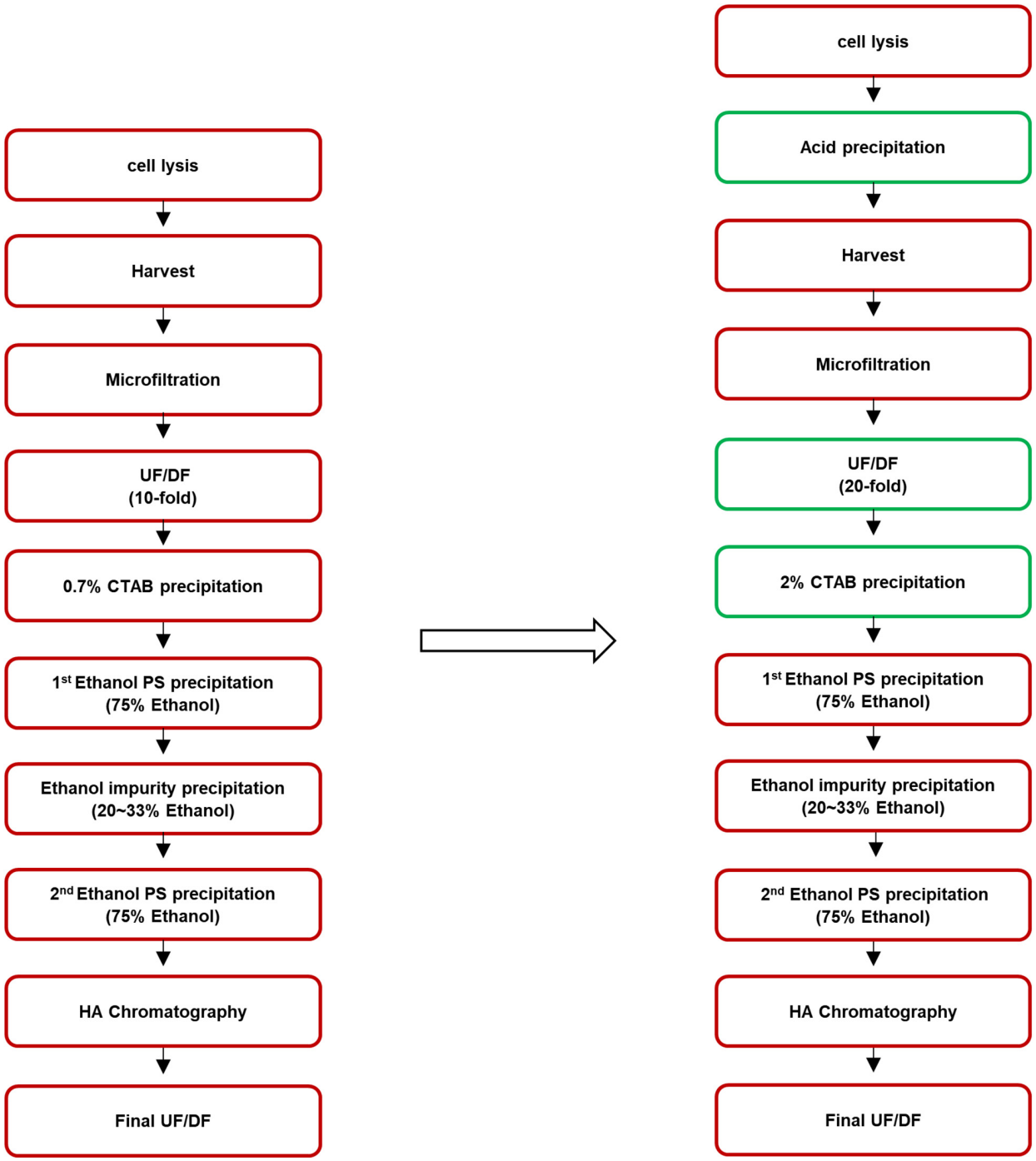

FIGURE 1 | Process flowchart of pneumococcal polysaccharide purification. The method before improvement is presented in the left and the improved steps are indicated in the green box in the right.

was performed using the Waters e2695 system equipped with the TSKgel G6000PW/5000PWXL column (2× bed column). Dextran standard (American Polymer Standard Corporation) was used to calculate the molecular weight of CPS, as dextran and pneumococcal CPS have similar characteristics.

Nuclear Magnetic Resonance (NMR) Spectroscopy

Concentrations of CWPS were measured by 1D ^{1}H-NMR spectroscopy. CPS samples were dissolved in 10% D_2O solution, and the 1D spectra were recorded with a Bruker Avance Neo 600 (600 MHz) spectrometer. NMR data were

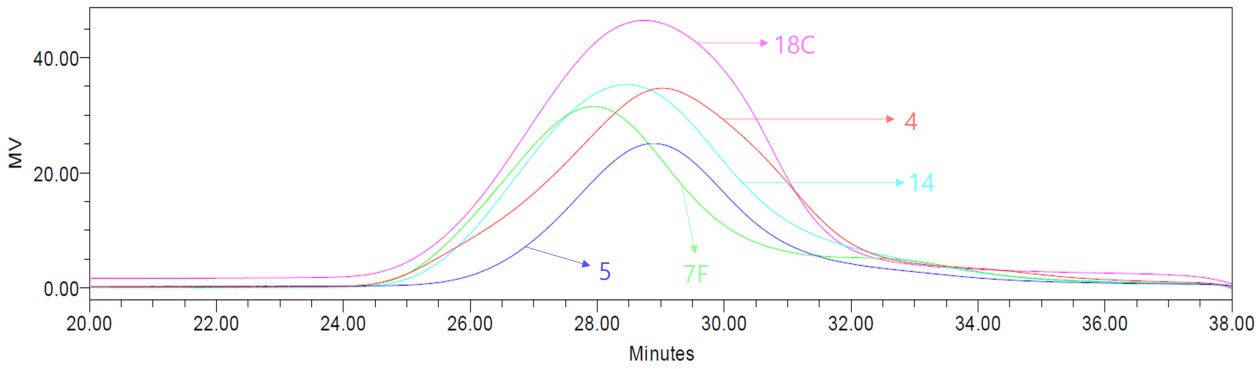

FIGURE 2 | Molecular weights of serotypes 4, 5, 7F, 14, 18C measured by GPC. The serotypes of 4, 5, 7F, 14, and 18C are shown in red, blue, green, cyan, and pink colors, respectively.

processed, and the spectra were analyzed in Topspin® software. CWPS content was calculated as the relative peak area ratio of CWPS to CPS.

Measurement of Proteins and Nucleic Acids

Proteins and nucleic acids as contaminants in CPS were measured by a Lowry protein assay kit (Thermo Fisher Scientific, Waltham, MA, United States) and NanoDrop spectrophotometer.

Activation of PnPSs

Purified CPS larger than 700 kDa was fragmented by a Microfluidizer® (Microfluidics, United States) at 30.000 psi to reduce the size. An ADH linker molecule was covalently bound to 5 mg/mL of fragmented CPS between 250 and 700 kDa in size using 1-cyano-4-diethylaminopyridinium (CDAP) and tri-ethylene amine (TEA) as described in literatures (Lees et al., 1996; Suárez et al., 2008). Briefly, CDAP in acetonitrile was added to 5 mg/mL of the polysaccharide solution at 1/10 of the volume (50 mg/mL), and after 1 min, 0.21 M of TEA was added at the same volume of CDAP (50 mg/mL, in acetonitrile). After 3 min, the same volume of 0.5 M ADH with 50 mg/mL CDAP (in acetonitrile) was added to the solution, and the activation reaction was performed for 15 h at 4–10°C with shaking at 200–300 rpm using a magnetic stirrer. Activated polysaccharides were confirmed by measuring the degree of activation, which shows the concentration of ADH molecules bound on the polysaccharide chains, by TNBS (2,4,6-trinitrobenzene sulfonic acid) assay (Snyder and Sobocinski, 1975).

TABLE 1 | Calculated molecular weights of serotypes 4, 5, 7F, 14, and 18C measured by GPC.

Serotype	4	5	7F	14	18C
Molecular weight (kDa)	951.0	1002.1	1275.1	1153.8	1128.3

Conjugation of Activated PnPSs to CRM_{197}

Activated PnPSs were conjugated to CRM_{197} using 1-ethyl-3-(-3dimethylaminopropyl) carbodiimide hydrochloride (EDAC) as a catalyst in 0.1 M MES buffer (pH 6.0). After the conjugation reaction proceeded at 4°C, EDAC and unbound CRM_{197} were removed by DF with a 100-kDa cut-off membrane filter, and Polysorbate 80 was added to a final concentration of 0.005%.

Formulation of 15-Valent Pneumococcal Conjugate Vaccines

All 15 CPS-CRM_{197} conjugates were adsorbed on aluminum phosphate adjuvant. Each vial of vaccine (0.5 mL) contained 125 μg of aluminum phosphate and 2.2 μg of CPS (except 6B, which contained 4.4 μg).

Animal Study

All animal studies were approved by the Institutional Animal Care and Use Committee (approval No.: 17B025) according to Animal Protection Law (13023, January 20th, 2015). To test the immunogenicity of the 15-valent pneumococcal conjugate vaccines, 0.5 mL of Prevnar 13® and formulated vaccine were intramuscularly injected into New Zealand white rabbits weighing 1.16–1.30 kg. After the first injection, two boosting injections were conducted at 2-week intervals, and serum samples were collected 6 weeks after the first injection.

Enzyme-Linked Immunosorbent Assay (ELISA)

Enzyme-linked immunosorbent assay units for 15 serotypes were measured by a modified method described by Concepcion and Frasch (2001). Microtiter plates were coated with 1 μg/mL of serotype-specific pneumococcal CPS antigens and incubated for 5 h at 37°C. Rabbit sera were pre-absorbed with pneumococcal C-polysaccharide (Statens Serum Institut) and each serotype of CPSs (American Type Culture Collection) for 30 min at room temperature before serial dilution. Serially diluted serum was added onto a washed plate, and the plates were incubated at room temperature for 1 h. After 1 h of incubation, the plates were

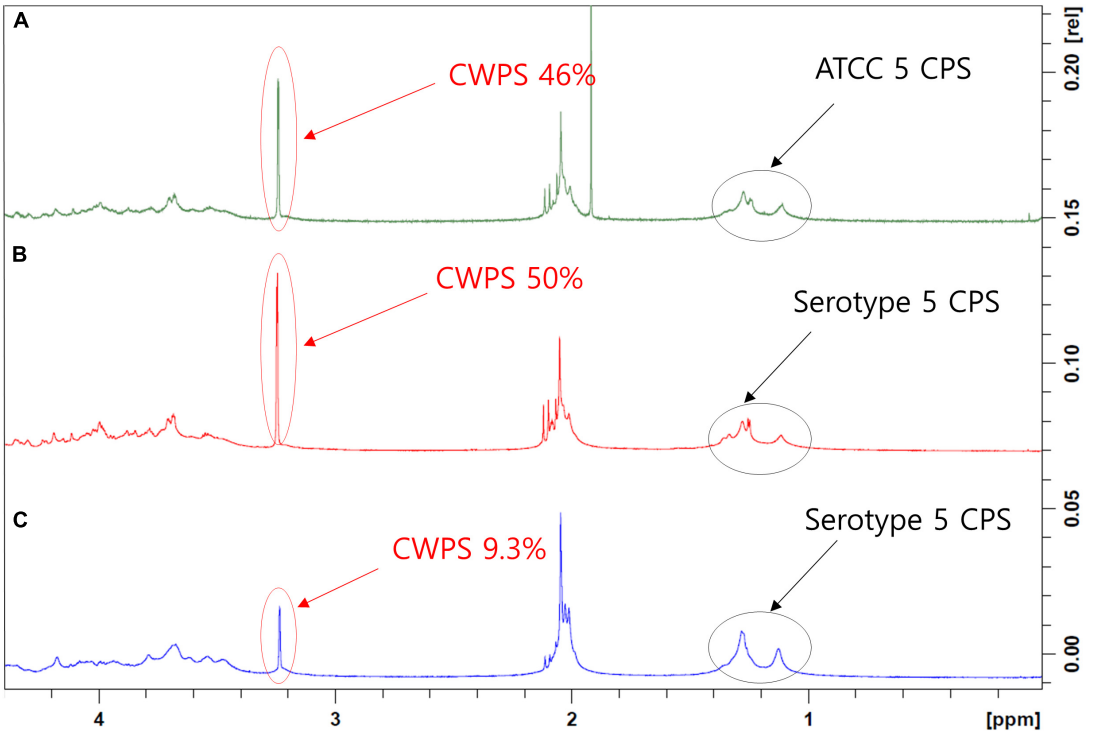

FIGURE 3 | 1D ^{1}H-NMR spectra of pneumococcal polysaccharide of serotype 5. **(A)** Pneumococcal polysaccharide of ATCC standard. **(B)** Pneumococcal polysaccharide purified using the method before improvement. **(C)** Pneumococcal polysaccharide purified using improved method. The peaks from CPSs and cell wall polysaccharides are indicated by arrows. The peaks in the 1–1.5 ppm region are three methyl groups in type 5 CPS, and the peak that appeared at 3–3.5 ppm is phosphocholine groups in CWPS.

washed, and HRP-conjugated goat anti-rabbit IgG (AB Frontier) was added. Following a 1-h incubation and washing, substrate (3,3′,5,5′-tetramethylbenzidine, TMB) was added to all wells. The optical density of each well was measured at 450 nm using an ELISA plate reader. *t*-test was used to evaluate the increase of the serotype specific IgG levels in the sera. p values of <0.05 was considered as statistically significant and all statistical analysis was performed by GraphPad Prism v5.01 (GraphPad, La Jolla, CA, United States).

Opsonophagocytic Activity Assay (OPA)

The functional activity of antibodies in sera was measured by the standard opsonophagocytic activity assay (OPA) (Burton and Nahm, 2006). HL-60 cells (Korean Cell Line Bank, KCLB No. 10240) were used as effector cells, which express complement receptors CR1 and CR3 (for iC3b and C3b). HL-60 cells were maintained, passaged, and differentiated into granulocytes with dimethylformamide. HL-60 cells were allowed to phagocytose bacteria in the presence of sera containing anticapsular antibodies

TABLE 2 | Comparison of the yields and content of impurities of serotype 5 before and after process optimization.

	Before improved	After improved
CPS yield (g/L)	0.26 ± 0.05	0.17 ± 0.07
Proteins (%)	3.16 ± 2.08	4.34 ± 1.19
Nucleic acids (%)	5.13 ± 1.78	0.03 ± 0.01
CWPS (%)	≥50	9.3

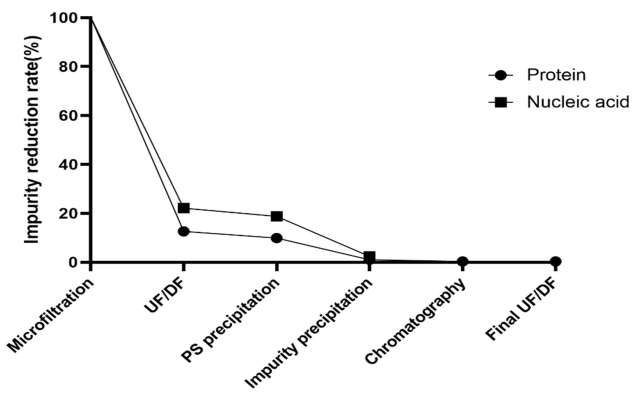

FIGURE 4 | Reduction rates of impurities in each steps of improved method. Reductions of protein and nucleic acid contaminants are indicated by circle and square dots, respectively. Microfiltration is a filtering process using 0.2 μm cut-off capsule filter while UF/DF process is a process to remove low molecular contaminants using 50 kDa cut-off filter. PS and impurity precipitation were carried out by using CTAB and ethanol, respectively. Hydroxyapatite (HA) column was used in chromatography process and buffer exchange to the final formulation was performed in final UF/DF process.

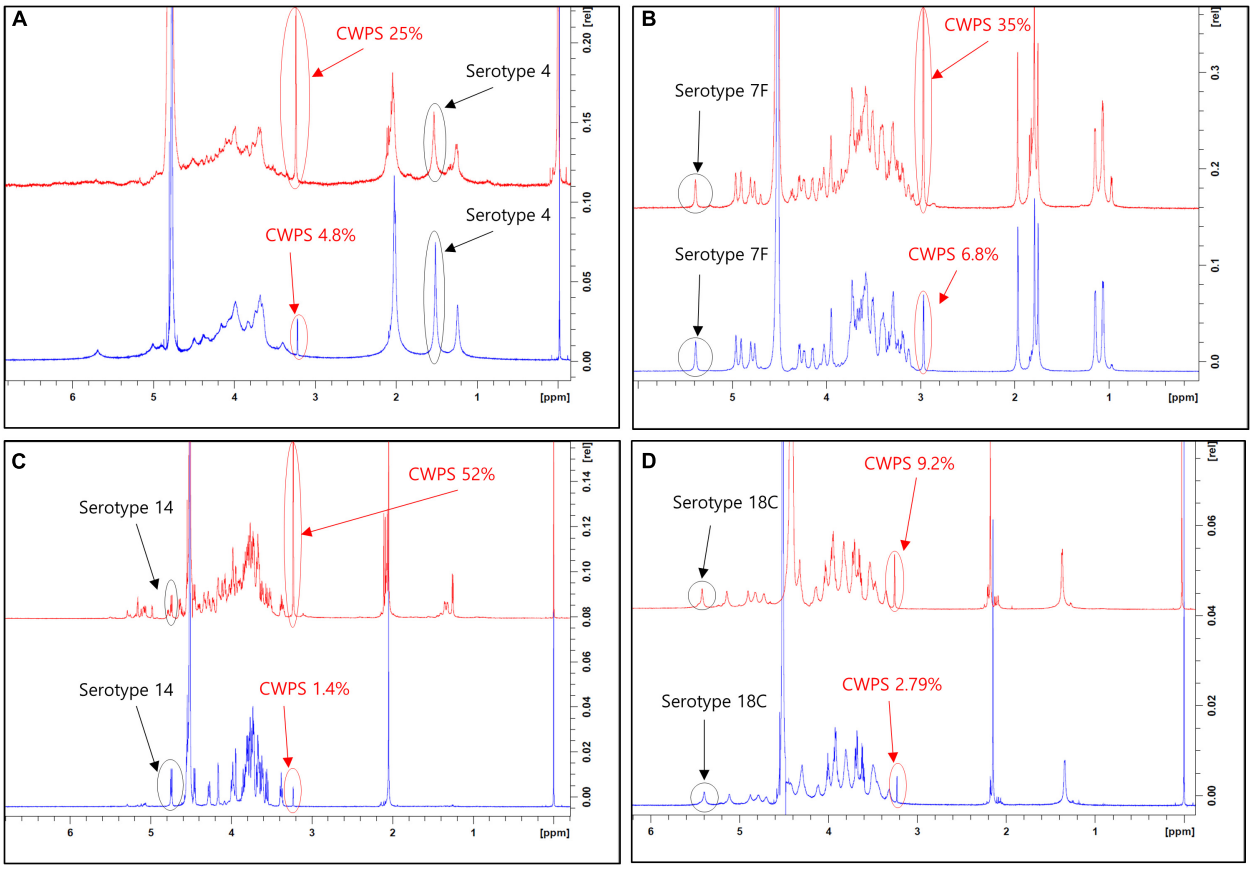

FIGURE 5 | 1D ^{1}H-NMR spectra of pneumococcal polysaccharide of serotypes **(A)** 4, **(B)** 7F, **(C)** 14, **(D)** 18C. Peaks from capsular polysaccharides and cell wall polysaccharides are indicated by arrows in each panel. The peaks from pyruvyl ketal (type 4) and anomeric protons (types 7F, 14, and 18C) are chosen and identified in the spectra since these chemical groups are unique and easily identifiable from the peaks from phosphocholine groups in CWPS.

TABLE 3 | Comparison of the yields and content of impurities of serotypes 4, 7F, 14, and 18C.

	CPS yield (g/L)		Proteins (%)		Nucleic acids (%)	
	Before	After	Before	After	Before	After
Serotype 4	0.26 ± 0.01	0.24 ± 0.02	0.95 ± 0.15	0.86 ± 0.03	0.19 ± 0.06	0.20 ± 0.02
Serotype 7F	1.59 ± 0.18	1.36 ± 0.01	0.94 ± 0.18	0.69 ± 0.07	0.09 ± 0.01	0.04 ± 0.01
Serotype 14	0.19 ± 0.02	0.10 ± 0.02	3.47 ± 0.34	2.73 ± 0.57	0.12 ± 0.05	0.11 ± 0.05
Serotype 18C	0.88 ± 0.06	1.17 ± 0.04	0.03 ± 0.01	0.01 ± 0.01	0.07 ± 0.05	0.04 ± 0.03

and baby rabbit complement (Pel-Freez Biologicals). The assay was performed on microtiter plates, and duplicate samples from each well were plated on THYE agar plates. The results were expressed as an opsonic index, which is the reciprocal of the serum dilution at 50% killing as compared to bacterial growth in controls without serum.

RESULTS

Molecular Weights of CPS and CWPS

The molecular weights of CWPS were measured by GPC to determine if CWPS can be separated from CPS based on size differences (**Figure 2**). As summarized in **Table 1**, the molecular weights of CPS were 951.0, 1002.1, 1275.1, 1153.8, and 1128.3 kDa for serotypes 4, 5, 7F, 14, and 18C, respectively. CWPS has a molecular weight of approximately 10 kDa, indicating that the large difference in size can be utilized for separation.

Concentrations of CWPS, Nucleic Acids, and Protein Impurities in Serotype 5 CPS

Cell wall polysaccharide content in serotype 5, determined to be 50% by NMR, was the highest among all 15 serotypes (data not shown) and similar to that of a comparator CPS (ATCC standard pneumococcal serotype 5 polysaccharide) (**Figures 3A,B**). After

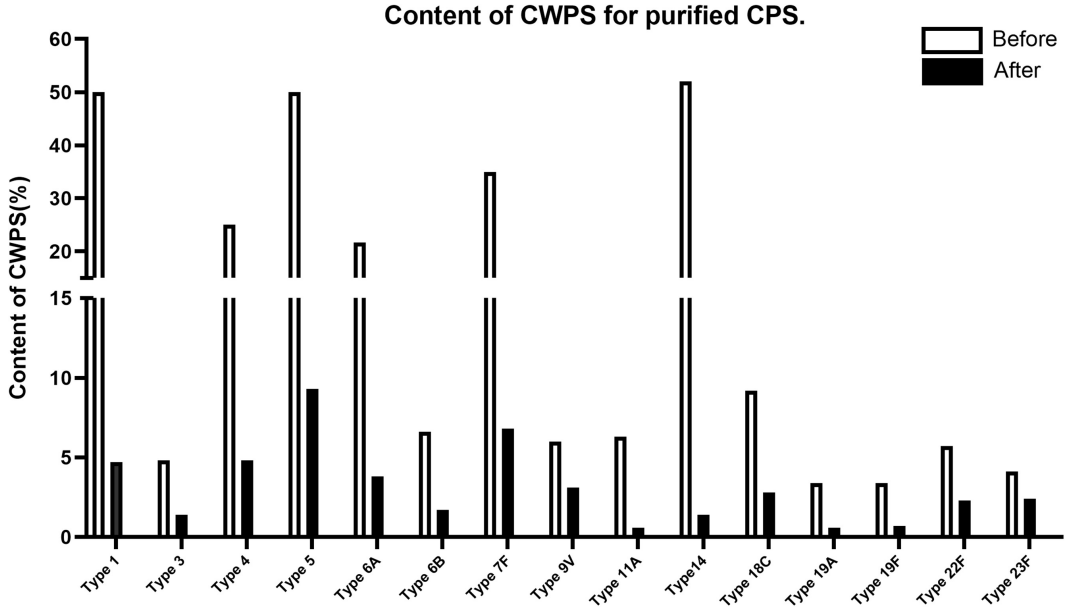

FIGURE 6 | CWPS contents in each of 15 pneumococcal polysaccharides (1, 3, 4, 5, 6A, 6B, 7F, 9V, 11A, 14, 18C, 19A, 19F, 22F, 23F). CWPS contents are presented as a percentage of the ratios of cell wall polysaccharides to capsular polysaccharides. The comparison of before and after the process improvement are presented in the graph for each serotype.

optimization of the purification processes, which included changes in the conditions of CTAB addition and ultrafiltration, the CWPS concentration fell to 9.3% (**Figure 3C**). Despite the decrease in CPS yield, the levels of other contaminants such as nucleic acids were also reduced, as was the concentration of CWPS, after applying the improved processes (**Table 2**). There was a small increase in protein contamination after process optimization; however, it is thought to be within a batch variation range. The reduction rates of nucleic acids and proteins in CPS from serotype 5 were monitored step-by-step in each process, revealing that the majority of the impurities were removed by the intensive microfiltration step (**Figure 4**). During UF/DF, proteins and nucleic acids were reduced by 85.7 and 75.6%, respectively. When impurity precipitation was performed using ethanol, proteins and nucleic acids decreased by 98.6 and 96.7%, while in the chromatography step, levels decreased by 99.3 and 99.6%. Therefore, changes in UF/DF and impurity precipitation processes resulted in the most dramatic decreases in nucleic acid contaminants from serotype 5.

Concentrations of CWPS, Nucleic Acids, and Protein Impurities in 14 Other Serotypes

This improved purification method was then applied to four other serotypes (4, 7F, 14, and 18C) that also exhibited high CWPS concentrations used the previous method. The NMR spectra of CPS produced by each method were compared (**Figure 5**). CWPS concentration was decreased from 25 to 4.8% for serotype 4 (**Figure 5A**), 35–6.8% for 7F (**Figure 5B**), 52–1.4% for 14 (**Figure 5C**), and 9.2–2.8% for 18C (**Figure 5D**). The production yield of CPS and concentrations of nucleic acids and proteins from serotypes 4, 7F, 14, and 18C were not affected by modification of the processes (**Table 3**), indicating that CWPS concentrations were efficiently reduced by the improved method, without affecting other factors. When the improved method was applied to other serotypes (1, 3, 6A, 6B, 9V, 11A, 19A, 19F, 22F, and 23F), decreases in CWPS were consistently observed, indicating that the method is generally applicable (**Figure 6**). In particular, notable decreases were observed in serotypes 1, 4, 5, 6A, 7F, and 14.

Impact of the Increased Quality of CPS on Immunogenicity

A 15-valent conjugate vaccine prepared using CPS produced without process optimization was injected into rabbits, and sera were subsequently analyzed by ELISA and OPA. Significantly lower IgG levels for serotypes 1, 3, 5, 6A, 6B, 18C, 19A, and 23F were observed in the sera compared with those following administration of a comparator vaccine (Prevnar 13®), while IgG for serotypes 4, 7F, 9V, and 19F showed no significant differences (**Figure 7A**). When the CPS produced by the improved method was used in the conjugate vaccine, the concentration of IgG for most serotypes was equivalent to or higher than those observed after administration of Prevnar 13®, except for serotype 7, indicating that the polishing of the CPS production steps dramatically improved the quality of the vaccine and thus increased the immunogenicity of the vaccine (**Figure 7B**). In addition, IgG levels for serotypes 11A and 22F, which are not covered by Prevnar 13®, were similar to those for other serotypes covered by the 15-valent pneumococcal conjugate vaccine. OPA

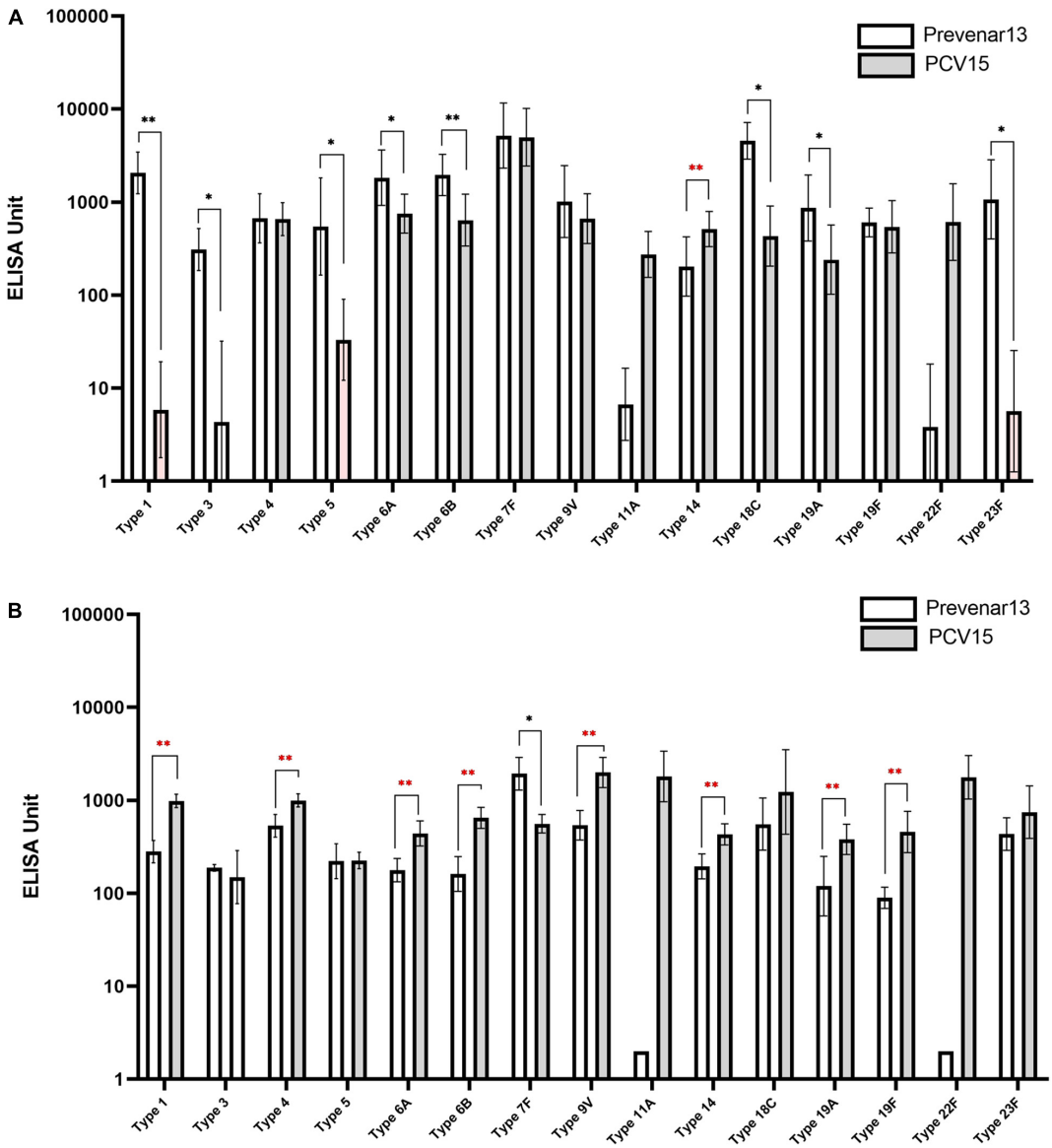

FIGURE 7 | Immune responses against pneumococcal polysaccharides in mice measured by ELISA. **(A)** Before the process optimization. **(B)** After the process optimization. Prevenar 13® was used as a comparator vaccine and PCV15 indicates the polysaccharide-carrier protein conjugate produced in this study by Eubiologics. (*$p < 0.05$, **$p < 0.01$).

to measure the functional antibody levels in the sera also showed results similar to those of ELISA. Notably, serotypes 1, 5, 6B, 9V, 19A, and 23F in the method before improvement demonstrated lower opsonophagocytic killing activity than a comparator vaccine (**Figure 8A**); however, by improving the purification method and decreasing the CWPS, these serotypes showed higher or similar fold increases of OPA index (**Figure 8B**).

DISCUSSION

Several methods for purification of CPS from *S. pneumoniae* have been reported, and advances in technology have enabled production of CPS with high purity and yield (Suárez et al., 2001; Macha et al., 2014; Yuan et al., 2014; Zanardo et al., 2016; Morais et al., 2018). However, while these methods were optimized for specific serotypes of CPS such as type14 (Suárez et al., 2001; Zanardo et al., 2016), types 3, 6B, 14, 19F, and 23F (Macha et al., 2014), and types 1, 4, 5, 6A, 6B, 7F, 9V, 14, 18C, 19A, 19F, and 23F (Yuan et al., 2014), our method can be universally applied to all 15 serotypes (1, 3, 4, 5, 6A, 6B, 7F, 9V, 11A, 14, 18C, 19A, 19F, 22F, and 23F) contained in a newly developing 15-valent conjugate vaccine, although there is one determination step whether to use supernatant or precipitant depending on the charge of the target CPS after CTAB precipitation. Methods mentioned above do not use traditional

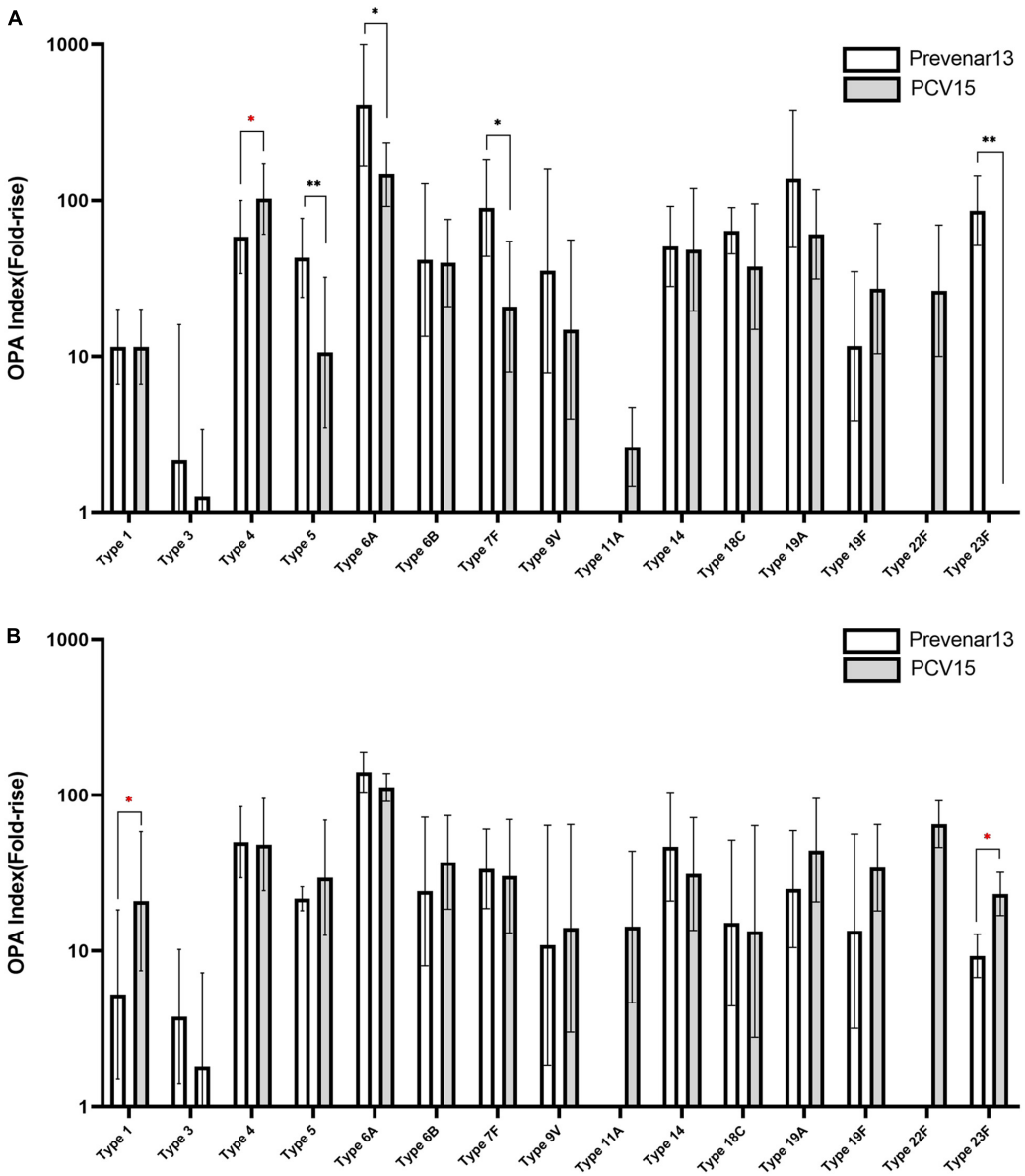

FIGURE 8 | Immune responses against pneumococcal polysaccharides in mice measured by OPA. **(A)** Before the process optimization. **(B)** After the process optimization. Prevenar 13® was used as a comparator vaccine and PCV15 indicates the polysaccharide-carrier protein conjugate produced in this study by Eubiologics. (*$p < 0.05$, **$p < 0.01$).

CTAB precipitation which is our main separation step, and we combined this with other techniques including acid precipitation, ethanol precipitation, and HA chromatography and this ensured high purity of CPS and low CWPS contamination. Moreover, while most studies in the literature focus on reducing nucleic acid and protein impurities, we focused on the CWPS, which is one of the major contaminants in the process of CPS purification and remains a concern in the production of pneumococcal vaccines. Although CPS yield could have been compromised due to many steps which is the case in traditional methods (Morais et al., 2018), we substantially reduced CWPS contaminations in CPS. The method used in the development of Prevenar 13®, which is a comparator vaccine in our animal immunogenicity study, is based on CTAB precipitation as our technique (Hausdorff et al., 2010); however, the main difference is that it uses NaI to precipitate CTAB after CTAB precipitation and our method uses ethanol precipitation to specifically precipitate CPS.

CONCLUSION

In conclusion, we developed our own pneumococcal CPS purification method by combining several traditional separation techniques such as ultrafiltration, CTAB precipitation,

and chromatography; however, concerns about CWPS contamination remained, as high CWPS concentrations in CPS were observed by NMR spectroscopy. To solve this problem and reduce CWPS and other impurities, process optimization was carried out, which resulted in lower CWPS, leading to higher immunogenicity when used in a conjugate vaccine. By optimizing only the main purification processes, including extensive UF/DF and impurity precipitation, concentrations of CWPS were notably decreased. Moreover, in animal models, ELISA and OPA analyses revealed that the higher-quality CPS affected the immunogenicity of the multivalent pneumococcal conjugate vaccine in which CPS was used as an antigen. Our results reveal that the reduced levels of CWPS contamination of CPS by our optimized method significantly improved the quality of the CPS which can contribute to the development of new multivalent conjugate vaccines to prevent pneumococcal diseases.

DATA AVAILABILITY STATEMENT

The datasets generated for this study are available on request to the corresponding author.

ETHICS STATEMENT

The animal study was reviewed and approved by the Institutional Animal Care and Use Committee of Chuncheon Bioindustry Foundation.

AUTHOR CONTRIBUTIONS

CL, SC, YB, and IL: conceptualization. CL, IL, and SP: data curation, supervision, and writing – review and editing. HC and CL: formal analysis. HC and RK: investigation. HC, MP, RK, and YW: methodology. HC: writing – original draft.

FUNDING

This study was supported by a grant of the Korea Health Technology R&D Project through the Korea Health Industry Development Institute (KHIDI), funded by the Ministry of Health and Family Welfare, South Korea.

REFERENCES

Beuvery, E. C., Rossum, F. V., and Nagel, J. (1982). Comparison of the induction of immunoglobulin M and G antibodies in mice with purified pneumococcal type 3 and meningococcal group C polysaccharides and their protein conjugates. *Infect. Immun.* 37, 15–22. doi: 10.1128/iai.37.1.15-22.1982

Blasi, F., Mantero, M., Santus, P., and Tarsia, P. (2012). Understanding the burden of pneumococcal disease in adults. *Clin. Microbiol. Infect.* 18, 7–14. doi: 10.1111/j.1469-0691.2012.03937.x

Brown, S., Santa Maria, J. P., and Walker, S. (2013). Wall teichoic acids of gram-positive bacteria. *Annu. Rev. Microbiol.* 67, 313–336. doi: 10.1146/annurev-micro-092412-155620

Burton, R. L., and Nahm, M. H. (2006). Development and validation of a fourfold multiplexed opsonization assay (MOPA4) for Pneumococcal antibodies. *Clin. Vaccine Immunol.* 13, 1004–1009. doi: 10.1128/CVI.00112-06

Concepcion, N. F., and Frasch, C. E. (2001). Pneumococcal type 22F polysaccharide absorption improves the specificity of a Pneumococcal-polysaccharide Enzyme-linked immunosorbent assay. *Clin. Vaccine Immunol.* 8, 266–272. doi: 10.1128/cdli.8.2.266-272.2001

Dubos, R., and Avery, O. T. (1931). Decomposition of the capsular polysaccharide of pneumococcus type II by a bacterial enzyme. *J. Exp. Med.* 54, 51–71. doi: 10.1084/jem.54.1.51

Geno, K. A., Gilbert, G. L., Song, J. Y., Skovsted, I. C., Klugman, K. P., Jones, C., et al. (2015). Pneumococcal capsules and their types: past present, and future. *Clin. Microbiol. Rev.* 28, 871–899. doi: 10.1128/CMR.00024-15

Grabenstein, J. D., and Klugman, K. P. (2012). A century of pneumococcal vaccination research in humans. *Clin. Microbiol. Infect.* 18, 15–24. doi: 10.1111/j.1469-0691.2012.03943.x

Hausdorff, W. P., Siber, G. R., Paradiso, P. R., and Prasad, A. K. (2010). *Multivalent Pneumococcal Polysaccharide-Protein Conjugate Composition*. United States Patent #US 7709001B2.

Henrichsen, J. (1995). Six newly recognized types of *Streptococcus pneumoniae*. *J. Clin. Microbiol.* 33, 2759–2762. doi: 10.1128/jcm.33.10.2759-2762.1995

Hortal, M., Camou, T., Palacio, R., Dibarboure, H., and García, A. (2000). Ten-year review of invasive pneumococcal diseases in children and adults from uruguay: clinical spectrum, serotypes, and antimicrobial resistance. *Int. J. Infect. Dis.* 4, 91–95. doi: 10.1016/S1201-9712(00)90100-90100

Larson, T. R., and Yother, J. (2017). *Streptococcus pneumoniae* capsular polysaccharide is linked to peptidoglycan via a direct glycosidic bond to β-D- N -acetylglucosamine. *Proc. Natl. Acad. Sci. U.S.A.* 114, 5695–5700. doi: 10.1073/pnas.1620431114

Lees, A., Nelson, B. L., and Mond, J. J. (1996). Activation of soluble polysaccharides with 1-cyano-4-dimethylaminopyridinium tetrafluoroborate for use in protein—polysaccharide conjugate vaccines and immunological reagents. *Vaccine* 14, 190–198. doi: 10.1016/0264-410X(95)00195-7

Lesinski, G. B., and Westerink, M. A. J. (2001). Novel vaccine strategies to T-independent antigens. *J. Microbiol. Methods* 2001, 135–149. doi: 10.1016/s0167-7012(01)00290-1

Macha, C., Lavanya, A., and Nanna, R. (2014). Purification of *Streptococcus pneumoniae* capsular polysaccharides using aluminium phosphate and ethanol. *Int. J. Pharm. Pharm. Sci.* 6, 664–670.

Melegaro, A., Edmunds, W., Pebody, R., Miller, E., and George, R. (2006). The current burden of pneumococcal disease in England and Wales. *J. Infect.* 52, 37–48. doi: 10.1016/j.jinf.2005.02.008

Mitchell, A. M., and Mitchell, T. J. (2010). *Streptococcus pneumoniae*: virulence factors and variation. *CMI* 2010, 411–418. doi: 10.1111/j.1469-0691.2010.03183.x

Morais, V., Dee, V., and Suárez, N. (2018). Purification of capsular polysaccharides of *Sterptococcus pneumoniae*: traditional and new methods. *Front. Bioeng. Biotechnol.* 12:145. doi: 10.3389/fbioe.2018.00145

Nielsen, S. V., Sørensen, U. B., and Henrichsen, J. (1993). Antibodies against pneumococcal C-polysaccharide are not protective. *Microb. Pathog.* 14, 299–305. doi: 10.1006/mpat.1993.1029

Örtqvist, Å (1999). Pneumococcal disease in Sweden: experiences and current situation. *Am. J. Med.* 107, 44–49. doi: 10.1016/S0002-9343(99)00101-101

Snyder, S. L., and Sobocinski, P. Z. (1975). An improved 2,4,6-trinitrobenzenesulfonic acid method for the determination of amines. *Anal. Biochem.* 64, 284–288. doi: 10.1016/0003-2697(75)90431-5

Sørensen, U. B., Henrichsen, J., Chen, H.-C., and Szu, S. C. (1990). Covalent linkage between the capsular polysaccharide and the cell wall peptidoglycan of *Streptococcus pneumoniae* revealed by immunochemical methods. *Microb. Pathog.* 8, 325–334. doi: 10.1016/0882-4010(90)90091-90094

Suárez, N., Fraguas, L. F., Texeira, E., Massaldi, H., Batista-Vieira, F., and Ferreira, F. (2001). Production of capsular polysaccharide of *Streptococcus pneumoniae* type 14 and its purification by affinity ahromatography. *Appl. Microbiol.* 67, 969–971. doi: 10.1128/aem.67.2.969-971.2001

Suárez, N., Massaldi, H., Frguas, L. F., and Ferreira, F. (2008). Improved conjugation and purification strategies for the preparation of protein-polysaccharide conjugates. *J. Chromatogr. A* 1213, 169–175. doi: 10.1016/j.chroma.2008.10.030

Tuomanen, E., Rich, R., and Zak, O. (1987). Induction of pulmonary inflammation by components of the Pneumococcal cell surface 1– 2. *Am. Rev. Respir. Dis.* 135, 869–874. doi: 10.1164/arrd.1987.135.4.869

Vialle, S., Sepulcri, P., Dubayle, J., and Talaga, P. (2005). The teichoic acid (C-polysaccharide) synthesized by *Streptococcus pneumoniae* serotype 5 has a specific structure. *Carbohydr. Res.* 340, 91–96. doi: 10.1016/j.carres.2004.10.021

Xu, Q., Abeygunawardana, C., Ng, A. S., Sturgess, A. W., Harmon, B. J., and Hennessey, J. P. (2005). Characterization and quantification of C-polysaccharide in *Streptococcus pneumoniae* capsular polysaccharide preparations. *Anal. Biochem.* 336, 262–272. doi: 10.1016/j.ab.2004.10.019

Yuan, Y., Ruppen, M., Sun, W.-Q., Chu, L., Simpson, J., Patch, J., et al. (2014). *Shortened Purification Process for the Production of Capsular Sreptococcus pneumoniae Polysaccharide*. United States Patent #US 8999697B2.

Zanardo, R. T., Figueiredo, D. B., Kraschowetz, S., Cabrera-Crespo, J., and Gonçalves, V. M. (2016). Development of a new process for purification of capsular polysaccharide from *Streptococcus pneumoniae* serotype 14. *Braz. J. Chem. Eng.* 33, 435–443. doi: 10.1590/0104-6632.20160333s20150140

Conflict of Interest: CL, HC, MP, RK, YW, SC, YB, and IL were employed by the company R&D Center, EuBiologics Co., Ltd.

The remaining author declares that the research was conducted in the absence of any commercial or financial relationships that could be construed as a potential conflict of interest.

frontiers in Bioengineering and Biotechnology

REVIEW
published: 24 March 2020
doi: 10.3389/fbioe.2020.00222

Laccases in Food Industry: Bioprocessing, Potential Industrial and Biotechnological Applications

Karla Mayolo-Deloisa[1†], Mirna González-González[2†] and Marco Rito-Palomares[2]*

[1] Tecnologico de Monterrey, Escuela de Ingeniería y Ciencias, Monterrey, Mexico, [2] Tecnologico de Monterrey, Escuela de Medicina y Ciencias de la Salud, Monterrey, Mexico

Laccase is a multi-copper oxidase that catalyzes the oxidation of one electron of a wide range of phenolic compounds. The enzyme is considered eco-friendly because it requires molecular oxygen as co-substrate for the catalysis and it yields water as the sole by-product. Laccase is commonly produced by fungi but also by some bacteria, insects and plants. Due it is capable of using a wide variety of phenolic and non-phenolic substrates, laccase has potential applications in the food, pharmaceutical and environmental industries; in addition, it has been used since many years in the bleaching of paper pulp. Fungal laccases are mainly extracellular enzyme that can be recovered from the residual compost of industrial production of edible mushrooms as *Agaricus bisporus* and *Pleurotus ostreatus.* It has also been isolated from microorganisms present in wastewater. The great potential of laccase lies in its ability to oxidize lignin, one component of lignocellulosic materials, this feature can be widely exploited on the pretreatment for agro-food wastes valorization. Laccase is one of the enzymes that fits very well in the circular economy concept, this concept has more benefits over linear economy; based on "reduce-reuse-recycle" theory. Currently, biorefinery processes are booming due to the need to generate clean biofuels that do not come from oil. In that sense, laccase is capable of degrading lignocellulosic materials that serve as raw material in these processes, so the enzyme's potential is evident. This review will critically describe the production sources of laccase as by-product from food industry, bioprocessing of food industry by-products using laccase, and its application in food industry.

Keywords: agro-food wastes, by-products, bioprocessing, food industry, laccase

OPEN ACCESS

Edited by:
Sónia Patrícia Marques Ventura, University of Aveiro, Portugal

Reviewed by:
Alessandro Pellis, University of Natural Resources and Life Sciences, Austria
Ana Paula Mora Tavares, University of Aveiro, Portugal

***Correspondence:**
Marco Rito-Palomares
mrito@tec.mx

[†]These authors have contributed equally to this work

Specialty section:
This article was submitted to Industrial Biotechnology, a section of the journal Frontiers in Bioengineering and Biotechnology

Received: *18 September 2019*
Accepted: *05 March 2020*
Published: *24 March 2020*

Citation:
Mayolo-Deloisa K, González-González M and Rito-Palomares M (2020) Laccases in Food Industry: Bioprocessing, Potential Industrial and Biotechnological Applications. Front. Bioeng. Biotechnol. 8:222. doi: 10.3389/fbioe.2020.00222

INTRODUCTION

Laccase (benzenediol:oxygen oxidoreductase; EC 1.10.3.2) is a blue-copper oxidoreductase that catalyze the oxidation of wide range of substrates including phenolic compounds with the concomitant reduction of molecular oxygen to water (Nunes and Kunamneni, 2018). Fungal laccases contain two disulfide bonds and four copper atoms distributed in three cupper centers: T1, T2, and T3. Type I (T1) is mononuclear and has an absorption band at around 610 nm, which

is responsible for the characteristic blue color of such enzyme. T2/T3 are a trinuclear cluster. The oxidation of the substrate is carried out in T1, through a His-Cys-His tripeptide sequence, the extracted electrons are transferred to the T2/T3 site where the reduction of molecular oxygen to water finally occurs (Osma et al., 2010; Hautphenne et al., 2016; Nunes and Kunamneni, 2018). That is the reason why laccase is considered as a "green tool," due to it is able to perform the catalysis process using molecular oxygen as the only co-substrate rather than hydrogen peroxide like other oxidoreductases (*v.gr.* lignin peroxidase and manganese peroxidase) (Agrawal et al., 2018). Laccase can cooperate with small compounds called "mediators" and oxidize non-phenolic compounds, so that its activity is not limited only to phenolic compounds (Chio et al., 2019). Mediator is oxidized giving one or more electrons to laccase, after the mediator oxidized form diffuses away from the catalytic pocket, where it is capable of oxidizing the substrate. Mediator is able of oxidizing substrates inaccessible for the laccase due to its small size (Rochefort et al., 2004; Munk et al., 2018). Most biotechnologically useful laccases are fungal origin, however, the enzyme has been found in plants, insects and some bacteria (Nunes and Kunamneni, 2018). Around 150 laccases have been fully characterized. The most studied have been isolated from fungi capable of destroying wood, especially white-rot fungi as: *Pleurotus pulmonarius*, *Pleurotus ostreatus*, *Agaricus bisporus*, *Trametes versicolor*, etc. (Bertrand et al., 2016; Nunes and Kunamneni, 2018). The production of the enzyme can be influenced for the type of culture (submerged or solid state), type of microelements and the source of nitrogen. Generally, the enzyme is produced during the fungi secondary metabolism (Brijwani et al., 2010). Laccases are secreted, with typical molecular weight around of 60 kDa. Typical fungal laccases have an isoelectric point around 4.0, however there are some laccases with basic isoelectric points (Mukhopadhyay and Banerjee, 2015). The optimal temperature of fungal laccases may vary in a range of 40–70°C (Debaste et al., 2018). They are generally glycosylated, which contributes to the high stability of the enzyme (Osma et al., 2010). Owing its versatility, stability, and wide range of substrates; a large number of laccase industrial applications have been explored in the past years, including delignification and brightening of pulp paper, decolorization of dyes in textile industry, bioremediation of soils, organic synthesis of medications, biosensor technology, and in food processing (Upadhyay et al., 2016).

In nature, laccase is secreted by the fungus to access carbohydrates (cellulose and hemicellulose) in the wood through the degradation of lignin (Osma et al., 2010). Lignin, which is a phenylpropanoid biopolymer, it is considered the most abundant polymer in nature (Chio et al., 2019). Lignin has an extremely complex structure; it is recalcitrant and difficult to degrade. In its natural state it has practically no applications, however, it can be burned to get energy. That is why one of the great challenges to allow the use of lignin is its depolymerization. Currently, there are different methods of lignin depolymerization: thermo-chemical, mechanical, chemical, and biological (Chio et al., 2019). Naturally, biological treatments have been classified as "environmental friendly catalyst" since they are developed by microorganisms or enzymes that are generally not toxic (Chio et al., 2019). In addition, biological treatments have low energy requirements, reduced waste streams and low downstream cost (Albornoz et al., 2018). In this way, the role of laccases in the production of bioethanol through the pretreatment of ligninolytic residues has been studied. Since the treatment with laccase allows the degradation of lignin which increases the fermentability of such ligninolytic residues (Agrawal et al., 2018). It is known that with help of mediators, laccase degrades almost 80–90% of lignin structure (Chio et al., 2019). The conversion of lignin moieties into biofuels is one of the objectives of biorefinery (Ponnusamy et al., 2019). In general, biorefinery has been defined as a facility for converting lignocellulosic materials into bioenergy and chemicals with potential industrial significance (Roth and Spiess, 2015; Sperandio and Ferreira Filho, 2019). As mentioned earlier, lignocellulosic materials are very abundant and therefore represent a much more suitable resource as a raw material for biorefineries. Thus eliminating the problem of using feedstock for producing biofuel that can be used in food production (Roth and Spiess, 2015).

In this review paper; we analyzed the production sources of laccase, together with the state of the art in the recovery of laccase from by-products generated mainly by the food industry. The bioprocessing of the food industry by-products using laccase and the potential applications of the enzyme in the food industry are presented. Potential trends and current challenges of the potential application of laccase are critically described.

LACCASE AS BY-PRODUCT FROM FOOD INDUSTRY

The biological pretreatment of lignocellulosic biomass is cost-effective and eco-friendly. Lignin can be degraded by enzymes secreted through the metabolism of wide variety of fungi. For example, white-rot fungi show more significant effects in the degradation of lignocellulose materials (Ponnusamy et al., 2019). Traditionally, laccase has been produced by white-rot fungi using submerged fermentation batch culture. This strategy is very convenient due it makes possible to control the conditions and enhance the production of the enzyme. Nevertheless, sometimes it can be an expensive process, especially if the enzyme requires a high fold purification. The production of laccase at laboratory level has been widely reported, however in the market, there are only some presentations from fungi available such as *Agaricus bisporus*, *Coriolus versicolor*, *Pleurotus ostreatus*, *Trametes versicolor,* and *Rhus vernicifera* (Osma et al., 2010). A great alternative to obtain laccase from agro-food wastes is the residual compost used for the commercial production of edible mushrooms; because laccase is secreted to the compost during the growth of the fungus.

Royse et al. (2017) reported that in the last 40 years the cultivation of edible mushrooms in the world increased about 30-fold, which gives an idea of the commercial value of this type of food. In 2013, the mushroom production industry was valued about of $63 billion and in *per capita* consumption it

exceeds 4.7 kg annually. Cultivated mushroom are saprophytes, capable of growing on lignocellulosic materials as they have the ability to degrade them, such materials are generally abundant and may come from industrial or agricultural wastes (Kertesz and Thai, 2018). Residual compost is available in huge amounts; when 1 kg of mushrooms is produced, about 5 kg of residual compost are obtained (Grimm and Wösten, 2018). Among the main edible mushrooms produced around the world are the genera: *Lentinula*, *Pleutorus*, *Auricularia*, *Agaricus,* and *Flammulina*. *Lentinula edodes* (Wong et al., 2013), *Agaricus bisporus,* and *Pleurotus ostreatus* have been recognized as laccase-producing basidiomycetes and they are produced at industrial scale (Yang et al., 2017).

Agaricus bisporus is one of the most produced mushrooms worldwide, capable of using different substrates for its growth (Trejo-Hernandez et al., 2001). The compost used is a complex mixture prepared using horse manure and/or straw added with nitrogen sources such as poultry manure, urea, ammonium nitrate and plaster (Kertesz and Thai, 2018). The production of laccase during the growth of *A. bisporus* on this type of compost has been reported previously so it is known that large quantities of laccase are secreted. Once the fungus production is finished, the compost can be discarded (Trejo-Hernandez et al., 2001; Mayolo-Deloisa et al., 2009). There are some studies demonstrating the presence of laccase in the residual compost. Trejo-Hernandez et al. (2001) evaluated the oxidative capacity of an aqueous crude extract from compost using various phenolic compounds which are laccase typical substrates. On such studies, they worked with an aqueous extract of the residual compost; that is to say, the enzyme was not pure. That represents an advantage, if the future application does not require a high pure laccase, as it is the case of decolorization of textile dyes. Further, the use of aqueous two phase systems (ATPS) for the primary recovery of laccase from residual compost of *A. bisporus* has been reported (see **Figure 1**; Mayolo-Deloisa et al., 2009). The most commonly used ATPS are formed by two polymers or one polymer and one salt, which mixed in critical concentrations demonstrate incompatibility (Mayolo-Deloisa et al., 2017). The components of each phase are immiscible despite containing about 80% water (molal base). Each phase has different characteristics, which allows them to partition a sample with different molecules (Zaslavsky et al., 2016). They are considered as a primary recovery stage for the separation of biological molecules, due to the large amount of water they contain. ATPS have been used for the treatment of complex samples such as the aqueous extract of residual compost. In that work, polyethylene glycol (PEG) - phosphate ATPS were utilized and the presence of laccase in the PEG rich-phase (top-phase) was proved. It is known that PEG prevents aggregation and gives some stability to proteins, so it was not separated from laccase and the top-phase was used to oxide several Polycyclic Aromatic Hydrocarbons (PAHs), which are generally present in the most recalcitrant fraction of crude oil. The best results were reached with the oxidation of benzo[a]pyrene (BaP), which is formed by a very complex structure difficult to degrade. During the treatment, no interference was observed due to the presence of PEG, on the contrary, a higher oxidation percentage was achieved than the one obtained with the crude extract (Mayolo-Deloisa et al., 2011).

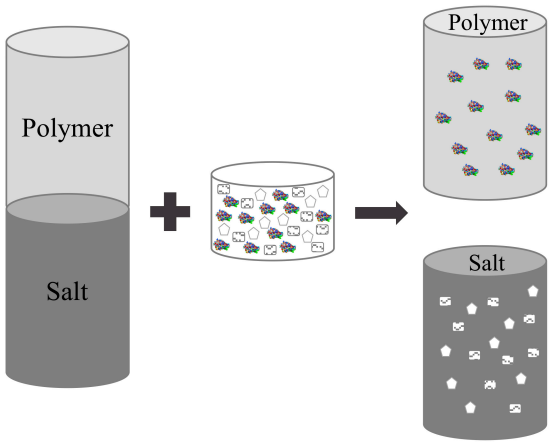

FIGURE 1 | Aqueous two-phase systems (ATPS). ATPS can be formed through the combination of two polymers or a polymer and a salt at critical concentrations. Many parameters are involved in the partition, however in general the enzyme is concentrated in one of the phases.

On the other hand, *Pleurotus ostreatus* is one of the most-produced species in the world. It is cultivated mainly on sawdust but it is capable of a rapid conversion of other substrates, including bagasse and cornstalks. Generally the fungus grows by competing with other microorganisms since it is not very common to sterilize the compost before being inoculated (Kertesz and Thai, 2018). The residual compost from *Pleurotus ostreatus* has been used in the production of bioethanol as it is a rich source of sugars such as glucose and xylose (Grimm and Wösten, 2018). Additionally, the presence of laccase in this waste has also been proved. Bertrand et al. (2016) evaluated the potential of different ATPS in the partial recovery of laccase including PEG-phosphate, UCON-salts and polymer-polymer ATPS. The UCON-salts ATPS, specially UCON-$(NH_4)_2SO_4$, reached a recovery percentage and purification factor up to 98.31% and 9.97, respectively. This demonstrates the potential of systems to recover laccase. UCON is a random copolymer (composed by 50% ethylene oxide and 50% propylene oxide) with a cloud point temperature as low as 40°C. It is a thermoresponsive polymer so it is easier to recover it after a temperature change, where laccase can be separated and the polymer can be recycled (Pereira et al., 2003). Additionally, polymer-polymer systems as PEG10,000/Dextran 10,000 and PEG10,000/Dextran 100,000 have also proved their potential in the recovery of the enzyme; reaching high purification factors. In general, polymer-polymer systems are more expensive, so their application will depend on the final destination of the enzyme.

Laccase can be recovered from residual compost, a lignocellulosic material waste from food industry. After the recovery, laccase can be used for different applications including the degradation of other lignocellulosic materials. It is clear that ATPS represents a viable alternative to be applied in the primary recovery of this enzyme from waste. ATPS-based processes can

be formed through a large combination of polymers and salts, are often inexpensive and easy to scale up for commercial purposes.

PRODUCTION OF LACCASE USING AGRORESIDUES

The generation of waste from the processing of fruits and vegetables represents up to 60% of its production, which highlights the importance of developing new alternatives for the use of this material (Pleissner et al., 2016). There are also other sources of waste production such as those generated by the processing of palm oil and rubber wood that are discharged in large quantities into the environment (Vikineswary et al., 2006). Many of them are lignocellulosic residues. The potential of using such residues in the growth of the *Pycnoporus sanguineus* fungus through solid state fermentation (SSF) has been previously reported, proving that it is a route for the production of laccase (**Figure 2**). Laccase can be produced with high yields through the degradation of sago and oil palm parenchyma tissue (Rajagopalu et al., 2016). There are also other residues that have been reported for the growth of the *Ganoderma lucidum* fungus, including sunflower seed hulls and rice residues (straw and husk). *G. lucidum* is a laccase-producing fungus, recognized as a medicinal mushroom and highly valued in the market. Pilot-scale studies demonstrated the bioconversion of these substrates during the production process of *G. lucidum*, additionally the presence of laccase in the different crude extracts was also detected. This suggests that there is an area of opportunity in the optimization of enzyme production (Postemsky et al., 2017). There is also evidence of the use of paddy straw and coir pith in combination with biogas digester residue (anaerobically digested plant material) in the cultivation of *Pleurotus ostre*atus and *Pleurotus florida*; reaching high levels of fungus production and demonstrating effectiveness in the degradation of lignin, cellulose, and hemicellulose. Although in this case, the production of laccase was not directly measured, its activity is implicit due to the degradation of lignin (Chanakya et al., 2015). In addition, there are other substrates of agro-industrial origin that can be used for the growth of ligninolytic fungi and therefore for the production of laccase. These may include: barley bran, chestnut shell waste, potato pulp, banana skins, mandarin peels, kiwifruit wastes, and grape seeds (Strong and Claus, 2011).

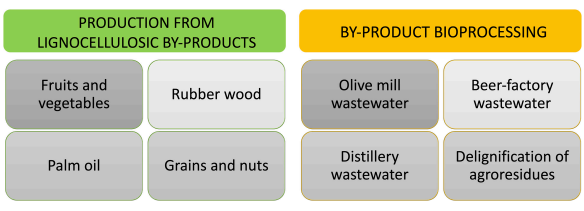

FIGURE 2 | Laccase in food industry. Laccase can be used for the bioprocessing of different food industry by-products, as well as produced in agroresidues by laccase producing fungi.

BIOPROCESSING OF FOOD INDUSTRY BY-PRODUCTS USING LACCASE

Many by-products generated by food industry have high content of phenolic compounds, low pH, as well as high biochemical oxygen demand (BOD) and chemical oxygen demand (COD). Due such complex characteristics is difficult to apply directly a treatment using microorganisms hence enzymatic treatments are more appropriate. Thus, this section will review the main applications of laccase in the processing of by-products from food industry (summarized in **Figure 2**).

Olive-Oil Mill Wastewater

The olive-oil production process contributes significantly to the pollution of the Mediterranean area, because it generates a large amount of both solid and liquid wastes with a concentration of organic compounds that is toxic to nature (Osma et al., 2010; Jurado et al., 2011). The biggest problem in olive-oil wastewater treatment is principally related to the low pH, high BOD, COD, the high concentration of phenols (from 1.5 to 8.0 g/L) and other organic substances (Chiacchierini et al., 2004). Chemical treatments have so far been the most used to treat this waste. However, due to the toxicity of the residue, biological treatments directly with ligninolytic fungi and/or their enzymes have been studied (Berrio et al., 2007). Laccase from white-rot fungi as *Pleurotus ostreatus*, *Trametes versicolor, Lentinula edodes, Cerrena unicolor*, and *Pycnoporus coccineus* have been able to oxidize different phenolic compounds present in olive-oil mill wastewaters (Osma et al., 2010), and such activity can be enhanced by enzyme immobilization (Berrio et al., 2007). A strong impact of the enzyme on color removal and phytotoxicity has also been reported (Strong and Claus, 2011).

Distillery Wastewater

During the fermentation of molasses from sugarcane, ethanol is produced, which leads to the generation of distillery wastewater (Osma et al., 2010). Due to its extreme physicochemical characteristics such as high content of organic and inorganic matter, high values of BOD and COD, acidic pH, high concentration of ash, high temperature, and dark color; distillery wastewater is one of the most polluting waste and difficult to degrade (Kharayat, 2012). The effectiveness of the laccase in removing phenolic compounds and the color of different distillery wastewater has been evaluated, however it has been found that the fungal culture is more effective than the laccase alone (Strong and Burgess, 2008). Which suggests that this residue can also be used for the production of ligninolytic enzymes (as laccase) using it as a substrate for the growth of white-rot fungi.

Beer-Factory Wastewater

Another residue contaminated with a high load of polyphenolic compounds (especially tannins) is that generated from beer production (Chiacchierini et al., 2004). Tannins are one of the very abundant phenolic compounds in plants, only surpassed by lignin. There are studies that shown the efficiency of *Corolopsis*

gallica in the decolorization and a reduction of the COD of a beer-industry effluent containing a high tannins proportion (Yagüe et al., 2000). *C. gallica* fungus is able to grow on beer-factory wastewater because it has a high tolerance to tannins which even allows the production of laccase. It has been observed that when this residue is added to the fungus culture, laccase secretion is increased (Chiacchierini et al., 2004).

Delignification of Agroresidues

Laccase is one of the enzymes that fits very well in the circular economy concept, this concept has more benefits over linear economy; based on "reduce-reuse-recycle" theory (Agrawal et al., 2018; Giacobbe et al., 2018). In that sense and as mentioned before, laccase can be recovered from waste materials after industrial mushroom cultivation but can also be used to treat lignocellulosic residues generated by agro-industrial activities (Jurado et al., 2011). Agroresidues contain high concentrations of cellulose and hemicellulose that can be a raw material used in biorefinery processes (Giacobbe et al., 2018). It has been reported that the use of laccase for the degradation of lignin present in food residues, such as apple pomace and coffee silverskin, allows the hydrolysis of hemicellulose generating a high sugar content (Giacobbe et al., 2018). In the same way the use of laccase from *Myrothecium verrucaria* in the delignification of agroresidues (like wheat straw, rice straw, and sugar cane bagasse) has been reported, reaching efficient delignification in the absence of mediators (Agrawal et al., 2018).

FOOD INDUSTRY APPLICATION OF LACCASE

Over the years, laccase has been used in the food industry especially in the determination of different phenolic compounds that can affect the quality of some products. **Table 1** summarizes some of the most important applications of laccase in the processing of foods.

Beverage Processing

The content and quantity of phenolic compounds present in juices affects their quality, changing their color and taste and thus decreasing their value. Darkening of these products is very common due to the presence of polyphenols. In that sense, it has been demonstrated the high efficacy of laccase to remove phenols, avoiding the use of other chemical treatments such as activated carbon adsorption (Ribeiro et al., 2010). Color stability can be greatly increased after the treatment with the enzyme (Brijwani et al., 2010).

TABLE 1 | Direct applications of laccase in food processing industry.

Food application	Objective	References
Beverage processing	Enhance or modify color appearance	Osma et al., 2010
Wine stabilization	Selective polyphenol removal	Minussi et al., 2007
Beer stabilization	Removal of oxygen in finished beer	Osma et al., 2010
Baking	Increase strength, stability, and reduce stickiness improving machinability of the dough	Selinheimo et al., 2006; Osma et al., 2010
Sugar beet pectin gelation	Crosslink the beet pectin through the oxidative coupling of the feruloyl groups	Micard and Thibault, 1999; Minussi et al., 2002

Wine Stabilization

One of the best known applications of laccase in the food industry is in the wine stabilization through the control of phenolic compounds (Osma et al., 2010). The maintenance of flavor in this type of products is fundamental for quality control. Besides, the oxidative reactions that may occur due to the complexity of the mixture of chemicals in the wines can even intensify the color, especially in red wines (Minussi et al., 2007). Chemical methods for the elimination of phenolic compounds, such as the addition of polyvinylpolypyrrolidone (PVPP) and sulfur dioxide, have been used to stabilize the wines and prevent the loss of flavor and color quality (Minussi et al., 2002). Due laccase has good stability at low pH and it is possible to reverse its inhibition with sulfite, the treatment of wines with the enzyme is widely used (Osma et al., 2010). It has been reported that the treatment of white wine with laccase is also feasible, this represents an alternative to ensure the quality of the wines that remain stored for a long time, avoiding their deterioration and reducing the costs of their production. In addition to the advantage of using an ecological treatment (Minussi et al., 2007).

Beer Stabilization

Another product that needs to be stored for long time periods is beer. The control of temperature, oxygen and a cloudy appearance are factors that can affect its quality (Osma et al., 2010). The presence of phenolic compounds such as proanthocyanidins can provoke the precipitation of proteins favoring haze formation (Brijwani et al., 2010). The half-life of the beer can be prolonged through laccase treatment, which can be added at the end of the production process allowing the oxidation of the phenolic compounds (Osma et al., 2010).

Baking

Enzymes have been widely used in the bakery industry because they improve the texture of bread. Laccase is no exception and its usage has been reported to improve dough consistency and enhancing strength of gluten structures. It has also been observed how the structure of the crumb changes, the volume and softness of the dough is improved when the laccase is added (Brijwani et al., 2010).

Sugar Beet Pectin Gelation

This product is a gel formed by the oxidative cross-linking of ferulic acid, widely used in the food industry due to its functional properties. The oxidative process can be carried out by oxidoreductases such as laccase and peroxidase. There is a fundamental difference between these enzymes, laccase only needs molecular oxygen for the oxidation process while peroxidase requires the presence of H_2O_2. The obtained gel after the process with laccase is thermo-irreversible and can be used in products like luncheon meat (Norsker et al., 2000; Minussi et al., 2002).

The main applications of laccase directly in food processing were aforementioned. However, alternative indirect applications have been reported. These applications may include: laccase amperometric biosensors to measure polyphenols concentration (Osma et al., 2010); the detection and quantification of ascorbic acid in different products and other biosensors for glucose and aromatic amines determination (Minussi et al., 2002). Additionally, laccase has also been applied in the synthesis of medications such as analgesic, sedatives, anti-inflammatory and antibiotics (Upadhyay et al., 2016).

POTENTIAL TRENDS AND CURRENT CHALLENGES

The use of by-products from food industry is a growing trend due to the prevailing need to combat environmental pollution and follow the trend of "reduce-reuse-recycle." So, researchers have a shared responsibility with the private initiative to explore ways for the proper disposal of waste and its reuse in the generation of new products.

Edible mushrooms production represents one of the most important food industries around the world. As already mentioned, the production of laccase during the cultivation of different species of fungi has been proven through different studies. However, not many studies are known about the increase in laccase concentration during the industrial production of these fungi without altering their nutritional value. Which represents an area of opportunity in the optimization of the production of the fungus, while optimizing the production of laccase and even other ligninolytic enzymes. In turn, it is necessary to optimize the recovery process of the enzyme from the residual compost, explore other primary recovery techniques and purification stages that allow high purities to be achieved. This represents a real challenge, since the crude extract is very complex and not well characterized. In that sense, the integration of ultrasonication in the primary recovery of laccase using ATPS can be a suitable option for to increase the yield. It has been reported that its use can increase the yield, especially of phenolic compounds, in addition to increasing the activity; so, it could be an excellent strategy to treat the crude extract from the residual compost and evaluate its impact in the laccase activity.

Laccase production at the laboratory level in submerged cultivation has been widely reported in recent years. However, in the market there are few presentations of the enzyme, with low levels of purity and from extracts that are not fully characterized, which complicates the reproducibility of many processes that were mentioned throughout this work. Therefore, it is necessary to increase the interest in the area of production and purification of commercial laccases for the development of new products.

The potential of laccase in the pretreatment of lignocellulosic residues to integrate them into biorefinery processes in order to obtain biofuels has been well established in the literature. However, it is necessary to further consider the optimization of conditions to obtain the highest degradation yields, since in many occasions the effectiveness of the fungus is greater than the enzyme. This may be due to the presence of other ligninolytic enzymes, so the possibility of using enzyme cocktails, increase the affinity of laccase through different chemical modifications or realize changes in the parameters of the reactions that are being carried out should be explored.

Additionally, the modification of the laccase through the covalent attachment of one molecule of PEG, known as PEGylation, can be considered to improve its stability. PEGylation is common process reported for the modification of protein drugs and its efficiency has been widely demonstrated. Even though, there are few reports about laccase PEGylation, they present evidence on the improvement of its catalytic activity (Mayolo-Deloisa et al., 2015; Su et al., 2018). This can be an alternative when the process justifies it, especially when the enzyme is used for the detection of certain compounds using biosensors. In that sense, one of the applications of laccase is the detection of various compounds in certain foods. However, it is also used for the synthesis of chemical compounds, their detection and recently it has been reported that the enzyme is capable of removing morphine from aqueous systems (Huber et al., 2018). This reflects the great potential of the enzyme not only in the food industry but also for the recovery of contaminated areas, hence the importance and relevance of the information presented here.

CONCLUDING REMARKS

Laccase is one of the most studied enzymes in the world. Its low substrate specificity and capacity to degrade phenolic compounds using just oxygen, make it suitable for different industrial applications. In addition, it is secreted by several microorganisms to degrade lignin, especially the white-rot fungi. The enzyme can be recovered from residual compost of edible mushroom as *Agaricus bisporus* and *Pleurotus ostreat*us using aqueous two-phase systems; thereby this technique can be applied for the extraction of the enzyme from other food by-products. Laccase is also capable of degrading phenolic compounds present in wastewaters from food processing such as olive oil, fermentation of sugarcane molasses, and brewing. However, laccase can also be produced using many of the agro-residues from the food industry, as lignocellulosic waste can serve as a substrate for many enzyme-producing fungi, generating a cycle of production and reuse suitable to be applied in the circular economy. This makes the enzyme highly valued in biorefinery processes for its already recognized ability to degrade lignin naturally. In addition, laccase is widely used in various food industry processes such as beverage processing, baking, stabilization of wine and beer, and sugar beet pectin gelation. This potential justifies the need to deepen the sources of production and purification processes of the enzyme. Furthermore, the opportunity to establish a complete process where the enzyme is obtained from a waste material, recovered purified and placed on the market for a new application, is still available.

AUTHOR CONTRIBUTIONS

KM-D and MG-G defined the general objective and the topics to be discussed. KM-D wrote and discussed the sections "Laccase as By-Product From Food Industry," "Production of Laccase

Using Agroresidues," and "Concluding Remarks." MG-G wrote the sections "Introduction" and "Bioprocessing of Food Industry By-Products Using Laccase." MR-P wrote the sections "Food Industry Application of Laccase" and "Potential Trends and Current Challenges." All authors contributed to the final review of the manuscript.

ACKNOWLEDGMENTS

The authors would like to thank the Translational Omics (Grant No. 002EICCB01) and Bioengineering and Regenerative Medicine (Grant No. 0020609M07) strategic focus group of Tecnologico de Monterrey.

REFERENCES

Agrawal, K., Chaturvedi, V., and Verma, P. (2018). Fungal laccase discovered but yet undiscovered. *Bioresour. Bioprocess.* 5:4. doi: 10.1186/s40643-018-0190-z

Albornoz, S., Wyman, V., Palma, C., and Carvajal, A. (2018). Understanding of the contribution of the fungal treatment conditions in a wheat straw biorefinery that produces enzymes and biogas. *Biochem. Eng. J.* 140, 140–147. doi: 10.1016/j.bej.2018.09.011

Berrio, J., Plou, F. J., Ballesteros, A., Martínez, Á. T., and Martínez, M. J. (2007). Immobilization of *Pycnoporus coccineus* laccase on Eupergit C: stabilization and treatment of olive oil mill wastewaters. *Biocatal. Biotransform.* 25, 130–134. doi: 10.1080/10242420701379122

Bertrand, B., Mayolo-Deloisa, K., González-González, M., Tinoco-Valencia, R., Serrano-Carreón, L., Martínez-Morales, F., et al. (2016). *Pleurotus ostreatus* laccase recovery from residual compost using aqueous two-phase systems. *J. Chem. Technol. Biotechnol.* 91, 2235–2242. doi: 10.1002/jctb.4995

Brijwani, K., Rigdon, A., and Vadlani, P. V. (2010). Fungal laccases: production, function, and applications in food processing. *Enzyme Res.* 2010:149748. doi: 10.4061/2010/149748

Chanakya, H. N., Malayil, S., and Vijayalakshmi, C. (2015). Cultivation of *Pleurotus* spp. on a combination of anaerobically digested plant material and various agro-residues. *Energy Sustain. Dev.* 27, 84–92. doi: 10.1016/j.esd.2015.04.007

Chiacchierini, E., Restuccia, D., and Vinci, G. (2004). Bioremediation of food industry effluents: recent applications of free and immobilised polyphenoloxidases. *Food Sci. Technol. Int.* 10, 373–382. doi: 10.1177/1082013204049388

Chio, C., Sain, M., and Qin, W. (2019). Lignin utilization: a review of lignin depolymerization from various aspects. *Renew. Sustain. Energy Rev.* 107, 232–249. doi: 10.1016/j.rser.2019.03.008

Debaste, F., Flahaut, S., Penninckx, M., and Songulashvili, G. (2018). "Chapter 15 – using laccases for food preservation," in *Food Packaging and Preservation*, eds A. M. Grumezescu, and A. M. Holban (Cambridge, MA: Academic Press).

Giacobbe, S., Pezzella, C., Lettera, V., Sannia, G., and Piscitelli, A. (2018). Laccase pretreatment for agrofood wastes valorization. *Bioresour. Technol.* 265, 59–65. doi: 10.1016/j.biortech.2018.05.108

Grimm, D., and Wösten, H. A. B. (2018). Mushroom cultivation in the circular economy. *Appl. Microbiol. Biotechnol.* 102, 7795–7803. doi: 10.1007/s00253-018-9226-8

Hautphenne, C., Penninckx, M., and Debaste, F. (2016). Product formation from phenolic compounds removal by laccases: a review. *Environ. Technol. Innov.* 5, 250–266. doi: 10.1016/j.eti.2016.04.001

Huber, D., Bleymaier, K., Pellis, A., Vielnascher, R., Daxbacher, A., Greimel, K. J., et al. (2018). Laccase catalyzed elimination of morphine from aqueous systems. *New Biotechnol.* 42, 19–25. doi: 10.1016/j.nbt.2018.01.003

Jurado, M., Martínez, Á. T., Martínez, M. J., and Saparrat, M. C. N. (2011). Application of white-rot fungi in transformation, detoxification, or revalorization of agriculture wastes: role of laccase in the processes. *Comprehen. Biotechnol.* 6, 595–603. doi: 10.1016/b978-0-08-088504-9.00398-6

Kertesz, M. A., and Thai, M. (2018). Compost bacteria and fungi that influence growth and development of *Agaricus bisporus* and other commercial mushrooms. *Appl. Microbiol. Biotechnol.* 102, 1639–1650. doi: 10.1007/s00253-018-8777-z

Kharayat, Y. (2012). Distillery wastewater: bioremediation approaches. *J. Integr. Environ. Sci.* 9, 69–91. doi: 10.1080/1943815X.2012.688056

Mayolo-Deloisa, K., Benavides, J., and Rito-Palomares, M. (2017). "General concepts and definitions of aqueous two-phase systems," in *Aqueous Two-Phase Systems for Bioprocess Development for the Recovery of Biological Products*, eds M. Rito-Palomares, and J. Benavides (Cham: Springer International Publishing).

Mayolo-Deloisa, K., González-González, M., Simental-Martínez, J., and Rito-Palomares, M. (2015). Aldehyde PEGylation of laccase from *Trametes versicolor* in route to increase its stability: effect on enzymatic activity. *J. Mol. Recognit.* 28, 173–179. doi: 10.1002/jmr.2405

Mayolo-Deloisa, K., Machin-Ramirez, C., Rito-Palomares, M., and Trejo-Hernandez, M. R. (2011). Oxidation of polycyclic aromatic hydrocarbons using partially purified laccase from residual compost of *Agaricus bisporus*. *Chem. Eng. Technol.* 34, 1368–1372. doi: 10.1002/ceat.201000205

Mayolo-Deloisa, K., Trejo-Hernández, M. R., and Rito-Palomares, M. (2009). Recovery of laccase from the residual compost of *Agaricus bisporus* in aqueous two-phase systems. *Process Biochem.* 44, 435–439. doi: 10.1016/j.procbio.2008.12.010

Micard, V., and Thibault, J. F. (1999). Oxidative gelation of sugar-beet pectins: use of laccases and hydration properties of the cross-linked pectins. *Carbohyd. Polym.* 39, 265–273. doi: 10.1016/S0144-8617(99)00012-0

Minussi, R. C., Pastore, G. M., and Durán, N. (2002). Potential applications of laccase in the food industry. *Trends Food Sci. Technol.* 13, 205–216. doi: 10.1016/S0924-2244(02)00155-3

Minussi, R. C., Rossi, M., Bologna, L., Rotilio, D., Pastore, G. M., and Durán, N. (2007). Phenols removal in musts: strategy for wine stabilization by laccase. *J. Mol. Catal. B Enzym.* 45, 102–107. doi: 10.1016/j.molcatb.2006.12.004

Mukhopadhyay, M., and Banerjee, R. (2015). Purification and biochemical characterization of a newly produced yellow laccase from *Lentinus squarrosulus* MR13. *3 Biotech* 5, 227–236. doi: 10.1007/s13205-014-0219-8

Munk, L., Larsen, M., and Meyer, A. S. (2018). Influence of mediators on laccase catalyzed radical formation in lignin. *Enzyme Microb. Technol.* 116, 48–56. doi: 10.1016/j.enzmictec.2018.05.009

Norsker, M., Jensen, M., and Adler-Nissen, J. (2000). Enzymatic gelation of sugar beet pectin in food products. *Food Hydrocoll.* 14, 237–243. doi: 10.1016/S0268-005X(00)00016-3

Nunes, C. S., and Kunamneni, A. (2018). "Chapter 7 – laccases—properties and applications," in *Enzymes in Human and Animal Nutrition*, eds C. S. Nunes, and V. Kumar (Cambridge, MA: Academic Press), 133–161. doi: 10.1016/b978-0-12-805419-2.00007-1

Osma, J. F., Toca-Herrera, J. L., and Rodríguez-Couto, S. (2010). Uses of laccases in the food industry. *Enzyme Res.* 2010:918761. doi: 10.4061/2010/918761

Pereira, M., Wu, Y. T., Venâncio, A., and Teixeira, J. (2003). Aqueous two-phase extraction using thermoseparating polymer: a new system for the separation of endo-polygalacturonase. *Biochem. Eng. J.* 15, 131–138. doi: 10.1016/S1369-703X(02)00190-0

Pleissner, D., Qi, Q., Gao, C., Rivero, C. P., Webb, C., Lin, C. S. K., et al. (2016). Valorization of organic residues for the production of added value chemicals: a contribution to the bio-based economy. *Biochem. Eng. J.* 116, 3–16. doi: 10.1016/j.bej.2015.12.016

Ponnusamy, V. K., Nguyen, D. D., Dharmaraja, J., Shobana, S., Banu, J. R., Saratale, R. G., et al. (2019). A review on lignin structure, pretreatments, fermentation reactions and biorefinery potential. *Bioresour. Technol.* 271, 462–472. doi: 10.1016/j.biortech.2018.09.070

Postemsky, P. D., Bidegain, M. A., González-Matute, R., Figlas, N. D., and Cubitto, M. A. (2017). Pilot-scale bioconversion of rice and sunflower agro-residues into medicinal mushrooms and laccase enzymes through solid-state fermentation with *Ganoderma lucidum*. *Bioresour. Technol.* 231, 85–93. doi: 10.1016/j.biortech.2017.01.064

Rajagopalu, D., Show, P. L., Tan, Y. S., Muniandy, S., Sabaratnam, V., and Ling, T. C. (2016). Recovery of laccase from processed *Hericium erinaceus* (Bull.:Fr) Pers. fruiting bodies in aqueous two-phase system. *J. Biosci. Bioeng.* 122, 301–306. doi: 10.1016/j.jbiosc.2016.01.016

Ribeiro, D. S., Henrique, S. M. B., Oliveira, L. S., Macedo, G. A., and Fleuri, L. F. (2010). Enzymes in juice processing: a review. *Int. J. Food Sci. Technol.* 45, 635–641. doi: 10.1111/j.1365-2621.2010.02177.x

Rochefort, D., Leech, D., and Bourbonnais, R. (2004). Electron transfer mediator systems for bleaching of paper pulp. *Green Chem.* 6, 14–24. doi: 10.1039/B311898N

Roth, S., and Spiess, A. C. (2015). Laccases for biorefinery applications: a critical review on challenges and perspectives. *Bioprocess. Biosyst. Eng.* 38, 2285–2313. doi: 10.1007/s00449-015-1475-7

Royse, D. J., Baars, J., and Tan, Q. (2017). "Current overview of mushroom production in the world," in *Edible and Medicinal Mushrooms: Technology and Applications*, eds C. Z. Diego, and A. Pardo−Giménez (Hoboken, NJ: Wiley-Blackwell).

Selinheimo, E., Kruus, K., Buchert, J., Hopia, A., and Autio, K. (2006). Effects of laccase, xylanase and their combination on the rheological properties of wheat doughs. *J. Cereal Sci.* 43, 152–159. doi: 10.1016/j.jcs.2005.08.007

Sperandio, G. B., and Ferreira Filho, E. X. (2019). Fungal co-cultures in the lignocellulosic biorefinery context: a review. *Int. Biodeter. Biodegr.* 142, 109–123. doi: 10.1016/j.ibiod.2019.05.014

Strong, P. J., and Burgess, J. E. (2008). Treatment methods for wine-related and distillery wastewaters: a review. *Bioremediat. J.* 12, 70–87. doi: 10.1080/10889860802060063

Strong, P. J., and Claus, H. (2011). Laccase: a review of its past and its future in bioremediation. *Crit. Rev. Environ. Sci. Technol.* 41, 373–434. doi: 10.1080/10643380902945706

Su, J., Noro, J., Fu, J., Wang, Q., Silva, C., and Cavaco-Paulo, A. (2018). Exploring PEGylated and immobilized laccases for cathecol polimerization. *AMB Express* 8:134. doi: 10.1186/s13568-018-0665-5

Trejo-Hernandez, M. R., Lopez-Munguia, A., and Quintero Ramirez, R. (2001). Residual compost of *Agaricus bisporus* as a source of crude laccase for enzymic oxidation of phenolic compounds. *Process Biochem.* 36, 635–639. doi: 10.1016/s0032-9592(00)00257-0

Upadhyay, P., Shrivastava, R., and Agrawal, P. K. (2016). Bioprospecting and biotechnological applications of fungal laccase. *3 Biotech* 6:15. doi: 10.1007/s13205-015-0316-3

Vikineswary, S., Abdullah, N., Renuvathani, M., Sekaran, M., Pandey, A., and Jones, E. B. G. (2006). Productivity of laccase in solid substrate fermentation of selected agro-residues by *Pycnoporus sanguineus*. *Bioresour. Technol.* 97, 171–177. doi: 10.1016/j.biortech.2005.02.015

Wong, K.-S., Cheung, M.-K., Au, C.-H., and Kwan, H.-S. (2013). A novel *Lentinula edodes* laccase and its comparative enzymology suggest guaiacol-based laccase engineering for bioremediation. *PLoS One* 8:e66426. doi: 10.1371/journal.pone.0066426

Yagüe, S., Terrón, M. C., González, T., Zapico, E., Bocchini, P., Galletti, G. C., et al. (2000). Biotreatment of tannin-rich beer-factory wastewater with white-rot basidiomycete *Coriolopsis gallica* monitored by pyrolysis/gas chromatography/mass spectrometry. *Rapid Commun. Mass Spectrom.* 14, 905–910. doi: 10.1002/(SICI)1097-0231(20000530)14:10<905::AID-RCM963<3.0.CO;2-7

Yang, J., Li, W., Ng, T. B., Deng, X., Lin, J., and Ye, X. (2017). Laccases: production, expression regulation, and applications in pharmaceutical biodegradation. *Front. Microbiol.* 8:832. doi: 10.3389/fmicb.2017.00832

Zaslavsky, B. Y., Uversky, V. N., and Chait, A. (2016). Analytical applications of partitioning in aqueous two-phase systems: exploring protein structural changes and protein–partner interactions in vitro and in vivo by solvent interaction analysis method. *Biochim. Biophys. Acta Proteins Proteom.* 1864, 622–644. doi: 10.1016/j.bbapap.2016.02.017

Conflict of Interest: The authors declare that the research was conducted in the absence of any commercial or financial relationships that could be construed as a potential conflict of interest.

frontiers in Bioengineering and Biotechnology

ORIGINAL RESEARCH
published: 30 April 2020
doi: 10.3389/fbioe.2020.00314

Methane Production From Different Parts of Corn Stover via a Simple Co-culture of an Anaerobic Fungus and Methanogen

Yuqi Li[1,2], Zhesheng Hou[3], Qicheng Shi[1,2], Yanfen Cheng[1,2] and Weiyun Zhu[1,2]*

[1] Laboratory of Gastrointestinal Microbiology, National Center for International Research on Animal Gut Nutrition, Nanjing Agricultural University, Nanjing, China, [2] Joint International Research Laboratory of Animal Health and Food Safety, Nanjing Agriculture University, Nanjing, China, [3] College of Mechanical and Electrical Engineering, Jilin Institute of Chemical Technology, Jilin, China

To determine ways to improve the utilization of corn stover, this study investigated methane production from different parts of corn stover using a simple co-culture of an anaerobic fungus (*Pecoramyces* species) and methanogen (*Methanobrevibacter* species). The simple co-culture was incubated with the stem pith, leaf blade, or stem bark of corn stover (as substrates) at 39°C for 72 h. The results showed that the stem bark had the lowest ($P < 0.05$) digestibility (38.0 ± 1.36%) and neutral detergent solubles, that is, cell solubles (31.6 ± 0.45%), and the highest ($P < 0.05$) lignin content (4.8 ± 0.56%). The leaf blade had a significantly higher methane conversion rate (56.6 ± 0.76 mL/g digested substrate) than the stem pith (49.2 ± 1.60 mL/g digested substrate), even though they showed similar levels of methane production (42.4 ± 1.0 mL and 40.9 ± 1.35 mL, respectively). Both the leaf blade and stem pith of corn stover have the potential to produce methane in a simple co-culture of an anaerobic fungus and methanogen.

Keywords: anaerobic fungus, methanogen, corn stover, leaf blade, stem pith

OPEN ACCESS

Edited by:
Jorge Fernando Brandão Pereira, Chemical Process Engineering and Forest Products Research Centre (CIEPQPF), Portugal

Reviewed by:
Artur Ribeiro, University of Minho, Portugal
Guilherme Peixoto, São Paulo State University, Brazil

****Correspondence:***
Yanfen Cheng
yanfencheng@njau.edu.cn

Specialty section:
This article was submitted to Industrial Biotechnology, a section of the journal Frontiers in Bioengineering and Biotechnology

Received: *14 September 2019*
Accepted: *23 March 2020*
Published: *30 April 2020*

Citation:
Li Y, Hou Z, Shi Q, Cheng Y and Zhu W (2020) Methane Production From Different Parts of Corn Stover via a Simple Co-culture of an Anaerobic Fungus and Methanogen. Front. Bioeng. Biotechnol. 8:314. doi: 10.3389/fbioe.2020.00314

INTRODUCTION

The rational exploitation and utilization of energy are vital for sustainable social development. The increasing depletion of fossil fuels is one of the biggest challenges for the future development of the economy and society. The production of non-petroleum sources of energy has attracted increased attention in several countries. Today, dedicated energy crops, such as maize, sorghum, and wheat, are widely used to produce methane (Riva et al., 2014). However, an increasing energy demand has led to the need to consume large amounts of such energy crops to produce methane. This makes the cost of methane production very high, and leads to an inevitable conflict between the use of limited supplies of energy crops for both food/feed and energy production (Croce et al., 2016).

The use of corn stover, instead of energy crops, to produce methane is one way to address this challenge. Corn stover stores half of the organic matter of an entire crop and has a reasonably high nutritional value (Li et al., 2017). However, cellulose, which is complexed with lignin in crop residues, is highly resistant to anaerobic fermentation and thus to methane production (Berchem et al., 2017; Wu and Tian, 2018). Although there are many limitations in the production of methane

from corn stover, it is still considered a good potential substrate for anaerobic fermentation. Furthermore, the production of methane from corn stover is greater than that produced from other crop straws (Croce et al., 2016). In recent years, corn stover has been used to produce methane in anaerobic digestors or in batch cultures (Haag et al., 2015).

Methane production from corn stover depends on its chemical composition (Fernando et al., 2006). At present, some physical and chemical pretreatment methods can improve the degradation of straw and thus improve the efficiency of methane production. Steam explosion, microwave, and other heat treatment methods can dissolve lignin, but they also produce toxic substances, which can inhibit anaerobic fermentation (Sapci et al., 2013; Theuretzbachera et al., 2015). Although cold treatment methods, such as extrusion and comminution, do not produce harmful substances, they do not remove lignin from the fiber structure, which leads to poor methane production (Hjorth et al., 2011).

Other processes, such as acid and alkali pretreatment, may also be applied separately before anaerobic fermentation. The application of acid for pretreatment is great extent restricted by high acid and energy consumption, equipment corrosion, and obligation for acid recovery (Ibrahim, 2012). Moreover, alkaline treatment can even produce secondary products, thereby reducing the production of methane during fermentation (Croce et al., 2016). When combined with some physical and chemical methods to simultaneously pretreat straw, the above listed drawbacks could be alleviated, and methane production increased. However, such pretreatment itself violates the original intention of producing new energy sustainably, owing to the considerable consumption of energy. In addition, the application of such treatments can be expensive.

Anaerobic fungi (AF), a constituent of the natural microbial communities found in the rumen of herbivores, are known for their fiber-degrading ability. Unlike fiber-degrading bacteria, AF have unique rhizoid systems that can colonize and degrade the plant cell wall for effective degradation (Gruninger et al., 2014; Solomon et al., 2016). Anaerobic fungi use many carbohydrate-degrading enzymes and their unique rhizoid system to physically destroy the ultrastructure of the plant cell wall to degrade lignocellulose. This action is considered to increase the surface area for bacterial colonization and further enzymatic digestion (Gruninger et al., 2018). The use of AF could preclude the requirement for pretreatment in methane production.

Compared with industrial preparations, AF are natural, harmless, efficient, and convenient and can be easily obtained. Methanogens can be found toward the end of the metabolic process in the rumen, which can utilize the metabolic products of AF and fibrolytic bacteria to produce methane (Jin et al., 2017). Many studies using co-cultured AF and methanogens have shown that co-cultured methanogens could not only use fungal metabolites to produce methane, but also shift the fungal metabolic pathway to confer significantly higher levels of fiber-degrading ability to the AF (Joblin et al., 1990). Thus, co-cultures of AF and methanogens have the potential for use in the degradation of lignocellulosic substrates for methane production (Theodorou et al., 1996; Bootten et al., 2011; Shi et al., 2019).

Zhou et al. (2015) reported that the structural components and nutrient utilization rates of different parts of the same straw were significantly different. Zhao et al. (2011) demonstrated that the content and structure of cellulose and hemicellulose in the stem bark (SB), leaf blade (LB), and stem pith (SP) of corn stover also differed. In order to improve the utilization of corn stover, this study investigated the methane production from different parts of corn stover using a simple co-culture of an anaerobic fungus and methanogen.

MATERIALS AND METHODS

Co-culture of Anaerobic Fungus and Methanogen

The co-culture of an anaerobic fungus and methanogen used in the present study was isolated from a goat (Jin et al., 2011). The fungus was identified as *Pecoramyces* species (Li et al., 2017), and the methanogen was identified as *Methanobrevibacter* species (Jin et al., 2011). The anaerobic fungus was identified to the genus level through the use of traditional morphological identification and molecular phylogenetic analyses. Morphological identification included rhizoid, mycelium, and flagella identification and nuclear staining with DAPI (4′,6-diamidino-2-phenylindole). Molecular phylogenetic analyses were based on the amplification and sequencing of the genes encoding the 28S rRNA (*LSU*) and ITS (internal transcribed spacer) sequences with AF-LSU primers (Li et al., 2019). The 16S rRNA genes amplified from the total DNA extracted from the cultures were used for gene sequencing to evaluate the specific type of methanogen, using the Met86F and Met1340R primers, according to the methods of Jin et al. (2011).

The co-culture was maintained in liquid media (Davies et al., 1993) with rice straw as a substrate and transferred every 3 days. Briefly, this method entailed the transfer of 1 mL of co-cultured anaerobic fungus and methanogen solution into a roll tube with 9 mL of fresh medium, according to the methods of Cheng et al. (2009). Each 1,000 mL of medium contained 150 mL of buffer solution A, 150 mL of buffer solution B, 550 mL of basal medium, (2.5 g yeast extract, 100 g tryptone, and 6 g $NaHCO_3$), 150 mL of cell-free rumen fluid (centrifuged at 16,000*g* for 20 min at 4°C, with the supernatant decanted and stored at −20°C), 1 g of L-cysteine hydrochloride, and 1 mL of 0.1% (wt/vol) resazurin. Buffer solution A contained 0.3 g of K_2HPO_4 per 100 mL, and buffer solution B contained 0.3 g of KH_2PO_4, 0.6 g of NaCl, 0.6 g of $(NH_4)_2SO_4$, 0.06 g of $MgSO_4 \cdot 7H_2O$, and 0.06 g of $CaCl_2 \cdot 2H_2O$ per 100 mL. This medium was sterilized by autoclaving at 115°C for 20 min.

Penicillin–streptomycin solution was added to the medium to inhibit bacterial growth. The final concentrations of penicillin and streptomycin were 1,915 and 2,031 U mL^{-1}, respectively. Antibiotic solution was sterilized by using a filtration membrane (size 0.22 μm, SCAA-102; ANPEL, Shanghai, China). At the end of the fermentation process, an aliquot of 10 mL of the supernatant from each bottle was transferred to new media, to which chloramphenicol was added to determine whether the medium became clear after 3 days of incubation. If the medium

became clear, this indicated the presence of methanogens in the fermentation medium, and if the medium remained turbid, this indicated the presence of bacteria.

Different Parts of Corn Stover

The corn stover was collected, air dried, and separated into the LB, SP, and SB. The three parts were separately oven dried at 65°C and ground to be passed through a sieve (∼1 mm) for further use as substrates.

Experimental Design and Sample Collection

The experiment comprised three groups, each containing 1 g of SP, LB, or SB as substrates. Each group had four replicates. The media (90 mL) was pre-warmed at 39°C and inoculated with 10 mL of 3-day-old anaerobic fungus and methanogen co-culture. Based on the established growth characteristics of the anaerobic fungus (Li et al., 2017), the co-culture of the anaerobic fungus and methanogen was conducted under strict anaerobic conditions under a headspace of 100% CO_2 at 39°C in a butyl rubber-stoppered 180 mL serum bottle containing 90 mL of media without shaking for 72 h. A blank group without inoculation was prepared for gas and analyte correction.

Before the fermentation process, 2 mL of the supernatants was collected from the SP, LB, and SB vessels and used to measure the concentrations of reducing sugars, glucose, and xylose. Gas production and methane production were measured every 6 h (at 0, 6, 12, 18, 24, 30, 36, 42, 48, 54, 60, 66, and 72 h). At the end of fermentation, the pH was immediately measured, and the supernatant was collected for the analysis of fermentation end products, fiber-degrading enzyme activities, and reducing sugars. The remaining substrates were collected for the analysis of the digestibility of dry matter (DM), neutral detergent fiber (NDF), acid detergent fiber (ADF), cellulose, and hemicellulose.

Analysis of Chemical Composition of Different Parts of Corn Stover

The contents of NDF, ADF, and lignin of the LB, SP, and SB were determined according to the methods of Van Soest et al. (1991). The cell solubles or the soluble solutes in the neutral detergent solution (NDS), cellulose, and hemicellulose were calculated according to the methods of Niu et al. (2018). In addition, NDF and ADF were determined using a fiber analyzer (Ankom A200i; Ankom Technology, Macedon, NY, United States). First, the samples were treated with NDS; the dissolved part was NDS, and the residue was NDF. The NDF was further treated with acid detergent solution to dissolve the hemicellulose and obtain the ADF. The ADF thus obtained was digested with 72% sulfuric acid, which dissolves cellulose, and the residue comprised a mixture of lignin and silicate. This residue was ashed, which removes the lignin, thereby facilitating the determination of silicate. The digestibility of DM, NDF, ADF, cellulose, and hemicellulose was calculated according to the methods of Li et al. (2016).

Each 1,000 mL of NDS contained 30 g of sodium dodecyl sulfate, 18.6 g of disodium ethylenediamine tetraacetic acid (Na_2EDTA), 6.8 g of $Na_2B_4O_7$, 4.6 g of Na_2HPO_4, and 10 mL of $C_6H_{14}O_4$. Each 1,000 mL of acid detergent solution contained 20 g of cetrimonium bromide dissolved in 1,000 mL of 0.5 mol/L sulfuric acid solution.

Measurement of Gas and Methane Production

Gas production was determined using a pressure transducer, according to the methods of Theodorou et al. (1994). The pressure transducer determined the levels of gas production during fermentation at the top surface of the serum bottles with a capacity of 180 mL. Gas production was recorded every 6 h, and the gas was then released to bring the air pressure within the bottle to 0, to facilitate the determination of gas production at the next time point. The gas production volumes at each time point were added to determine the cumulative gas production. By recording the gas production at intermittent time points, a complete growth curve of the co-culture of the anaerobic fungus and methanogen was obtained. After each time point at which gas production was determined, 5 mL of gas was collected in an air bag to determine the methane concentration in the gas.

Methane content in the gas was determined by gas chromatography (Agilent 7890B; Agilent, Palo Alto, CA, United States), according to the methods of Hu et al. (2006). The conditions used were as follows: column temperature of 80°C; vaporization chamber temperature of 100°C; H_2 ion flame detector, with a detection temperature of 120°C; and carrier gas (N_2) pressure of 0.05 MPa; air pressure of 0.05 MPa; and H_2 pressure of 0.05 MPa. The volume of methane was calculated according to the method of Li et al. (2018).

Analysis of Fermentation End Products

The reducing sugars were analyzed using the 3,5-dinitrosalicylic acid (DNS) method (Lowe et al., 1987b). The ratio of the sample to DNS reagent was 1:2, and absorbance was read at 640 nm. The concentrations of glucose, xylose, formate, acetate, and lactate were determined according to the protocol described by Shi et al. (2019). Glucose was determined using the glucose oxidase method, xylose was measured using the phloroglucinol color-developing method, and lactate was determined by the NAD^+ transformation method. These analytes were all determined using the applicable assay kits (Nanjing Jiancheng Bioengineering Institute, Nanjing, China).

Formate was measured with the Formate Assay Kit (Sigma, Santa Clara, CA, United States). Acetate was measured by gas chromatography (Daojin GC- 2014AFsc Instrument; Shimadzu, Kyoto, Japan) using a capillary column. An aliquot of 0.2 mL of crotonate metaphosphate solution (0.25 g/mL) was mixed with 1 mL of supernatant from the fermentation medium and centrifuged at 16,000*g* for 10 min. The supernatant was then analyzed by gas chromatography with a column temperature of 130°C; vaporization temperature of 180°C; H_2 ion flame detector and detection temperature of 180°C; N_2 carrier gas at a pressure of 60 kPa; H_2 pressure of 50 kPa; and O_2 pressure of 50 kPa. Ethanol was determined by gas chromatography (TRACE GC Ultra; Thermo Fisher, Waltham, Massachusetts, United States) using the method described by Edgardo et al. (2008).

Analysis of Fiber-Degrading Enzyme Activity

The activities of carboxymethyl cellulase (CMCase), a cellulose-degrading enzyme, and xylanase, a hemicellulose-degrading enzyme, were measured according to the method of Lowe et al. (1987a). The fermentation supernatant was used to measure enzyme activities. To an appropriate volume of the supernatant solution (preheated at 50°C), either 1 mL of xylan solution or 10 mg of carboxymethylcellulose sodium in 0.1 mol/L citric acid disodium hydrogen phosphate buffer solution was added. After 30 min of reaction at 50°C, DNS reagent was added, and the mixture was then boiled for 10 min, and the absorbance was read at 640 nm. The ratio of the sample to DNS reagent was 1:2. One unit of CMCase activity was defined as 1 μmol of glucose released per mL of supernatant per minute (U mL^{-1} min^{-1}). One unit of xylanase enzyme activity was defined as 1 μmol of xylose released per mL of supernatant per minute (U mL^{-1} min^{-1}).

Statistical Analysis

Statistical analysis was performed using the SPSS 20.0 software (IBM SPSS Statistics, version 20.0; IBM Corp, Armonk, NY, United States) with one-way analysis of variance at a confidence interval of 95%. Duncan new multiple-range test was then used to compare the differences among the three groups. Data were presented as the mean ± standard error of the mean.

RESULTS

Chemical Composition and Digestibility of the SB, LB, and SP of Corn Stover

The results are presented in **Table 1**. The SB had the lowest ($P < 0.05$) NDS content (31.6 ± 0.45%) and highest ($P < 0.05$) cellulose (40.9 ± 0.30%) and lignin (4.8 ± 0.56%) contents. The LB had the lowest ($P < 0.05$) cellulose (26.5 ± 0.09%) and lignin contents (2.4 ± 0.07%), and highest ($P < 0.05$) hemicellulose content (27.4 ± 0.55%). The SP had the highest ($P < 0.05$) NDS content (45.4 ± 0.55%).

TABLE 1 | Chemical composition of the stem bark, leaf blade, and stem pith of corn stover.

Items	Corn stover parts			SEM	*P*
	SB	LB	SP		
NDS (%)	31.6^{c}	42.8^{b}	45.4^{a}	0.73	<0.001
NDF (%)	68.4^{a}	57.2^{b}	54.6^{c}	0.73	<0.001
ADF (%)	46.6^{a}	29.8^{c}	31.4^{b}	0.48	<0.001
Cellulose (%)	40.9^{a}	26.5^{c}	28.0^{b}	0.42	<0.001
Hemicellulose (%)	21.8^{b}	27.4^{a}	23.3^{b}	0.90	0.002
Lignin (%)	4.8^{a}	2.4^{b}	2.6^{b}	0.62	0.013

Values in the same row with different superscript letters are significantly different ($P < 0.05$). SB, stem bark; LB, leaf blade; SP, stem pith; NDS, neutral detergent soluble solute; NDF, neutral detergent fiber; ADF, acid detergent fiber; SEM, standard error of the mean (n = 4).

The degradation values of the SB, LB, and SP of corn stover in the co-culture are shown in **Table 2**. The DM digestibility (DMD) of the SP was the highest (82.0 ± 1.95%, $P < 0.05$), followed by those of the LB (74.8 ± 1.95%) and SB (38.0 ± 1.36%). The hemicellulose digestibility of the SP was highest (78.6 ± 1.64%), followed by those of the LB (77.4 ± 0.95%) and SB (25.7 ± 0.75%). As shown in **Figure 1**, the concentrations of reducing sugars, glucose, and xylose in the SP were the highest ($P < 0.05$), followed by those in the LB and SB.

Gas and Methane Production From the SB, LB, and SP of Corn Stover

Figure 2 shows the cumulative gas production, over 72 h of fermentation, from the SB, LB, and SP of corn stover using the co-culture. The curves of methane production were similar to those of overall gas production. At the end of fermentation, the total gas production values of the LB (184.6 ± 3.74 mL) and SP (188.8 ± 2.60 mL) were significantly higher than those of the SB (105.8 ± 5.06 mL, $P < 0.05$), and no significant difference was observed between those of the LB and SP ($P > 0.05$) (**Figure 3**). Total methane production values from the LB (42.4 ± 0.99 mL) and SP (40.9 ± 1.35 mL) were significantly higher than those from the SB (25.8 ± 1.85 mL, $P < 0.05$), and no significant difference was observed between those from the LB and SP ($P > 0.05$) (**Figure 3**). The LB and SP showed similar levels of methane production, but the DMD of the LB was significantly lower than that of the SP ($P < 0.05$). This indicated that the methane conversion rate of the LB (56.6 ± 0.76 mL/g digested substrate) was significantly higher than that of the SP (49.2 ± 1.60 mL/g digested substrate) ($P < 0.05$).

Fiber-Degrading Enzyme Activity and Fermentation Metabolites Following Incubation of the SB, LB, and SP of Corn Stover

As shown in **Table 3**, the activity of CMCase in the LB group was significantly higher ($P < 0.05$) than that in the SP and SB

TABLE 2 | Degradation of the stem bark, leaf blade, and stem pith of corn stover in a co-culture of an anaerobic fungus and methanogen.

Items	Corn stover parts			SEM	*P*
	SB	LB	SP		
DMD (%)	38.0^{c}	74.8^{b}	82.0^{a}	2.51	<0.001
NDFD (%)	32.7^{c}	63.3^{b}	79.5^{a}	0.17	<0.001
ADFD (%)	36.0^{c}	50.3^{b}	80.2^{a}	0.12	<0.001
NDSD (%)	62.4^{c}	81.4^{b}	86.9^{a}	0.07	<0.001
HD (%)	25.7^{b}	77.4^{a}	78.6^{a}	0.30	0.002
CD (%)	24.2^{c}	60.1^{b}	75.0^{a}	0.75	< 0.001

Values in the same row with different superscript letters are significantly different ($P < 0.05$). SB, stem bark; LB, leaf blade; SP, stem pith; DMD, digestibility of dry matter; NDFD, digestibility of neutral detergent fiber; ADFD, digestibility of acid detergent fiber; NDSD, digestibility of neutral detergent solubles; HD, digestibility of hemicellulose; CD, digestibility of cellulose; SEM, standard error of the mean (n = 4).

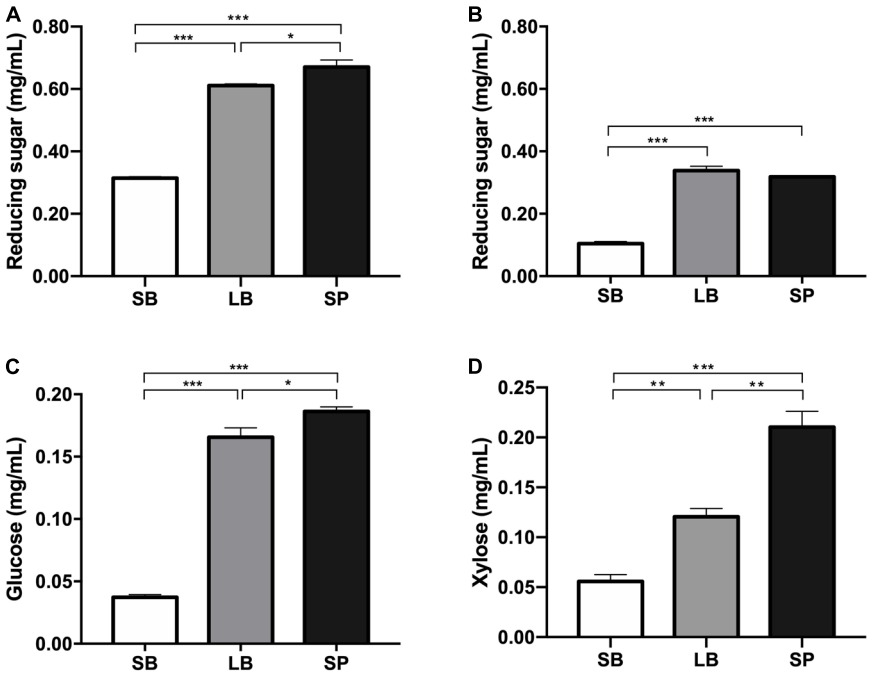

FIGURE 1 | Concentrations of reducing sugar before **(A)** and after **(B)** fermentation and of glucose **(C)** and xylose **(D)** in the supernatant, following incubation using the stem bark (SB), leaf blade (LB), and stem pith (SP) of corn stover as substrates. The error bars represent the standard error of the mean ($n = 4$). *$P < 0.05$, **$P < 0.01$, and ***$P < 0.001$.

groups. Xylanase activity in the SB group was significantly lower ($P < 0.05$) than that in the LB and SP groups, and no significant difference ($P > 0.05$) was observed between the values in the LB and SP groups.

The pH values showed significant differences among the three groups ($P < 0.05$). The SB had the highest pH value (6.6 ± 0.01), which was significantly higher than those of the LB (6.4 ± 0.02) and SP (6.3 ± 0.01) ($P < 0.05$). The pH value of the LB was also significantly higher than that of the SP ($P < 0.05$). The concentrations of water-soluble metabolites in the supernatant of the co-culture of the anaerobic fungus and methanogen when incubated with SB, LB, and SP as substrates are shown in **Figure 4**. Acetate was the dominant metabolite in the supernatant, followed by formate, ethanol, and lactate. The concentrations of formate, ethanol, lactate, and acetate all showed significant differences among the three groups ($P < 0.05$).

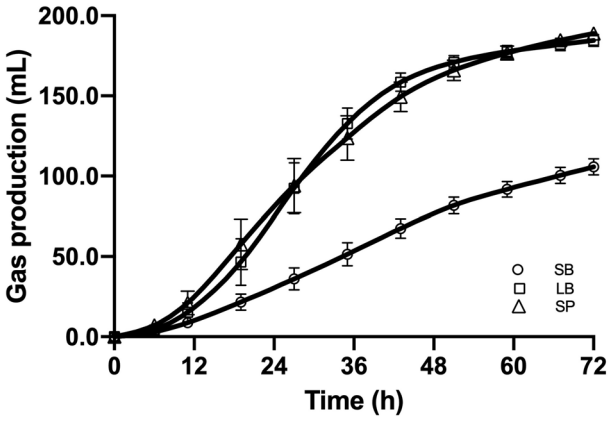

FIGURE 2 | Cumulative gas production from the stem bark (SB), leaf blade (LB), and stem pith (SP) of corn stover using a co-culture of anaerobic fungus and methanogen. The error bars represent the standard error of the mean ($n = 4$).

DISCUSSION

The DMD of substrates reflects their utilization (Hao, 2011). In the present study, the DMD of the SP, LB, and SB of corn stover showed significant differences ($P < 0.05$). The DMD of the SB was significantly lower than that of the SP and LB, and the DMD of the LB was significantly lower than that of the SP ($P < 0.05$). These findings might be due to the differences in cell-soluble and lignin contents among the three parts. According to Ma et al. (2018), NDS mainly contains protein, fat, starch, and sugar, all of which can be easily degraded by microorganisms (Teunissen et al., 1992).

In the present study, NDS in the SP was the highest, and that in the SB was the lowest. In plant fibers, lignin and hemicellulose are assembled into a complex supramolecular network, which coats the cellulose fibrils. This complex network reduces the digestibility of plant fiber and is the major constraint in the sustainable production of biofuels (Gruber, 2009;

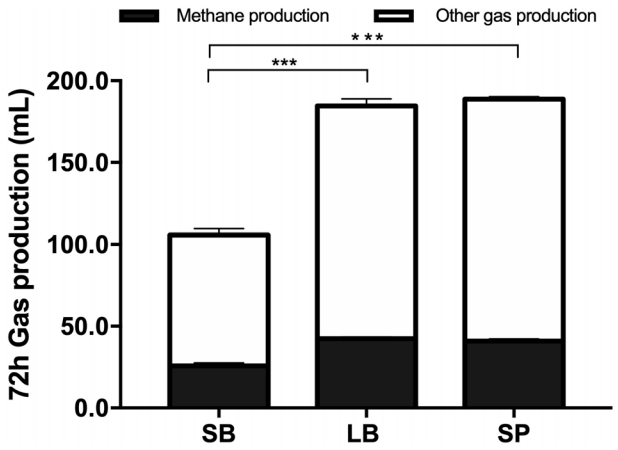

FIGURE 3 | Total gas and methane production from the stem bark (SB), leaf blade (LB), and stem pith (SP) of corn stover using a co-culture of anaerobic fungus and methanogen. The error bars represent the standard error of the mean ($n = 4$). ***$P < 0.001$.

TABLE 3 | Activities of fiber-degrading enzymes of an anaerobic fungus following incubation using the stem bark, leaf blade, and stem pith of corn stover as substrates.

Items	Corn stover parts			SEM	*P*
	SB	LB	SP		
CMCase (U mL^{-1} min^{-1})	0.37^{c}	0.50^{a}	0.45^{b}	0.01	<0.001
Xylanase (U mL^{-1} min^{-1})	9.51^{b}	14.53^{a}	13.80^{a}	0.71	<0.001

Values in the same row with different superscript letters are significantly different ($P < 0.05$). SB, stem bark; LB, leaf blade; SP, stem pith; SEM, standard error of the mean ($n = 4$); CMCase, carboxymethyl cellulase.

Silveira et al., 2015). In the present study, the digestibility of hemicellulose and cellulose in the LB and SP was significantly higher than that in the SB, which might be due to the significantly higher lignin content in the SB compared with that in the LB and SP.

Sun et al. (2005) investigated the attachment on and fermentation profiles of substrates with different lignin contents exposed to ruminal AF. They found that the growth of AF was decreased with increasing lignin content in the substrates. Lignin is a complex compound composed of phenylpropane. It is the most difficult part of the plant cell wall to be degraded. Lignin and polysaccharide are linked by hydroxycinnamic acid, which forms an ester bond and ether linkage with carbonyl and phenolic groups of hydroxycinnamic acid. Although AF can degrade arabinoxylan and release hydroxycinnamic acid, they can neither break the ether bond between lignin and hydroxycinnamic acid, nor degrade lignin (Borneman et al., 1990). Therefore, AF can degrade plant tissues with a relatively low lignin content to a greater extent and at a higher rate.

Methane production by the SB was the lowest in this study, which might be due to the low DMD of the SB, resulting in less substrates (H_2/CO_2/formate) for the co-cultured methanogens. Zhu et al. (2001) determined the total gas and methane production in their study of the degradation of straw by an anaerobic fungus. They found that the DMD was positively correlated with total gas production and methane production. Jin (2009) also reported that methane production was positively correlated with the DMD of substrates following the co-culture of an anaerobic fungus and methanogen. The process of anaerobic fungal growth and the utilization of crude fiber can be divided into two stages: in the first phase, the polysaccharide hydrolytic enzyme secreted by the anaerobic fungus hydrolyzes the crude fiber into fermentable sugars (mainly glucose and xylose); in the second stage, the anaerobic fungus absorbs or transports these fermentable sugars into the cell and finally metabolizes them into H_2, CO_2, formate, acetate, lactate, and ethanol (Solomon et al., 2016). In this study, each part of corn stover was first degraded into a large number of fermentable carbon sources, and then these carbon sources generated H_2, CO_2, and soluble metabolites in the cytosol and hydrogenosome of anaerobic fungus. At the end of the fermentation, the measured amount of H_2 accumulation was very low, accounting for only 2% of the total gas production, indicating that most of the H_2 produced was used by methanogens, H_2 reduces CO_2 to generate methane.

Li (2017) reported that during co-culture methane production is accelerated during the period from 32 to 64 h, and methanogens can utilize both the H_2 and formate produced by the anaerobic fungus. In our current study, the LB fraction with the highest methane conversion efficiency had the lowest formate concentration in the medium. In addition, gas production from the LB fraction was highest at 30–64 h of fermentation. These results suggest that a large amount of formate produced by the anaerobic fungus was utilized by methanogens during this fermentation stage, which is consistent with previous results.

The SP had the highest DMD in the present study, which might be explained by the higher content of NDS and lower contents of cellulose and lignin, as discussed above. It is interesting that the LB had a significantly lower DMD than the SP but showed similar levels of gas and methane production. Thus, the methane conversion efficiency of the LB was higher than that of the SP, which might be attributed to higher levels of hemicellulose degradation in the LB compared with that in the SP. Without considering economic performance, the methane conversion efficiency of the co-culture pretreatment strategy used in the present study was lower than that of the physical and chemical pretreatment mentioned in the introduction. Whether sulfuric acid, hydrochloric acid, sodium hydroxide, extrusion, or steam explosion pretreatment is used, the conversion efficiency of methane is consistently higher than 100 mL/g, which is more than twofold the conversion efficiency of the pretreatment strategy used in the present study. However, the pretreatment of sulfuric acid, hydrochloric acid, and sodium hydroxide took 9 days (7 days of acid treatment and 2 days of drying), and the following anaerobic digestion was up to 35 days, which indicated that the whole procedure was 44 days (Song et al., 2014; Croce et al., 2016). Meanwhile, the present strategy provided in this study took only 3 days for the whole procedure, which is much more efficient than the above discussed pretreatments.

Compared with the NDS, hemicellulose and cellulose in plants need to be gradually degraded into usable sugars by plant

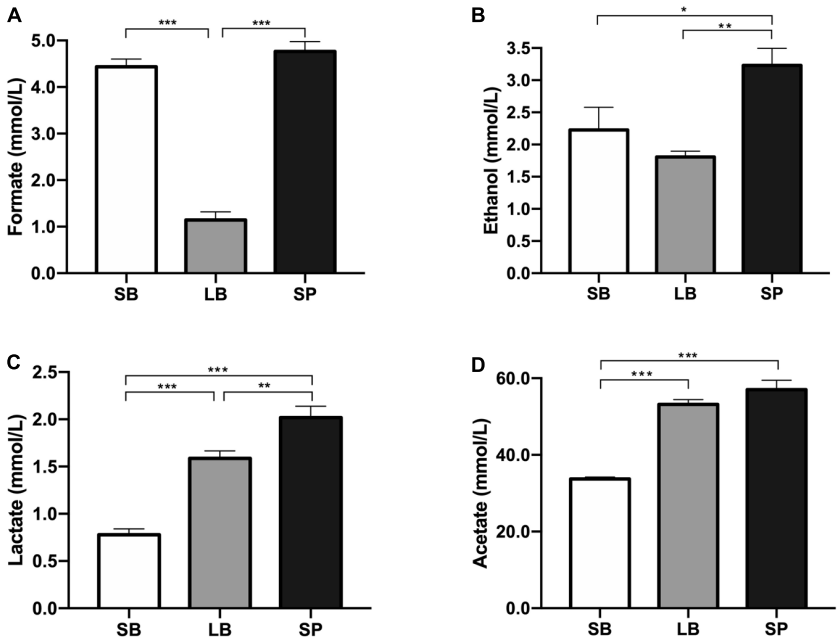

FIGURE 4 | Concentrations of formate **(A)**, ethanol **(B)**, lactate **(C)**, and acetate **(D)** in the supernatant of a co-culture of anaerobic fungus and methanogen, following incubation using the stem bark (SB), leaf blade (LB), and stem pith (SP) of corn stover as substrates. The error bars represent the standard error of the mean ($n = 4$). $^{*}P < 0.05$, $^{**}P < 0.01$, and $^{***}P < 0.001$.

cell wall-degrading enzymes secreted by the anaerobic fungus (Mountfort and Asher, 1985; Haitjema et al., 2014). These usable sugars are then metabolized by the anaerobic fungus into H_2, CO_2, formate, acetate, ethanol, and succinic acid (Li et al., 2016). Methanogens use H_2, reduce the partial pressure of H_2 in the system, remove the inhibition of hydrogenase, and thus catalyze more NAD(P)H to H_2, which results in increased methane production (Bernalier et al., 1991). The formation of lactate and ethanol requires the participation of NAD(P)H; thus, the production of lactate and ethanol should be inhibited. In this study, the concentrations of ethanol and lactate in the LB group were significantly lower than those in the SP group ($P < 0.05$).

Solomon et al. (2016) showed that hemicellulase expression is more easily regulated than cellulolytic enzymes in AF. Recent studies have also found that under the same conditions the activity of xylanase produced by AF in the rumen is six times that of cellulase (Li et al., 2017) and four times more than that of the xylanase produced in some industrial fermentations (Lee et al., 1999). Yu (2017) studied the activity of plant cell wall–degrading enzymes in 12 strains of an anaerobic fungus and found that the xylanase activity in *Piromyces* species CN6 was significantly higher than that of cellulase. Jin (2009) studied the activities of several enzymes after 96 h of fermentation of rice straw by AF and found that xylanase activity of the AF was much higher than that of cellulase. The results of our current study also reflect this situation, in which xylanase activity was much higher than that of cellulase.

At the end of fermentation, the difference in pH values was due to the differences in the concentrations of metabolites. The accumulation of metabolites (acetate, lactate, and formate) can result in a reduction of the pH. Formate, lactate, acetate, and ethanol are reportedly the main water-soluble metabolites of AF (Boxma et al., 2004; Li et al., 2016). Ethanol and lactate are the end products of cytoplasmic metabolism by AF. Compared with the SP, the low concentrations of ethanol and lactate in the LB indicate that cytoplasmic metabolism by the anaerobic fungus was reduced, and more metabolites entered the hydrogenosome to generate H_2 and acetate, which promoted the co-cultured methanogen to produce methane, as discussed above. When co-cultured with methanogen, the formate in the supernatant might be utilized to produce methane when H_2 is limited (Jin, 2012; Wei et al., 2016).

In the present study, significantly lower levels of formate were observed in the LB group, which implied that the formate was used by the co-cultured methanogen to produce methane, resulting in higher levels of methane in this group. Previous studies have shown that the co-culture of an anaerobic fungus and methanogen could degrade lignocellulosic substrates and produce methane with very limited amounts of formate in the supernatant within 3 days (Kim et al., 2011; Tapio et al., 2017). In the present study, the concentrations of formate were all greater than 1 mmol/L, which implies that the co-culture needed more time to utilize formate to produce methane. Moreover, a large amount of acetate was accumulated in the culture. If acetate-utilizing methanogens could be added to the culture, much higher levels of methane could be produced.

The SB, LB, and SP showed significantly different chemical compositions, which resulted in different levels of digestibility and methane production. The LB and SP of corn stover had

higher levels of digestibility and methane production, as they had higher levels of NDS and hemicellulose, which could be easily degraded by the anaerobic fungus. The co-culture of an anaerobic fungus and methanogen has the potential to degrade lignocellulosic substrates to produce methane. More studies are needed in this area to pave the way toward sustainable methane production from lignocellulosic substrates.

DATA AVAILABILITY STATEMENT

All datasets generated for this study are included in the article/supplementary material.

AUTHOR CONTRIBUTIONS

YL and QS completed the experiment and data analysis. YC and ZH conceived and designed the manuscript. YL, YC, and WZ wrote and revised the manuscript.

FUNDING

This work was supported by the Natural Science Foundation of China (31772627), the Fundamental Research Funds for the Central Universities (KYDK201701) and the "Belt and Road" Cooperation Program of Jiangsu Province (BZ2018055).

REFERENCES

Berchem, T., Roiseux, O., Vanderghem, C., Boisdenghien, A., Foucart, G., and Richel, A. (2017). Corn stover as feedstock for the production of ethanol: chemical composition of different anatomical fractions and varieties. *Biofuel. Bioprod. Biorefin. Biofpr.* 11, 430–440. doi: 10.1002/bbb.1755

Bernalier, A., Fonty, G., and Gouet, P. (1991). Cellulose degradation by two rumen anaerobic fungi in monoculture or in coculture with rumen bacteria. *Anim. Feed Sci. Technol.* 32, 131–136. doi: 10.1016/0377-8401(91)90016-l

Bootten, T. J., Joblin, K. N., McArdle, B. H., and Harris, P. J. (2011). Degradation of lignified secondary cell walls of lucerne (*Medicago sativa* L.) by rumen fungi growing in methanogenic co-culture. *J. Appl. Microbiol.* 111, 1086–1096. doi: 10.1111/j.1365-2672.2011.05127.x

Borneman, W. S., Hartley, R. D., Morrison, W. H., Akin, D. E., and Ljungdahl, L. G. (1990). Feruloyl and p-coumaroyl esterase from anaerobic fungi in relation to plant cell wall degradation. *Appl. Microbiol. Biotechnol.* 33, 345–351. doi: 10.1007/BF00164534

Boxma, B., Voncken, F., Jannink, S., van Alen, T., Akhmanova, A., van Weelden, S. W., et al. (2004). The anaerobic chytridiomycete fungus *Piromyces* sp. E2 produces ethanol via pyruvate:formate lyase and an alcohol dehydrogenase E. *Mol. Microbiol.* 51, 1389–1399. doi: 10.1046/j.1365-2958.2003.03912.x

Cheng, Y. F., Edwards, J. E., Allison, G. G., Zhu, W. Y., and Theodorou, M. K. (2009). Diversity and activity of enriched ruminal cultures of anaerobic fungi and methanogens grown together on lignocellulose in consecutive batch culture. *Bioresour. Technol.* 100, 4821–4828. doi: 10.1016/j.biortech.2009.04.031

Croce, S., Wei, Q., D'Imporzano, G., Dong, R., and Adani, F. (2016). Anaerobic digestion of straw and corn stover: the effect of biological process optimization and pre-treatment on total bio-methane yield and energy performance. *Biotechnol. Adv.* 34, 1289–1304. doi: 10.1016/j.biotechadv.2016.09.004

Davies, D. R., Theodorou, M. K., Lawrence, M. I., and Trinci, A. P. (1993). Distribution of anaerobic fungi in the digestive tract of cattle and their survival in faeces. *J. Gen. Microbiol.* 139(Pt 6), 1395–1400. doi: 10.1099/00221287-139-6-1395

Edgardo, A., Carolina, P., Manuel, R., Juanita, F., Baeza, J. J. E., and Technology, M. (2008). Selection of thermotolerant yeast strains *Saccharomyces cerevisiae* for bioethanol production. *Enzyme Microb. Technol.* 43, 120–123. doi: 10.1016/j.enzmictec.2008.02.007

Fernando, S., Adhikari, S., Chandrapal, C., and Murali, N. (2006). Biorefineries: current status, challenges, and future direction. *Energy Fuel* 20, 1727–1737. doi: 10.1021/ef060097w

Gruber, L. (2009). Chemical composition, analyses and relevance of plant cell walls in the nutrition of ruminant livestock. *Uebers. Tierernaehr.* 37, 45–86.

Gruninger, R. J., Nguyen, T. T. M., Reid, I. D., Yanke, J. L., Pan, W., Abbott, D. W., et al. (2018). Application of transcriptomics to compare the carbohydrate active enzymes that are expressed by diverse genera of anaerobic fungi to degrade plant cell wall carbohydrates. *Front. Microbiol.* 9:1581. doi: 10.3389/fmicb.2018.01581

Gruninger, R. J., Puniya, A. K., Callaghan, T. M., Edwards, J. E., Youssef, N., Dagar, S. S., et al. (2014). Anaerobic fungi (phylum Neocallimastigomycota): advances in understanding their taxonomy, life cycle, ecology, role and biotechnological potential. *FEMS Microbiol. Ecol.* 90, 1–17. doi: 10.1111/1574-6941.12383

Haag, N. L., Nagele, H. J., Fritz, T., and Oechsner, H. (2015). Effects of ensiling treatments on lactic acid production and supplementary methane formation of maize and amaranth–an advanced green biorefining approach. *Bioresour. Technol.* 178, 217–225. doi: 10.1016/j.biortech.2014.08.048

Haitjema, C. H., Solomon, K. V., Henske, J. K., Theodorou, M. K., and O'Malley, M. A. (2014). Anaerobic gut fungi: Advances in isolation, culture, and cellulolytic enzyme discovery for biofuel production. *Biotechnol. Bioeng* 111, 1471–1482. doi: 10.1002/bit.25264

Hao, J. X. (2011). *Study on Nutritional Evaluation of Feed for Ruminants by in vitro*. Nanjing: Nanjing agricultural university.

Hjorth, M., Gränitz, K., Adamsen, A. P. S., and Møller, H. B. (2011). Extrusion as a retreatment to increase biogas production. *Bioresour. Technol.* 102, 4989–4994. doi: 10.1016/j.biortech.2010.11.128

Hu, W. L., Wang, J. K., Lv, J. M., Guo, Y. Q., and Liu, J. X. (2006). Rapid gas chromatogram determination of methane, organic acid in in vitro ruminal fermentation products. *J. Z. Univ*. 32, 217–221.

Ibrahim, A. H. (2012). Pretreatment of straw for bioethanol production. *Energy Procedia* 14, 542–551. doi: 10.1016/j.egypro.2011.12.973

Jin, W. (2009). *Isolation and Identification of Anaerobic Fungi and Their Associated Mehanogens from Herbivorous Animals and Their Characteristics of In Vitro Fermentation*. Nanjing: Nanjing Agricultural University.

Jin, W. (2012). *Rumen Cluster C: Distribution, Isolation and Hydrogenotrpphy*. Nanjing: Nanjing Agricultural University.

Jin, W., Cheng, Y. F., Mao, S. Y., and Zhu, W. Y. (2011). Isolation of natural cultures of anaerobic fungi and indigenously associated methanogens from herbivores and their bioconversion of lignocellulosic materials to methane. *Bioresour. Technol.* 102, 7925–7931. doi: 10.1016/j.biortech.2011.06.026

Jin, W., Liu, J. H., Li, Y. F., Cheng, Y. F., and Zhu, W. Y. (2017). Effect of methanogens on carbon metabolism of anaerobic fungi. *Acta Microbiol. Sin.* 57, 162–167.

Joblin, K. N., Naylor, G. E., and Williams, A. G. (1990). Effect of methanobrevibacter smithii on xylanolytic activity of anaerobic ruminal fungi. *Appl. Environ. Microbiol.* 56, 2287–2295. doi: 10.1128/aem.56.8.2287-2295.1990

Kim, M., Morrison, M., and Yu, Z. (2011). Status of the phylogenetic diversity census of ruminal microbiomes. *FEMS Microbiol. Ecol.* 76, 49–63. doi: 10.1111/j.1574-6941.2010.01029.x

Lee, S. S., Shin, K. J., Kim, W. Y., Ha, J. K., and Han, I. K. (1999). The rumen ecosystem: as a fountain source of nobel enzymes - Review. *AsianAustr. J. Anim. Sci.* 12, 988–1001. doi: 10.5713/ajas.1999.988

Li, Y. (2017). *Investigation of the Effect of Methanogens on the Metabolism of Anaerobic Fungi by Co-culture Technique*. Nanjing: Nanjing Agricultural University.

Li, Y., Cheng, Y., and Zhu, W. (2018). Enhancing the resistance of anaerobic fungus *Piromyces* sp. F1 to nitrovin by co-culture with *Methanobrevibacter thauer* F1. *Microbiol. China* 45, 111–119. doi: 10.13344/j.microbiol.china.170143

Li, Y., Jin, W., Cheng, Y., and Zhu, W. (2016). Effect of the associated methanogen methanobrevibacter thaueri on the dynamic profile of end and intermediate metabolites of anaerobic fungus *Piromyces* sp. F1. *Curr. Microbiol.* 73, 434–441. doi: 10.1007/s00284-016-1078-1079

Li, Y., Jin, W., Mu, C., Cheng, Y., and Zhu, W. (2017). Indigenously associated methanogens intensified the metabolism in hydrogenosomes of anaerobic fungi with xylose as substrate. *J. Basic Microbiol.* 57, 933–940. doi: 10.1002/jobm.201700132

Li, Y., Li, Y., Jin, W., Sharpton, T. J., Mackie, R. I., Cann, I., et al. (2019). Combined Genomic, transcriptomic, proteomic, and physiological characterization of the growth of *Pecoramyces* sp. F1 in Monoculture and Co-culture with a syntrophic methanogen. *Front. Microbiol.* 10:435. doi: 10.3389/fmicb.2019.00435

Lowe, S. E., Theodorou, M. K., and Trinci, A. P. (1987a). Cellulases and xylanase of an anaerobic rumen fungus grown on wheat straw, wheat straw holocellulose, cellulose, and xylan. *Appl. Environ. Microbiol.* 53, 1216–1223. doi: 10.1128/aem.53.6.1216-1223.1987

Lowe, S. E., Theodorou, M. K., and Trinci, A. P. J. (1987b). Growth and fermentation of an anaerobic rumen fungus on various carbon-sources and effect of temperature on development. *Appl. Environ. Microbiol.* 53, 1210–1215. doi: 10.1128/aem.53.6.1210-1215.1987

Ma, S. N., Xu, G. S., Cui, K., Ma, T., and Diao, Q. Y. (2018). Correlation analysis of CF, NDF and ADF in ruminant feedstuffs. *Feed Ind.* 39, 52–59. doi: 10.13302/j.cnki.fi.2018.21.012

Mountfort, D. O., and Asher, R. A. (1985). Production and regulation of cellulase by two strains of the rumen anaerobic fungus *Neocallimastix frontalis*. *Appl. Environ. Microbiol.* 49, 1314–1322. doi: 10.1128/aem.49.5.1314-1322.1985

Niu, D., Zuo, S., Jiang, D., Tian, P., Zheng, M., Xu, C. J. A. F., et al. (2018). Treatment using white rot fungi changed the chemical composition of wheat straw and enhanced digestion by rumen microbiota in vitro. *Anim. Feed Sci. Technol.* 237:S0377840117308350.

Riva, C., Schievano, A., D'Imporzano, G., and Adani, F. (2014). Production costs and operative margins in electric energy generation from biogas. Full-scale case studies. *Waste Manag.* 34, 1429–1435. doi: 10.1016/j.wasman.2014.04.018

Sapci, Z., Morken, J., and Linjordet, R. (2013). An investigation of the enhancement of biogas yields from lignocellulosic material using two pretreatment methods: microwave Ir- radiation and steam explosion. *Bioresources* 8, 1976–1985. doi: 10.15376/biores.8.2.1976-1985

Shi, Q., Li, Y., Li, Y., Cheng, Y., and Zhu, W. (2019). Effects of steam explosion on lignocellulosic degradation of, and methane production from, corn stover by a co-cultured anaerobic fungus and methanogen. *Bioresour. Technol.* 290:121796. Epub ahead., doi: 10.1016/j.biortech.2019.121796

Silveira, R. L., Stoyanov, S. R., Gusarov, S., Skaf, M. S., and Kovalenko, A. (2015). Supramolecular interactions in secondary plant cell walls: effect of lignin chemical composition revealed with the molecular theory of solvation. *J. Phys. Chem. Lett.* 6, 206–211. doi: 10.1021/jz502298q

Solomon, K. V., Haitjema, C. H., Henske, J. K., Gilmore, S. P., Borges-Rivera, D., Lipzen, A., et al. (2016). Early-branching gut fungi possess a large, comprehensive array of biomass-degrading enzymes. *Science* 351, 1192–1195. doi: 10.1126/science.aad1431

Song, Z., Yang, G., Liu, X., Yan, Z., Yuan, Y., and Liao, Y. (2014). Comparison of seven chemical pretreatments of corn straw for improving methane yield by anaerobic digestion. *PLoS One* 9:e93801. doi: 10.1371/journal.pone.0093801

Sun, Y. Z., Mao, S. Y., Jie, C., Zhou, L. F., and Zhu, W. Y. (2005). Effect of substrates with different lignin content on rumen fungal attachment and fermentation in the rumen of goats. *Acta Pratac. Sci.* 3, 56–61.

Tapio, I., Snelling, T. J., Strozzi, F., and Wallace, R. J. (2017). The ruminal microbiome associated with methane emissions from ruminant livestock. *J. Anim. Sci. Biotechnol.* 8:7. doi: 10.1186/s40104-017-0141-140

Teunissen, M. J., Kets, E. P., Op den Camp, H. J., Huis in't Veld, J. H., and Vogels, G. D. (1992). Effect of coculture of anaerobic fungi isolated from ruminants and non-ruminants with methanogenic bacteria on cellulolytic and xylanolytic enzyme activities. *Arch. Microbiol.* 157, 176–182. doi: 10.1007/bf00245287

Theodorou, M. K., Williams, B. A., Dhanoa, M. S., Mcallan, A. B., and France, J. (1994). A simple gas-production method using a pressure transducer to determine the fermentation kinetics of ruminant feeds. *Anim. Feed Sci. Technol.* 48, 185–197. doi: 10.1016/0377-8401(94)90171-90176

Theodorou, M. K., Zhu, W. Y., Rickers, A., Nielsen, B. B., Gull, K., and Trinci, A. P. J. (1996). *Biochemistry and Ecology of Anaerobic Fungi*. Berlin: Springer.

Theuretzbachera, F., Lizasoaina, J., Lefevera, C., Saylora, M. K., Enguidanosa, R., Weranc, N., et al. (2015). Steam explosion pretreatment of wheat straw to improve methane yields: investigation of the degradation kinetics of structural com- pounds during anaerobic digestion. *Bioresour. Technol.* 179, 299–305. doi: 10.1016/j.biortech.2014.12.008

Van Soest, P. J., Robertson, J. B., and Lewis, B. A. (1991). Methods for dietary fiber, neutral detergent fiber, and nonstarch polysaccharides in relation to animal nutrition. *J. Dairy Sci.* 74, 3583–3597. doi: 10.3168/jds.S0022-0302(91)78551-78552

Wei, Y. Q., Long, R. J., Yang, H., Yang, H. J., Shen, X. H., Shi, R. F., et al. (2016). Fiber degradation potential of natural co-cultures of Neocallimastix frontalis and Methanobrevibacter ruminantium isolated from yaks (*Bos grunniens*) grazing on the Qinghai Tibetan Plateau. *Anaerobe* 39, 158–164. doi: 10.1016/j.anaerobe.2016.03.005

Wu, Y. N., and Tian, H. P. (2018). Advances in utilization of crop straw as forage resource for ruminants. *Livestock Poul. Ind.* 29:26.

Yu, D. D. (2017). Isolation, Identification and enzymatic characteristics of rumen fungi. *J. Agric. Biotechnol.* 120, 571–587. doi: 10.1111/jam.13035

Zhao, M. M., Jiang, M., and Zhou, Z. W. (2011). the components analysis of several kinds of agricultural residues. *Mater. Rev.* 25, 122–125.

Zhou, T., Yang, Q. L., Zhang, T. Y., and Ren, L. P. (2015). Chemical composition, energetic values and ruminal degradation characteristics of different portions of cornstalks derived from skin-pith separation. *Chin. J. Anim. Nutr.* 27, 320–326.

Zhu, W., Mao, S., Wang, Q., and Wen, Y. (2001). Study on the screening of anaerobic fungi by in vitro fermentation. *J. Nanjing Agric. Univ.* 3, 44–48.

Conflict of Interest: The authors declare that the research was conducted in the absence of any commercial or financial relationships that could be construed as a potential conflict of interest.

frontiers in Bioengineering and Biotechnology

ORIGINAL RESEARCH
published: 14 October 2020
doi: 10.3389/fbioe.2020.547857

Insights on the DNA Stability in Aqueous Solutions of Ionic Liquids

Teresa B. V. Dinis[1], Fani Sousa[2] and Mara G. Freire[1]**

[1] Department of Chemistry, CICECO – Aveiro Institute of Materials, University of Aveiro, Aveiro, Portugal, [2] CICS-UBI – Health Sciences Research Center, Universidade da Beira Interior, Covilhã, Portugal

Deoxyribonucleic acid (DNA) carries the genetic information essential for the growth and functioning of living organisms, playing a significant role in life sciences research. However, the long-term storage and preservation of DNA, while ensuring its bioactivity, are still current challenges to overcome. In this work, aqueous solutions of ionic liquids (ILs) were investigated as potential preservation media for double stranded (dsDNA). A screening of several ILs, by combining the cholinium, tetrabutylammonium, tetrabutylphosphonium, and 1-ethyl-3-methylimidazolium, cations with the anions bromide, chloride, dihydrogen phosphate, acetate, and glycolate, was carried out in order to gather fundamental knowledge on the molecular features of ILs that improve the dsDNA stability. Different IL concentrations and the pH effect were also addressed. Circular dichroism (CD) spectroscopy was used to evaluate the conformational structure and stability of dsDNA. IL-DNA interactions were appraised by UV-Vis absorption spectrophotometry and ^{31}P nuclear magnetic resonance (NMR) spectroscopy. The results obtained demonstrate that pH has a significant effect towards the dsDNA stability. Amongst the ILs investigated, cholinium-based ILs are the most promising class of ILs to preserve the dsDNA structure, in which electrostatic interactions between the cholinium cation and the DNA phosphate groups play a significant role as demonstrated by the ^{31}P NMR data, being more relevant at higher IL concentrations. On the other hand, the denaturation of dsDNA mainly occurs with ILs composed of more hydrophobic cations and able to establish dispersive interactions with the nucleobases environment. Furthermore, the IL anion has a weaker impact when compared to the IL cation effect to interact with DNA molecules. The experimental data of this work provide relevant fundamental knowledge for the application of ILs in the preservation of nucleic acids, being of high relevance in the biotechnology field.

Keywords: DNA, interactions, ionic liquids, native conformation, nucleic acid, stability

OPEN ACCESS

Edited by:
Nicolas Papaiconomou, Université Côte d'Azur, France

Reviewed by:
Ana B. Pereiro, New University of Lisbon, Portugal
Diego O. Hartmann, New University of Lisbon, Portugal

****Correspondence:***
Fani Sousa
fani.sousa@fcsaude.ubi.pt
Mara G. Freire
maragfreire@ua.pt

Specialty section:
This article was submitted to Industrial Biotechnology, a section of the journal Frontiers in Bioengineering and Biotechnology

Received: *31 March 2020*
Accepted: *23 September 2020*
Published: *14 October 2020*

Citation:
Dinis TBV, Sousa F and Freire MG (2020) Insights on the DNA Stability in Aqueous Solutions of Ionic Liquids. Front. Bioeng. Biotechnol. 8:547857. doi: 10.3389/fbioe.2020.547857

INTRODUCTION

Deoxyribonucleic acid (DNA) is one of the most important macromolecules in cells, carrying the genetic information essential for the growth and functioning of living organisms. DNA is arranged in a helical stranded structure, but it can adopt different three-dimensional conformations. Because of this structural polymorphism (Renčiuk et al., 2009), experimentally, DNA can be designed

to create specific structures, being a powerful tool in many fields of application, such as in the development of advanced materials (Tateishi-Karimata and Sugimoto, 2014), templated chemical synthesis, nanomachines, and biosensors (Gartner et al., 2004; Yamada et al., 2005; Liu and Liu, 2009). On the other hand, the biological significance of DNA as a genetic information carrier places this biopolymer as a hot topic of research in life sciences.

In the past decades, several studies pointed out DNA as a relevant biopharmaceutical for genetic therapy purposes (Uludag et al., 2019), namely in the development of DNA vaccination, in pluripotent stem cells research, cellular therapy in psychiatric diseases (Lissek, 2017) and to induce the expression of therapeutic transgenes (Yin et al., 2014). However, the therapeutic efficacy and biological activity of DNA mainly depends on its structural stability and integrity (Diamantino et al., 2016). Due to its degradation by nucleobases and chemical instability, DNA is not stable in aqueous solutions at room temperature for long periods (Lindahl and Nyberg, 1972; Sasaki et al., 2007). Furthermore, temperature, ionic strength, pH and solvent type, and concentration are critical factors that lead to DNA destabilization (Lindahl and Nyberg, 1972; Cheng and Pettitt, 1992). Long-term storage and preservation of DNA at room temperature, while ensuring its bioactivity, are therefore important issues, motivating the research on effective and sustainable solvents for DNA preservation.

With the appearance of the first air- and water-stable ionic liquids (ILs), the scientific community focused the research on the finding of alternative applications for these compounds (Plechkova and Seddon, 2008), namely in organic chemistry (Sheldon, 2001; Jain et al., 2005; Zhao et al., 2005; Wong et al., 2006), new materials formulations (Hussey, 1994; Bowlas et al., 1996; Gordon et al., 1998; Endres and El Abedin, 2006), biocatalysis (Ventura et al., 2012) and as improved solvation media for a plethora of solutes and biomolecules (Freire et al., 2012; Padrino et al., 2018; Shamshina and Berton, 2020). Despite the relevant properties of most ILs, such as low flammability, and high thermal, and chemical stabilities (Seddon, 1997), they also display tunable properties, being generally described as "designer solvents" (Freire et al., 2012). For instance, the physicochemical properties of ILs can be adjusted to provide adequate aqueous microenvironments for biological applications, such as in gene delivery (Satpathi et al., 2015; Freyer et al., 2016) and long-term storage and structural preservation of nucleic acids (Vijayaraghavan et al., 2010; Mukesh et al., 2013; Pedro et al., 2018).

Several research groups have studied the interactions between DNA molecules and ILs, most of the times focused on the finding of novel solvents for DNA preservation. For instance, Ding et al. (2010) suggested a mechanism of interaction between IL and DNA mainly dependent on the IL concentration in water: for IL concentrations lower than 1.05 wt%, the IL cation is localized at several angstroms of distance from DNA phosphate strand, while the IL hydrophobic chains are in parallel arrangement to the DNA molecule surface; however, for higher IL concentrations, the IL cationic head group is near to the DNA phosphate strand and the IL hydrocarbon chains are perpendicularly attached to the DNA molecule surface. Chandran et al. (2012) described that the electrostatic interactions between ILs and DNA phosphate groups as well as hydrophobic and polar interactions between ILs and DNA major and minor grooves are responsible for dehydration and high stability of DNA macromolecules. More recently, Sahoo et al. (2018) reported the molecular mechanism of binding between DNA and non-toxic ILs composed of a cholinium cation and amino-acid-derived anions, namely glycine, alanine, and proline. The authors showed that IL anions have a negligible effect on binding to DNA, when compared with the cholinium cation. On the other hand, Satpathi et al. (2015) proposed that the IL guanidinium tris(pentafluoroethyl)trifluorophosphate is not involved in specific interactions with DNA but instead leads to the compaction of the DNA structure from coil-to-globule conformation.

Although relevant manuscripts have been published (Ding et al., 2010; Chandran et al., 2012; Satpathi et al., 2015; Sahoo et al., 2018), the existence of variable discussions on the mechanisms responsible for the interactions occurring between ILs and DNA is also affected by a still limited number of studies regarding the IL chemical structure effects. Furthermore, a more comprehensive description of the importance of water molecules in the DNA native structure and stability is still missing when dealing with hydrated ILs or IL-water mixtures. In this work, we investigated a series of hydrophilic ILs (combining different cations and anions) in aqueous solutions in order to extend the scientific knowledge about the DNA stability and binding phenomenon occurring between IL and DNA in aqueous solutions, aiming at identifying promising ILs and adequate concentrations to be used in formulations and extraction/separation processes. Although neat ILs have been investigated as well (Zhao, 2015), the use of IL aqueous solutions presents several advantages when compared with neat ILs. Aqueous solutions of ILs may improve the solubility of biomolecules (Cláudio et al., 2013, 2015), provide a more amenable environment and reduced viscosity (Passos et al., 2014) to maintain the biological activity and structural stability of bioactive compounds, and also represent more sustainable solvents since water is used. Circular dichroism (CD) spectroscopy was used to evaluate the conformational structure and stability of DNA in presence of different ILs at different concentrations. The pH and buffer concentration effects were also investigated. The binding characteristics and molecular mechanisms of IL-DNA interactions were studied by UV-Vis absorption spectrophotometry and ^{31}P nuclear magnetic resonance (NMR) spectroscopy. To the best of our knowledge, this work comprises for the first time a screening of several ILs with different cations and anions combinations, allowing a deeper understanding of the ILs molecular features responsible for the DNA stability and structural conformation in aqueous solutions.

MATERIALS AND METHODS

Materials

Double stranded deoxyribonucleic acid (dsDNA) sodium salt extracted from Salmon testes (CAS no. 9007-49-2), of analytical

grade, was purchased from TCI Chemicals. The 260/280 nm absorbance ratio of the DNA stock solution was found to be 1.896, indicating the absence of proteins as contaminants (Saenger, 1984). The ILs studied were: tetrabutylammonium bromide, $[N_{4444}]Br$, tetrabutylphosphonium bromide, $[P_{4444}]Br$, 1-ethyl-3-methylimidazolium bromide, $[C_2C_1im]Br$, (2-hydroxyethyl)-trimethylammonium (cholinium) bromide, $[N_{111(2OH)}]Br$, cholinium chloride, $[N_{111(2OH)}]Cl$, cholinium dihydrogen phosphate, $[N_{111(2OH)}][DHP]$, cholinium acetate, $[N_{111(2OH)}][Ac]$, and cholinium glycolate, $[N_{111(2OH)}][Gly]$. The molecular structures of the investigated ILs are illustrated in **Figure 1**. $[C_2C_1im]Br$ (99 wt%), $[N_{111(2OH)}][DHP]$ (>98 wt%), $[N_{111(2OH)}][Ac]$ (>99 wt%), and $[P_{4444}]Br$ (95 wt%) were purchased from Iolitec. $[N_{4444}]Br$ (98 wt%) was purchased from Fluka. $[N_{111(2OH)}]Br$ (>98 wt%) was purchased from TCI chemicals. $[N_{111(2OH)}]Cl$ (98 wt%) was provided by Acros Organics. $[N_{111(2OH)}][Gly]$ was synthetized by us, by the neutralization of cholinium hydroxide ($[N_{111(2OH)}]OH$) with the respective acid, glycolic acid (1:1.10 mole ratio), at room conditions according to published protocols (Sintra et al., 2015). $[N_{111(2OH)}]OH$ (in methanol solution at 45 wt%) was purchased from Sigma-Aldrich. Glycolic acid (99 wt%) was acquired from Acros Organics. Tris (hydroxymethyl) aminomethane (Tris buffer) (>99.8 wt%) was purchased from Pronalab. Hydrochloric acid (HCl) (in water solution at 37 wt%) was from Sigma-Aldrich. Acetone (100 wt%) and ethanol absolute were acquired from Thermo Fisher Scientific. The water used was double distilled, passed by a reverse osmosis system and further treated with a Milli-Q plus 185 water purification apparatus (18.2 MΩ cm at 25°C).

Experimental Procedure

CD Spectroscopy

CD experiments were performed using a Jasco J-1500 CD spectrophotometer. Aqueous solutions containing 1 g dm^{-3} of DNA in 10 mM of Tris–HCl (pH ≈ 7.2) were incubated during 12 h at 25°C with different concentrations of ILs (5, 15, and 30 wt%), and CD spectra were acquired at a constant temperature of 25°C using a scanning speed of 100 nm min^{-1}, with a response time of 4 s over wavelengths ranging from 220 to 350 nm. Due to the high interference caused by $[C_2C_1im]Br$ in the CD spectrum in the studied wavelengths, for this particular IL, DNA was regenerated using ice cold ethanol (EtOH) in a sample:EtOH ratio of 1:6. The CD spectrum of 10 mM of Tris–HCl (pH ≈ 7.2) was firstly taken as a blank. The recording bandwidth was of 1 nm with a step size of 0.5 nm using a quartz cell with an optical path length of 1 mm. Three scans were averaged *per* spectrum to improve the signal-to-noise ratio. Measurements were performed under a constant nitrogen flow, which was used to purge the ozone generated by the light source of the instrument.

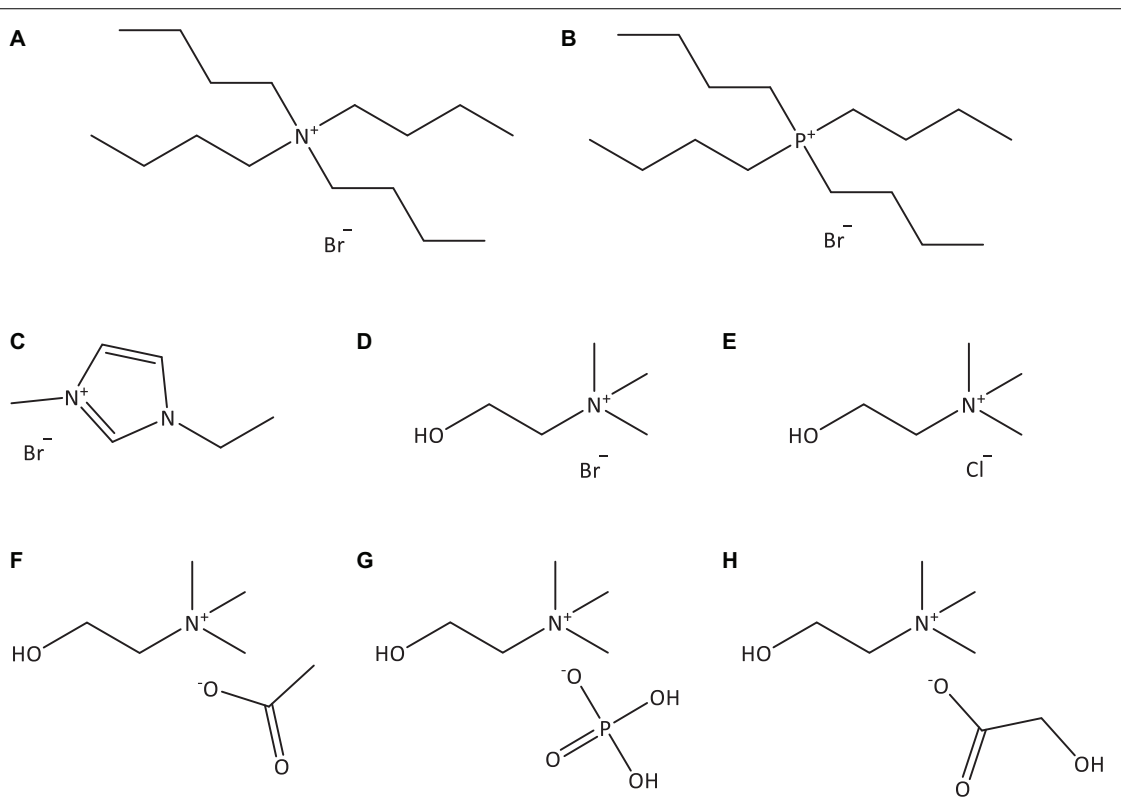

FIGURE 1 | Chemical structures of the ILs used in this work: **(A)** $[N_{4444}]Br$; **(B)** $[P_{4444}]Br$; **(C)** $[C_2C_1im]Br$; **(D)** $[N_{111(2OH)}]Br$; **(E)** $[N_{111(2OH)}]Cl$; **(F)** $[N_{111(2OH)}][Ac]$; **(G)** $[N_{111(2OH)}][DHP]$; **(H)** $[N_{111(2OH)}][Gly]$.

UV-Vis Spectrophotometry

The UV-Vis absorption spectra were obtained with a Shimadzu UV-1800, Pharma-Spec Spectrophotometer. To prepare the samples, different weights of ILs were added to a constant concentration of DNA in aqueous solutions, namely 0.03 g dm^{-3} in 10 mM of Tris–HCl (pH ≈ 7.2) (0.21 g dm^{-3} of DNA for the samples composed of $[C_2C_1im]Br$ due to the high UV absorption caused by this IL), in order to have IL final concentrations of 5 and 30 wt%. The concentrations of DNA used were chosen to avoid absorbance saturation. Each sample was allowed to stand for equilibration during 12 h at 25°C before the UV absorption spectra were recorded. To remove the background of each IL in UV absorption, solutions of ILs at the same concentrations, yet with no DNA added, were used as standard controls, while 10 mM of Tris–HCl (pH ≈ 7.2) was taken as blank reading. All measurements were performed from 200 to 400 nm and carried out in a quartz cuvette with optical path length of 10 mm.

^{31}P NMR

A total of 35 g dm^{-3} of DNA in 10 mM of Tris–HCl (pH ≈ 7.2) aqueous solutions were prepared in different concentrations of ILs (5 and 30 wt%). These solutions were left to stabilize during 12 h at 25°C. NMR spectra of DNA were recorded in a Bruker Avance III operating at 300 MHz, using deuterium oxide (D_2O) as solvent containing trimethylsilyl propanoic acid (TSP) as the internal reference. The phosphorus chemical shifts of DNA were externally referenced to 5 vol% of orthophosphoric acid.

pH Measurements

pH values of the DNA/IL samples were monitored at (25 ± 1)°C using a SevenMulti (METTLER TOLEDO Instruments) with a relative accuracy of ±0.02. All the aforementioned measurements were performed in triplicate.

RESULTS AND DISCUSSION

The evaluation of the dsDNA stability in aqueous solutions of ILs is of high complexity, particularly when aiming the understanding of the interactions occurring between dsDNA and each IL. In the first place, hydration itself has an important impact on the dsDNA structure (McDermott et al., 2017). The helical structure of dsDNA is stabilized by a solvation environment, where changes on hydration can lead to significant changes in the DNA conformation. Furthermore, several hydrophilic ILs composed of distinct ions were investigated in this work, being organized into four classes: cholinium-, $[N_{111(2OH)}]^+$, tetrabutylammonium-, $[N_{4444}]^+$, tetrabutylphosphonium-, $[P_{4444}]^+$, and 1-ethyl-3-methylimidazolium-, $[C_2C_1im]^+$, based ILs. All classes of ILs have bromide as a similar anion. ILs with cholinium as cation were further combined with bromide, chloride, acetate, $[Ac]^-$, dihydrogen phosphate, $[DHP]^-$, and glycolate, $[Gly]^-$, anions.

dsDNA Conformational Structure in ILs Aqueous Solutions

The dsDNA conformational structure was firstly evaluated by CD assays in order to infer the stability of this macromolecule in aqueous solutions of ILs at different concentrations: 5, 15, and 30 wt%. Apart from the IL concentration and chemical structure, the buffer concentration and pH were evaluated in order to address their impact on the dsDNA stability. It is well-known that the pH influences the dsDNA stability and structural integrity (Lindahl and Nyberg, 1972; Cheng and Pettitt, 1992). In this work, the pH was controlled by the use of Tris–HCl buffer (pH ≈ 7.2) in all solutions, in which different concentrations were also investigated.

Circular dichroism spectroscopic measurements allow to gather information on the DNA secondary structure (Satpathi et al., 2015), being commonly used to monitor nucleic acids structure perturbations (Tateishi-Karimata and Sugimoto, 2014). The dsDNA from salmon testes, used in this work, presents a β-form conformation, exhibiting two characteristic peaks: one positive band at approximately 275–280 nm associated to π–π base stacking and a negative band around 245 nm corresponding to helicity (Williams and Kielland, 1975; Evdokimov et al., 1976).

Double stranded deoxyribonucleic acid aqueous solutions were prepared in Tris–HCl buffered solutions at different concentrations (from 10 to 1000 mM) to initially appraise the buffer concentration effect in the dsDNA structural conformation. Since no significant changes were observed in the DNA secondary structure when increasing the buffer concentration (cf. **Supplementary Figure 1**), 10 mM of Tris–HCl was selected and used in the following assays.

For almost all ILs and at the three concentrations investigated, dsDNA maintains its β-form conformation with no transition of the native double-helical structure, as shown in **Figures 2**, **3**. Regarding the IL cation effect, shown in **Figure 2**, and with the exception of $[P_{4444}]Br$, when the remaining ILs are added to DNA aqueous buffered solutions, no significant variations in the CD signal and spectrum of dsDNA are observed. However, with $[P_{4444}]Br$, a significant perturbation in the dsDNA structural conformation is observed at 15 wt% of IL, with a slightly higher effect reflected in the helicity peak than in the base stacking corresponding peak. Furthermore, when using 30 wt% of this IL, no CD spectrum of dsDNA in solution was acquired due to the complete precipitation of DNA.

When dealing with the IL anion effect, being these studies carried out with cholinium-based ILs, less significant changes in the CD signal were observed in the same range of IL concentrations, with the exception of $[N_{111(2OH)}][DHP]$ (**Figure 3**). Aqueous solutions of $[N_{111(2OH)}][DHP]$ are highly acidic, being the pH a main factor leading to the destabilization of DNA as demonstrated below.

The effect of the IL concentration on the CD data of nucleic acids has already been reported. Sahoo et al. (2018) reported no conformational changes in both positive and negative bands of β-form DNA along with the increase of $[N_{1111(2OH)}][Gly]$ concentration, up to 1.8 wt%. Pabbathi and Samanta (2015) demonstrated no significant modifications on the DNA β-form structure when ranging the *N*-ethyl-*N*-methyl-morpholinium bromide ([Mor1,2]Br) concentration from 6 to 20 wt%. These

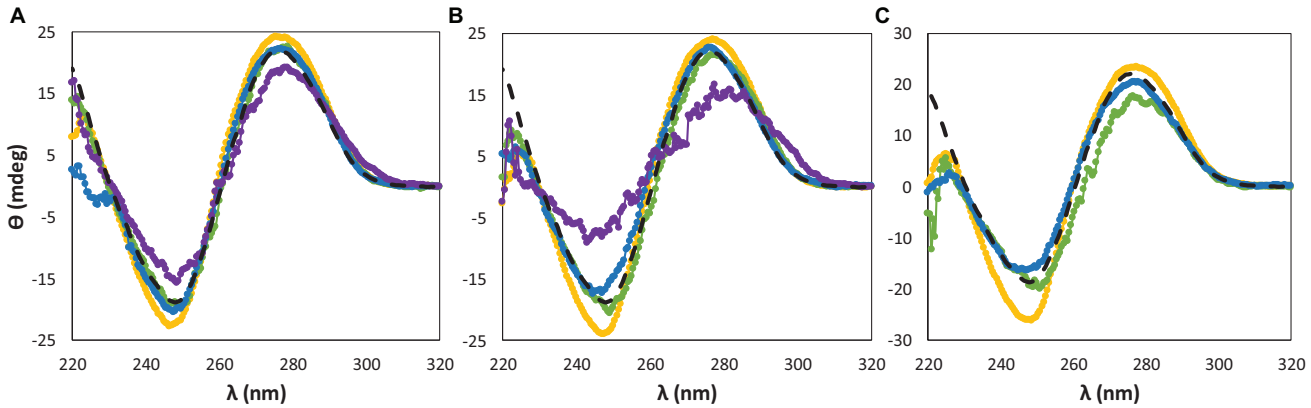

FIGURE 2 | CD spectra regarding the ellipticity, θ, of 0.01 g dm^{-3} of β-DNA (from salmon testes) as a function of wavelength, λ, in 10 mM of Tris–HCl buffer (pH ≈ 7.2) aqueous solutions at different concentrations of bromide-based ILs: **(A)** 5 wt%; **(B)** 15 wt%; **(C)** 30 wt%. (—) only buffer; (•) $[N_{111(2OH)}]Br$; (•) $[N_{4444}]Br$; (•) $[C_2C_1im]Br$; (•) $[P_{4444}]Br$.

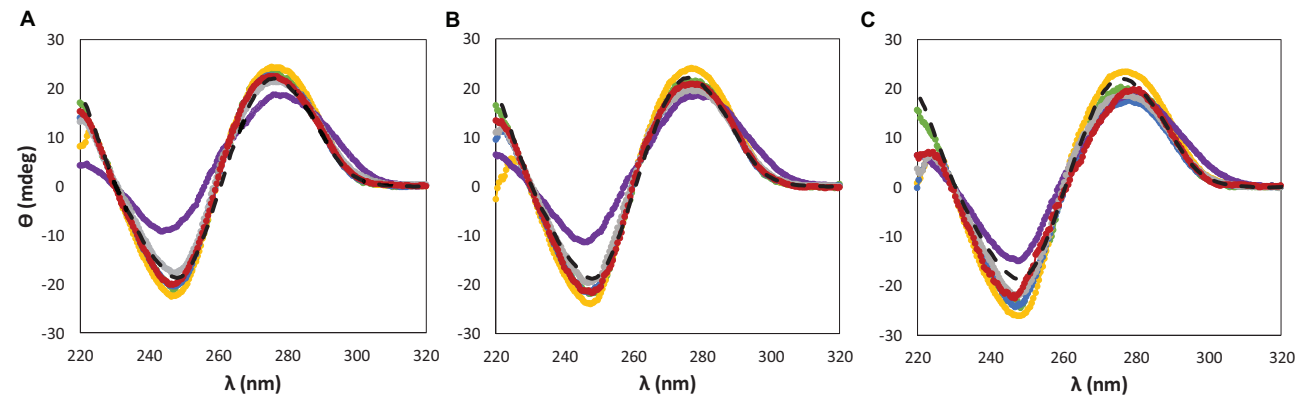

FIGURE 3 | CD spectra regarding the ellipticity, θ, of 0.01 g dm^{-3} of β-DNA (from salmon testes) as a function of wavelength, λ, in 10 mM of Tris–HCl buffer (pH ≈ 7.2) aqueous solutions at different concentrations of cholinium-based ILs: **(A)** 5 wt%; **(B)** 15 wt%; **(C)** 30 wt%. (—) only buffer; (•) $[N_{111(2OH)}]Br$; (•) $[N_{111(2OH)}]Cl$; (•) $[N_{111(2OH)}][Ac]$; (•) non-buffered $[N_{111(2OH)}][DHP]$; (•) buffered $[N_{111(2OH)}][DHP]$; (•) $[N_{111(2OH)}][Gly]$.

results are in agreement with the results obtained in this work, at least in the range of IL concentrations studied.

Effect of pH on the dsDNA Conformational Stability

According to the aforementioned results (**Figures 2**, **3**), both $[P_{4444}]Br$ and non-buffered $[N_{111(2OH)}][DHP]$ induce significant perturbations in the dsDNA native conformation. Although 10 mM of Tris–HCl (pH ≈ 7.2) was used to keep the pH of all ILs solutions, these two ILs provide highly acidic conditions, with the respective aqueous solutions with pH values ranging between 2 and 4 (cf. **Supplementary Table 1** with detailed data). The commercial $[P_{4444}]Br$ used contains phosphines as main impurities, whereas $[N_{111(2OH)}][DHP]$ provides acidic medium due to the IL anion. It should be noted that the presence of DNA in the aqueous solutions of ILs does not influence the pH values, as experimentally verified. Accordingly, the results obtained in terms of the dsDNA loss of stability seem to be highly affected by the pH and not by the IL chemical structure alone. Some authors already associated acidic properties, along with the increase of the IL concentration, to a significant perturbation of the nucleic acids structure. For instance, Pedro et al. (2018) observed that the structural integrity of ribonucleic acid (RNA) is destabilized in presence of non-buffered $[N_{111(2OH)}][DHP]$ that confers acidic conditions to the aqueous medium. However, by the addition of cholinium hydroxide to $[N_{111(2OH)}][DHP]$ aqueous solutions to reach a pH *ca.* 7, the authors (Pedro et al., 2018) demonstrated significant improvements in the RNA stability. In the same line, in this work, the stability of dsDNA was further evaluated in buffered $[N_{111(2OH)}][DHP]$ by adding cholinium hydroxide up to pH 7. By increasing the pH of the medium there is the improvement of the stability of dsDNA, as shown in **Figure 3**. These results demonstrate that the IL chemical structure alone is not responsible for the DNA destabilization, but yet the pH plays a significant role.

In order to better address the pH effect, a set of studies was additionally performed on the dsDNA stability in aqueous solutions of $[P_{4444}]Br$, since this was the IL that provided the most acidic conditions due to the present impurities (cf. **Supplementary Table 1**), and where DNA precipitation was

observed at 30 wt% of IL. Different concentrations of Tris–HCl buffer were used in 30 wt% [P_{4444}]Br aqueous solutions. As shown in **Supplementary Figure 2**, only with Tris–HCl concentrations from 500 mM it is possible to reach the physiological pH in aqueous solutions containing 30 wt% of [P_{4444}]Br. Furthermore, in aqueous solutions composed of [P_{4444}]Br at 30 wt% in 1000 mM of Tris–HCl (pH ≈ 7.2) it was observed that the solubility of DNA increases (**Figure 4A** – the tendency followed by the arrow), thus avoiding the DNA precipitation initially observed, reinforced by the improvement in the maintenance of the dsDNA native conformation (**Figure 4B**). Our results are in agreement with those published by Vijayaraghavan et al. (2010), who performed a set of experiments to demonstrate the effect of pH on the fluorescence emission intensity of aqueous solutions of DNA. Since fluorescence is the result of the presence of the hydrogen-bonded adenine base in native DNA, its intensity depends on the pH of the medium. In acidic conditions, the authors attributed the increase of the intensity to the increased protonation of adenine (Vijayaraghavan et al., 2010). Overall, and although pH plays a significant role since the protonation of DNA is an important factor for maintaining the stability of the macromolecule, the IL chemical structure influence and the existence of specific interactions occurring between IL and DNA should not be dismissed, as shown below.

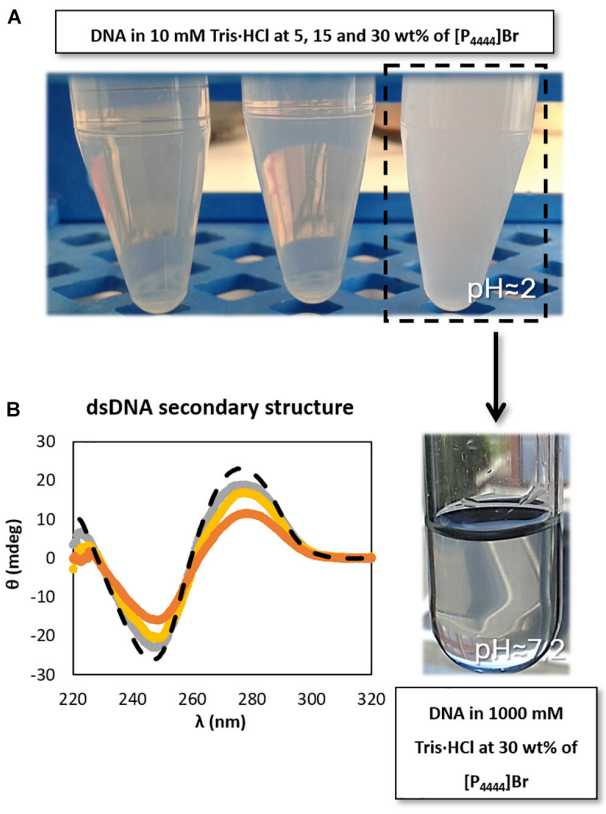

FIGURE 4 | Schematic representation of **(A)** DNA dissolution process with the increase of buffer concentration (increase of pH value) and **(B)** CD spectra regarding the ellipticity, θ, of 0.01 g dm^{-3} of β-DNA (from salmon testes) as a function of wavelength, λ, in 1000 mM Tris–HCl buffer (pH ≈ 7.2). (—) only buffer; (•) 5 wt% of [P_{4444}]Br; (•) 15 wt% of [P_{4444}]Br; (•) 30 wt% of [P_{4444}]Br.

DNA-IL Interaction Studies

Considering the set of results presented before, it is still required a deeper analysis of the molecular mechanisms and interactions occurring between ILs and DNA. Only with this information it will be possible a proper design of IL-based media for the long-term preservation of nucleic acids. In this line, UV-Vis absorption measurements were carried out to investigate interaction patterns between DNA and ILs.

Figure 5 shows the effect of adding different concentrations of IL, namely at the minimum and maximum concentrations used in the previous studies, i.e., 5 and 30 wt%, on the dsDNA absorption spectra. **Figures 5A,C** represent the IL cation effect, whereas **Figures 5B,D** represent the IL anion effect. It should be noted that changes in position (shift) and absorbance maximum of dsDNA is associated to DNA-IL interactions and/or DNA gains and losses of stability (Haque et al., 2017; Sahoo et al., 2018). For all the absorption spectra acquired an hyperchromic effect is observed, where the absorption of dsDNA in aqueous solutions of ILs is higher than that for dsDNA in 10 mM of Tris–HCl buffer (pH ≈ 7.2). In what concerns the IL cation effect (**Figures 5A,C**), a specific trend of the cation structure is observed independently of the IL concentration. At 260 nm, and at the two concentrations of ILs investigated, the hyperchromicity increases in the following order: [$N_{111(2OH)}$]Br < [C_2C_1im]Br ≈ [N_{4444}]Br < [P_{4444}]Br. An increase of the dsDNA absorption spectrum is due to the unstacking of nucleobases, as a consequence of uncoiling or denaturation processes of dsDNA, which seems to be affected by the IL chemical structure. Overall, and among the bromide-based ILs investigated, [P_{4444}]Br is the IL that leads to a higher unstacking of the DNA bases, whereas [$N_{111(2OH)}$]Br is the most promising IL to promote the DNA stability. In what concerns the IL anion effect (**Figures 5B,D**), a specific trend associated to the anion structure is not observed considering its impact on the dsDNA structure. Different patterns are observed when changing the IL concentration. However, amongst the cholinium-based ILs investigated, [$N_{111(2OH)}$][Gly] is the IL that leads to a higher unstacking of nucleobases in DNA, as confirmed by the higher hyperchromic effect observed with this IL. On the other hand, [$N_{111(2OH)}$]Br and [$N_{111(2OH)}$][Ac] seem to be the most appropriate ILs to keep the DNA structure at the two concentrations investigated.

Although the UV absorption results demonstrate that the IL influences the dsDNA helical structure, a quantitative approach was additionally carried out by ^{31}P NMR analysis of the DNA phosphate backbone with aqueous solutions of ILs at 5 and 30 wt%. The intensity values of the ^{31}P NMR peaks express the DNA phosphate backbone and the exposition of phosphate groups in a given environment. **Figure 6** depicts the ^{31}P NMR intensity values of DNA phosphate groups, in aqueous solutions of ILs at 5 and 30 wt%, as a function of dsDNA ellipticity at 245 nm that represents the helicity, whose values were taken from the data given in **Figures 2**, **3**. Regardless the IL concentration, there is a correlation between the helicity and the ^{31}P NMR intensity

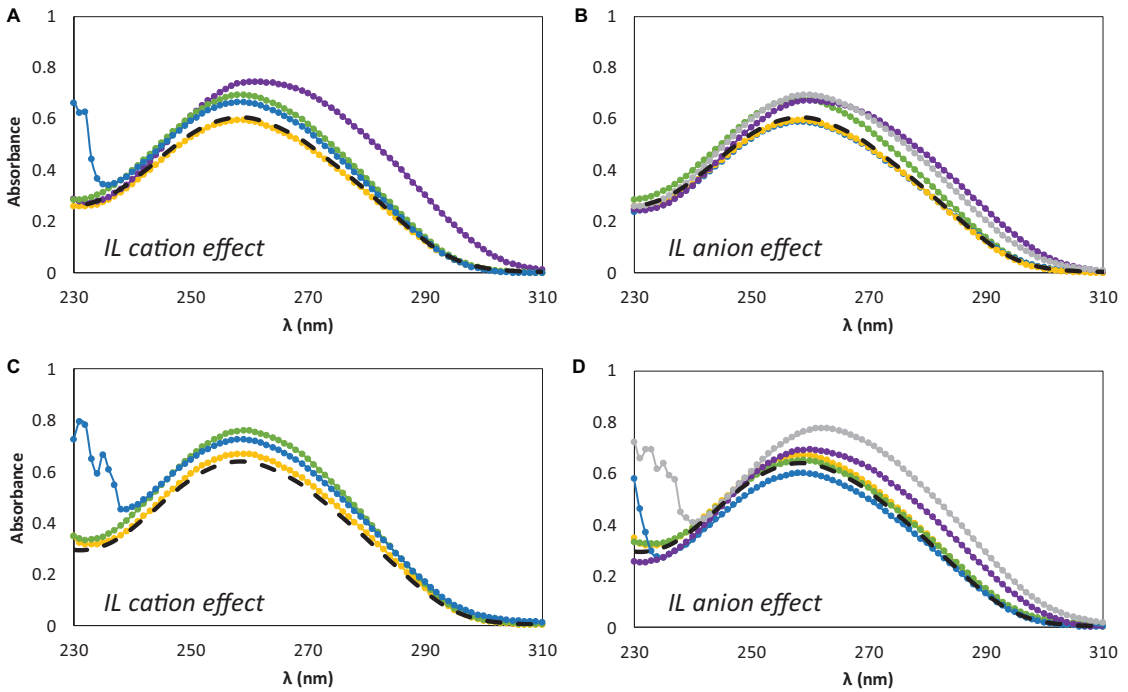

FIGURE 5 | Absorption spectra of β-DNA (from salmon testes) as a function of wavelength, λ, in 10 mM of Tris–HCl buffer (pH ≈ 7.2) aqueous solutions at different concentrations of IL. **(A)** 5 wt% of bromide-based ILs: (—) only buffer; (•) [$N_{111(2OH)}$]Br; (•) [C_2C_1im]Br; (•) [N_{4444}]Br; (•) [P_{4444}]Br; **(B)** 5 wt% of cholinium-based ILs. (—) only buffer; (•) [$N_{111(2OH)}$]Br; (•) [$N_{111(2OH)}$][Ac]; (•) non-buffered [$N_{111(2OH)}$][DHP]; (•) [$N_{111(2OH)}$]Cl; (•) [$N_{111(2OH)}$][Gly]; **(C)** 30 wt% of bromide-based ILs: (—) only buffer; (•) [$N_{111(2OH)}$]Br; (•) [C_2C_1im]Br; (•) [N_{4444}]Br; **(D)** 30 wt% of cholinium-based ILs. (—) only buffer; (•) [$N_{111(2OH)}$]Br; (•) [$N_{111(2OH)}$][Ac]; (•) non-buffered [$N_{111(2OH)}$][DHP]; (•) [$N_{111(2OH)}$]Cl; (•) [$N_{111(2OH)}$][Gly].

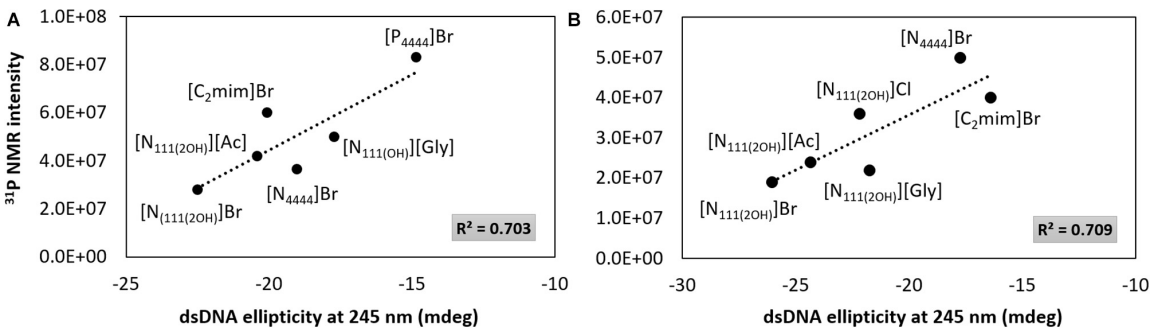

FIGURE 6 | ^{31}P NMR intensity peaks of DNA as a function of dsDNA ellipticity at 245 nm. **(A)** IL at 5 wt%; **(B)** IL at 30 wt%.

peaks of DNA. The higher the ellipticity of dsDNA, the higher the phosphorous peaks intensity of phosphate groups of DNA. According to **Figure 6**, [$N_{111(2OH)}$]Br presents the lowest value of ellipticity and the lowest intensity peak of DNA phosphate groups, supporting the possibility of the IL cation being more strongly interacting with the phosphate backbone of dsDNA, thus lowering the phosphorous exposition to the aqueous environment. These results reinforce the higher capability of [$N_{111(2OH)}$]Br to better stabilize dsDNA in aqueous solutions, being in agreement with the CD and UV absorption analysis (**Figures 2**, **3**, **5**). At the IL concentration of 5 wt% (**Figure 6A**), [P_{4444}]Br presents the highest values of ellipticity and ^{31}P NMR intensity associated to the phosphate groups of DNA. With [P_{4444}]Br, the dsDNA macromolecule surface is more exposed to the aqueous environment and the IL cation is not preferentially interacting with the phosphate groups of the biopolymer. Accordingly, the perturbation on the dsDNA conformation due to [P_{4444}]Br are not due to electrostatic interactions, but yet by dispersive interactions that may be established between the alkyl side chains of the IL cation and the nucleobases. However, with this ILs, it should be remarked that the pH effect cannot be discarded. Since $[P_{4444}]^+$ is also detected in ^{31}P NMR spectra, an example of the obtained spectrum for the samples composed of dsDNA in 5 wt% of [P_{4444}]Br in 10 mM of Tris–HCl buffer (pH ≈ 7.2) is provided

in the **Supplementary Figure 3**, allowing to demonstrate that ^{31}P NMR peaks values of DNA phosphate groups are distinguished from $[P_{4444}]^+$ peaks. At higher concentrations of IL (**Figure 6B**), i.e., at 30 wt%, there is a general trend of the cholinium-based ILs to display lower ^{31}P NMR peaks intensity, reinforcing that the cholinium cation preferentially interacts with the DNA phosphate groups when compared with imidazolium and tetrabutylphosphonium/ammonium cations.

Figure 7 depicts the ^{31}P NMR intensity values of DNA phosphate groups (in aqueous solutions of ILs at 5 and 30 wt%) as a function of the dsDNA ellipticity at 280 nm, representing π–π base stacking, whose values were taken from the data provided in **Figures 2**, **3**. As dsDNA ellipticity at 280 nm represents the binding strength occurring between bases, the higher this value is the more consistent the base stacking, thus fostering a more stable double strand conformation of dsDNA. Overall, at 5 wt% of IL (**Figure 7A**), the ^{31}P NMR peak intensity values decrease with the increase in the dsDNA ellipticity at 280 nm. This trend supports that favorable interactions of the IL cation with the DNA phosphate groups, expressed by a decrease in the NMR peak intensity, improve the DNA π–π base stacking. At 5 wt% of IL, $[N_{111(2OH)}]$Br induces the highest dsDNA ellipticity value at 280 nm and the lowest NMR intensity peak of DNA phosphate groups, meaning that π–π base stacking occurring in dsDNA molecules are better preserved and that interactions of the IL cation with the DNA phosphate groups are preferentially established. This trend reinforces the preferential interactions of cholinium with the DNA phosphate backbone. On the other hand, π–π base stacking seems to be more relaxed in presence of $[P_{4444}]$Br, being this the IL with the lowest ability to preserve the DNA structure as discussed above. However, at 30 wt% of IL (**Figures 7B,C**), no correlation between the ^{31}P NMR intensity values of DNA phosphate groups as a function of the dsDNA ellipticity at 280 nm was found. These results support that at higher concentrations of ILs the molecular-level phenomenon is more complex and that other interactions different from electrostatic may play a role in the stabilization of DNA.

Overall, taking into account the data shown in **Figures 6**, **7**, the main molecular-level mechanisms occurring in aqueous solutions containing ILs and dsDNA can be summarized as follows: (i) electrostatic interactions – at lower IL concentrations higher ^{31}P NMR intensity peak values are observed, meaning that the DNA phosphate backbone is more exposed, and thus less electrostatic interactions are established between the IL cation and the DNA phosphate groups, which may be due to difficulties in "breaking" the DNA hydration shell. At higher IL concentrations, IL cations compete stronger with water molecules for the dsDNA phosphate backbone, thus decreasing the ^{31}P NMR intensity peak values; (ii) dispersive interactions – the hydrophobicity of the IL cation plays a role since an increase in the DNA ellipticity and a decrease in π–π base stacking is observed with more hydrophobic ILs cations, therefore causing perturbation on the dsDNA native conformation; and (iii) the IL anion has a weaker impact when compared to the IL cation effect on interacting with DNA molecules since no correlation was found at higher concentrations of IL (**Figure 7C**).

The hypothesis previously addressed is in accordance with previously published results. Ding et al. (2010) demonstrated that at IL concentrations lower than 1.05 wt%, the IL cation is localized at several angstroms of distance from DNA phosphate strand, while the IL hydrophobic chains are in parallel arrangement to the DNA molecule surface. On the other hand, at higher IL concentrations, the IL cation is near to the DNA phosphate strand and the IL hydrocarbon chains are perpendicularly attached to the DNA molecule surface. Sahoo et al. (2018) described that when using cholinium-based ILs with anions derived from amino acids, the cholinium cation interacts with DNA through with an independent effect of the anions. According to the experimental and theoretical data gathered by the authors, they suggested a heterogeneity in binding modes of

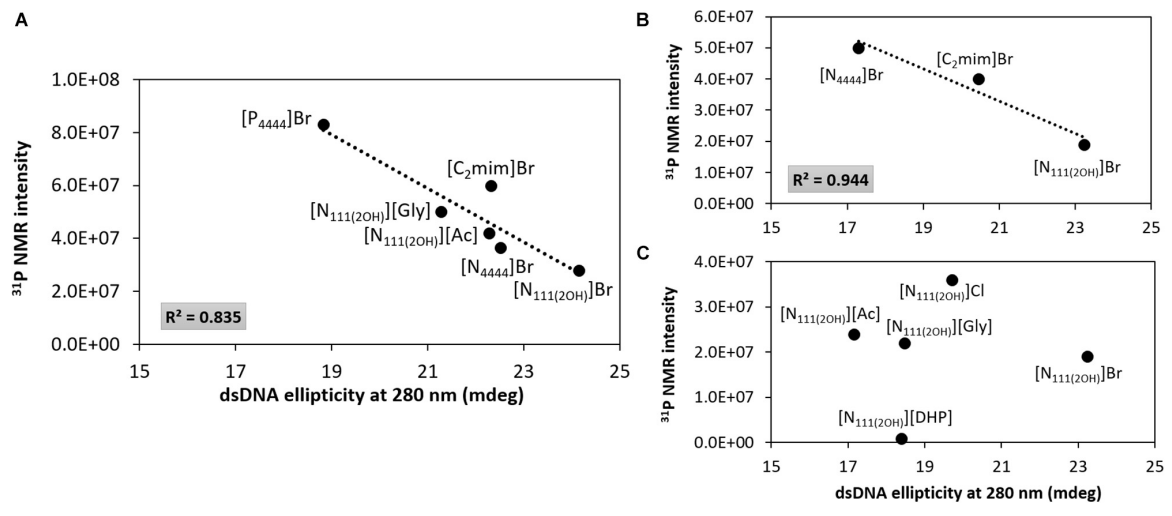

FIGURE 7 | ^{31}P NMR intensity peak of DNA as a function of dsDNA ellipticity at 280 nm. **(A)** IL at 5 wt%; **(B)** bromide-based ILs at 30 wt%; **(C)** cholinium-based ILs at 30 wt%.

IL to DNA, where electrostatic interactions and H-bonding with the phosphate groups occur, while binding modes in the minor groove of dsDNA were predominantly stabilized by van der Waals interactions. Pabbathi and Samanta (2015) demonstrated that the morpholinium cation binds to the minor grooves of dsDNA and its binding is weaker when compared with the imidazolium cation. Singh et al. (2012) suggested not only the presence of electrostatic interactions between DNA and IL by fluorescence intensity measurements, but also that non-electrostatic interactions between the IL cation alkyl chain and the dsDNA base pairs are relevant. Overall, the data previously published by different authors together with the results presented in this manuscript correspond to relevant fundamental insights on the ILs effects toward DNA in aqueous solution. The gathered data are of high relevance for the preparation of effective DNA preservation media and for the design of IL-based separation processes from biological media.

CONCLUSION

In this work, a screening of several ILs with different cations and anions combinations, and at different concentrations and pH values, was carried out for a deeper understanding on the molecular features responsible for the dsDNA stability and structural conformation in aqueous solutions. CD, UV absorption, and ^{31}P NMR spectroscopic studies were performed, where it was observed that the pH, type, and IL concentration contribute to changes in the dsDNA conformational structure. It was observed that higher IL concentrations and hydrophobicity of the corresponding cation lead to perturbations on the structural conformation of dsDNA. Overall, the best IL identified to preserve the stability of dsDNA was $[N_{111(2OH)}]$Br.

The obtained results allowed us to identify main interactions and phenomena responsible for the dsDNA stability in IL aqueous solutions. At lower IL concentrations, less electrostatic interactions are established between the IL cation and the DNA phosphate groups, which may be due to difficulties in "breaking" the dsDNA hydration shell. On the other hand, at higher IL concentrations, IL cations compete stronger with water molecules for the dsDNA phosphate backbone, as verified with the decrease in the ^{31}P NMR intensity peak values. The hydrophobicity of the IL cation plays a main role since an increase in the DNA ellipticity and a decrease in π–π base stacking is observed with more hydrophobic ILs cations, leading to the perturbation of the dsDNA native conformation. Finally, the IL anion has a weaker impact when compared to the IL cation effect on interacting with DNA molecules. In summary, the results presented in this work provide fundamental knowledge for the application of adequate ILs in the preservation and separation and purification of nucleic acids, with significant impact in the biotechnology field.

DATA AVAILABILITY STATEMENT

The raw data supporting the conclusions of this article will be made available by the authors, without undue reservation.

AUTHOR CONTRIBUTIONS

TD, MF, and FS conceived and planned the work. TD carried out the experimental assays, analyzed the data, and prepared the first draft of the manuscript. All authors contributed to the interpretation and discussion of the acquired data and to the manuscript preparation.

FUNDING

This work was developed within the scope of the project CICECO – Aveiro Institute of Materials, UIDB/50011/2020 and UIDP/50011/2020, financed by national funds through the Portuguese Foundation for Science and Technology/MCTES. TD acknowledges the Ph.D. grant SFRH/BD/130958/2017. FS acknowledges the CICS-UBI project UIDB/00709/2020 and the project PTDC/BII-BBF/29496/2017 (PUREmiRSILs) funded by FEDER, through COMPETE2020 – Programa Operacional Competitividade e Internacionalização (POCI), and by national funds (OE), through FCT/MCTES. The authors acknowledge the financial support from the European Union Framework Programme for Research and Innovation HORIZON 2020, under the TEAMING Grant Agreement No. 739572 – The Discoveries CTR.

SUPPLEMENTARY MATERIAL

The Supplementary Material for this article can be found online at: https://www.frontiersin.org/articles/10.3389/fbioe.2020.547857/full#supplementary-material

REFERENCES

Bowlas, C. J., Bruce, D. W., and Seddon, K. R. (1996). Liquid-crystalline ionic liquids. *ChemComm* 1996, 1625–1626. doi: 10.1039/cc9960001625

Chandran, A., Ghoshdastidar, D., and Senapati, S. (2012). Groove binding mechanism of ionic liquids: a key factor in long-term stability of DNA in hydrated ionic liquids?. *J. Am. Chem. Soc.* 134, 20330–20339. doi: 10.1021/ja304519d

Cheng, Y. K., and Pettitt, B. M. (1992). Stabilities of double-strand and triple-strand helical nucleic-acids. *Prog. Biophys. Mol. Biol.* 58, 225–257. doi: 10.1016/0079-6107(92)90007-s

Cláudio, A. F. M., Ferreira, A. M., Freire, M. G., and Coutinho, J. A. P. (2013). Enhanced extraction of caffeine from guaraná seeds using aqueous solutions of ionic liquids. *Green Chem.* 15, 2002–2010. doi: 10.1039/C3GC40437D

Cláudio, A. F. M., Neves, M. C., Shimizu, K., Canongia Lopes, J. N., Freire, M. G., and Coutinho, J. A. P. (2015). The magic of aqueous solutions of ionic liquids: ionic liquids as a powerful class of catanionic hydrotropes. *Green Chem.* 17, 3948–3963. doi: 10.1039/C5GC00712G

Diamantino, T., Pereira, P., Queiroz, J. A., Sousa, Â, and Sousa, F. (2016). Minicircle DNA purification using a CIM® DEAE-1 monolithic support. *J. Sep. Sci* 39, 3544–3549. doi: 10.1002/jssc.201600375

Ding, Y. H., Zhang, L., Xie, J., and Guo, R. (2010). binding characteristics and molecular mechanism of interaction between ionic liquid and DNA. *J. Phys. Chem. B.* 114, 2033–2043. doi: 10.1021/jp9104757

Endres, F., and El Abedin, S. Z. (2006). Air and water stable ionic liquids in physical chemistry. *Phys. Chem. Chem. Phys.* 8, 2101–2116. doi: 10.1039/b600519p

Evdokimov, Y. M., Pyatigorskaya, T. L., Polyvtsev, O. F., Akimenko, N. M., Kadykov, V. A., Tsvankin, D. Y., et al. (1976). A comparative X-ray diffraction and circular dichroism study of DNA compact particles formed in water-salt solutions, containing poly(ediylene glycol). *Nucleic Acids Res.* 3, 2353–2366. doi: 10.1093/nar/3.9.2353

Freire, M. G., Cláudio, A. F. M., Araújo, J. M. M., Coutinho, J. A. P., Marrucho, I. M., Canongia Lopes, J. N., et al. (2012). Aqueous biphasic systems: a boost brought about by using ionic liquids. *Chem. Soc. Rev.* 41, 4966–4995. doi: 10.1039/c2cs35151j

Freyer, J. L., Brucks, S. D., Gobieski, G. S., Russell, S. T., Yozwiak, C. E., Sun, M., et al. (2016). Clickable Poly(ionic liquids): a materials platform for transfection. *Angew. Chem. Int. Ed.* 55, 12382–12386. doi: 10.1002/anie.201605214

Gartner, Z. J., Tse, B. N., Grubina, R., Doyon, J. B., Snyder, T. M., and Liu, D. R. (2004). DNA-templated organic synthesis and selection of a library of macrocycles. *Science* 305, 1601–1605. doi: 10.1126/science.1102629

Gordon, C. M., Holbrey, J. D., Kennedy, A. R., and Seddon, K. R. (1998). Ionic liquid crystals: hexafluorophosphate salts. *J. Mater. Chem.* 8, 2627–2636. doi: 10.1039/a806169f

Haque, A., Khan, I., Hassan, S. I., and Khan, M. S. (2017). Interaction studies of cholinium-based ionic liquids with calf thymus DNA: spectrophotometric and computational methods. *J. Mol. Liq.* 237, 201–207. doi: 10.1016/j.molliq.2017.04.068

Hussey, C. L. (1994). "The electrochemistry of room- temperature haloaluminate molten salts," in *Chemistry of Nonaqueous Solutions*, eds G. Mamantov and A. I. Popov (Weinheim: VCH), 227–276.

Jain, N., Kumar, A., Chauhan, S., and Chauhan, S. M. S. (2005). Chemical and biochemical transformations in ionic liquids. *Tetrahedron* 61, 1015–1060. doi: 10.1016/j.tet.2004.10.070

Lindahl, T., and Nyberg, B. (1972). Rate of depurination of native deoxyribonucleic acid. *Biochemistry* 11, 3610–3618. doi: 10.1021/bi00769a018

Lissek, T. (2017). Interfacing neural network components and nucleic acids. *Front. Bioeng. Biotech.* 5:13. doi: 10.3389/fbioe.2017.00053

Liu, H., and Liu, D. S. (2009). DNA nanomachines and their functional evolution. *ChemComm* 6, 2625–2636. doi: 10.1039/b822719e

McDermott, M. L., Vanselous, H., Corcelli, S. A., and Petersen, P. B. (2017). DNA's chiral spine of hydration. *ACS Cent. Sci.* 3, 708–714. doi: 10.1021/acscentsci.7b00100

Mukesh, C., Mondal, D., Sharma, M., and Prasad, K. (2013). Rapid dissolution of DNA in a novel bio-based ionic liquid with long-term structural and chemical stability: successful recycling of the ionic liquid for reuse in the process. *ChemComm* 49, 6849–6851. doi: 10.1039/c3cc42829j

Pabbathi, A., and Samanta, A. (2015). Spectroscopic and molecular docking study of the interaction of DNA with a morpholinium ionic liquid. *J. Phys. Chem. B* 119, 11099–11105. doi: 10.1021/acs.jpcb.5b02939

Padrino, B., Lara-Serrano, M., Morales-delaRosa, S., Campos-Martin, J. M., Fierro, J. L. G., Martinez, F., et al. (2018). Resource recovery potential from lignocellulosic feedstock upon lysis with ionic liquids. *Front. Bioeng. Biotech.* 6:119. doi: 10.3389/fbioe.2018.00119

Passos, H., Freire, M. G., and Coutinho, J. A. P. (2014). Ionic liquid solutions as extractive solvents for value-added compounds from biomass. *Green Chem.* 16, 4786–4815. doi: 10.1039/C4GC00236A

Pedro, A. Q., Pereira, P., Quental, M. J., Carvalho, A. P., Santos, S. M., Queiroz, J. A., et al. (2018). Cholinium-Based Good's buffers ionic liquids as remarkable stabilizers and recyclable preservation media for recombinant small RNAs. *ACS Sustain. Chem. Eng.* 6, 16645–16656. doi: 10.1021/acssuschemeng.8b03900

Plechkova, N. V., and Seddon, K. R. (2008). Applications of ionic liquids in the chemical industry. *Chem. Soc. Rev.* 37, 123–150. doi: 10.1039/b006677j

Renčiuk, D., Kejnovská, I., Kypr, J., and Vorlíčková, M. (2009). Circular dichroism and conformational polymorphism of DNA. *Nucleic Acids Res.* 37, 1713–1725. doi: 10.1093/nar/gkp026

Saenger, W. (1984). *Principles of Nucleic Acid Structure*. New York, NY: Springer-Verlag New York.

Sahoo, D. K., Jena, S., Dutta, J., Chakrabarty, S., and Biswal, H. S. (2018). Critical assessment of the interaction between DNA and choline amino acid ionic liquids: evidences of multimodal binding and stability enhancement. *ACS Cent. Sci.* 4, 1642–1651. doi: 10.1021/acscentsci.8b00601

Sasaki, Y., Miyoshi, D., and Sugimoto, N. (2007). Regulation of DNA nucleases by molecular crowding. *Nucleic Acids Res.* 35, 4086–4093. doi: 10.1093/nar/gkm445

Satpathi, S., Sengupta, A., Hridya, V. M., Gavvala, K., Koninti, R. K., Roy, B., et al. (2015). A green solvent induced DNA package. *Sci. Rep.* 5:9137. doi: 10.1038/srep09137

Seddon, K. R. (1997). Ionic liquids for clean technology. *J. Chem. Technol.* 68, 351–356.

Shamshina, J. L., and Berton, P. (2020). Use of ionic liquids in chitin biorefinery: a systematic review. *Front. Bioeng. Biotech.* 8:14. doi: 10.3389/fbioe.2020.00011

Sheldon, R. (2001). Catalytic reactions in ionic liquids. *ChemComm* 7, 2399–2407. doi: 10.1039/b107270f

Singh, P. K., Sujana, J., Mora, A. K., and Nath, S. (2012). Probing the DNA–ionic liquid interaction using an ultrafast molecular rotor. *J. Photochem. Photobiol. A* 246, 16–22. doi: 10.1016/j.jphotochem.2012.07.006

Sintra, T. E., Luís, A., Rocha, S. N., Ferreira, A., Goncalves, F., Santos, L., et al. (2015). Enhancing the antioxidant characteristics of phenolic acids by their conversion into cholinium salts. *ACS Sustain. Chem. Eng.* 3, 2558–2565. doi: 10.1021/acssuschemeng.5b00751

Tateishi-Karimata, H., and Sugimoto, N. (2014). Structure, stability and behaviour of nucleic acids in ionic liquids. *Nucleic Acids Res.* 42, 8831–8844. doi: 10.1093/nar/gku499

Uludag, H., Ubeda, A., and Ansari, A. (2019). At the intersection of biomaterials and gene therapy: progress in non-viral delivery of nucleic acids. *Front. Bioeng. Biotech.* 7:131. doi: 10.3389/fbioe.2019.00131

Ventura, S. P. M., Santos, L. D. F., Saraiva, J. A., and Coutinho, J. A. P. (2012). Ionic liquids microemulsions: the key to *Candida antarctica* lipase B superactivity. *Green Chem.* 14, 1620–1625. doi: 10.1039/c2gc35197h

Vijayaraghavan, R., Izgorodin, A., Ganesh, V., Surianarayanan, M., and MacFarlane, D. R. (2010). Long-term structural and chemical stability of DNA in hydrated ionic liquids. *Angew. Chem. Int. Ed.* 49, 1631–1633. doi: 10.1002/anie.200906610

Williams, R. E., and Kielland, S. L. (1975). Water-soluble lysine-containing polypeptides. II. the interaction of several sequential lysine–glycine polypeptides with DNA. A circular dichroism study of DNA conformation in annealed complexes. *Can. J. Chem.* 53, 542–548. doi: 10.1139/v75-074

Wong, H. T., Han, S. J., and Livingston, A. G. (2006). The effect of ionic liquids on product yield and catalyst stability. *Chem. Eng. Sci.* 61, 1338–1341. doi: 10.1016/j.ces.2005.08.019

Yamada, M., Yokota, M., Kaya, M., Satoh, S., Jonganurakkun, B., Nomizu, M., et al. (2005). Preparation of novel bio-matrix by the complexation of DNA and metal ions. *Polymer* 46, 10102–10112. doi: 10.1016/j.polymer.2005.07.086

Yin, H., Kanasty, R. L., Eltoukhy, A. A., Vegas, A. J., Dorkin, J. R., and Anderson, D. G. (2014). Non-viral vectors for gene-based therapy. *Nat. Rev. Genet.* 15, 541–555. doi: 10.1038/nrg3763

Zhao, H. (2015). DNA stability in ionic liquids and deep eutectic solvents. *J. Chem. Technol. Biotechnol.* 90, 19–25. doi: 10.1002/jctb.4511

Zhao, H., Xia, S. Q., and Ma, P. S. (2005). Use of ionic liquids as 'green' solvents for extractions. *J. Chem. Technol. Biotechnol.* 80, 1089–1096. doi: 10.1002/jctb.1333

Conflict of Interest: The authors declare that the research was conducted in the absence of any commercial or financial relationships that could be construed as a potential conflict of interest.

Advantages of publishing in Frontiers

OPEN ACCESS
Articles are free to read for greatest visibility and readership

FAST PUBLICATION
Around 90 days from submission to decision

HIGH QUALITY PEER-REVIEW
Rigorous, collaborative, and constructive peer-review

TRANSPARENT PEER-REVIEW
Editors and reviewers acknowledged by name on published articles

Frontiers
Avenue du Tribunal-Fédéral 34
1005 Lausanne | Switzerland

Visit us: www.frontiersin.org
Contact us: frontiersin.org/about/contact

REPRODUCIBILITY OF RESEARCH
Support open data and methods to enhance research reproducibility

DIGITAL PUBLISHING
Articles designed for optimal readership across devices

FOLLOW US
@frontiersin

IMPACT METRICS
Advanced article metrics track visibility across digital media

EXTENSIVE PROMOTION
Marketing and promotion of impactful research

LOOP RESEARCH NETWORK
Our network increases your article's readership